Smithsonian Institution
Scholarly Press

SMITHSONIAN CONTRIBUTIONS TO PALEOBIOLOGY • NUMBER 98

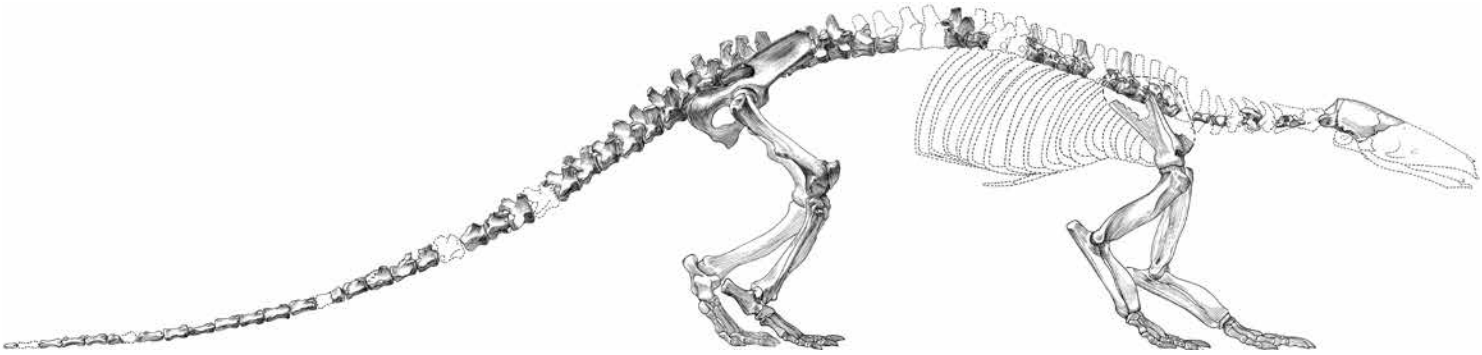

Skeletal Anatomy of the North American Pangolin *Patriomanis americana* (Mammalia, Pholidota) from the Latest Eocene of Wyoming (USA)

Timothy J. Gaudin, Robert J. Emry, and Jeremy Morris

SERIES PUBLICATIONS OF THE SMITHSONIAN INSTITUTION

Emphasis upon publication as a means of "diffusing knowledge" was expressed by the first Secretary of the Smithsonian. In his formal plan for the Institution, Joseph Henry outlined a program that included the following statement: "It is proposed to publish a series of reports, giving an account of the new discoveries in science, and of the changes made from year to year in all branches of knowledge." This theme of basic research has been adhered to through the years by thousands of titles issued in series publications under the Smithsonian imprint, commencing with Smithsonian Contributions to Knowledge in 1848 and continuing with the following active series:

Smithsonian Contributions to Anthropology
Smithsonian Contributions to Botany
Smithsonian Contributions to History and Technology
Smithsonian Contributions to the Marine Sciences
Smithsonian Contributions to Museum Conservation
Smithsonian Contributions to Paleobiology
Smithsonian Contributions to Zoology

In these series, the Institution publishes small papers and full-scale monographs that report on the research and collections of its various museums and bureaus. The Smithsonian Contributions Series are distributed via mailing lists to libraries, universities, and similar institutions throughout the world.

Manuscripts intended for publication in the Contributions Series undergo substantive peer review and evaluation by SISP's Editorial Board, as well as evaluation by SISP for compliance with manuscript preparation guidelines (available on SISP's "Author Resources" page at www.scholarlypress.si.edu). For open access, fully searchable PDFs of volumes in the Smithsonian Contributions Series, visit Open SI (http://opensi.si.edu).

SMITHSONIAN CONTRIBUTIONS TO PALEOBIOLOGY • NUMBER 98

Skeletal Anatomy of the North American Pangolin *Patriomanis americana* (Mammalia, Pholidota) from the Latest Eocene of Wyoming (USA)

Timothy J. Gaudin, Robert J. Emry, and Jeremy Morris

Smithsonian Institution
Scholarly Press
WASHINGTON D.C.
2016

ABSTRACT
Gaudin, Timothy J., Robert J. Emry, and Jeremy Morris. Skeletal Anatomy of the North American Pangolin *Patriomanis americana* (Mammalia, Pholidota) from the Latest Eocene of Wyoming (USA). *Smithsonian Contributions to Paleobiology*, number 98, viii + 102 pages, frontispiece + 52 figures, 1 appendix with 13 tables, 2016.—*Patriomanis americana* is the only pangolin (Mammalia, Pholidota), living or extinct, known from the Western Hemisphere. It derives from latest Eocene (Chadronian North American Land Mammal Age) deposits from central Wyoming and western Montana. Since its initial description more than 40 years ago based on a partial skeleton, several nearly complete skeletons have been discovered, together including nearly every bone in the skeleton. This taxon is thus not only the most completely preserved fossil pangolin but is also among the best preserved of any Eocene mammal taxon. In the present study we have prepared a detailed, bone-by-bone description of the osteology of *Patriomanis,* comparing it with other well-known fossil pangolin skeletons (*Eomanis*, *Euromanis, Cryptomanis,* and *Necromanis*), as well as representatives of the three extant pangolins genera (*Manis, Smutsia, Phataginus*). We provide a catalog of all known *Patriomanis* specimens and their provenance and an extensive series of measurement tables incorporating the comparative taxa. We analyze the alpha-level taxonomy of the genus, concluding that all specimens should be kept in a single species, *Patriomanis americana,* based on currently available fossil material. We summarize the taxonomic and phylogenetic position of *Patriomanis* and discuss its implications for the biogeographic history of the order Pholidota. We analyze the paleobiology of *Patriomanis*, concluding that it was likely a myrmecophagous, arboreal animal with a prehensile tail. Last, we discuss its paleoecology, suggesting that its late appearance in the Eocene record, during a time of global cooling, may imply that earlier pangolins are waiting to be discovered in the Eocene record of Asia and North America. KEY WORDS: Eocene, fossils, morphology, osteology, pangolins, *Patriomanis,* Pholidota, skeleton, skull.

Cover image: Drawing of *Patriomanis americana* skeleton (detail from Figure 1).

Published by SMITHSONIAN INSTITUTION SCHOLARLY PRESS
P.O. Box 37012, MRC 957
Washington, D.C. 20013-7012 USA
www.scholarlypress.si.edu

Library of Congress Cataloging-in-Publication Data
Names: Gaudin, Timothy J., author. | Emry, Robert J., author. | Morris, Jeremy, 1981—author. | Smithsonian Institution Scholarly Press, publisher.
Title: Skeletal anatomy of the North American Pangolin Patriomanis americana (Mammalia, Pholidota) from the latest Eocene of Wyoming (USA) / Timothy J. Gaudin, Robert J. Emry, and Jeremy Morris.
Other titles: Smithsonian contributions to paleobiology; no. 98.
Description: Washington, D.C.: Smithsonian Institution Scholarly Press, 2016. | Series: Smithsonian contributions to paleobiology, ISSN 0081-0266; number 98 | Includes bibliographical references.
Identifiers: LCCN 2016024058
Subjects: LCSH: Pangolins, Fossil—North America. | Extinct mammals—North America.
Classification: LCC QE882.P45 G38 2016 | DDC 569/.31—dc23 | SUDOC SI 1.30:98 LC record available at https://lccn.loc.gov/2016024058

ISSNs: 1943-6688 (online); 0081-0266 (print)
ZooBank Registration: 8 September 2016 (LSID: urn:lsid:zoobank.org:pub:0E6025B4-6E40-452A-A333-25D39FE616A4)

Publication date: 22 September 2016

♾ The paper used in this publication meets the minimum requirements of the American National Standard for Permanence of Paper for Printed Library Materials Z39.48–1992.

Contents

Figures

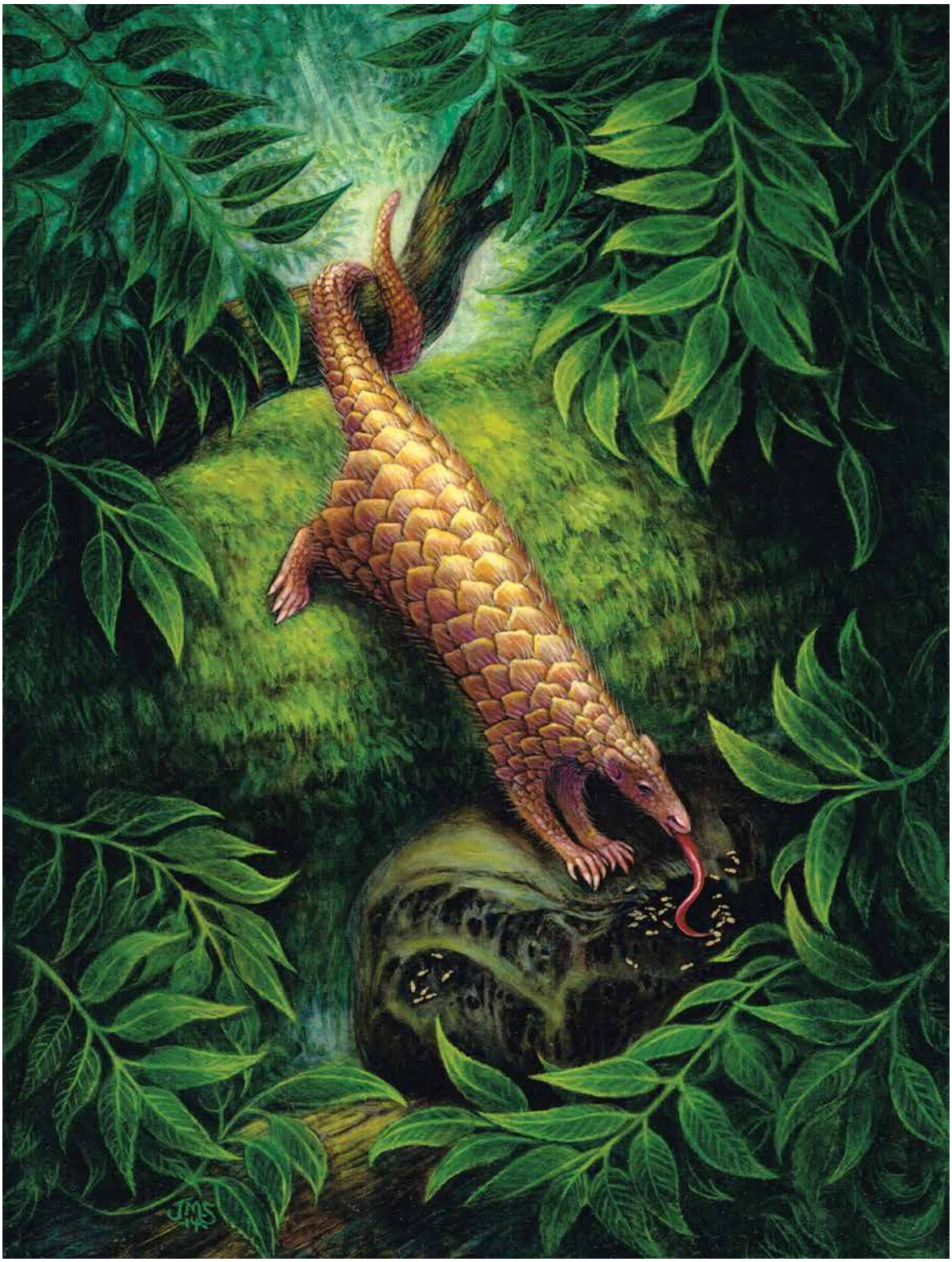

FRONTISPIECE. Life reconstruction of *Patriomanis americana* foraging for termites in the treetops. The tree is from the genus *Carya*, which, according to Prothero (1994), was present in this part of Wyoming during the Chadronian North American Land Mammal Age (latest Eocene). Illustration by Julia Morgan Scott for Smithsonian Institution.

Skeletal Anatomy of the North American Pangolin *Patriomanis americana* (Mammalia, Pholidota) from the Latest Eocene of Wyoming (USA)

Timothy J. Gaudin,[1] Robert J. Emry,[2] and Jeremy Morris[1,3]*

INTRODUCTION

One of the more remarkable and unexpected findings to emerge from the past 100 years of detailed study of the North American Cenozoic fossil mammal record is the discovery of a fossil pangolin in latest Eocene deposits of central Wyoming (Emry, 1970). The pangolins themselves, relegated to their own order, the Pholidota, are an extraordinary group of placental mammals. Rare, secretive, solitary, and largely nocturnal, the animals in this group comprise only eight living species distributed across sub-Saharan Africa, the Indian subcontinent, Southeast Asia, Indonesia, and the westernmost Philippines (Corbet and Hill, 1991; Nowak, 1999; Gaubert and Antunes, 2005, Schlitter, 2005; Gaudin et al., 2009). Thus, they are relatively poorly known even in the parts of the globe they frequent and virtually unheard of outside those areas. Their external appearance is truly bizarre, for they are the only mammals to be covered in an epidermal armor of large overlapping keratinous scales, earning them such nicknames as "perambulating artichoke." And their list of oddities does not end there. They have enormously enlarged salivary glands producing copious, sticky saliva; a portion of their stomach is converted into a cornified "gizzard" for grinding their preferred food, ants and termites; their tongue is remarkably elongated, taking its origin from a xiphisternal cartilage that may itself extend far back into the abdominal cavity; and one species, the long-tailed pangolin (*Phataginus tetradactyla*), has the most caudal vertebrae of any living mammal, its prehensile organ formed around 47–49 vertebral elements (Flower, 1885; Kingdon, 1974, 1997).

Pangolins are fossorially adapted for excavating ant and termite nests, and most species are either arboreal or semiarboreal/scansorial, with the exception of the two terrestrial African ground pangolins (*Smutsia* spp.). Their terrestrial progression is generally slow (Kingdon, 1974; Heath 1992a, 1992b; Nowak,

[1] Department of Biological and Environmental Sciences, University of Tennessee at Chattanooga, 615 McCallie Avenue, Chattanooga, Tennessee 37403-2598 USA.

[2] Department of Paleobiology, MRC 121, National Museum of Natural History, Smithsonian Institution, P.O. Box 37012, Washington, D.C. 20013, USA.

[3] Present address: Department of Biology, University of Utah, 257 South 1400 East, Rm. 201, Salt Lake City, Utah 84112-0840, USA.

[*] Correspondence: timothy-gaudin@utc.edu

Manuscript received 15 January 2016; accepted 17 March 2016.

1999). Given their slow movements, alongside the low diversity and abundance at which their populations exist, and their sluggish reproductive rate (litter size typically one, occasionally two or three in Asiatic species, birthed once a year in all but African tree pangolins, which may breed two or three times in a year; Kingdon, 1974, 1997; Heath, 1992a, 1992b, 1995; Nowak, 1999), they do not seem like a group that would be likely to spread quickly or to have a broad, global distribution. Indeed, the presence of different species of myrmecophagous mammals on different continents, with vermilinguans restricted to South and Central America, aardvarks and aardwolves in Africa, and echidnas and numbats in Australia, has become an iconic example of convergent evolution in undergraduate textbooks (e.g., Vaughan et al., 2011), even at the introductory level (e.g., Solomon et al., 2011). Extant pangolins are the only one of these groups to be broadly distributed on two continents (although vermilinguans do extend their range into southern parts of Central America, and aardvarks were distributed into Europe and Asia historically; Holroyd and Mussell, 2005). Until the recent report of the new extinct taxon *Cryptomanis* from the late Eocene of northern China, the *Patriomanis* localities lay on the other side of the world from the only other known Paleogene pangolins, the middle Eocene *Eomanis* and *Euromanis* from central Europe (Gaudin et al., 2006, 2009). To the present day, all but one of the Paleogene pangolin records (the exception being several isolated ungual phalanges from the Fayum of Egypt of questionable value; see discussion in Gaudin et al., 2009) pertain to localities in the midlatitudes of the Northern Hemisphere, outside the range not only of the modern pangolins but of all other extant myrmecophagous mammals (although these areas were characterized by a subtropical climate in the Eocene; Prothero, 1994). Thus, the presence of pangolins throughout northern Laurasia and into western North America in the Eocene is a startling finding.

Emry (1970, 2004) describes the somewhat circuitous route by which the first partial remains of a creature from the modern day midlatitudes of North America were recognized as pertaining to this group from the Old World tropics. He notes that the original identification was based largely on postcranial remains, although the type specimen included a well-preserved braincase (Emry, 1970). He subsequently reported on the remains of an additional specimen that preserved the front end of the skull, which demonstrated that this fossil pangolin was edentulous like its modern relatives (Emry, 2004). There are, in fact, three primary specimens, including the incomplete type housed in the Frick Collections at the American Museum of Natural History (F:AM 78999) and two later recovered by Emry from same vicinity (see below) housed at Smithsonian's Natural History Museum (USNM-P 299960, 494439), both relatively complete but in combination representing almost every skeletal element in the body.

Articulated, well-preserved skeletons are a rarity in vertebrate paleontology, complete skeletons even more so. These remains of *Patriomanis* not only represent the most complete known fossil pholidotan skeleton but are also among the best-known skeletons of any fossil mammal from the Eocene. Such finds are, of course, invaluable for understanding phylogenetic relationships among living and extinct mammals, although in this case, an exhaustive phylogenetic treatment of *Patriomanis* and other living and extinct pangolins has already been conducted by Gaudin et al. (2009). That work is an essential companion to the present study and is frequently cited in the material that follows. However, these *Patriomanis* skeletons are significant beyond what can be ascertained from them concerning pangolin phylogenetic relationships. They show us the skeletal morphology of a pangolin significantly more primitive than that of any alive today and hence should prove valuable in any subsequent investigations of morphological evolution in the group. To the degree that function can be inferred from these remains, they provide insight into the paleobiology of *Patriomanis* and into paleobiological aspects of pangolin evolution. Finally, given the relative rarity of complete fossil mammal skeletons, especially from the early parts of the Cenozoic, they have the potential to yield insight into broader aspects of skeletal evolution and supraordinal phylogeny across placental mammals as a whole, including, for example, their putative relationship to Carnivora in the supraordinal clade Ferae (see O'Leary et al., 2013, and references therein).

The primary goal of the present study is to describe in detail the skeletal anatomy of the North American fossil pangolin *Patriomanis americana*. We describe all the known material of *Patriomanis* and compare its anatomy to that of the other fossil pangolins. As has been noted elsewhere (e.g., Gaudin et al., 2006; Gaudin, 2010), the fossil record of Pholidota is poor, with very few extinct taxa (McKenna and Bell, 1997; Gaudin et al., 2009). That said, the taxa that do exist are reasonably well known, including *Eomanis* (middle Eocene of Germany; Storch, 1978, 2003), *Euromanis* (middle Eocene of Germany; Storch and Martin, 1994; Gaudin et al., 2009), *Cryptomanis* (late Eocene of China; Gaudin et al., 2006), and *Necromanis* (Oligocene-Miocene of central Europe; Koenigswald and Martin, 1990; Koenigswald, 1999; see also Storch, 2003; Gaudin et al., 2009; Hoffmann et al., 2009;

Hoffmann, 2011, for new, undescribed material). Because *Patriomanis* is more complete than any of the other fossil pangolin taxa, however, and the whole group Pholidota is rather small, we also compare *Patriomanis* to each of the three extant pangolin genera, the African tree pangolins (two species in genus *Phataginus*), the African ground pangolins (two species in the genus *Smutsia*), and the Asian pangolins (four species in the genus *Manis*; Gaudin et al., 2009). Last, some comparisons are included, where appropriate, to the metacheiromyid palaeanodonts *Metacheiromys* and *Palaeanodon* and the enigmatic "edentate" *Eurotamandua*. According to Gaudin et al. (2009), Palaeanodonta is the sister taxon to Pholidota (see also Matthew, 1918; Emry, 1970; Rose, 1979; Rose et al., 2005; O'Leary et al., 2013), forming a more inclusive clade Pholidotamorpha, whereas *Eurotamandua* falls within Pholidota proper, although the latter is a more debatable conclusion. It is hoped that these broad-based comparisons will yield additional insight into the evolution of skeletal anatomy in pangolins. We also examine in brief the paleobiological implications of the *Patriomanis* remains, as well as their potential to inform us about the Paleogene history of pangolins and the terrestrial ecosystems of the late Eocene.

Institutional Abbreviations

AMNH	American Museum of Natural History, New York, NY
CM	Carnegie Museum of Natural History, Pittsburgh, PA
F:AM	Frick Collection, American Museum of Natural History, New York, NY
FMNH	Field Museum of Natural History, Chicago, IL
SMF	Senckenberg Museum, Frankfurt am Main, Germany
USNM	National Museum of Natural History, Smithsonian Institution, Washington, D.C.
UTCM	University of Tennessee at Chattanooga Natural History Museum, Chattanooga, TN

Other Abbreviations

C1, C2, C3, …	cervical vertebra
Ca1, Ca2, Ca3, …	caudal vertebra
char(s).	character(s)
CN	cranial nerve
GL	greatest length
GSL	greatest skull length
L	left
L1, L2, L3, …	lumbar vertebrae
m., mm.	muscle, muscles
mc	metacarpal
MML	maximum mandibular length
mt	metatarsal
MYA	million years ago
NALMA	North American Land Mammal Age
R	right
T1, T2, T3, …	thoracic vertebrae

Catalog of Specimens

There are six specimens of *Patriomanis,* five of which comprise multiple skeletal elements, two of those representing nearly complete skeletons. All but one are housed in the Department of Paleobiology at the U.S. National Museum of Natural History of the Smithsonian Institution. The remaining specimen, the holotype, is part of the Frick Collection at the American Museum of Natural History. The type and four of the five other specimens come from three different sites in the Chadronian NALMA (latest Eocene) deposits of the White River Formation in the Flagstaff Rim area of Natrona County, Wyoming (Emry, 1970, 1973, 2004). The remaining specimen is from Chadronian NALMA strata at Pipestone Springs, Montana. For the convenience of the reader, a complete catalog of specimens and their provenance is provided below.

F:AM 78999 (holotype; see Emry, 1970; Figure 1, skull): White River Formation, Flagstaff Rim, Natrona County, Wyoming; Chadronian NALMA, latest Eocene; stratigraphic level, 5 m above Ash F, is in the late middle Chadronian part of the section (Emry, 1973, 2004; Unit 21 of Emry, 1973); assigned to Chadronian Biochron Ch3, 34.8–35.8 MYA, in Rose (2008) and Janis et al. (2008, appendix 1; = middle Chadronian)—Braincase (endocranium visible, endocast available), L and R mandibular fragments, incomplete atlas and axis, cervical vertebrae fragments, 8 thoracic vertebrae (3 articulated with ribs, 1 partial anterior, 4 partial posterior), 7 caudal vertebra (1 compete anterior, 6 partial), rib fragments (including 3 mediolaterally expanded ribs), 2 pelvic fragments (one including the pubic symphysis, the other preserving the left ischium ventral to the obturator foramen), fragments of L femur, partial L patella, partial L and R tibia, proximal R fibula, R calcaneus, L cuboid, R proximal mt I and V, 2 distal mt, partial R scapula, partial L and R

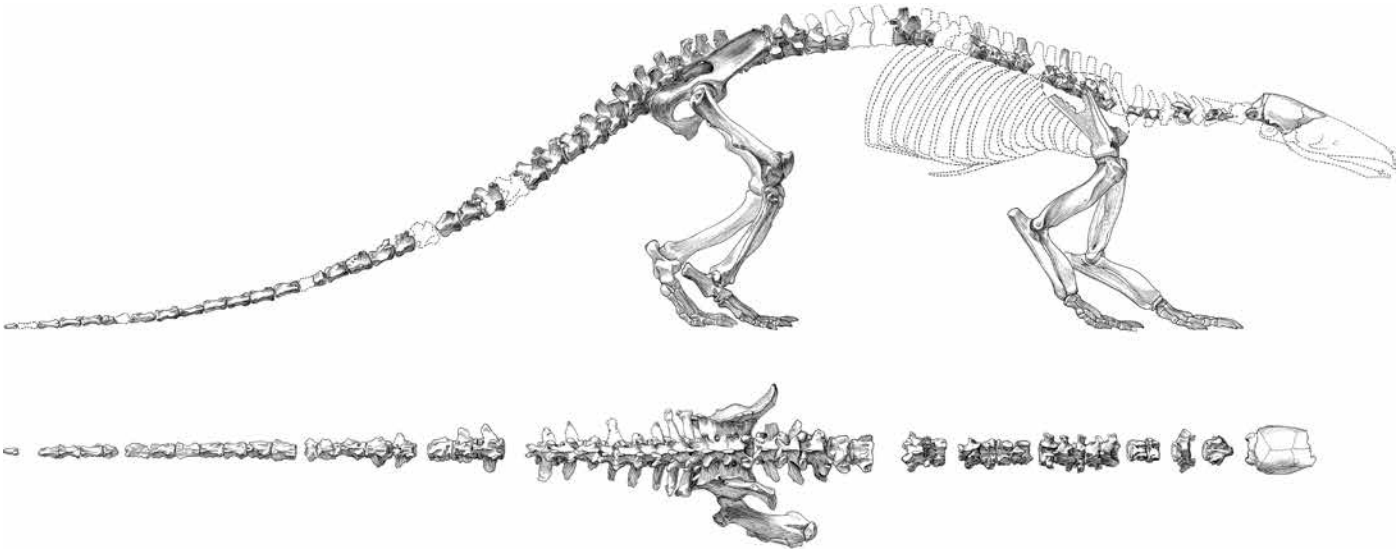

FIGURE 1. Drawing of skeleton of *Patriomanis americana* in right lateral (top) and dorsal (bottom) views based on the skull of the holotype (F:AM 78999) and the skeleton of USNM-P 299960. Drawn by Larry Isham and digitized by Mary Parrish for Smithsonian Institution.

humerus, partial L and R ulna, partial L and R radius, partial R scapholunar, R pisiform, L hamate, manual phalanges (including 2 proximal phalanges, 1 partial and 1 complete intermediate phalanx, 4 ungual phalanges [digits I, II, III, V]).

USNM-P 299960 (Figure 1, postcrania): White River Formation, Flagstaff Rim, Natrona County, Wyoming; Chadronian NALMA, latest Eocene; stratigraphic level near base of claystone immediately below Ash A (Unit 4 of Emry, 1973) or about 16 m below Ash B, which is radiometrically dated at 35.9 Ma (Swisher and Prothero, 1990; Prothero and Swisher, 1992). This specimen occurred almost exactly at the early Chadronian–middle Chadronian transition as defined by Prothero and Emry (1996, 2004); assigned to Chadronian Biochron Ch2-3, 34.8–36.6 MYA in Rose (2008) and Janis et al. (2008, appendix 1) but, given stratigraphic position, likely in the older part of this range—Skull fragments (including frontal bone with 8 grooves on underside for ethmoturbinals; L posterolateral corner of skull showing parietal, squamosal, occipital, and petrosal; basisphenoid–basioccipital with sella turcica dorsally and groove for musculotubal canal ventrally; R junction of parietal, squamosal, and occipital, and 3 miscellaneous fragments), partial axis, 3 cervical vertebrae (1 complete, 2 centra only), 11 thoracic vertebrae (9 anterior, 2 posterior, range from partial to nearly complete), 5 lumbar vertebrae (3 partial, last 3 in articulation, last 2 nearly complete), complete sacrum (3 sacrals), 28 caudal vertebrae (9 complete anteriorly, including first 5 in articulation, the remainder more posterior, many composed only of centra or partial centra), 4–5 chevron bones, 11 ribs with proximal end preserved (including 2 L, 4 R), many rib fragments, 3 sternebrae, complete pelvis, L and R femur, L and R patella, L and R tibia, R fibula, partial L fibula, complete R pes (except entocuneiform), L pes (missing astragalus, ungual phalanx I, damaged calcaneus, cuboid, mt I and II), miscellaneous sesamoids, partial L and R scapula, R humerus, R ulna, L and R radius, complete R manus (triquetrum damaged), L manus (missing hamate, mc III, proximal phalanx II, intermediate phalanx IV, damaged triquetrum), miscellaneous sesamoids, ?hyoid element.

USNM-P 460256: Renova Formation, Climbing Arrow Member, Pipestone Springs Local Fauna, Jefferson River Basin, Montana; Chadronian NALMA, latest Eocene; assigned to Chadronian Biochron Ch3 (= middle Chadronian), 34.8–35.8 MYA in Rose (2008) and Janis et al. (2008, appendix 1)—Partial R ulna.

USNM-P 494439 (Figure 2): White River Formation, Flagstaff Rim, Natrona County, Wyoming; Chadronian NALMA, latest Eocene; stratigraphic level 5 m above Ash F (at the same stratigraphic level and only 3–4 m away from the spot where the type was discovered; Emry, 1973, 2004; Unit 21 of Emry, 1973) assigned to Chadronian Biochron Ch3 (= middle Chadronian), 34.8–35.8 MYA in Rose (2008) and Janis et al. (2008, appendix 1)—Partial skull (including premaxilla, rostrum, partial L and R dentary, complete L

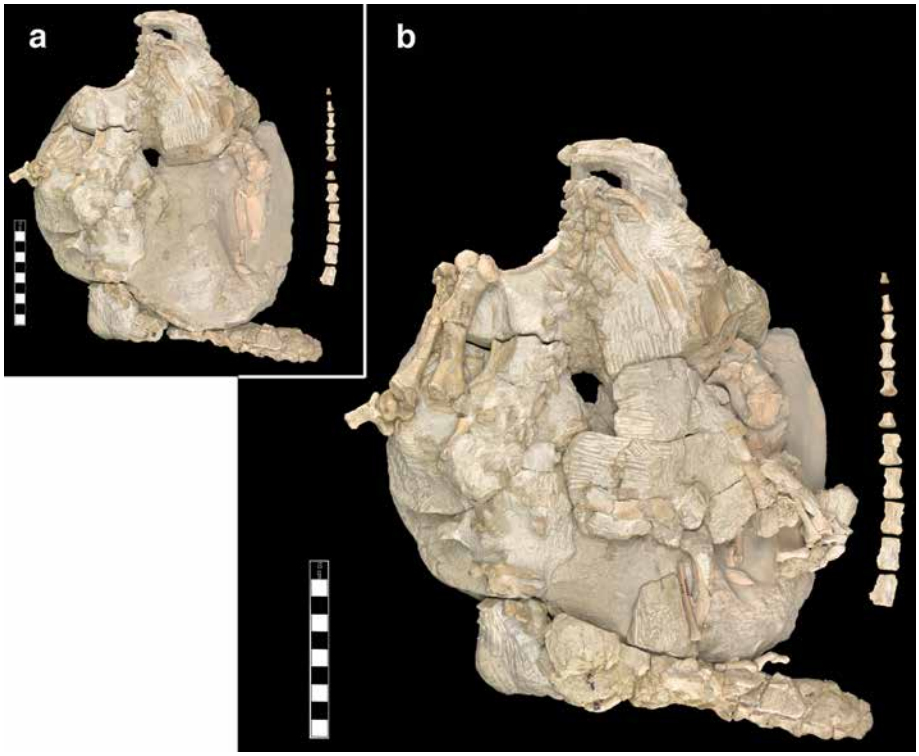

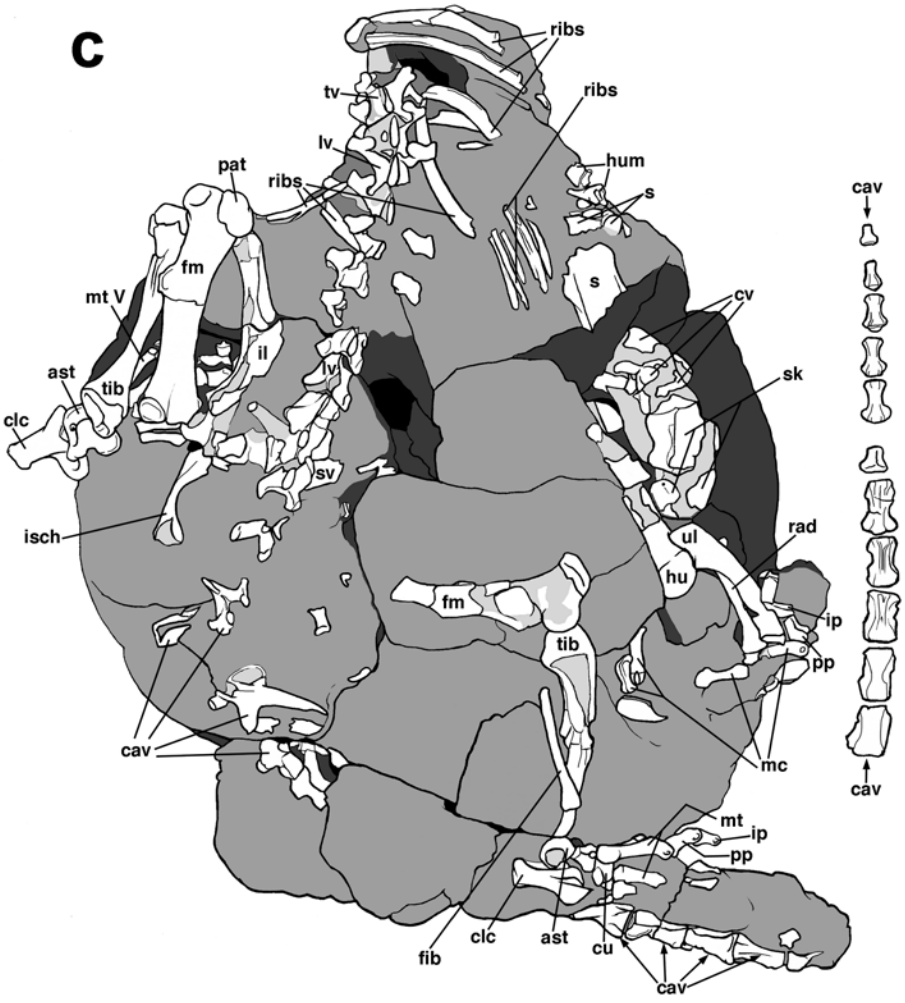

FIGURE 2. Partially prepared skeleton of *Patriomanis americana* (in block), USNM-P 494439: (a) dorsal view with more superficial elements of block removed to show position of skull; (b) full specimen in dorsal view; (c) line drawing of full specimen in dorsal view with skeletal elements highlighted. Abbreviations: **ast,** astragalus; **cav,** caudal vertebrae; **clc,** calcaneus; **cu,** cuboid; **cv,** cervical vertebrae; **fib,** fibula; **fm,** femur; **hu,** humerus; **il,** ilium; **ip,** intermediate phalanx; **isch,** ischium; **lv,** lumbar vertebra; **mc,** metacarpal; **mt,** metatarsal; **mt V,** fifth metatarsal; **pat,** patella; **pp,** proximal phalanx; **rad,** radius; **s,** scapula; **sk,** skull; **sv,** sacral vertebra; **tib,** tibia; **tv,** thoracic vertebra; **ul,** ulna. Gray areas represent matrix. Scale bar = 5 cm. Photos (a), (b) by James DiLoreto; illustration (c) by Tim Gaudin and Julia Morgan Scott for Smithsonian Institution.

and R petrosals, partial L and R orbital walls), partial atlas and axis, at least 5 thoracic vertebrae (perhaps 1 or 2 more, last 3 in articulation with lumbars), 6 articulated lumbar vertebrae (lumbars 3–5 damaged, 6 articulated with sacrum), partial sacrum (3 sacrals), 26 caudal vertebrae (include fragment of first, 14 anterior and mid-caudals in articulation likely starting with Ca3, 11 posterior), 11 ribs (4 L, 7 R) plus multiple rib fragments, partial L pelvis, nearly complete L femur, damaged R femur, L patella, damaged L and R tibia, damaged R fibula, distal L fibula, L calcaneus, L astragalus, L and R mesocuneiform, L and R ectocuneiform, partially articulated L pes (including cuboid, isolated tarsal [?mesocuneiform or prehallux], mt I–V, proximal phalanges II–V, intermediate phalanges ?IV and ?V), articulated R pes (including calcaneus, astragalus, cuboid, mt I–V, proximal phalanx II–III, intermediate phalanx II–IV, ungual phalanges I and III), partial L and R scapula, damaged R humerus, L and R ulna, L and R radius, partial L manus (including mt I, proximal phalanx II, intermediate phalanx II, ungual phalanx IV), partial R manus (including triquetrum, trapezium, capitate, hamate, mc I–IV, proximal phalanges I–IV, intermediate phalanx II–IV, ungual phalanges I–IV), miscellaneous isolated phalanges (1 proximal, 1 intermediate, 1 ungual).

USNM-P 531556: White River Formation, Flagstaff Rim, Natrona County, Wyoming; Chadronian NALMA, latest Eocene; stratigraphic level just below Ash D (Unit 17 of Emry, 1973) assigned to Chadronian Biochron Ch3 (= middle Chadronian), 34.8–35.8 MYA in Rose (2008) and Janis et al. (2008, appendix 1)—Complete R mt V, incomplete ungual phalanx, complete L humerus, partial R humerus, partial R ulna, partial L radius, complete R radius, miscellaneous fragments.

USNM-P 531557: White River Formation, Flagstaff Rim, Natrona County, Wyoming; Chadronian NALMA, latest Eocene; stratigraphic level 8 m [25 feet] below Ash D (Unit 17 of Emry, 1973)—Distal fibula, distal R mt II, left capitate, 3 ungual phalanges, miscellaneous fragments.

Acknowledgments

We thank the following institutions and individuals for providing access to the specimens that were used for comparative purposes in this study: Ross MacPhee, Richard Monk, Nancy Simmons, and Eileen Westwig, Department of Mammalogy, American Museum of Natural History, New York, NY; John Flynn and Meng Jin, Department of Vertebrate Paleontology, American Museum of Natural History, New York, NY; Bruce Patterson, Larry Heaney, and Bill Stanley, Division of Mammals, Field Museum of Natural History, Chicago, IL; Gerhard Storch, Senckenberg Forschungsinstitut und Naturmuseum, Frankfurt am Main, Germany; Norbert Micklich and Connie Kurz, Hessisches Landesmuseum Darmstadt, Darmstadt, Germany; Ken Rose, Johns Hopkins University, Baltimore, MD; Richard Thorington, Linda Gordon, and Helen Kafka, Department of Mammalogy, National Museum of Natural History, Washington, D.C.; and Eberhard "Dino" Frey, Staatliches Museum für Naturkunde, Karlsruhe, Germany. We especially thank John Flynn and Meng Jin of the American Museum of Natural History for providing access to the type material of *Patriomanis* (and *Cryptomanis*). Special thanks are also owed to Gerhard Storch, who provided access to undescribed material of *Necromanis* for the Gaudin et al. (2009) study and who also provided us casts of several specimens of *Eomanis waldi* and the type of *Euromanis krebsi* and showed us his three-dimensional X-ray photographs of *Eurotamandua joresi*. His material help and insightful comments were critical to the success of this project.

All of the USNM specimens of *Patriomanis* from Flagstaff Rim were collected between 1971 and 1991, and during that interval Emry was assisted in the field by various staff of the museum and volunteers; among these, he especially thanks Frederick Grady, USNM preparator, who in 1975 found USNM 299960 and helped to collect it, and Wang Banyue of the Institute of Vertebrate Paleontology and Paleoanthropology, Beijing, who helped collect USNM 494439 in 1991. For help with the preparation and casting of *Patriomanis* and *Cryptomanis* specimens, we thank Fred Grady, Pete Kroehler, and Steve Jabo of the Department of Paleobiology at the National Museum of Natural History.

This work was greatly improved by the comments of Ken Rose; we thank him for his excellent and thorough review. We thank Julia Morgan Scott, Mary Parrish, and the late illustrator Larry Isham for their skillful work in the preparation of illustrations. Mary Parrish and Larry Isham prepared Figure 1, and Larry Isham prepared Figures 24b, 33, 36, 39b, 42, 45, 47a,b, and 49a (T.J.G. prepared Figure 48c). Julia Morgan Scott prepared the frontispiece and the remaining drawings and formatted and labeled all the figures. B. Ammons and L. Boykin assisted with the formatting of the tables, and L. Boykin assisted with the preparation of the figure captions and other editing tasks. For housing T. Gaudin during his 2002

period of sabbatical study and again during the summer of 2004, special thanks are owed to the Department of Paleobiology at the National Museum of Natural History. T. Gaudin's work on this project was supported by a sabbatical grant from the University of Chattanooga Foundation and by NSF RUI Grant DEB 0107922 and NSF AToL Grant 0629959.

DESCRIPTION

Axial Skeleton: Skull

FIGURES 3–9; TABLE A1

The skull of *Patriomanis* has been described and illustrated in several previous publications. Emry (1970:466) described the type specimen (F:AM 78999), an uncrushed isolated braincase in excellent condition, broken through "at the level of the cribriform plate, which is also missing." It displays much of the basicranial and endocranial anatomy, although the former is not everywhere well preserved and the latter can be observed only through the anterior opening into the braincase or the foramen magnum, limiting which structures are visible. The same skull was illustrated in Rose and Emry (1993: fig. 7.1, right lateral view), where it was used to show the separation between the alisphenoid and parietal bones at the back of the orbit and the enclosure of the foramen ovale by the alisphenoid in pangolins. Emry (2004) described the other good skull for *Patriomanis,* that of USNM-P 494439. He noted (p. 131) that "the skull is distorted," mainly through some mediolateral crushing, and that "some of the individual bones are broken and displaced, especially in the interorbital region and the dorsal part of the braincase." His description focused almost entirely on the bones of the rostrum (premaxilla, maxilla, nasal) and the mandible since these were elements missing from the type and, more importantly, these elements showed that *Patriomanis* was edentulous like the modern forms. This skull was also used to code characters in Gaudin and Wible's (1999) cladistic phylogenetic analysis of pangolins (although it was misattributed to USNM-P 299960). The other *Patriomanis* specimen with well-preserved postcrania, USNM-P 299960, includes only disarticulated skull fragments, including a portion of the frontal bone, marked on the inside with grooves to accommodate the ethmoturbinals; the left posterolateral corner of the skull, including portions of the parietal, squamosal, petrosal, and occipital; and portions of the basisphenoid and basioccipital.

Since the publication of Emry's (2004) description, additional preparation of the skull from USNM-P 494439 has been undertaken, particularly in the orbital wall, posterior palate, nasopharynx, basicranium, auditory region, and occiput (Figures 3, 5–7). Therefore, the following description will focus mainly on these areas, although the skull bones and portions of the mandible already described by Emry (1970, 2004; Rose and Emry, 1993) will be given at least cursory treatment. For terminology we largely follow that of Wible and Gaudin (2004) and Wible (2010).

Premaxilla

The edentulous premaxilla of *Patriomanis* has been described in detail by Emry (2004), so we will limit our discussion here to comparisons with a somewhat wider variety of fossil and extant pangolins than those considered in the previous work. Emry (2004) has already noted the strong resemblance of the premaxilla in *Patriomanis* to that of *Manis javanica.* As in all the modern forms, the prominent dorsal process of the premaxilla is oriented posterodorsally; that is, the anterior edge extends anteroventrally to posterodorsally (Figure 3c). In the only other fossil pangolin that preserves the premaxilla, *Eomanis waldi,* the leading edge of the bone is roughly vertical and distinctly concave anteriorly, giving the whole dorsal process a C shape in lateral view (Storch, 2003; Rose et al., 2005). This morphology is also present in the palaeanodont *Metacheiromys* and in the enigmatic edentate mammal *Eurotamandua,* making it a synapomorphy of Pholidotamorpha (as defined by Gaudin et al., 2009) that is subsequently modified in patriomanids and manids. Emry (2004:131) described the incomplete posteromedian process on the palatal portion of the premaxilla as "essentially like that of *M. javanica."* However, the form of the anterior edge of the maxilla, with its rather short median V-shaped notch (Figure 4b), makes it likely that *Patriomanis* did not possess an elongate median process like that found in *M. javanica, M. crassicaudata,* and the two extant African genera (Figure 5b; Gaudin et al., 2009) and, moreover, that the incisive foramen lay between the premaxilla and maxilla, rather than being completely enclosed in the former, a derived condition found in *Smutsia, M. pentadactyla,* and in some, but not all, specimens of *M. javanica* (Gaudin et al., 2009).

Nasal

Emry (2004) describes these elements in detail, and there is little to add here. The notch described by Emry between the medial and lateral anterior processes of the

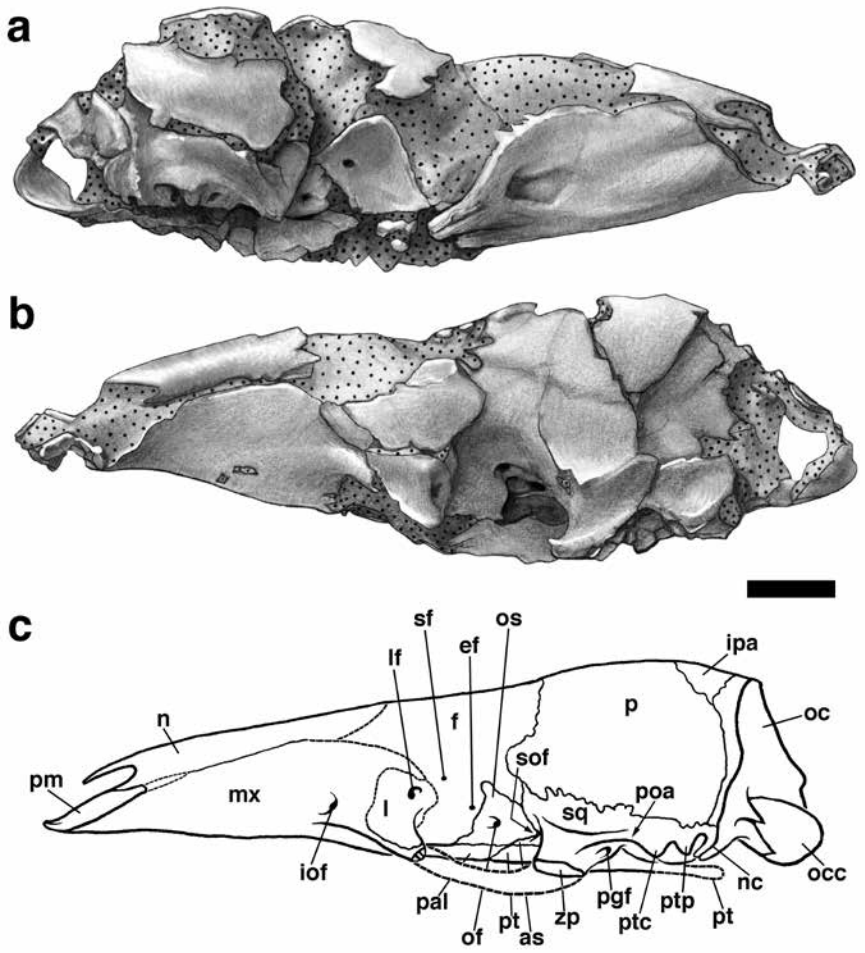

FIGURE 3. Skull of *Patriomanis americana*: (a) USNM-P 494439 in right lateral view; (b) USNM-P 494439 in left lateral view; (c) reconstruction of the skull in left lateral view. Abbreviations: **as,** alisphenoid; **ef,** ethmoid foramen; **f,** frontal; **iof,** infraorbital foramen; **ipa,** interparietal; **l,** lacrimal; **lf,** lacrimal foramen; **mx,** maxilla; **n,** nasal; **nc,** nuchal crest; **oc,** occipital; **occ,** occipital condyle; **of,** optic foramen; **os,** orbitosphenoid; **p,** parietal; **pal,** palatine; **pgf,** postglenoid foramen; **pm,** premaxilla; **pt,** pterygoid; **sf,** supraorbital foramen; **sq,** squamosal; **zp,** zygomatic process of squamosal. Stippled areas represent matrix. Scale bar = 1 cm. Illustrations by Julia Morgan Scott for Smithsonian Institution.

nasal is quite deep (Figures 3, 4a,c), like that of *Manis* and *Smutsia*, whereas the notch is present but much shallower in *Phataginus* (Figure 5a,c) and *Eomanis waldi,* the only other fossil pangolin that preserves the anterior nasal region (Gaudin et al., 2009). Emry (2004) notes that the posterior parts of both nasals are missing in *Patriomanis*. It appears, however, that on the left side of USNM-P 494439 the upper sutural edge of the maxilla, that is, the portion in contact with the nasal, is preserved intact. The right maxilla is not as well preserved (Figure 3) yet in outline appears roughly symmetrical with the left in dorsal view (Figure 4a,c). In addition, the matrix underlying the missing right nasal bears a ridge that may represent a cast of the underside of the frontonasal suture. If the posterior region of the nasal is reconstructed on this basis (Figure 4c), it would appear to flare posteriorly and form a broad, shallow U-shaped suture with the frontal. This is very reminiscent of the posterior nasal morphology illustrated by Koenigswald and Martin (1990: fig. 3a,b) for *E. waldi* and *Necromanis edwardsi*. In extant manids, the posterior portions of the nasals together form a narrow V-shaped or U-shaped extension of variable width that deeply indents the anterior edge of the frontal (Figure 5a).

Maxilla

Emry (2004) provides a very extensive description of the maxilla in *Patriomanis*, noting its characteristic pholidotan morphology, as indicated by the complete loss of the upper dentition, and the presence of both an alveolar sulcus and a median longitudinal palatal trough (Figure 4b,d). All three are basal apomorphies of Pholidota (Gaudin et al., 2009). Additional preparation of the posterior reaches of the palate failed to reveal any remains of the palatine bones, so the location and form of both the maxillary–palatine suture and the palatine foramina cannot be ascertained. Similarly, further preparation in the anteroventral orbital wall yielded only a few isolated bone fragments, leaving it unclear whether *Patriomanis*, like

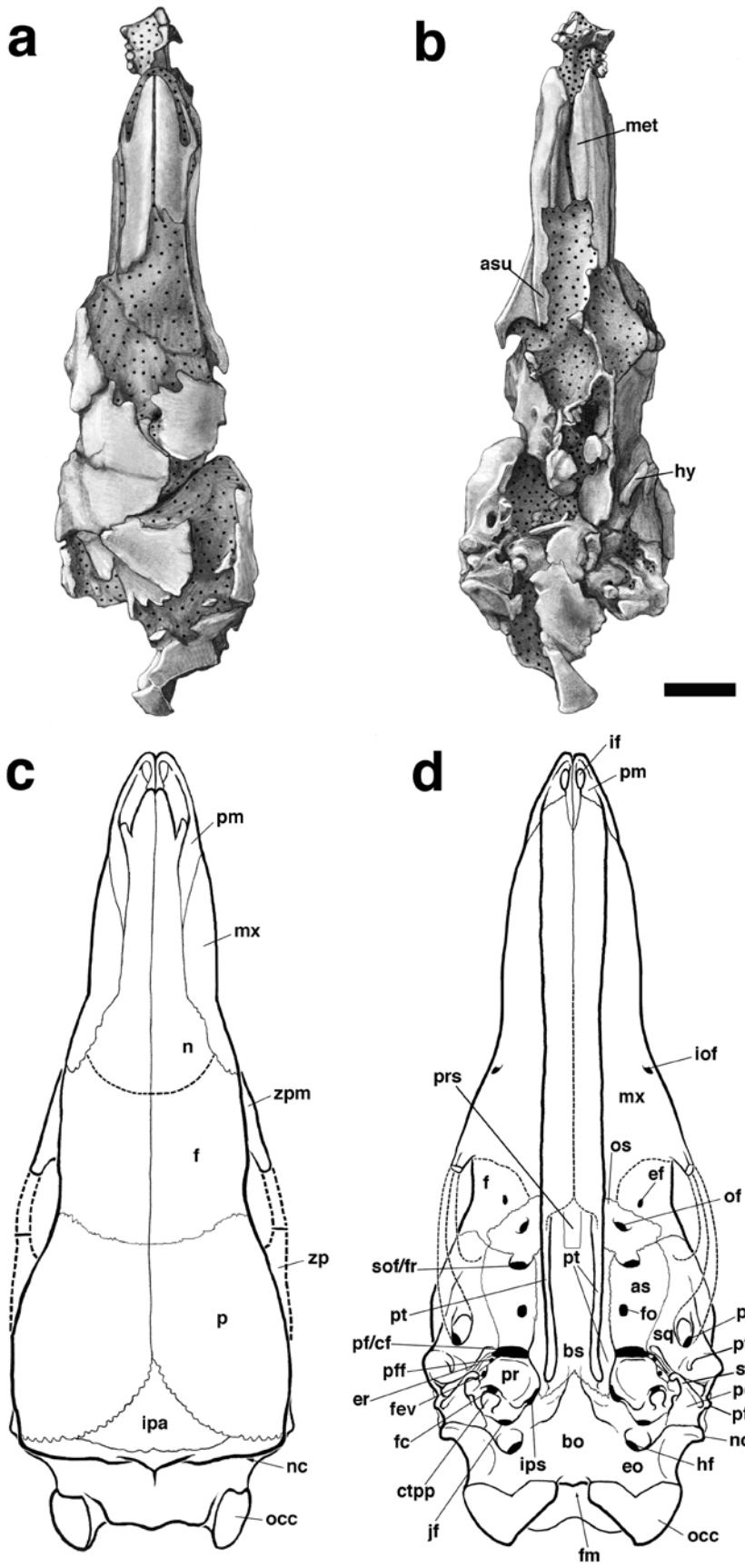

FIGURE 4. Skull of *Patriomanis americana*: (a) USNM-P 494439 in dorsal view; (b) USNM-P 494439 in ventral view; (c) reconstruction of the skull in dorsal view; (d) reconstruction of the skull in ventral view. Abbreviations: **as,** alisphenoid; **asu,** alveolar sulcus; **bo,** basioccipital; **bs,** basisphenoid; **ctpp,** caudal tympanic process of petrosal; **ef,** ethmoid foramen; **eo,** exoccipital region of occipital bone; **er,** epitympanic recess; **f,** frontal; **fc,** fenestra cochleae; **fev,** fenestra vestibuli; **fm,** foramen magnum; **fo,** foramen ovale; **hf,** hypoglossal foramen; **hy,** hyoid fragment; **if,** incisive foramen; **iof,** infraorbital foramen; **ipa,** interparietal; **ips,** opening for inferior petrosal sinus; **jf,** jugular foramen; **met,** median trough; **mx,** maxilla; **n,** nasal; **nc,** nuchal crest; **occ,** occipital condyle; **of,** optic foramen; **os,** orbitosphenoid; **p,** parietal; **pf/cf,** piriform fenestra/carotid foramen; **pff,** primary facial foramen; **pgf,** postglenoid foramen; **pm,** premaxilla; **pop,** paraoccipital process of petrosal (= mastoid process of Evans and Christensen, 1979); **pr,** promontorium of petrosal; **prs,** presphenoid; **pt,** pterygoid; **ptc,** posttympanic crest; **ptp,** posttympanic process of squamosal; **sof/fr,** fused sphenorbital fissure and foramen rotundum; **sq,** squamosal; **stmn,** stylomastoid notch; **zp,** zygomatic process of squamosal; **zpm,** zygomatic process of maxilla. Stippled areas represent matrix. Scale bar = 1 cm. Illustrations by Julia Morgan Scott for Smithsonian Institution.

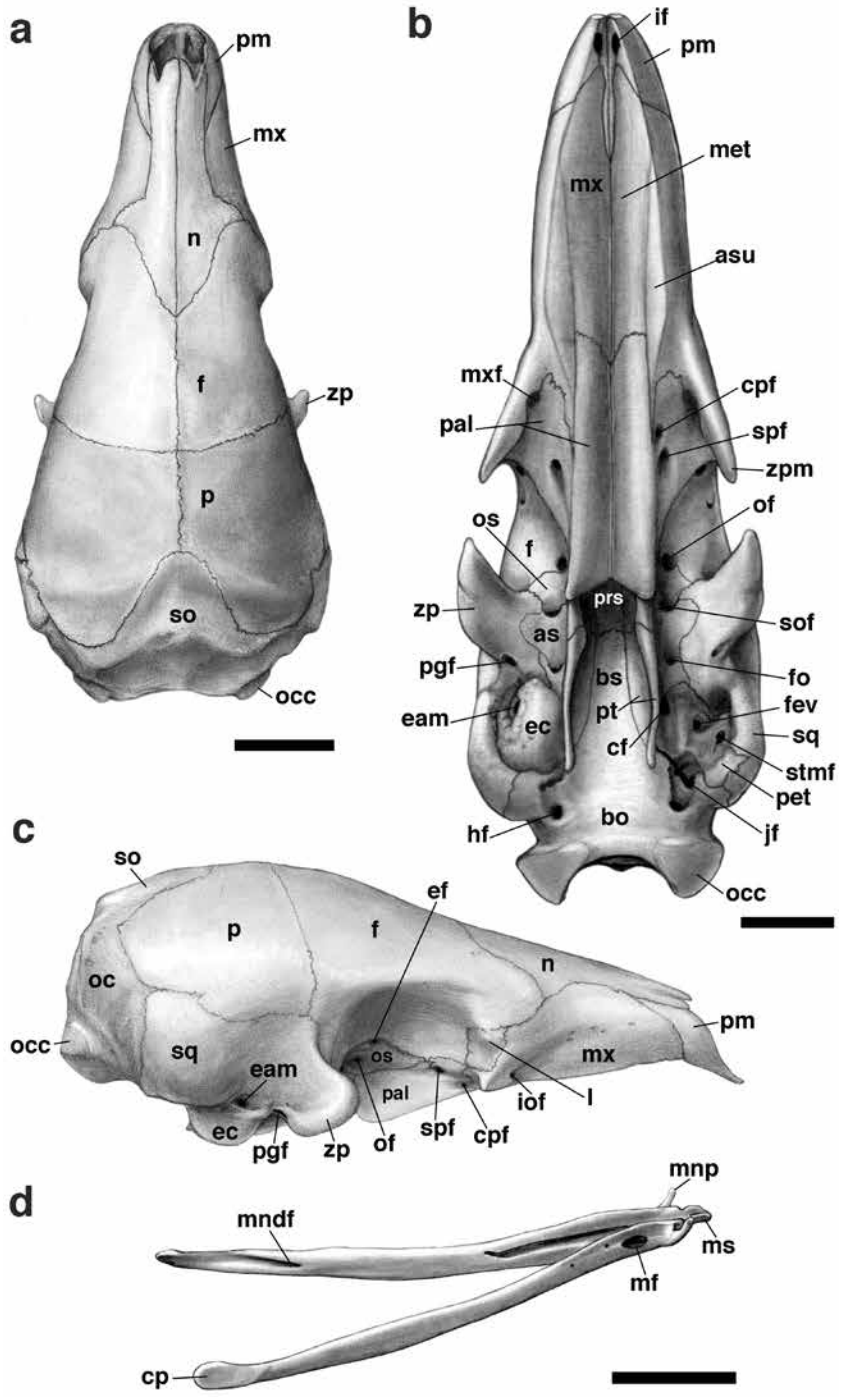

FIGURE 5. Skulls and mandible of modern pangolins: (a) *Phataginus tricuspis*, UTCM 1695, in dorsal view; (b) *Manis javanica*, USNM 198852, in ventral view; (c) *Phataginus tricuspis*, UTCM 1695, in right lateral view; (d) mandible of *Phataginus tricuspis*, CM 86715, in right dorsolateral view. Abbreviations: **as,** alisphenoid; **asu,** alveolar sulcus; **bo,** basioccipital; **bs,** basisphenoid; **cf,** carotid foramen; **cp,** condylar process; **cpf,** caudal palatine foramen; **eam,** external auditory meatus; **ec,** ectotympanic; **ef,** ethmoid foramen; **f,** frontal; **fev,** fenestra vestibuli; **fo,** foramen ovale; **hf,** hypoglossal foramen; **if,** incisive foramen; **iof,** infraorbital foramen; **jf,** jugular foramen; **l,** lacrimal; **met,** median trough; **mf,** mental foramen; **mndf,** mandibular foramen; **mnp,** mandibular prong; **ms,** mandibular symphysis; **mx,** maxilla; **mxf,** maxillary foramen; **n,** nasal; **nc,** nuchal crest; **oc,** occipital; **occ,** occipital condyle; **of,** optic foramen; **os,** orbitosphenoid; **p,** parietal; **pal,** palatine; **pet,** petrosal; **pgf,** postglenoid foramen; **pm,** premaxilla; **prs,** presphenoid; **pt,** pterygoid; **so,** supraoccipital region of occipital bone; **sof,** sphenorbital fissure; **spf,** sphenopalatine foramen; **sq,** squamosal; **stmf,** stylomastoid foramen; **zp,** zygomatic process of squamosal; **zpm,** zygomatic process of maxilla. Scale bars = 1 cm. Panels (b) and (c) modified from Gaudin et al. (2009). Illustrations by Julia Morgan Scott for Smithsonian Institution.

modern pangolins, lacked an orbital exposure of the maxilla (Gaudin, 2004; this study shows that an orbital wing of the maxilla is also missing in *Metacheiromys* and vermilinguan anteaters). The infraorbital foramen lies toward the back of the facial process of the maxilla in *Patriomanis* (Figure 3). It is displaced forward in *Smutsia* and even more so in *E. waldi*, where it is located near the anteroposterior midpoint of the bone (Gaudin et al., 2009).

Palatine

The only portion of the palatine that is preserved in USNM-P 494439 is a portion of perpendicular process (= orbital wing of Gaudin et al., 2009). We believe there are fragments preserved of the perpendicular process on both the left and right sides, although it is difficult to determine which portions of these fragments pertain to the

palatine and which to the pterygoid. In modern pangolins, the suture between the perpendicular process of the palatine and the pterygoid lies at or just posterior to the level of the sphenorbital fissure (Figure 5; Jollie, 1968; Gaudin et al., 2009: char. 376). There is a crack in approximately this position on the larger, better-preserved palatine fragment from the left side, suggesting that roughly the anterior two-thirds of this piece is from the palatine's perpendicular process. Moreover, the preserved morphology suggests that the palatine of *Patriomanis* has a low, anteroposteriorly elongate exposure in the ventral wall of the orbit (Figure 3) as in extant pangolins (Novacek and Wyss, 1986; Gaudin, 2004). The left palatine fragment ends anteriorly at a broken surface marked by two grooves that presumably led to foramina, the upper being the sphenopalatine foramen and the lower the caudal palatine foramen (Jollie, 1968). These foramina were likely completely enclosed within the perpendicular process of the palatine, as they are in extant taxa (Jollie, 1968).

Although the anterior parts of the perpendicular process and the entire horizontal process are missing, the palatine certainly possessed its normal contacts with the horizontal process of the maxilla and at least the base of the maxilla's zygomatic process if an orbital exposure of the maxilla was indeed lacking (see above). In addition, USNM-P 494439 preserves dorsal contacts between the perpendicular process and the frontal and orbitosphenoid and, as noted, likely a posterior contact with the pterygoid (Figure 3), as in extant pangolins (Figure 5; Jollie, 1968). The orbital portion of the palatine is unknown in other fossil pangolins.

Lacrimal

The lacrimal of USNM-P 494439 is preserved only on the left side of the skull (Figure 3b,c). In lateral view it is a triangular element with its apex pointing anteriorly. It has a large facial process extending forward from the prominent, rounded orbital rim that crosses the bone dorsoventrally and a smaller semicircular orbital exposure that houses a small lacrimal foramen immediately posterior to the orbital rim. It contacts the zygomatic process of the maxilla anteroventrally and the frontal both dorsally and posteriorly. It could conceivably have had a small, posteroventral contact with either the maxilla or, more likely, the palatine within the orbit, but that portion of the orbital wall is badly damaged on both sides of the skull and does not permit a more definitive assessment. There is a small pit between lacrimal and frontal within the orbit, near the posteroventral corner of the former. This is likely the lacrimal fenestra that accommodates the origin of the inferior oblique muscle in other mammals (Wible and Gaudin, 2004).

It is noteworthy that the lacrimal foramen is missing in all modern pangolins, and the bone itself is absent in both *Manis* and *Smutsia* (Figure 5; Jollie, 1968; Gaudin et al., 2009; the lacrimal is indistinguishably fused to the maxilla in these genera according to Grassé, 1955). In this regard, *Patriomanis* is more similar to *Eomanis waldi* and nonpholidotan eutherians (Evans and Christensen, 1979; Novacek, 1993). Interestingly, although the bone is absent, the lacrimal fenestra is at least variably present in all extant species of *Manis* and *Smutsia,* whereas it is absent in both species of *Phataginus,* despite the fact that both species retain a separate lacrimal element (Jollie, 1968; Gaudin et al., 2009). Whether *E. waldi* possessed this opening is unknown (Gaudin et al., 2009). In *Phataginus*, the orbital portion of the lacrimal is much larger than its almost nonexistent facial exposure (Figure 5c). The facial exposure is also small in the palaeanodont *Metacheiromys* and the enigmatic edentate *Eurotamandua,* whereas the large facial process of the lacrimal in *Patriomanis* is more like the condition in cingulate and vermilinguan xenarthrans (Gaudin and Branham, 1998; Gaudin, 2004).

Jugal

Emry (2004) describes a sutural surface for the jugal carried dorsally on the zygomatic process of the maxilla, although the bone itself is not known to be preserved in any *Patriomanis* specimen. Because of this, it is not known definitively whether *Patriomanis* had a complete zygomatic arch like *E. waldi* (Storch, 2003) and some *M. pentadactyla* (Emry, 2004; we also observed a complete zygoma in one specimen of *M. javanica,* USNM 14448) or an incomplete zygoma like all remaining modern pangolins (Figure 5). However, we are reconstructing a complete zygoma on the basis of the presence of the jugal bone (Figures 3 and 4; but see discussion below of the zygomatic process of the squamosal). The jugal is present in *E. waldi* and many, if not most, of those *M. pentadactyla* specimens with a complete zygomatic arch (it is presumably synostosed to the maxilla and squamosal in the remaining examples). The other extant pangolin species lack a jugal and are characterized by an incomplete arch (except for the aforementioned specimen of *M. javanica,* with both a jugal and complete zygoma, and *M. crassicaudata* FMNH 98232, with the jugal attached to maxilla but an incomplete zygoma). Weber (1928) suggests the bone is fused early in ontogeny to the squamosal, whereas Grassé (1955) asserts that it is fused to the maxilla.

Frontal

Only the posterodorsal regions of the frontal bone are preserved in the type (F:AM 78999), from the skull roof immediately behind the interorbital constriction to the frontoparietal suture (Emry, 1970), which, in turn, lies just anterior to the level of the zygomatic process of the squamosal. Consequently, Emry (1970) has little to say about its morphology. The frontal is damaged on both sides of USNM-P 494439, especially on the right, where large chunks are missing from the skull roof and dorsal orbital wall, whereas on the left the bone is present in its entirety but cracked and distorted. Nevertheless, its morphology and sutural contacts can be largely reconstructed on the basis of the available material (Figures 3, 4).

On the rostrum, the frontal contacts the nasals anteriorly (see above), the maxilla anterolaterally, and the lacrimal laterally (Figures 3c, 4c). The frontal has an extensive exposure in the medial wall of the orbit, being by far the largest component of the orbital mosaic, as is the case in modern manids (Figure 5; Jollie, 1968; Novacek and Wyss, 1986). Within the orbit it contacts the lacrimal anteriorly, the palatine and orbitosphenoid laterally, and the squamosal and parietal posteriorly (Figure 3c). The dorsal portion of the alisphenoid closely approaches, but appears not to contact, the frontal (Figure 3c) because of the presence of a small orbitosphenoid–squamosal contact (Gaudin and Wible, 1999; Gaudin et al., 2009; see also fig. 7.1 in Rose and Emry, 1993). A similar condition prevails in *E. waldi, Phataginus, S. gigantea,* and some *S. temminckii,* whereas in other *S. temminckii* and in *Manis* the orbitosphenoid and squamosal share a broad sutural contact (Figure 5b; Gaudin and Wible, 1999; Gaudin et al., 2009). Because of poor preservation (see above), it is not possible to determine whether there was also an anterolateral contact with the maxilla in the orbital wall.

The orbital surface of the frontal is smooth except for a single relatively large ethmoid foramen located entirely within the frontal but close to the frontal–orbitosphenoid suture, anterodorsal to the optic foramen (Figures 3c, 4d). In the older extinct forms *Eomanis* and *Eurotamandua*, the ethmoid foramen actually lies on the suture between the frontal and orbitosphenoid, as it does in the extant species *M. pentadactyla* and *M. javanica* and variably so in *M. crassicaudata, S. temminckii,* and *P. tricuspis* (Gaudin et al., 2009). As noted above, the frontal also participates in the lacrimal fenestra. In addition, just below the dorsal rim of the orbit, midway between the lacrimal and ethmoid foramina, is a very small supraorbital foramen. This foramen is also known in modern pangolins (Gaudin, 2004). We know of no record of its contents in pangolins, but in xenarthrans and carnivorans, this is an opening that houses the frontal diploic vein (Evans and Christensen, 1979; Wible and Gaudin, 2004), whereas in humans it transmits the supraorbital nerve (a branch of the ophthalmic nerve, CN V_1) and its accompanying vessels (Pick and Howden, 1977).

The frontal of *Patriomanis* is not marked by a postorbital process or temporal lines on the skull roof. These features are also absent in all known members of Pholidota, including *Eurotamandua* (Gaudin et al., 2009). This likely indicates that the temporalis muscle was strongly reduced in *Patriomanis,* although perhaps not to the same degree as in the modern forms, where Doran and Allbrook (1973:997; see also Weber, 1928) note "the almost total absence of masticatory muscles." *Patriomanis* also lacks a postorbital constriction and has instead a weak interorbital constriction in dorsal view (Figure 4c). This is the condition in all extant pangolins (Figure 5; except for some *S. gigantea*), whereas in other fossil taxa, namely, *Necromanis, Eomanis,* and *Eurotamandua,* a separate postorbital constriction is present (Gaudin and Wible, 1999; Gaudin et al., 2009).

Parietal

Although the parietals are preserved in their entirety in the type, Emry (1970) says little about them, apart from noting their sutural contacts with the frontal anteriorly and the occipital and interparietal posteriorly. In addition, they contact the squamosal laterally at an elongate suture (length ~30% GSL; Table A1). This suture is similarly elongated in extant *Phataginus* and some *S. temminckii* (Figure 5c; length >25% GSL), whereas the suture is much shorter in other *Smutsia,* in *Manis,* and in *E. waldi, Eurotamandua,* and other out-groups (Gaudin et al., 2009; Table A1). The frontoparietal suture is situated at or just behind the level of the zygomatic process of the squamosal (Figures 3c, 4c), as in all other pangolins except *E. waldi* (and *Eurotamandua*; Gaudin et al., 2009). The parietals themselves are relatively flat dorsally and in their anteroposterior profile and strongly convex laterally, and their lateral margins are slightly convex in dorsal view. USNM-P 494439 adds no real information to the description of the parietal since the bones are badly cracked and distorted on the left, and much of the medial and anterior portions are entirely missing on the right.

Interparietal

Emry (1970) notes the presence of a large, triangular interparietal element in *Patriomanis* that is suturally

distinct from the occipital (Figure 4c), whereas in modern pangolins the interparietal is fused to the occipital (marked as supraoccipital region of occipital in Figure 5; Jollie, 1968). The condition is unknown in other fossil pangolins except *E. waldi*, where a separate interparietal is not apparent (Gaudin, unpublished data). As discussed by Rose and Emry (1993), Novacek and Wyss (1986) had suggested the lack of an interparietal was a derived feature linking xenarthrans and pholidotans, before adding a note acknowledging its presence in pangolins based on Emry (1970) and Jollie (1968). The apical angle of the interparietal in *Patriomanis* is slightly obtuse (approximately 100°), as in modern *Manis* (where it is fused to the supraoccipital in adults, as noted by Jollie, 1968), whereas in *Phataginus* and some specimens of either *Smutsia* species, it forms a right angle or even a slightly acute angle (Figure 5a,c; Gaudin and Wible, 1999; Gaudin et al., 2009).

Squamosal

The squamosals are preserved nearly intact in the type specimen (Emry, 1970) and on the right in USNM-P 494439, whereas on the left the bone is broken and distorted, and its posterodorsal corner is missing (Figure 3). The zygomatic process is the only portion of the squamosal where the morphology is questionably known. The best-preserved process is on the left side of USNM-P 494439, although there is also a substantial process preserved on the right in the type. The latter is described by Emry (1970:468) as follows: "The zygomatic processes are small, directed downward, and, although somewhat weathered, appear to have ended in a rather sharp point. There was apparently no glenoid articular surface." The description fits the morphology of USNM-P 494439 well enough, although the zygomatic process in that specimen is somewhat more elongated ventrally and comes to a narrower point. The absence of a distinct glenoid fossa would match the morphology in modern pangolins, where the mandibular condyle "[contacts] lightly with the ventromedial side of the zygomatic process" (Emry, 1970:468); that is, it has a ligamentous attachment to the inner base of the process (and perhaps to the lateralmost portion of the alisphenoid) but does not attach to the moderately rugose, somewhat expanded distal end of the process (see *P. tricuspis,* UTCM 1695, Figure 6a; note that the distal tip of the zygomatic process is scored erroneously as an anteroposteriorly convex "glenoid fossa" in Gaudin and Wible, 1999: char. 51, and in Gaudin et al., 2009: char. 356). The left zygomatic process of USNM-P 494439 has a rodlike bone fragment attached by matrix to this "glenoid" region (Figure 4b), but given its rodlike shape and the fact that it is broken at either end, we interpret this as a displaced portion of the hyoid arch (probably stylohyal) rather than a portion of the mandible.

The distal tip of the zygomatic process resembles the morphology in modern pangolins and differs from that in *E. waldi, Eurotamandua,* and metacheiromyid palaeanodonts, in which the process is laterally and anteriorly directed, relatively short, and inflated at its base and terminates in a sharp point (Gaudin et al., 2009; see also Storch, 2003: fig. 1). The weathered condition of the tip in both the type and USNM-P 494439 leaves open the possibility that the zygomatic process is broken off in both specimens and thus incompletely preserved. Although its shape is like that of modern pangolins, the likely presence of a jugal bone (see above), lacking in modern forms, raises the possibility of a complete zygoma in *Patriomanis*. However, if a complete zygoma were present, a more

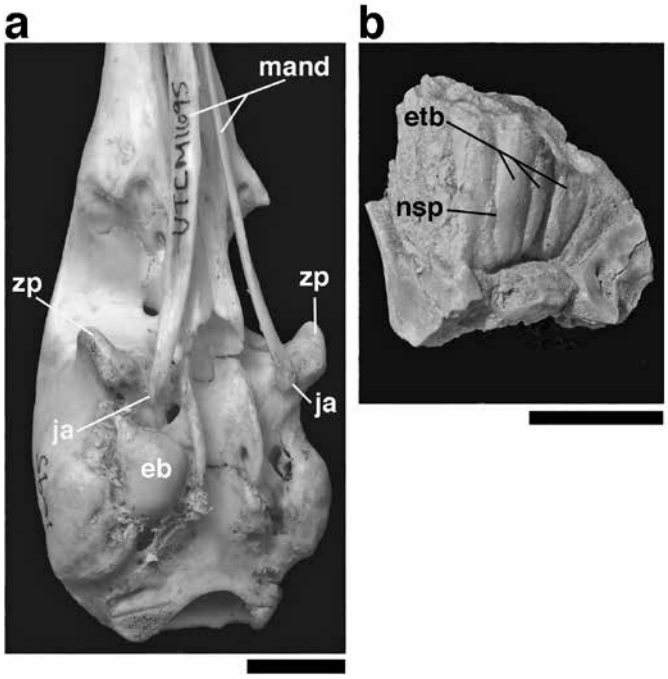

FIGURE 6. Skull of *Phataginus tricuspis* and skull fragment of *Patriomanis americana*: (a) skull of *Phataginus tricuspis* (UTCM 1695) in ventrolateral view; (b) skull fragment of *Patriomanis americana* (USNM-P 299960) showing cast of ethmoturbinals in dorsal view. Abbreviations: **eb,** ectotympanic bulla; **etb,** ethmoturbinal; **ja,** jaw articulation; **mand,** mandible; **nsp,** nasal septum; **zp,** zygomatic process of squamosal. Scale bars = 1 cm. Photos by Tim Gaudin, composed and labeled by Julia Morgan Scott for Smithsonian Institution.

anterolaterally elongated zygomatic process with a facet for the jugal would be expected, like that of *E. waldi*. The ventrally directed process in the two *Patriomanis* specimens shows no trace of a facet for the jugal as preserved. Thus, the evidence for a complete zygoma in *Patriomanis* is ambiguous, although we have chosen to reconstruct its presence in Figures 3 and 4.

The posterolateral surface of the zygomatic process is marked by a clearly delineated depression, the postglenoid fossa. The lateral margin of the fossa is defined by a strong ridge that passes from the tip of the zygomatic process (as preserved) posterodorsally, arching over the porus acousticus to terminate at the base of a prominent squamosal posttympanic crest (see below). In the middle of the postglenoid fossa is a large opening, the postglenoid foramen (Figures 3a,c, 4b,d, and 7), which in cingulate xenarthrans and other placental mammals transmits the capsuloparietal emissary vein (Evans and Christensen, 1979; Wible and Gaudin, 2004; this vein is one of the major drainage routes for the transverse sinus in eutherians; see Wible, 1990). In USNM-P 494439, there is an additional small foramen of unknown function medial to the postglenoid foramen (Figure 7). The postglenoid foramen is present in all pholidotans (except *Eurotamandua;* Gaudin et al., 2009) and in *Palaeanodon* but not *Metacheiromys* (Patterson et al., 1992), but its position varies. In *Patriomanis* and *Phataginus tetradactyla*, it lies posterior to the base of the zygomatic process. In *E. waldi, Smutsia, M. pentadactyla,* and some *M. crassicaudata* it lies on the lateral aspect of the process itself, whereas in *M. javanica,* some *M. crassicaudata,* and *P. tricuspis* it lies on the posterior aspect of the zygomatic process (Figure 5; Gaudin and Wible, 1999; Gaudin et al., 2009).

The portion of the squamosal bordering the ear region is quite different from that in modern manids. *Patriomanis* lacks the postauditory inflation of the squamosal characteristic of the extant taxa (Figure 5; Gaudin and Wible, 1999: char. 48, figs. 2, 4; Gaudin et al., 2009: char. 353; see also illustrations in Emry, 1970: figs. 9B, 10A), an inflation that largely hides the mastoid portion of the petrosal from external view (Novacek and Wyss, 1986; Patterson et al., 1992). Instead, the posteroventral squamosal margin, that is, the postglenoid area, is marked by three arches and two processes (Figures 3, 4b,d, and 7). This arrangement is quite reminiscent of that described for the late Cretaceous eutherian *Zalambdalestes* by Wible et al. (2004) and, to a lesser extent, that of the extant West Indian eulipotyphlan *Solenodon paradoxus* (Hispaniolan solenodon) described by Wible (2008).

As in these taxa, the first arch is undoubtedly the porus acousticus, the arch that would accommodate the external auditory meatus. Dorsal and medial to the ventromedial edge of the porus is a small shelf that forms the squamosal contribution to the roof of the epitympanic recess. The first process immediately behind the porus and carrying an anteroventral facet for the missing posterior crus of the ectotympanic is likely what Wible et al. (2004) and Wible (2008) label the "posttympanic crest," although in *Patriomanis* it abuts both the tympanohyal and the large, blocky paroccipital process of the petrosal (sensu Wible and Gaudin, 2004; equal "mastoid process" of Evans and Christensen, 1979) and is enlarged and rugose laterally, as if it may have served as a site for muscle attachment. In *Zalambdalestes* and *Solenodon,* it has the tympanohyal contact but is separated from the paroccipital process by the stylomastoid notch for cranial nerve VII, and it lacks any lateral expansion (Wible et al., 2004; Wible, 2008). The arch behind the posttympanic crest is semicircular and is well lateral to the stylomastoid notch of *Patriomanis*. It accommodates a significant lateral exposure of the paroccipital process of the petrosal, that is, a lateral mastoid exposure, a feature missing in modern pangolins (as noted above; Novacek and Wyss, 1986; Patterson et al., 1992) but present in *E. waldi, Eurotamandua,* and palaeanodonts (Gaudin et al., 2009). However, there is a ventral groove on the right paroccipital process of USNM-P 494439 that leads toward the back edge of this arch, which may imply that the arch is a kind of auxiliary stylomastoid notch. Immediately behind this second arch is a second process, smaller than the posttympanic crest and much smaller in USNM-P 494439, where it is preserved only on the right side and even then may be damaged distally, than in the type, where it is preserved apparently intact on the right but not the left. This process abuts the paroccipital process medially and posteriorly; hence, we identify it as the posttympanic process of the squamosal on the basis of its similarity to the morphology in *Zalambdalestes* and *Solenodon* (Wible et al., 2004; Wible, 2008). We make this conclusion despite the fact that in *Patriomanis* there is a tall, anteroposteriorly narrow arch separating the posttympanic process from the lower end of the nuchal crest on the occipital bone. This arch is not present in either *Zalambdalestes* or *Solenodon*. This third arch in the sequence accommodates a second, smaller lateral mastoid exposure and could conceivably have housed a tendon of insertion for the sternomastoid (the cleidomastoid is absent in modern pangolins; see Windle and Parsons, 1899), given that sternomastoid and cleidomastoid insert

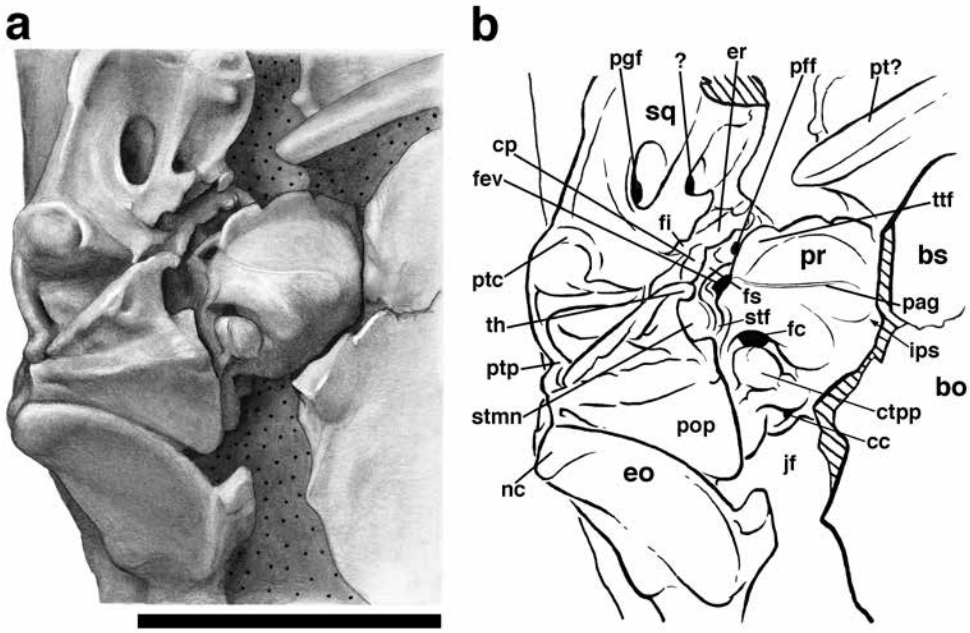

FIGURE 7. Close-up of right auditory region of *Patriomanis americana,* USNM-P 494439, in ventral view: (a) pencil drawing; (b) labeled line drawing. Abbreviations: **bo,** basioccipital; **bs,** basisphenoid; **cc,** cochlear canaliculus; **cp,** crista parotica; **ctpp,** caudal tympanic process of petrosal; **eo,** exoccipital; **er,** epitympanic recess; **fc,** fenestra cochleae; **fev,** fenestra vestibuli; **fi,** fossa incudis; **fs,** facial sulcus; **ips,** inferior petrosal sinus; **jf,** jugular foramen; **nc,** nuchal crest; **pag,** promontorial artery groove; **pff,** primary facial foramen; **pgf,** postglenoid foramen; **pop,** paraoccipital process of petrosal (= mastoid process of Evans and Christensen, 1979); **pr,** promontorium of petrosal; **pt,** pterygoid; **ptc,** posttympanic crest; **ptp,** posttympanic process of squamosal; **stf,** stapedius fossa; **sq,** squamosal; **stmn,** stylomastoid notch; **th,** tympanohyal; **ttf,** m. tensor tympani fossa; **?,** unknown foramen. Stippled areas represent matrix. Scale bar = 1 cm. Illustrations by Julia Morgan Scott for Smithsonian Institution.

on the posterior surface of the posttympanic process in *Solenodon* (Wible, 2008).

Like most placental mammals, the squamosal contacts the parietal dorsally, the occipital (i.e., exoccipital) posteriorly, the frontal anteriorly, and the alisphenoid and petrosal medially. As noted above, there is also a small anterior contact with the orbitosphenoid.

Ethmoid and Vomer

Neither the ethmoid nor vomer is available for study in any of our *Patriomanis* specimens, apart from some impressions of the ethmoturbinals on the underside of a fragment of the frontal bone preserved in USNM-P 299960 (Figure 6b). The type is broken posterior to these elements since the entire rostrum is absent, whereas in USNM-P 494439 they are covered by matrix and would be difficult to expose without damaging more superficial elements. The fragment from USNM-P 299960 preserves impressions of four ethmoturbinal scrolls on each side of the skull, but extant taxa are known to possess six ethmoturbinals (Grassé, 1955). Modern pangolins are one of several placental orders in which a separate mesethmoid ossification makes a sizable contribution to the osseous nasal septum (Novacek and Wyss, 1986; Novacek, 1993). This morphology is also known in carnivorans, the sister taxon to Pholidota in molecular-sequence-based placental phylogenies (Meredith et al., 2011) or combined morphology- and molecular-based phylogenies (O'Leary et al., 2013) but not xenarthrans (but see Ferigolo, 1981), a group often allied with Pholidota in exclusively morphology-based phylogenies (Gaudin and McDonald, 2008; O'Leary et al., 2013).

Orbitosphenoid and Presphenoid

Emry (1970) makes no mention of the orbitosphenoid since the type preserves no more than the posterodorsalmost fragments of the bone. Our additional preparation in the orbital region of USNM-P 494439, however, has revealed a sizable orbitosphenoid exposure in the medial wall of the orbit, as in modern pangolins (Jollie, 1968; Novacek, 1993: fig. 9.22C; Gaudin, 2004). The exposed surface is triangular with its apex dorsad (Figures 3c, 4d). In the middle of the bone is a large optic foramen, and the posteroventral portion of the orbitosphenoid forms the medial wall of the sphenorbital fissure. The optic foramen is similarly large in *E. waldi, Phataginus,* and *S. temminckii* but is relatively smaller in *Manis, S. gigantea,* and various out-groups (Gaudin et al., 2009).

The orbitosphenoid is sutured to the frontal along its anterodorsal edge and to the palatine along its ventral edge (where dorsal connections between the palatine and the frontal and alisphenoid clearly exclude any connection between orbitosphenoid and maxilla or pterygoid). Its posterodorsal edge is sutured to the frontal, squamosal, and alisphenoid. The connection to the squamosal is lacking in the out-groups and in *Eurotamandua* but is present in *E. waldi* and all of Manidae and is particularly broad in members of the genus *Manis* (Figure 5b; Gaudin et al., 2009). The right and left orbitosphenoids are fused in the ventral midline to form a rodlike presphenoid element that was likely exposed in the roof of the nasopharynx (visible in USNM 494439 but hidden in ventral view by matrix and bone fragments in Figure 4b). As in *M. javanica* (Figure 5b; Jollie, 1968), the presphenoid would be sutured to the basisphenoid posteriorly and the palatine laterally. It may also have had a posterolateral connection to the pterygoid and an anterior connection to the vomer, but this cannot be confirmed with the material presently in hand.

Alisphenoid

Despite the fact that most of the left and right alisphenoid bones are preserved in the type specimen (F:AM 78999), Emry's (1970) description focuses on the foramina in and around these elements rather than a description of the bones themselves. USNM-P 494439 provides additional information beyond what was preserved in the type, in that it retains intact the anteriormost portion of the bone on the left side of the skull, that is, the portion forming the lateral wall of the sphenorbital fissure, as well as some vestige of the bone's ventral connections to the palatine and pterygoid, whereas the palatines and pterygoids are missing from the type specimen. The left alisphenoid of USNM-P 494439 is damaged posteriorly, with a broad transverse crack running through the foramen ovale, and the posterior reaches of the bone appear to be lost. The right alisphenoid is not preserved in USNM-P 494439.

The main body of the alisphenoid is nearly transversely oriented, extending from its lateral contact with the squamosal along the inner base of the zygomatic process to its medial contact with the pterygoid (Figure 4d). At its anterior end, it becomes more vertical, forming the semicircular lateral margin of the sphenorbital fissure (= anterior lacerate foramen of Emry, 1970), as well its lateral and ventral walls. The floor of the fissure contacts the orbitosphenoid–presphenoid medially. It appears to be broken anteriorly but must have extended far enough forward to contact the perpendicular process of the palatine. As noted previously, there is a crack that may represent the palatine–pterygoid suture—it extends as far back as the posteriormost point on the sphenorbital fissure's lateral margin. If it is indeed the suture, then there is a clear orbital contact between alisphenoid and palatine. The dorsalmost portion of the alisphenoid extends upward between the orbitosphenoid and palatine, terminating where the orbitosphenoid and squamosal briefly contact. As noted by Rose and Emry (1993), there is no alisphenoid–parietal contact. The contact is absent in all extant manids as well but is present in *E. waldi* and metacheiromyid palaeanodonts (Gaudin et al., 2009). The posterior margin of the alisphenoid appears to contact the petrosal in USNM-P 494439, but this contact is likely due to postmortem breakage and distortion of the skull. In the type, where the posterior edge appears unbroken and the specimen is less distorted, there seems to be no contact with the petrosal, unless it is with the lateralmost extremity of the posterior edge. Instead, the alisphenoid forms the anterior edge of a confluent carotid foramen (= median lacerate foramen of Emry, 1970, comprising the medial half of the opening) and piriform fenestra (Figure 4d). The carotid foramen–piriform fenestra is present in a newborn *M. javanica,* but the fenestra is obliterated by an extensive suture between the alisphenoid and petrosal in the adult (Figure 5b; Jollie, 1968; see also Figure 8).

As in other mammals, several of the large orbital foramina are associated with the alisphenoid (Figure 4d). These have been described by Emry (1970), who notes that the foramen rotundum (for the maxillary nerve, CN V_2) is absent in *Patriomanis,* becoming confluent instead with the sphenorbital fissure (for CN III, IV, V_1, VI and several major orbital arteries and veins), as in modern Manidae (Figure 5; Jollie, 1968; a separate foramen

rotundum is retained in palaeanodonts; Gaudin et al., 2009). The sphenorbital fissure lies between the orbitosphenoid and alisphenoid. Rose and Emry (1993) note that the foramen ovale (for the mandibular nerve, CN V_3) lies wholly within the alisphenoid in *Patriomanis*. It is located centrally within the main body of this element. This is also the condition in palaeanodonts, *Phataginus,* and *M. crassicaudata*, whereas a squamosal contribution to the lateral margin of the foramen ovale is known to occur in *S. temminckii, M. pentadactyla,* and some specimens of *S. gigantea* and *M. javanica* (Gaudin et al., 2009). In some modern pangolins, the foramen ovale is also situated more posteriorly, even with the anterior edge of the ectotympanic (*M. pentadactyla, M. crassicaudata,* some specimens of *S. temminckii* and *P. tricuspis*; Gaudin et al., 2009).

Pterygoid

The pterygoid bones are not mentioned by name in Emry's (1970) description. Emry (1970:468) does note that the "sphenoidal wings that extend the narial channel backward to the basioccipital in *Manis* were apparently also present in *Patriomanis*, but the ventral part has been broken away." These so-called basisphenoid wings (Gaudin and Wible, 1999) were shown by Gaudin et al. (2009; see description of char. 347) to be tympanic processes of the pterygoid, not parts of the basisphenoid. In USNM-P 494439, the tympanic process of the pterygoids appears to be partially preserved (Figures 3, 4), and as in the type, the pterygoids appear to terminate just in front of the basisphenoid–basioccipital suture (the suture is preserved in USNM-P 494439; see below), where they are

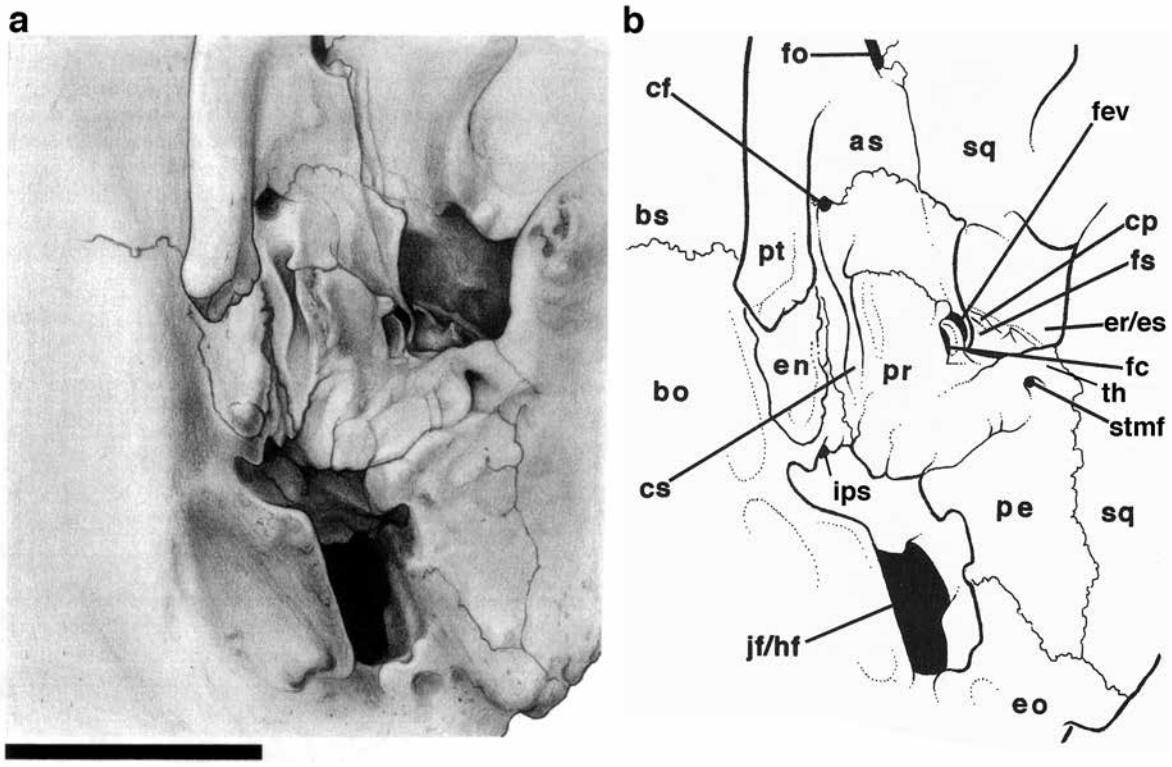

FIGURE 8. Close-up of left auditory region of *Smutsia gigantea*, AMNH 53858, in ventral view: (a) pencil drawing; (b) labeled line drawing. Abbreviations: **as,** alisphenoid; **bo,** basioccipital; **bs,** basisphenoid; **cf,** carotid foramen; **cp,** crista parotica; **cs,** sulcus for internal carotid artery; **en,** entotympanic; **eo,** exoccipital; **er/es,** epitympanic recess/epitympanic sinus; **fc,** fenestra cochleae; **fev,** fenestra vestibuli; **fo,** foramen ovale; **fs,** facial sulcus; **ips,** inferior petrosal sinus; **jf/hf,** confluent jugular foramen and hypoglossal foramen; **pe,** petrosal (paroccipital or "mastoid" exposure); **pr,** promontorium of petrosal; **pt,** pterygoid; **sq,** squamosal; **stmf,** stylomastoid foramen; **th,** tympanohyal. Scale bar = 1 cm. Modified from Gaudin and Wible (1999). Illustrations by Julia Morgan Scott for Smithsonian Institution.

fused to the lateral edge of the basisphenoid. This placement would suggest that in *Patriomanis* the auditory tube was displaced posteriorly and faced directly mediad, as in modern pangolins (Gaudin and Wible, 1999; Gaudin et al., 2009), and not anteromedially, as in most eutherians. This tympanic process of the pterygoid also likely formed the medial margin of the carotid foramen (= median lacerate foramen of Emry, 1970), whereas the alisphenoid and petrosal form the anterior and posterior margins of this opening, which, as noted above, is confluent laterally with the piriform fenestra.

The pterygoid hamulus is not preserved in any *Patriomanis* specimen. As was just noted, the pterygoid is fused to the basisphenoid posteromedially. It also was likely sutured to the palatine anteriorly and the alisphenoid dorsally and may also have attached to the presphenoid anteromedially.

Basisphenoid and Basioccipital

Emry (1970:468) describes these elements together, noting that they form a basicranial plate that is "rather narrow and decreases in width anteriorly." Although the suture between the two is fused in the type, it is preserved in USNM-P 494439, where it assumes a shallow V shape with its vertex pointing anteriorly, and in a fragment from USNM-P 299960, where it is straight, the difference in shape perhaps ontogenetic. It is located roughly where Emry (1970) suggests, at the midpoint of the ear region, terminating laterally at the anteromedial rim of the purported foramen for the inferior petrosal sinus just anterior to a large pair of basioccipital tubera (Figure 4c,d). Gaudin and Wible (1999) recognize small crests that extend posterolaterally from the tubera as tympanic processes of the basioccipital (= basioccipital "wings" of Gaudin and Wible, 1999). Although the processes are more extended ventrally and anteroposteriorly elongated in the modern forms, this characterization does not seem unreasonable. Immediately posterior to the basioccipital tubera in *Patriomanis* is a pair of shallow fossae. On the basis of the morphology in other eutherian mammals (see, e.g., *Homo,* Pick and Howden, 1977; *Canis,* Evans and Christensen, 1979; *Euphractus,* Wible and Gaudin, 2004; *Solenodon,* Wible, 2008), the basioccipital tubera likely served as attachment points for the longus capitis muscles, and the concavities immediately behind likely served as attachment sites for the rectus capitis ventralis muscles.

Emry (1970) identifies a narrow groove on the ventrolateral margin of the basisphenoid as housing the vidian nerve (= nerve of the pterygoid canal in Wible and Gaudin, 2004; = anterior portion of greater petrosal nerve in Pick and Howden, 1977; Evans and Christensen, 1979). This groove is also present on the left side of USNM-P 494439. In both the type and USNM-P 494439, it originates posterior to the tympanic process of the pterygoid, opposite the inferior petrosal sinus opening identified by Emry (1970). As Emry (1970) notes, this origin, which is shared with modern manids, is posterior to its more typical position in other eutherians, where it emerges from the carotid foramen (see, e.g., *Homo,* Pick and Howden, 1977 [emerges from foramen lacerum, homolog of carotid foramen as used here]; *Dasypus,* Wible, 2010; *Solenodon,* Wible, 2008; in *Canis* it emerges from a separate hiatus Fallopii just lateral to the carotid foramen, Evans and Christensen, 1979). The anterior termination of the groove, the pterygoid canal itself, is not preserved in *Patriomanis*.

Emry (1970) labels three openings associated with the lateral edge of the basisphenoid–basioccipital complex in his fig. 9: the foramen for the inferior petrosal sinus, the jugular foramen (following usage of Wible and Gaudin, 2004; = posterior lacerate foramen of Emry, 1970), and the hypoglossal foramen (following usage of Wible and Gaudin, 2004; = condylar foramen of Emry, 1970). He notes in the text, however, that the foramen assigned to the inferior petrosal sinus is continuous with a groove emerging from the hypoglossal foramen, a groove that would normally house either the internal carotid artery, the inferior petrosal sinus, or both but that would normally originate in the jugular rather than the hypoglossal foramen. The jugular foramen has been assigned to an opening lateral to this groove in Emry's (1970) fig. 9. The morphology is indeed difficult to interpret. There appear to be openings on the left side of USNM-P 494439 (Figure 4b,d) that correspond to those described by Emry (1970). There is a clearly marked, semiovate notch medial and slightly anterior to the basioccipital tuber that mirrors the inferior petrosal sinus opening (Figure 7). A second notch in the lateral margin of the basioccipital lies a short distance farther posteriorly and medially. This notch would appear to be the remnant of the hypoglossal foramen. There is no indication of the jugular foramen on the basioccipital; however, there is a vertical groove on the posteromedial surface of the petrosal. It houses the cochlear canaliculus (Figure 7), which typically opens in or near the jugular foramen (see, e.g., *Canis*, Evans and Christensen, 1979; *Dasypus*, Wible, 2010); hence, this groove almost certainly forms the lateral margin to the jugular foramen. The petrosal groove is displaced laterally relative to the inferior petrosal sinus and hypoglossal foramina, which would again be consistent with Emry's (1970) assessment

of the type specimen. Unfortunately, the morphology in both specimens is quite different from that in modern pangolins (Figures 5, 8), and the relevant features are not preserved in any other fossil pangolins. In the modern taxa, the internal carotid artery typically travels in a clearly marked sulcus on the ventromedial edge of the petrosal, the sulcus terminating anteriorly at the carotid foramen (Figure 8). If an inferior petrosal sinus foramen is present (as in *Manis* sp., *S. gigantea,* and some *S. temminckii*; Gaudin et al., 2009), it is generally found at the end of a dorsal canal, hidden in ventral view, that travels dorsal to the carotid sulcus and opens in the anterior margin of the jugular foramen (Figure 8). Moreover, the tympanic processes of the basioccipital (likely homologous at least in part with the basioccipital tubera of *Patriomanis*) form the medial margin of the jugular foramina. The groove emerging anteriorly from the hypoglossal foramen, when present, connects with the jugular foramen rather than passing medial to this opening (this groove is absent in *Phataginus* but present in *Manis* sp., *S. temminckii,* and those *S. gigantea* in which the jugular and hypoglossal foramina are not fused; Gaudin, unpublished data). Because of the difference in morphology between *Patriomanis* and the extant species, Gaudin et al. (2009) coded the inferior petrosal sinus foramen as being absent in the former. Ultimately, the identity of this "inferior petrosal sinus" opening cannot be conclusively established—it could, for instance, represent a patent basicochlear commissure, as in the armadillo *Dasypus novemcinctus* (Wible, 2010), an interpretation not considered by either Emry (1970) or Gaudin et al. (2009). That said, we now believe Emry's (1970) assignment of this opening to the inferior petrosal sinus is the most probable interpretation. We also accept his assignment of the remaining openings to the jugular and hypoglossal foramina, respectively.

Neither the type nor USNM-P 494439 preserves the posterior edge of the basioccipital, so the morphology of the ventral margin of the foramen magnum cannot be ascertained. The basisphenoid contacts the presphenoid anteriorly, the pterygoid and possibly the palatine laterally, and the basioccipital posteriorly. The basioccipital contacts the basisphenoid anteriorly and the exoccipital posterolaterally. Neither element appears to have a lateral connection with the petrosal, although both closely approach its medial margin (Figure 7).

Petrosal

Although both left and right petrosals are present in the type specimen, neither is well preserved. The left is better than the right, which is missing the entire ventral exposure of the pars canalicularis. Emry (1970) suggests that both petrosals have been displaced. He described several major foramina associated with the petrosal (see above) but not the bones themselves. Both left and right petrosals are much better preserved in USNM-P 494439 and have undergone extensive preparation as part of this study. A close-up illustration of the right petrosal is provided (Figure 7) since it is slightly more complete than the left.

The ventral surface of the petrosal is dominated by a globose promontorium. A similar morphology is present in *E. waldi* and *Metacheiromys*, but in modern pangolins the promontorium tends to be strongly reduced, with the lateral wall of the petrosal pars cochlearis (i.e., the portion that houses the cochlea and sacculus) nearly flat in ventral view (Figure 8; Gaudin and Wible, 1999; Gaudin et al., 2009). On the right side of USNM-P 494439 there is a weak groove originating at the ventral margin of the fenestra vestibuli and traveling medially across the promontorium, nearly transverse to its long axis. If anything, the groove is even less in evidence on the left side. Modern pangolins lack a transpromontorial internal carotid or stapedial artery (Gaudin et al., 2009)—indeed, the stapedial system is missing entirely (Bugge, 1979). Instead, as noted above, the internal carotid travels in a carotid sulcus along the ventromedial edge of the petrosal. In contrast, the promontorial groove, weak though it is, suggests that at least a vestige of the stapedial arterial system may have been retained in *Patriomanis* (Figure 7). The promontorium also bears a distinct, dorsally situated pit along its anterolateral margin. This is almost certainly a tensor tympani fossa, that is, an attachment point for the tensor tympani muscle. The anterior edge of the fossa is likely formed by a very narrow epitympanic wing of the petrosal anterior to the promontorium. An epitympanic wing is present in modern pangolins as well, ranging from a small shelf like that of *Patriomanis* (e.g., *P. tricuspis* UTCM 1695) to a prominent process (e.g., *M. javanica* USNM 198852, FMNH 33550; see also *Palaeanodon,* Patterson et al., 1992).

Immediately lateral and slightly anterior to the promontorium is a deep groove curving anteromedially, the facial sulcus, which houses the facial nerve (CN VII) and represents part of the ventral exposure of the pars canalicularis of the petrosal (i.e., the portion housing the semicircular canals and utricle). The anterior half of this sulcus is roughly horizontal and is bounded anterolaterally by a robust crista parotica, a condition found in some modern pangolins (*P. tricuspis*, some specimens of *P. tetradactyla,*

and *M. pentadactyla*), although in most the crista parotica is reduced (*Smutsia*; Figure 8) or the facial sulcus has been converted to a closed canal (*M. crassicaudata, M. javanica,* some specimens of *M. pentadactyla,* and *P. tetradactyla*; Gaudin and Wible, 1999; Gaudin et al., 2009). The posterior portion of the facial sulcus extends ventrally toward a well-defined stylomastoid notch that lies posterolateral to the small, cylindrical tympanohyal. The notch itself forms two-thirds of a circle, open medially, with its lateral and posterior walls formed by the paroccipital process of the petrosal. In extant Manidae, the tympanohyal bends medially at its distal extremity to fuse with the lateral surface of the petrosal, enclosing the exit of the facial nerve (CN VII) in a complete stylomastoid foramen (Figure 8; Gaudin and Wible, 1999; Gaudin et al., 2009).

Near the anterior terminus of the facial sulcus is an opening, the primary facial foramen, in the lateral wall of the petrosal's pars cochlearis (Figure 7). The space immediately lateral to this foramen, the cavum supracochleare, houses the geniculate ganglion of the facial nerve (Evans and Christensen, 1979; Wible, 2010). This space is open ventrally, although shielded somewhat in ventral view by the crista parotica itself, which bends medially toward its termination on the lateral wall of the pars cochlearis just anterior to the cavum supracochleare, and by the dorsal rim of the tensor tympani fossa. This dorsal rim stands out as a distinct ridge from the lateral surface of the pars cochlearis. In other eutherian mammals, the cavum supracochleare is completely floored ventrally by the petrosal, creating a secondary facial foramen posterior to the cavum and an anterior hiatus Fallopii that transmits the greater petrosal nerve (e.g., the extinct Late Cretaceous *Zalambdalestes,* Wible et al., 2004; *Solenodon,* Wible, 2008; some *Dasypus*, Wible, 2010). This is also the morphology in *P. tricuspis* (UTCM 1695) and *S. gigantea* (AMNH 53858), although the morphology varies in extant pangolins; for example, as noted above, many extant forms enclose the facial sulcus in a canal. In *Patriomanis*, there is a small ventral groove where the crista parotica meets the pars cochlearis that likely accommodated the greater petrosal nerve.

The posterior half of the facial sulcus is nearly twice the transverse width of the anterior half, largely because of the presence of a sizable pit along its medial edge. This pit, which faces laterally, anteriorly, and ventrally, is the stapedius fossa for the stapedius muscle. In modern pangolins the stapedius fossa is shielded from view ventrally by the contact between the tympanohyal and the pars cochlearis (Figure 8), but in *P. tricuspis* (UTCM 1695) it is somewhat more anteriorly directed than it is in *Patriomanis* (Figure 7).

The lateral surface of the crista parotica slopes anterodorsally, where it abuts a shelf extending medially from the inner wall of the squamosal, just dorsal to the porus acousticus. The shelf is actually separated from the crista by a narrow gap anteriorly (which may be a preservational artifact), whereas posteriorly the two are sutured. Together they form the roof to a triangular depression, the epitympanic recess (as noted above; Figure 7). The epitympanic recess houses the articulation between the mallear head and the body of the incus in basal eutherians (e.g., *Lepticitis,* Novacek, 1986; *Zalambdalestes,* Wible et al., 2004; *Solenodon,* Wible, 2008; *Maelestes,* Wible et al., 2009; see also extant *Canis*, Evans and Christensen, 1979; *Solenodon,* Wible, 2008). In modern pangolins, this area is not fully roofed over, opening rather into a sinus between the squamosal and petrosal, the epitympanic sinus, which is continuous with the inflation in the posterolateral corner of the squamosal (Figure 8; Jollie, 1968; Emry, 1970; Gaudin et al., 2009). An epitympanic sinus has also been reported for *E. waldi* (Rose et al., 2005; Gaudin et al., 2009) and *Palaeanodon* (Patterson et al., 1992). The latter authors suggested the presence of an epitympanic sinus might be considered a morphological synapomorphy of a cohort Edentata including xenarthrans, pangolins, and palaeanodonts, although its morphology is not uniform (e.g., it expands anterior to the porus acousticus in xenarthrans, posteriorly in pangolins, and in both directions in *Palaeanodon*), and it is absent in *Patriomanis,* in dasypodine and tolypeutine armadillos, and in mylodontid sloths (Patterson et al., 1989, 1992; Gaudin, 1995, 2004). The participation of the squamosal bone in the roof of the epitympanic recess or sinus is considered a unique synapomorphy of Pholidotamorpha (Pholidota + Palaeanodonta) by Gaudin et al. (2009).

Along the posterior wall of the epitympanic recess in *Patriomanis* lies a small circular pit that straddles the petrosal–squamosal suture and faces anteriorly. This depression represents the fossa incudis, which in modern manids is more medially located and faces laterally (Gaudin et al., 2009).

As in all mammals, there are two large foramina in the posterolateral and posteroventral walls of the promontorium. The more lateral of the two is the fenestra vestibuli, which in life accommodates the footplate of the stapes. As preserved on the right side of USNM-P 494439 (the only place where it is fully prepared), it is oval in shape, with a stapedial ratio of 1.63 (length/width; see Segall, 1970). In *P. tricuspis* (UTCM 1695) the ratio is somewhat lower, 1.50. It is deeply recessed and positioned midway between but slightly ventral to the primary facial foramen and the

stapedius fossa. The ventral edge of the fenestra forms a strong ridge that is continuous anteriorly with the dorsal ridge of the tensor tympani fossa, and there is a lower, broader ridge orthogonal to both that separates the anterior fenestra vestibuli from the posterior tensor tympani fossa. In *P. tricuspis* (UTCM 1695) and other modern forms, the strong ventral rim of the fenestra vestibuli does not extend anterior to the opening, and the opening itself is only slightly recessed.

The second large opening, situated at the back of the promontorium, is labeled here the fenestra cochleae (Figure 7; following Gaudin and Wible, 1999; Gaudin et al., 2009). It is actually, in all likelihood, the aperture for the cochlear fossula, which would contain an opening inside for the attachment of the round window, the true fenestra cochleae (see, e.g., Wible, 2010), as in the modern *M. javanica* (Jollie, 1968). However, since we have been unable to prepare the interior of this opening and cannot assess its morphology, we will retain the older usage in our description and figures. The fenestra cochleae faces mainly posteriorly and laterally to a small degree. It is separated from the fenestra vestibuli by a broad, superficially convex crista interfenestralis. This morphology differs strongly from that of modern pangolins, in which the crista interfenestralis is a narrow strut, the two fenestrae are in close proximity, and the fenestra cochleae faces almost directly lateral (Figure 8; Gaudin and Wible, 1999; Gaudin et al., 2009). The arrangement in *Patriomanis* is clearly less derived, resembling the condition in *E. waldi* and the palaeanodont *Metacheiromys* (Gaudin et al., 2009). The crista interfenestralis in *Patriomanis* bears a small, transverse ridge that is continuous anteriorly with the ventral rim of the fenestra vestibuli. Its function is unknown.

Part of the difficulty in preparing the fenestra cochleae stems from the fact that it is shielded posteriorly by a large, bulbous process with a rather square outline, the caudal tympanic process of the petrosal. The caudal tympanic process is present on both the left and right sides of the skull in USNM-P 494439 but is not in evidence in the type specimen, although we suspect its absence in the latter is due to postmortem damage. The process appears to be freestanding because it is bounded anteromedially and laterally by grooves. The latter is larger and deeper and undercuts the caudal tympanic process dorsally. On the basis of comparisons with other eutherians (*Canis,* Evans and Christensen, 1979; *Dasypus,* Wible 2010), this groove likely housed the auricular branch of the vagus nerve (CN X). The anteromedial groove does not undercut the caudal tympanic process. Again on the basis of comparisons with other eutherians (Evans and Christensen, 1979; Wible, 2010), it likely housed the tympanic nerve, a branch of the glossopharyngeal nerve (CN IX). The closest analog we found to this process is on the right side of a specimen of *M. pentadactyla* (FMNH 75878), where the caudal tympanic process of the petrosal is lower and blunter and rounded distally and situated farther laterally but appears to be flanked by the same two grooves. In other specimens we examined from extant species, the caudal tympanic process appeared as a low knob or flange and was often not clearly delineated by neural grooves. With the exception of a few specimens of *Phataginus* (*P. tetradactyla* FMNH 62209 and *P. tricuspis* FMNH 42680 but not *P. tricuspis* UTCM 1695), these knobs or flanges tended to be positioned at the lateral edge of the jugular foramen, as in *M. pentadactyla* (FMNH 32511), rather than at its anterior margin, as in *Patriomanis*.

The grooves flanking the caudal tympanic process of the petrosal in *Patriomanis* are roofed by a horizontal plate that also extends between the base of the caudal tympanic process and the dorsal rim of the fenestra cochleae. This plate represents the roof of the posttympanic sinus (Wible, 2010) and is a feature missing in modern pangolins because of the lateral reorientation of the fenestra cochleae. The junction of this roof with the promontorium is marked by a very small, shallow "hairline" groove that extends from the medial side of the fenestra cochleae opening to the medial side of the pars cochlearis, where it connects to a small foramen of unknown function just anterior to the foramen for the cochlear canaliculus. Both the roof of the posttympanic sinus and the caudal tympanic process are part of the pars canalicularis of the petrosal.

Posterior and medial to the base of the caudal tympanic process is a broad vertical groove that extends dorsally into the braincase. In the anterior wall of this groove is a foramen, the opening for the cochlear canaliculus (= cochlear aqueduct; see Evans and Christensen, 1979) that transmits the perilymphatic duct of the inner ear. In other extant eutherians (e.g., *Homo,* Pick and Howden, 1977; *Canis,* Evans and Christensen, 1979; *Dasypus,* Wible, 2010), the cochlear canaliculus opens into the lateral wall of the jugular foramen, so we identify this groove as the lateral wall to the jugular foramen as well, despite its lateral position relative to modern pangolins. As noted above, the medial margin of the jugular foramen is likely formed by the tympanic process of the basioccipital.

Although several portions of the ventral exposure of the pars canalicularis have already been described, including the facial sulcus, cavum supracochleare, crista parotica, and the caudal tympanic process, the largest

portion has not. It is manifested as a bulky, trapezoidal paroccipital process (following Wible and Gaudin, 2004; sometimes called the "mastoid process"; see Wible and Gaudin, 2004, for discussion). The paroccipital process has a nearly straight, elongate medial edge that is notched anteriorly. This notch, along with the tympanohyal, outlines the stylomastoid notch. The anterior and posterior edges of the paroccipital process approach one another laterally, lending the process its trapezoidal shape. The lateral edge is formed into two processes that are exposed in lateral view: an anterior process that is framed by the arch of the posttympanic crest of the squamosal and a posterior process that lies in the arch between the posttympanic process of the squamosal and the lower end of the nuchal crest of the exoccipital bone. The ventral surface of the paroccipital process is complex. It posteromedial portion is triangular, narrowing laterally, and its surface is anteroposteriorly convex. It ends at a transverse crest that marks its ventralmost extent. This crest is separated by a groove from a second similar but more anterior crest. The groove is broad medially, where it backs against the stylomastoid notch, then narrows laterally as it approaches the anterior margin of the posttympanic process. As noted above, this groove may be involved in transmitting the facial nerve. In front of the anterior crest, but raised dorsally, is the rather shapeless anterior lateral prong of the paroccipital process that is exposed beneath the posttympanic crest. In almost all modern Manidae, the paroccipital region of the petrosal is covered by the squamosal in lateral view (Gaudin et al., 2009) because of its expansion to accommodate internal sinuses (see above). However, there is at least one specimen of *S. gigantea* (AMNH 53858; Figure 8, labeled "pe") in which a small "mastoid exposure" of the paroccipital process is present. This exposure is triangular and extends farther dorsally than in *Patriomanis* and is simpler in its morphology. It abuts the anterior edge of the nuchal crest, as in *Patriomanis*, but lacks a posttympanic process or posttympanic crest of the squamosal, and the paroccipital process lies behind the enclosed stylomastoid foramen and does not participate in transmitting the facial nerve.

Ectotympanic/Entotympanic/Ear Ossicles

None of these elements is preserved in *Patriomanis*. Emry (1970) speculates that the ectotympanic element resembled the simple crescent-shaped form in the extant genus *Manis,* a form also present in *E. waldi* and the Paleocene palaeanodont *Palaeanodon,* as opposed to the inflated, bullate form evident in modern African pangolins, as well as the Eocene palaeanodont *Metacheiromys* and the enigmatic edentate *Eurotamandua* (Gaudin et al., 2009). Gaudin and Wible (1999) demonstrate that the entotympanic element present in *Smutsia* (Figure 8) and some specimens of *P. tricuspis* (as well as palaeanodonts; Gaudin et al., 2009) is almost certainly absent in *Patriomanis*.

Occipital

The occipital bone, including both exoccipital and supraoccipital regions, has been thoroughly described by Emry (1970), so we will not repeat that description here but instead make some broader taxonomic comparisons. Emry (1970) notes that a strong lambdoid or nuchal crest is present in *Patriomanis* but lacking in modern pangolins. The plesiomorphic condition is displayed not only by *Patriomanis* but also by *E. waldi, Eurotamandua,* and the metacheiromyid palaeanodonts (Gaudin et al., 2009). The latter authors also note that in some pangolins, the exoccipital bone is laterally constricted immediately anterior to the occipital condyle, forming a discrete condylar "neck." This feature is present in *E. waldi* and the extant giant pangolin (*S. gigantea*), as well as the species in the genus *Manis* (Figure 5b), but is not observed in *Patriomanis,* the extant genus and species *Phataginus* and *S. temminckii,* and metacheiromyid palaeanodonts (Gaudin et al., 2009). Last, the transversely oval foramen magnum of *Patriomanis* (Emry, 1970) is known to have quite a varying distribution among pholidotamorphs, with *Metacheiromys, S. gigantea,* and some *S. temminckii* and *M. javanica* sharing the condition in *Patriomanis,* whereas a more circular foramen magnum is present in *Palaeanodon, Phataginus, M. crassicaudata,* and *M. pentadactyla* (Gaudin et al., 2009).

Endocranium

The matrix was removed from the interior of the type skull of *Patriomanis,* and an endocast was made. This endocast is described briefly in Emry (1970). The removal of this matrix has allowed us limited access to assess the bony anatomy of the walls of the endocranial cavity. Access is limited in the sense that we can address only what is visible through the foramen magnum or the anterior opening where the skull is broken just behind the presumptive location of the cribriform plate. Gaudin and Wible (1999) and Gaudin et al. (2009) have already noted several phylogenetically relevant features. *Patriomanis* is plesiomorphic in its retention of venous grooves on the endocranial surface (including those for the transverse, sigmoid, and superior petrosal sinuses), these grooves being lost in modern Manidae. In addition, the flooring of the middle cranial

fossa by the sphenoid complex is plesiomorphic, in contrast to the derived squamosal floor found in manids. One of the cranial fragments from USNM-P 299960 preserves a clear, ovate hypophyseal fossa on the dorsal surface of the basisphenoid, flanked laterally by grooves for the internal carotid artery, those grooves in turn lying medial to a depression that presumably represents the cavum epipericum. This same fragment also has a clear groove running along the side of the basioccipital. This groove presumably accommodated the inferior petrosal sinus.

Patriomanis represents an intermediate condition in the development of a bony tentorium, that is, an osseous lamina formed within the sheet of connective tissue separating the cerebrum from the cerebellum. In most mammals (e.g., *Homo*, Pick and Howden, 1977; *Erinaceus*, Gaudin et al., 2009), this partition is composed entirely of membranous connective tissue. In *Patriomanis,* a partial bony tentorium is present in the form of an outgrowth from the inner surfaces of the squamosal and parietal bones, running posterodorsal to anteroventral along the anterior edge of the petrosal. In modern forms, the tentorium is a broad bony septum that extends all the way from the anteroventral edge of the petrosal to the roof of the cranial cavity, attaching again to the inner walls of the squamosal and parietal (anterior to their contact with the occipital). Curiously, an extensive bony tentorium like that of modern pangolins is also found in the most basal living carnivorans, *Nandinia* (Gaudin et al., 2009), and other extant Carnivora (Evans and Christensen, 1979; Wyss and Flynn, 1993; Homberger and Walker, 2004), with the Carnivora likely representing the sister taxon to Pholidotamorpha (Meredith et al., 2011; O'Leary et al., 2013). In both *Nandinia* and *Patriomanis*, the groove for the superior petrosal sinus passes between the petrosal and the tentorium, whereas in modern pangolins, there is a foramen piercing the tentorium that accommodates this vessel (Gaudin et al., 2009).

Mandible

The most completely preserved mandibular remains known for *Patriomanis* are those from USNM-P 494439 described in detail by Emry (2004). These remains include a nearly complete left dentary (Figure 9a,c) figured by Emry (2004: fig. 10.5A,B,D) in medial, lateral, and dorsal views, lacking only the posteriormost portions, including the condyle and angle. It also includes a much less complete right dentary, illustrated by Emry only in dorsal view (Emry, 2004: fig. 10.5D) but here in both medial and dorsal views (Figure 9b,c). It is missing the anterior part of the symphysis, the distal tip of the anterolateral mandibular "prong," and most of its posterior reaches. There are also two small fragments from the left and right dentaries of the type specimen. The largest of these preserves the ventral margin of the bone from the posteriormost part of the symphysis to the beginning of the ascending ramus. Emry (2004) has already drawn attention to its characteristic pangolin apomorphies, including its edentulous nature, its spout-like symphysis with an unfused, sutural attachment between the left and right dentaries, and the presence of the distinctive anterolateral bony prong in the symphyseal area, a feature that, according to Doran and Allbrook (1973:888), "gives attachment to the lower lip" in modern pangolins. Emry (2004) has also noted plesiomorphic features, like the retention of a weak coronoid process, lacking in the modern taxa. Emry (2004) also draws attention to the greater overall robusticity of the horizontal ramus relative to modern pangolins. The ramus is very thin transversely but deeper dorsoventrally than in extant manids. However, it should be noted that all known pholidotans, including the modern forms, *Necromanis, Patriomanis, E. waldi,* and *Eurotamandua*, have a maximum depth of the horizontal ramus less than 10% of overall maximum mandibular length.

One feature not described by Emry (2004) but illustrated here (Figure 9b) is a small bone fragment that we believe pertains to the right dentary of USNM-P 494439. It is not attached to the dentary, and indeed, we cannot fit it precisely to the existing broken posterior end of the bone. However, what we take to be its broken dorsal edge roughly matches the shape of the broken posteroventral edge of the right dentary. That would make this fragment a preserved angular process of the dentary. Note that it is robust and hooked posteriorly, with a convex leading edge, concave trailing edge, and rounded tip. The angular process is missing in *Necromanis* and modern manids but is retained in *E. waldi* and *Eurotamandua*. In *E. waldi* it forms either a short triangular process reminiscent of the coronoid in *Patriomanis* (see Storch, 2003: fig. 1, SMF MEA 263) or a blunt semicircular and slightly inflated process (type specimen, SMF Me 84, Storch, 1978), but in neither case is it as strong or posteriorly hooked as that of *Patriomanis*. The angular process is hooked in *Eurotamandua* (see especially Storch and Habersetzer, 1991: fig. 3a,b), but it is pointed at the tip instead of rounded, giving it a less robust appearance.

A few features of the symphyseal region not described by Emry (2004) are distinctive in *Patriomanis*. As in living pangolins, there are two mental foramina on the anterior dentary. The more posterior opens laterally on the

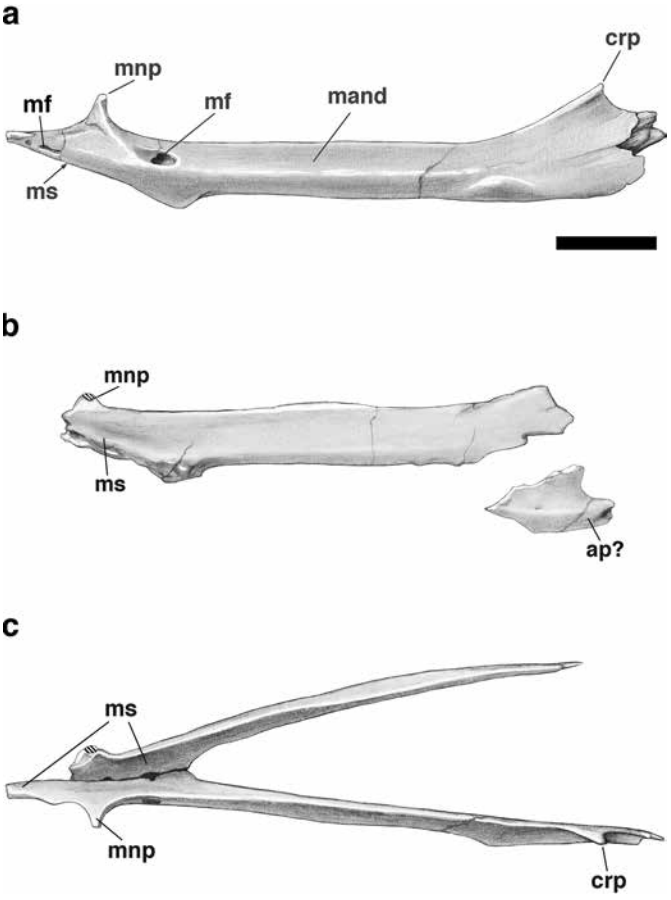

FIGURE 9. Mandible of *Patriomanis americana,* USNM-P 494439: (a) left mandible in lateral view; (b) right mandible in medial view; (c) left and right mandibles in occlusal view. Abbreviations: **ap,** angular process; **crp,** coronoid process; **mand,** mandible; **mf,** mental foramen; **mnp,** mandibular prong; **ms,** mandibular symphysis. Scale bar = 1 cm. Illustrations by Julia Morgan Scott for Smithsonian Institution.

horizontal ramus a short distance posterior to the anterolateral bony prong. The second, more anterior foramen typically perforates the base of the prong in extant forms, whereas in *Patriomanis* it is located well anterior and ventral to the prong, on the ventral surface of the symphysis. The morphology of the prong is itself unusual. In *Patriomanis* it arises from the dorsal edge of the symphysis, whereas in the extant manids it is separated by a groove from the dorsal rim and attaches much farther ventrally on the lateral sides of the symphysis. Finally, the symphysis itself is elongate with a straight ventral profile in lateral view in *Patriomanis* (Figure 9a). The symphysis is much shorter in *E. waldi, Eurotamandua,* and some individual specimens of the two species of African ground pangolins (*Smutsia*), and it has a convex profile in *E. waldi* and a concave profile in *M. javanica, M. pentadactyla*, and some specimens of *S. gigantea*.

Axial Skeleton: Vertebral Column

FIGURES 10–21; TABLES A2, A3

Atlas

Although not described by Emry (1970), a nearly complete atlas is available from the type specimen of *Patriomanis* (F:AM 78999; Figure 10a–c). The specimen is nearly complete ventrally but is missing the transverse processes laterally and the left anterior articular surface. It is also missing portions of the lamina, although the right side of the lamina is nearly complete. A second atlas is available from USNM-P 494439. It has not been prepared completely free of the matrix, but it preserves a complete transverse process and anterior articular facet on the left side (Figure 11).

In cranial view, the atlas is wider transversely than it is tall dorsoventrally (Table A2). This is the case in extant pangolins as well, although the discrepancy is somewhat less in the African forms. The dorsally bowed lamina is capped by a short, conical neural spine, whereas the ventral arch is nearly horizontal. As in other therian mammals (see, e.g., the early metatherian *Mayulestes*, Muizon, 1998; the early eutherian *Maelestes*, Wible et al., 2009; or the extant *Canis,* Evans and Christensen, 1979), the anterior articular facet for the occipital condyle is strongly concave dorsoventrally and faces strongly mediad and slightly craniad. The facet is broader dorsally than ventrally, taking on an inverted teardrop shape (Figure 10a). The left facet is widely separated ventrally from its counterpart on the right, the separation (~13 mm) equaling nearly 60% of the maximum width of the atlas (excluding the transverse process; Table A2). In *Smutsia, M. javanica,* and *M. crassicaudata,* this separation is much narrower, comprising less than 40% of the maximum atlas width (Gaudin et al., 2009). On its caudal surface, the atlas of *Patriomanis* bears a pair of posteromedially facing articular facets for the axis, situated at the intersection of the dorsal and ventral arches and the transverse process (Figure 10b). The surface contour of the facets is nearly flat, although in ventral view one can detect a slight transverse concavity. In outline, the facets take on the shape of a rounded equilateral triangle. The dorsolateral edge of this triangle forms a raised rim because of the presence of a short groove immediately anterior to this edge. The groove terminates

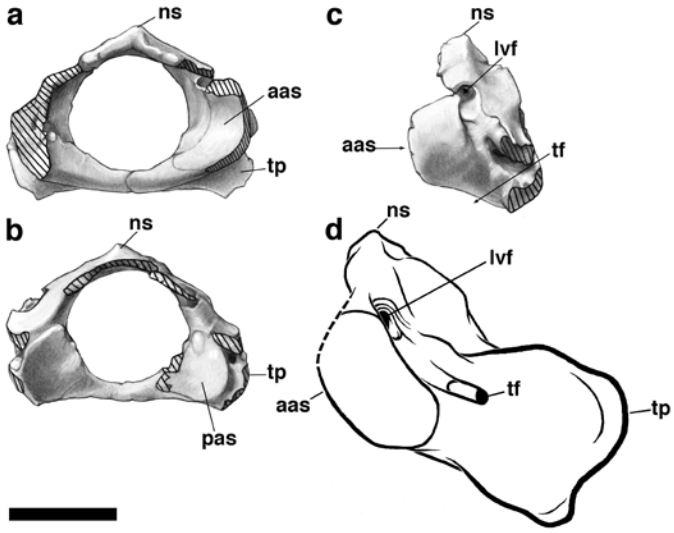

FIGURE 10. Atlas of *Patriomanis americana*: (a) atlas of F:AM 78999 (holotype) in anterior view; (b) in left lateral view; (c) in posterior view; (d) reconstruction of the atlas in left lateral view. Abbreviations: **aas,** anterior articular surface; **lvf,** lateral vertebral foramen; **ns,** neural spine; **pas,** posterior articular surface; **tf,** transverse foramen; **tp,** transverse process. Scale bar = 1 cm. Illustrations by Julia Morgan Scott for Smithsonian Institution.

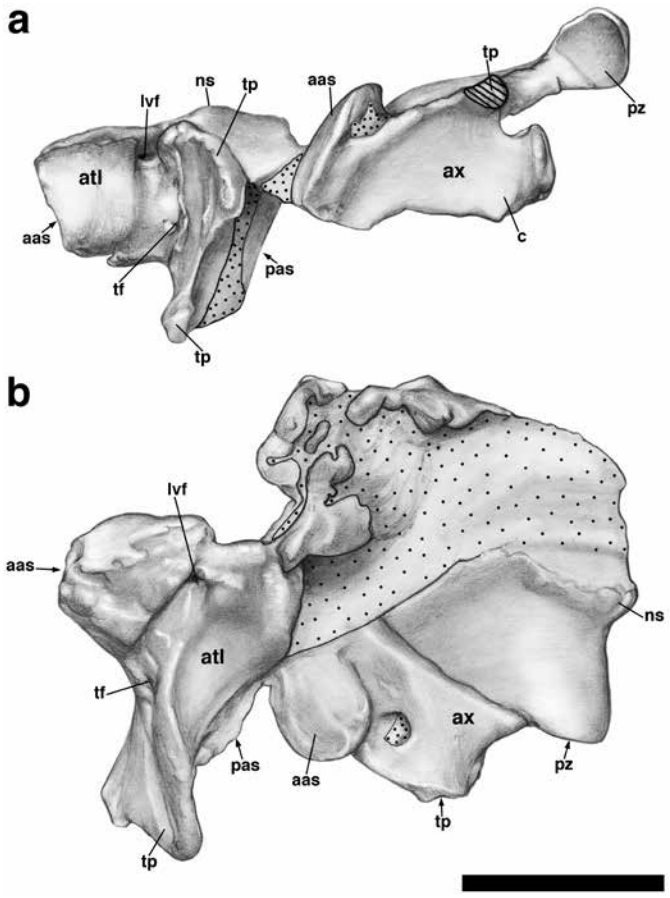

FIGURE 11. Atlas and axis of *Patriomanis americana,* USNM-P 494439: (a) axis in posterolateral view, axis in ventral view; (b) atlas in dorsal view, axis in dorsolateral view. Abbreviations: **aas,** anterior articular surface; **atl,** atlas; **ax,** axis; **c,** centrum; **lvf,** lateral vertebral foramen; **ns,** neural spine; **pas,** posterior articular surface; **pz,** posterior zygapophysis; **tf,** transverse foramen; **tp,** transverse process. Stippled areas represent matrix; the cross-hatched areas show broken surfaces. Scale bar = 1 cm. Illustrations by Julia Morgan Scott for Smithsonian Institution.

at the posterior opening to the transverse canal. The latter opening is thus situated at or near the lateral edge of the posterior articular facet, as in the extant *Phataginus* and *Smutsia,* whereas in *Manis* this opening is situated more medially, in a position dorsal to the midpoint of the facet.

In lateral view (Figure 10c), the height of the atlas is slightly greater than its anteroposterior length, as it is in most modern pangolin species except the two in the genus *Smutsia,* in which the atlas is anteroposteriorly elongated (Table A2). There is a prominent transverse process extending posterolaterally and slightly ventrad from the lateral surface of the bone in USNM-P 494439 (Figure 11). It extends at roughly a 30° angle from the lateral surface of the atlas in dorsal view and is flattened in a vertical plane, orthogonal to its long axis. From the side, it appears quite deep dorsoventrally, flaring toward its distal end before terminating in two rounded distal points. The process appears similarly deep in *Manis* (and variably so in *Phataginus*; see Gaudin et al., 2009), with *M. javanica* showing a distal bifurcation reminiscent of the condition in *Patriomanis*. The transverse process is flattened either anteroposteriorly or in a plane oblique to the anteroposterior axis in these modern taxa, giving it a deepened appearance in lateral view. In contrast, the transverse process of the atlas tends to be flattened dorsoventrally and expanded anteroposteriorly in *Eomanis* and *Smutsia* (Gaudin et al., 2009). The anterior opening of the transverse canal perforates the base of the transverse process, emptying into an open groove that travels anteriorly and dorsally onto the surface of the lamina, eventually reaching the lateral vertebral foramen. Although the latter seems to form only a partially closed foramen in the type (Figure 10), it is completely enclosed in bone in USNM-P 494439. In *Manis,* the groove connecting the transverse and lateral vertebral foramina is partially closed over by

a bridge of bone connecting the anteromedial edge of the transverse process to the lateral surface of the atlas (Gaudin et al., 2009). Such a bridge is also variably present in *Smutsia* and *Eomanis*, but *Phataginus* resembles the condition in *Patriomanis* (Gaudin et al., 2009).

In dorsal view, the lamina of the atlas appears to be relatively broad, with parallel anterior and posterior edges (Figure 11b). However, the middle portion of the posterior edge is missing, leaving open the possibility that there is some sort of notch or concavity in this area. *Patriomanis* lacks the prominent depressions anterolateral to the neural spine that are found in extant *Manis* and *S. gigantea* (Gaudin et al., 2009). These depressions likely house the origins of the m. rectus capitis dorsalis (see *Homo,* Pick and Howden, 1977; *Canis,* Evans and Christensen, 1979). *Patriomanis* also lacks any indication of an alar notch between the anterior edge of the transverse process and the lamina. Such a notch is evident in *Phataginus, M. crassicaudata,* and *S. temminckii* and is variably present in *S. gigantea*. The ventral arch, seen in ventral view, is narrower anteroposteriorly than the dorsal arch. It has a gently concave anterior margin, whereas the posterior margin is marked by a weak median spine flanked by lateral concavities. The ventral surface is otherwise unmarked.

Axis

Portions of the axis are preserved in all three of the most important specimens of *Patriomanis,* the type, F:AM 78999; USNM-P 494439; and USNM-P 299960. The centrum is preserved in both the type and in USNM-P 299960, but only USNM-P 494439 preserves any part of the neural arch. The partially prepared axis in this specimen preserves the posterior zygapophysis, the base of the transverse process, and portions of the neural spine. The axis of USNM-P 299960 is illustrated in Figure 12, and that of USNM-P 494439 is shown in Figure 11; these will largely serve as the basis for the following description.

The dens is reminiscent of that found in primitive therians (e.g., *Mayulestes,* Muizon, 1998; *Maelestes,* Wible et al., 2009). It is short and broad and thumb shaped in dorsal or ventral view, although slightly broader at its base than at its tip (Figure 12b). It bears a roughly triangular articular surface on its ventral surface that contacts a narrow corresponding surface on the floor of the atlantal vertebral canal. This facet abuts the anterior articular facets for the atlas along its posterolateralmost margins, resembling the condition in *Cryptomanis, Necromanis,* and most extant *Manis* (variably present in *M. pentadactyla*), whereas in the African pangolins the facet on the dens

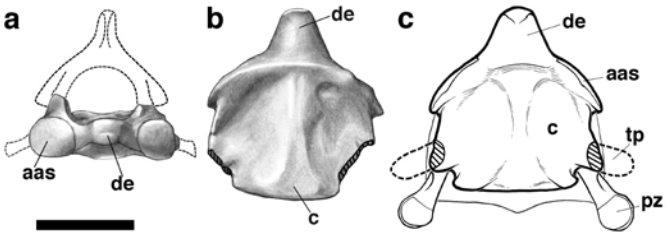

FIGURE 12. Axis of *Patriomanis americana*: (a) axis of USNM-P 299960 in anterior view (dorsal portion reconstructed on the basis of USNM-P 494439); (b) in ventral view; (c) reconstruction of the axis in ventral view. Abbreviations: **aas,** anterior articular surface; **c,** centrum; **de,** dens; **pz,** posterior zygapophysis; **tp,** transverse process. Cross-hatched areas represent broken surfaces. Scale bar = 1 cm. Illustrations by Julia Morgan Scott for Smithsonian Institution.

is completely separate from the anterior articular facets (Gaudin et al., 2009). In *Patriomanis*, the anterior articular facets are ovate, somewhat broader than they are tall, and have a slightly convex surface contour in both the transverse and dorsoventral planes (Figure 12a). The outline of these facets varies substantially among other pangolins. They are broader than tall in *Cryptomanis, Necromanis,* and *Manis,* whereas the maximum transverse width and maximum dorsoventral height are nearly equal in the extant African forms (Gaudin et al., 2009). The surface contour is transversely convex not only in *Patriomanis* but also in *Cryptomanis* and *Smutsia*. It is concave transversely in *Phataginus, M. javanica,* and *M. pentadactyla,* whereas in *Necromanis* and *M. crassicaudata,* it is convex medially and convex laterally; that is, it is largely convex but with a small concave depression immediately ventral and lateral to the dens (Gaudin et al., 2009).

The centrum is low and broad, as in other pangolins. In ventral view (Figure 12b), it is almost square, its transverse width nearly equal to its anteroposterior length. This shape resembles the condition in *Cryptomanis, Necromanis,* and *M. javanica* but stands in contrast to the condition in other extant manids, in which the centrum is wider than it is long, even when the dens is included in the length measurement (Gaudin et al., 2009; Table A2). The ventral surface of the centrum is marked by a prominent midline crest flanked by deep lateral excavations. The midline crest broadens posteriorly to form a raised triangular area. This kind of surface relief is missing in other pangolins with the exception of *Cryptomanis* and some *M. javanica* (Gaudin et al., 2009), in which the excavations tend to be weaker and more laterally situated and the midline crest is broader.

As noted above, the only specimen that preserves any portion of the neural arch is USNM-P 494439 (Figure 11). In this specimen the posterior zygapophysis is preserved in its entirety. Its surface faces ventrolaterally, and it is characterized by a concave surface contour like that of *P. tricuspis*. In contrast, the surface contour is convex in all other extant manids. Only the base of the transverse process and the base of the neural spine are present in USNM-P 494439, but there is enough of each process in place to demonstrate that the former extends posterolaterally from the neural arch and that the latter extends anteriorly to cover portions of the neural arch of the preceding atlas, as in most living pangolins (Gaudin et al., 2009).

Cervical Vertebrae (Exclusive of Atlas and Axis)

The remaining cervical vertebrae are poorly represented in the available material of *Patriomanis*. Only the type (F:AM 78999) and USNM-P 299960 preserve any of the cervicals other than the axis and atlas, and the former includes only fragments of these vertebrae, most notably a sizable fragment of C6 or C7 described and illustrated in Emry (1970). The latter specimen preserves what appears to be a nearly complete C4 or C5, along with two additional isolated cervical centra that likely represent C6 and C7 (Figures 1, 13). No complete cervical series is known for any fossil pangolin (Storch, 1978; Koenigswald and Martin, 1990; Storch and Martin, 1994; Gaudin et al., 2006). Although Storch (1978) states that the cervical count is "probably" seven in *Eomanis waldi*, it is difficult to tell from his illustrations of the type material, and indeed, in his reconstruction (Storch, 1978: plate 5, fig. 1) he illustrates only five or six cervicals. Nevertheless, given the near-universal presence of seven cervicals among modern mammals, including all eight species of modern pangolins, it is likely that *Patriomanis* (and the other fossil pangolin taxa) also possessed seven cervicals.

The cervical preserved in USNM-P 299960 (Figure 13) differs from that described by Emry (1970) in a number of respects. It is nearly complete bilaterally, unlike that from the type. The centrum is even more depressed, with rounded or squared off lateral edges, in contrast to the type, in which the lateral edge of the centrum appears to form a kind of lateral keel (Emry, 1970: fig. 11). The cervical centra in *Cryptomanis* are much wider and flatter than those of *Patriomanis,* which more closely resemble the condition in *Necromanis* and extant manids. The centrum in USNM-P 299960 is roughly the same relative length as that from the type. The neural arch bears a tall, vertical neural spine, a feature missing from the type. The transverse process is broken on both sides but is more complete on the left, missing roughly the distal half of the process. On both sides, the base of the transverse process is clearly perforated by a transverse foramen for the vertebral artery. The lack of a transverse foramen in the type specimen might be used to confirm its identity as a seventh cervical, although it should be noted that in all modern manids, the transverse foramen is present in C7 (Gaudin et al., 2007). The transverse process attaches to the side of the centrum and the base of the pedicle, in contrast to that of the type, in which it is attached more dorsally, at the junction of the pedicle and lamina. Furthermore, the shape and orientation of the transverse process are quite different in the two specimens. In the type it is directed dorsolaterally (in anterior view)

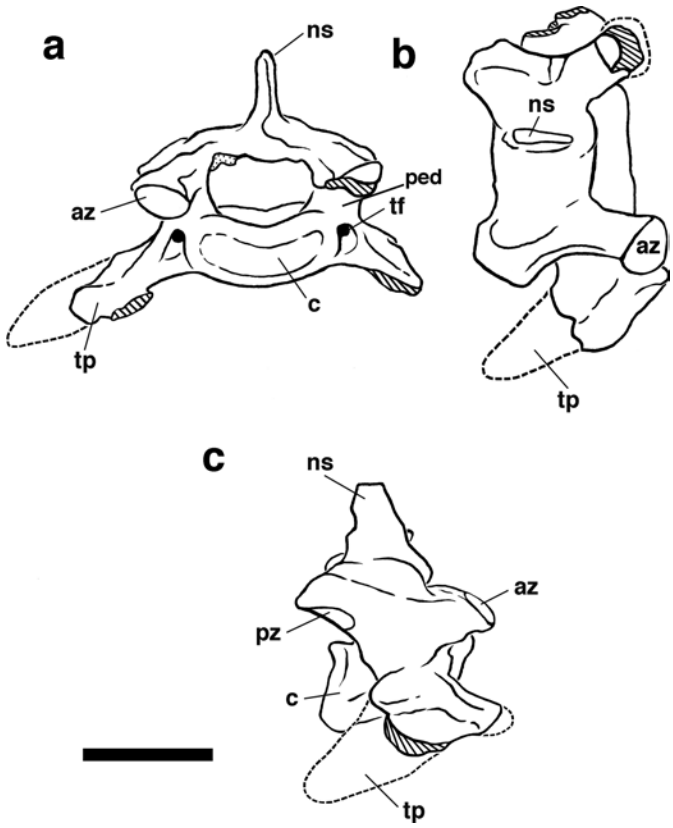

FIGURE 13. Cervical vertebra (C4 or C5?) of *Patriomanis americana,* USNM-P 299960: (a) in anterior view; (b) in dorsal view; (c) in right lateral view. Abbreviations: **az,** anterior zygapophysis; **c,** centrum; **ns,** neural spine; **ped,** pedicle; **pz,** posterior zygapophysis; **tf,** transverse foramen; **tp,** transverse process. Stippled areas represent matrix; the cross-hatched areas show broken surfaces. Scale bar = 1 cm. Illustrations by Julia Morgan Scott for Smithsonian Institution.

and is cylindrical in cross section. In USNM-P 299960, it is oriented ventrolaterally (in anterior view); it is dorsoventrally compressed and anteroposteriorly expanded. In dorsal view it has anterior and posterior extensions proximally, and the distal end is likely oriented posterolaterally (Figure 13). Both types of extensions are also present in most cervicals in living manids.

In extant pangolins and in *Cryptomanis* (but not in *Necromanis*; Gaudin et al., 2009) the processes that bear the anterior and posterior zygapophyseal articulations extend far anterior and posterior to the centra of their corresponding vertebra (Gaudin et al., 2009). The anterior processes, for example, typically extend to roughly one-third the length of the preceding centrum. The processes in *Patriomanis* are much shorter, extending only slightly beyond the margins of the centra in lateral view (Figure 13c). The anterior zygapophyseal facet in USNM-P 299960 is preserved only on the left side of the vertebra. It is egg shaped in outline, narrowing medially (Figure 13b), and faces dorsomedially (Figure 13a). The surface contour is almost flat (slightly convex), with the posterior zygapophyseal facet lacking even this slight curvature and facing ventrolaterally. Emry (1970) describes a similar surface contour for the zygapophyseal facets in the more posterior cervical preserved in the type specimen (F:AM 78999), but the orientation of the facets differs, with the posterior facet roughly horizontal and the anterior facet facing "outward and upward" (Emry, 1970:472). In extant pangolins, *Cryptomanis, Eomanis,* and *Euromanis*, the anterior zygapophyseal facets are usually concave, and the posterior zygapophyseal facets are convex, with an orientation similar to that of USNM-P 299960. In *Necromanis* the zygapophyseal facets are flatter, as in *Patriomanis* (Gaudin et al., 2009).

Thoracic Vertebrae

Emry (1970) described only one fragment of a posterior thoracic vertebra (= "dorsal" vertebra) from the type specimen (F:AM 78999). However, as reported in a footnote from that work, additional thoracics were later recovered, including parts of an anterior thoracic with a partial centrum, three thoracics still in articulation with one another and their corresponding ribs, and three other posterior thoracics. USNM-P 494439 preserves more thoracics, including the ultimate and penultimate still in articulation with the lumbar vertebrae but not fully prepared free of the matrix, as well as four free thoracics and perhaps one or two isolated thoracics still mostly embedded in matrix. The most complete thoracic series derives from USNM-P 299960, which preserves at least 13 fragmentary to nearly complete thoracic vertebrae from the anterior, middle, and posterior parts of the series (Figure 1). We have illustrated a representative, fairly complete thoracic vertebra from each of these regions in Figures 14 (anterior view), 15 (dorsal view), and 16 (lateral view). In our reconstruction (Figure 1), we estimate that at least 15 thoracic vertebrae were present in *Patriomanis,* which accords

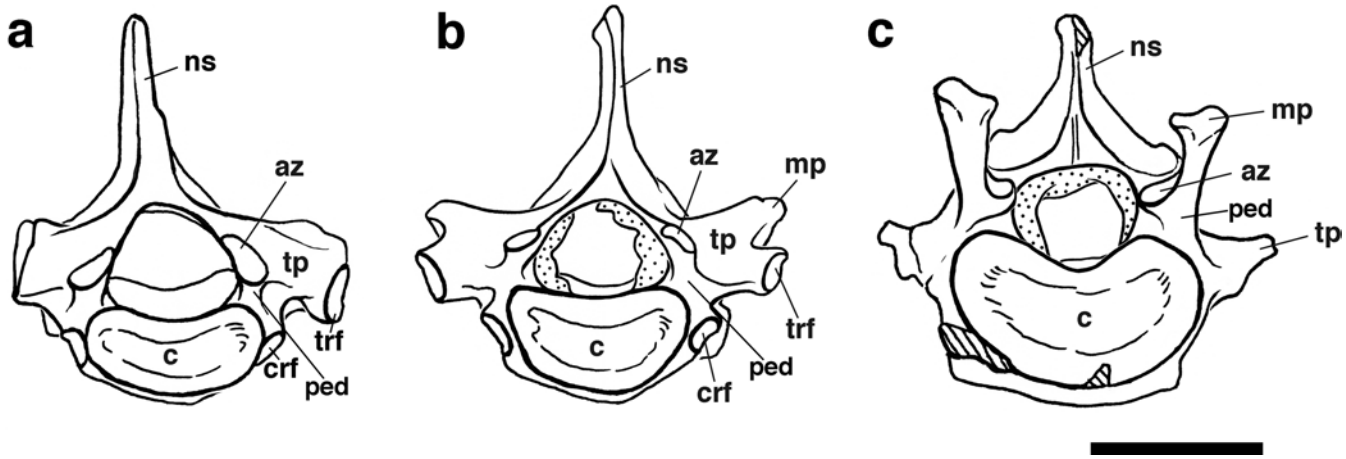

FIGURE 14. Thoracic vertebrae of *Patriomanis americana,* USNM-P 299960, in anterior view: (a) anterior thoracic (T4 or T5?) vertebra; (b) middle thoracic vertebra; (c) postdiaphragmatic thoracic vertebra. Abbreviations: **az,** anterior zygapophysis; **c,** centrum; **crf,** capitular rib facet; **mp,** metapophysis; **ns,** neural spine; **ped,** pedicle; **tp,** transverse process; **trf,** tubercular rib facet. Stippled areas represent matrix; the cross-hatched areas show broken surfaces. Scale bar = 1 cm. Illustrations by Julia Morgan Scott for Smithsonian Institution.

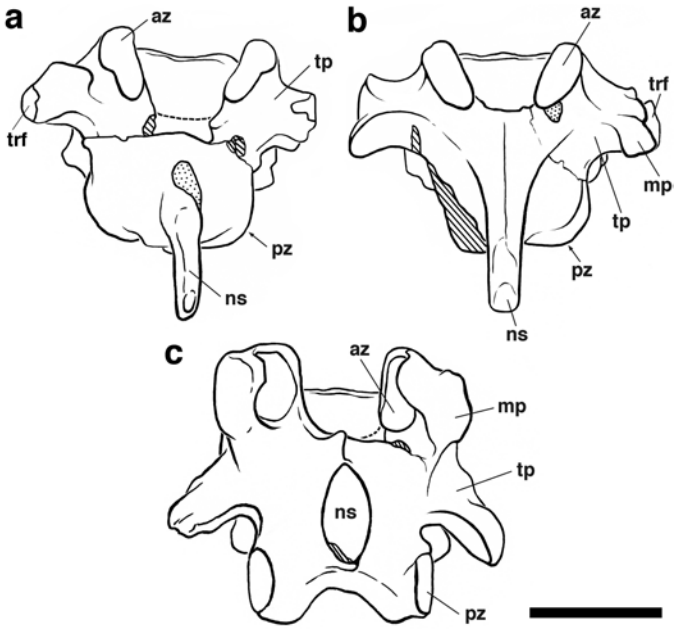

FIGURE 15. Thoracic vertebrae of *Patriomanis americana*, USNM-P 299960, in dorsal view: (a) anterior thoracic (T4 or T5?) vertebra; (b) middle thoracic vertebra; (c) postdiaphragmatic thoracic vertebra. Abbreviations: **az,** anterior zygapophysis; **mp,** metapophysis; **ns,** neural spine; **pz,** posterior zygapophysis; **tp,** transverse process; **trf,** tubercular rib facet. Stippled areas represent matrix; the cross-hatched areas show broken surfaces. Scale bar = 1 cm. Illustrations by Julia Morgan Scott for Smithsonian Institution.

well with the condition in most modern pangolin species, which have between 14 and 16 thoracics, although some *Phataginus tetradactyla* have only 13 and *Smutsia temminckii* has only 11 (Gaudin et al., 2009). *Eomanis waldi* has 13 thoracics (Storch, 1978, asserts there are 12, but better preserved specimens recovered subsequently show the presence of an extra vertebra; Gaudin et al., 2009), but only 12 are preserved in *Euromanis krebsi* (Storch and Martin, 1994; Gaudin et al., 2009).

As is evident in the reconstruction (Figure 1), the neural spines of the thoracic vertebrae are fairly uniform in height, although in the more anterior thoracics the spines are slightly longer and less broad anteroposteriorly (Figure 16). This condition also characterizes modern and extinct pangolins, with the exception of *Eomanis* and *Euromanis* (Gaudin et al., 2009). The distal tips of the spines take the form of a flat, anteroposteriorly elongate lenticular surface, especially in the more posterior vertebrae (Figures 15, 16). The neural spines are posterodorsally inclined in the anterior thoracics and nearly vertical in the posterior thoracics, but there is no real anticlinal vertebra, which is often present in other placental mammals (Slijper, 1946; for a classic example, see *Canis* in Evans and Christiansen, 1979). An anticlinal vertebra is present in the Asian pangolins *Manis javanica* and *M. crassicaudata* but is not in evidence in other extant forms or in *Eomanis* or *Euromanis*. The diaphragmatic vertebra is not preserved in *Patriomanis*, so

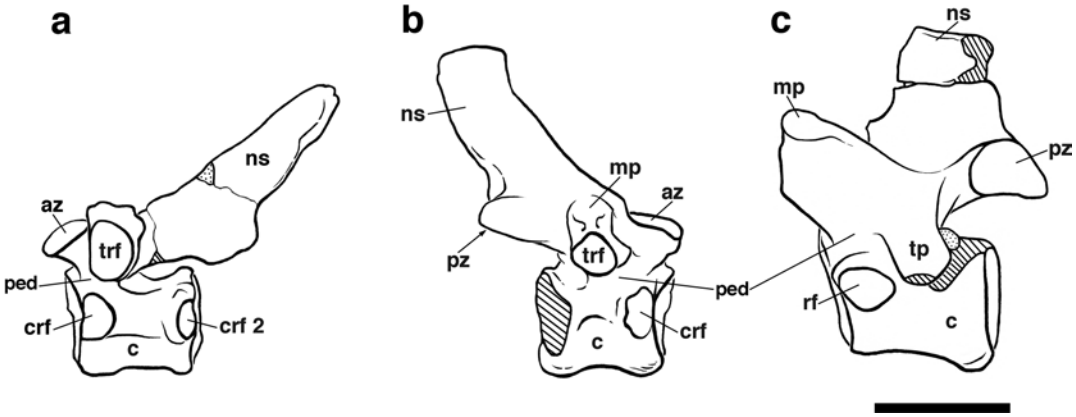

FIGURE 16. Thoracic vertebrae of *Patriomanis americana*, USNM-P 299960, in lateral view: (a) anterior thoracic (T4 or T5?) vertebra in left lateral view; (b) middle thoracic vertebra in right lateral view; (c) postdiaphragmatic thoracic vertebra in left lateral view. Abbreviations: **az,** anterior zygapophysis; **c,** centrum; **crf,** capitular rib facet; **crf 2,** second posterior capitular rib facet; **mp,** metapophysis; **ns,** neural spine; **ped,** pedicle; **pz,** posterior zygapophysis; **rf,** rib facet; **tp,** transverse process; **trf,** tubercular rib facet. Stippled areas represent matrix; the cross-hatched areas show broken surfaces. Scale bar = 1 cm. Illustrations by Julia Morgan Scott for Smithsonian Institution.

its position relative to that in other pholidotans cannot be ascertained, although it is clear from USNM-P 494439 that there are at least two thoracics behind the diaphragmatic vertebra. In all other pholidotans, the diaphragmatic vertebra is in the posterior part of the thoracic series, with two to three postdiaphragmatic thoracics in the extant taxa (Gaudin et al., 2006, 2009) and three in *Cryptomanis* (Gaudin et al., 2006), *Eomanis,* and *Euromanis* (Gaudin et al., 2009). It should be noted that the specific vertebra involved may vary among extant forms, even within species, and the diaphragmatic transition (i.e., the transition from horizontal, thoracic-type zygapophyses ["tangential" in terminology of O'Leary et al., 2013] to more upright, lumbar-type zygapophyses ["centric" in terminology of O'Leary et al., 2013]) may involve two vertebrae in some individuals (Gaudin et al., 2009).

The pedicles of the thoracic vertebrae are low and relatively narrow anteroposteriorly in the anterior thoracic vertebrae, becoming anteroposteriorly broader in more posterior thoracics (Figure 16). When viewed dorsally, the thoracic laminae are roughly rectangular in shape, broad transversely but even longer in their anteroposterior dimensions (Figure 15). As noted above, the zygapophyseal facets have a tangential orientation in the anterior thoracics; that is, they are approximately horizontal and parallel to the surface of the laminae, although with a slight dorsomedial to ventrolateral slant. The facets are flat and ovate in outline, with the long axes of the anterior facets running posteromedial to anterolateral. Consonant with Emry's (1970) observations on the type specimen, the zygapophyseal facets of the postdiaphragmatic thoracic vertebrae in *Patriomanis* begin to take on the "enrolled" or "embracing" morphology so typical of pangolins (Frechkop, 1949; Rose et al., 2005; Gaudin et al., 2006, 2009), with strongly concave anterior facets contacting the cylindrical posterior facets ventrally and laterally and barely overlapping their dorsal surfaces (Figures 14–16). *Euromanis* and *Eomanis* are the only pangolins, living or extinct, to lack these enrolled zygapophyses (Rose et al., 2005; Gaudin et al., 2009).

The anteriormost thoracic vertebra illustrated (probably T4 or T5; Figures 14a, 15a, and 16a) bears a robust diapophysis (= dorsally situated transverse process bearing an articular facet for the tubercle of the rib; see Homberger and Walker, 2004) extending laterally from the junction of the lamina and pedicle. It is marked distally by an oval, concave facet for the rib tubercle. A small ridge extends dorsal to the tubercular facet that represents a rudimentary metapophysis (= mammillary process of Homberger and Walker, 2004). The diapophysis of the midthoracic vertebra illustrated (Figures 14b, 15b, and16b) has a smaller tubercular facet but is attached to a much larger, more distinct metapophysis. In the postdiaphragmatic thoracic vertebra illustrated (Figures 14c, 15c, and 16c), the diapophysis is low, extending laterally and somewhat posteriorly from the side of the pedicle rather than the junction of the pedicle and lamina. It has also lost its association with the metapophysis, which is instead attached to the zygapophysis. Indeed, apart from the small tubercle extending dorsolaterally from the top of the zygapophyseal facet, which pertains solely to the metapophysis, it is not clear how much of the large process forming the lateral wall to this facet is composed of metapophysis and how much is composed of zygapophysis (the same could be said for many, if not most, therian mammals). It should be noted that the aforementioned "small tubercle" is apparently the broken remnant of a much larger, distally squared off metapophysis that extends a fair distance dorsally and laterally away from the zygapophyseal facet. The metapophyses are preserved in their entirety in the penultimate and ultimate thoracic vertebrae of USNM-P 494439. The disposition of these processes in *Patriomanis* is similar to that in other pangolins, as regards the separation of diapophysis and metapophysis in the posterior thoracic vertebrae. Although metapophyses are not well developed in the Messel pangolins or in extant *Manis* except for the posteriormost thoracics, they extend nearly to the front of the thoracic series in *Cryptomanis* and *Smutsia* and to the middle of the series in *Phataginus*.

The thoracic centra have a reniform cross section, with a dorsal depression for the capacious vertebral canal. The centra in the anterior thoracics are more depressed dorsoventrally and shorter anteroposteriorly and become progressively longer and deeper in more posterior thoracic vertebrae (Figures 14, 16), although the transverse dimension is the greatest in all (Table A3). As is evident in Table A3, the dimensions of the thoracic centra are very similar in *Patriomanis* and other extinct and extant pangolins, with the exception of the African tree pangolins (*Phataginus*), in which the centra are somewhat longer anteroposteriorly. The typical thoracic centrum bears part of two capitular facets for the heads of corresponding ribs, an anterior facet on the anterior dorsolateral margin of the centrum and a second on the posterior dorsolateral edge. However, in the more posterior centra, the posterior facet is lost, and the rib articulates entirely on one centrum rather than between two adjacent centra. It is unclear where this transition takes place, although in both USNM-P 299960 and 494439 there are at least two vertebrae with a single capitular facet. This is also the case in *Cryptomanis,* whereas in modern pangolins there may be

one (*Smutsia*), two (*Manis*), or three (*Phataginus*) thoracic centra with a single capitular facet.

Lumbar Vertebrae

The type specimen (F:AM 78999) preserves but a single fragment of vertebral arch from the lumbar series (Emry, 1970). USNM-P 494439 preserves six lumbar vertebrae in series, including the first lumbar, and USNM-P 299960 also preserves at least six, including the last two, both of which are well preserved and illustrated in Figures 17–19. We estimate *Patriomanis* had seven lumbar vertebrae, which matches the count from the other patriomanid genus *Cryptomanis* (Gaudin et al., 2006), whereas the older taxa *Euromanis* and *Eomanis* have only six lumbars each (Storch and Martin, 1994; Gaudin et al., 2009), as do most modern manids, with the exception of *Smutsia gigantea* and some *Phataginus tetradactyla*, which have only five (Gaudin et al., 2009).

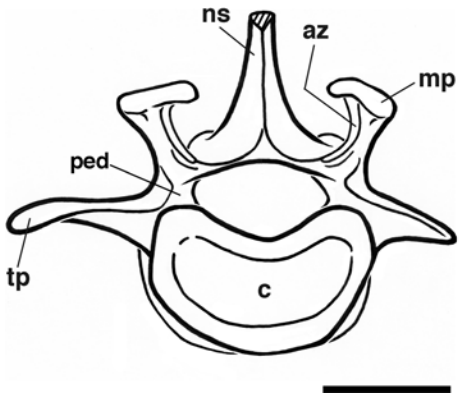

FIGURE 17. Penultimate lumbar vertebra (L6) of *Patriomanis americana,* USNM-P 299960, in anterior view. Abbreviations: **az,** anterior zygapophysis; **c,** centrum; **mp,** metapophysis; **ns,** neural spine; **ped,** pedicle; **tp,** transverse process. Scale bar = 1 cm. Illustration by Julia Morgan Scott for Smithsonian Institution.

The neural spines of the lumbar vertebrae are essentially upright, with their height roughly one and a half times their anteroposterior length (Figure 19; Table A3) and a flat, lenticular dorsal surface (Figure 18). The spines are roughly equivalent in height throughout the series. The lumbar neural spines exhibit similar dimensions in *Smutsia gigantea* and *Eomanis*. They are somewhat taller in *S. temminckii* and *Cryptomanis* and somewhat shorter in extant *Manis*, and in *Phataginus* the length of the neural spines actually exceeds their height (Table A3; Gaudin et al., 2009). The laminae and pedicles of the lumbar vertebrae are much like those described above for the posterior thoracics, the laminae broad and rectangular, the pedicles low and anteroposteriorly elongate. The posterior attachment of the pedicles is located well anterior to the posterior edge of the centrum and ventrolateral to the dorsal edge of the centrum. It is separated from the posterodorsolateral corner of the centrum by a deep groove for the spinal nerve (Figure 19b). This groove was first described in *Cryptomanis* (Gaudin et al., 2006) and is also present in *Necromanis* (Gaudin et al., 2009), but the condition is unknown in either *Eomanis* or *Euromanis* and is clearly absent in living pangolins (Gaudin et al., 2009).

Like the posterior thoracic vertebrae, the lumbar vertebrae bear large metapophyseal–zygapophyseal processes

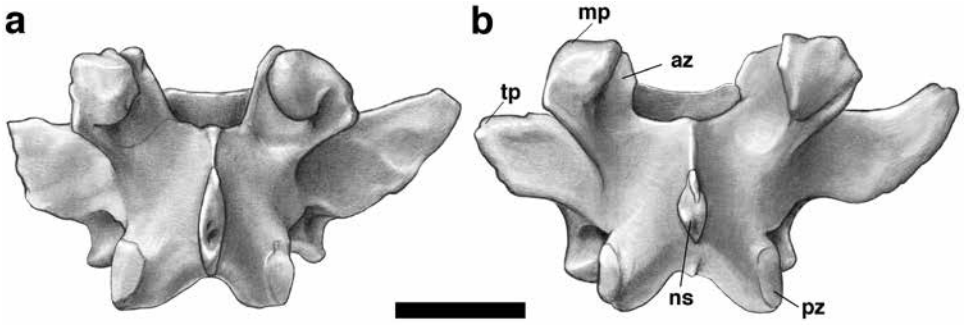

FIGURE 18. Lumbar vertebrae of *Patriomanis americana,* USNM-P 299960, in dorsal view: (a) penultimate vertebra (L6); (b) last lumbar vertebra (L7). Abbreviations: **az,** anterior zygapophysis; **mp,** metapophysis; **ns,** neural spine; **pz,** posterior zygapophysis; **tp,** transverse process. Scale bar = 1 cm. Illustrations by Julia Morgan Scott for Smithsonian Institution.

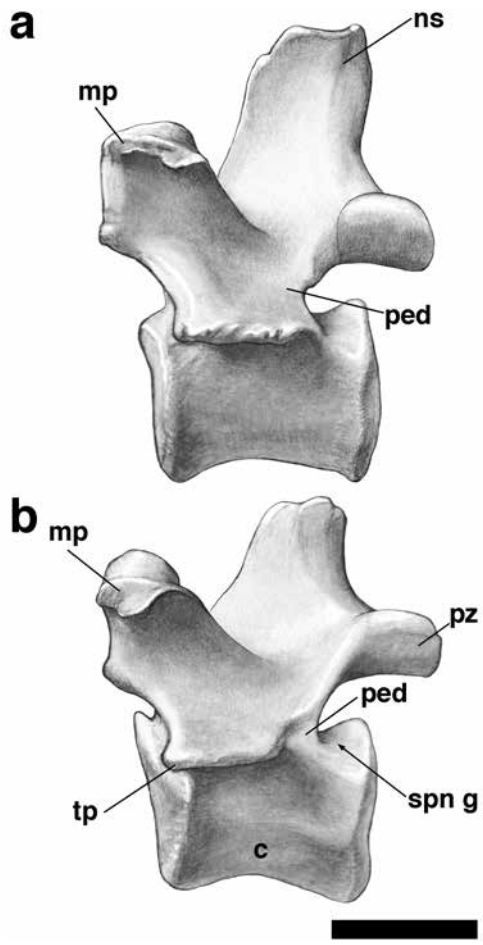

FIGURE 19. Lumbar vertebrae of *Patriomanis americana,* USNM-P 299960, in left lateral view: (a) penultimate vertebra (L6); (b) last lumbar vertebra (L7). Abbreviations: **c,** centrum; **mp,** metapophysis; **ns,** neural spine; **ped,** pedicle; **pz,** posterior zygapophysis; **spn g,** groove for spinal nerve; **tp,** transverse process. Scale bar = 1 cm. Illustrations by Julia Morgan Scott for Smithsonian Institution.

extending anterodorsally and slightly laterally from the anterior half of the laminae. These processes form the lateral margins to the strongly enrolled or embracing anterior zygapophyses, which contact the cylindrical posterior zygapophyses along their ventral, lateral, and dorsal surfaces. The illustrated lumbar vertebrae from USNM-P 299960 (Figures 17–19) lack large free-standing metapophyses extending beyond the zygapophyseal facets, carrying only short, laterally directed tubercles, but these are evidently broken remnants of larger processes. The lumbar metapophyses of USNM-P 494439 are like those described above for the posterior thoracics, extending a considerable distance dorsally and laterally, ending in squared distal tips. These metapophyses reach a height roughly one-half the height of the neural spines. The metapophyses are much shorter in *Eomanis* and *Euromanis* and somewhat taller in modern pangolins, in which they are nearly two-thirds the height of the neural spines. The transverse processes in the lumbar vertebrae represent pleurapophyses, that is, fused lumbar ribs (Homberger and Walker, 2004). They extend laterally from the junction between the pedicle and centrum (Figures 17, 19). In dorsal view, the transverse processes are wing shaped, with a straight to slightly concave anterior border and a convex posterior margin, and they are directed laterally and somewhat anteriorly (Figure 18). This morphology is generally similar to that found in *Manis javanica*, although in some individuals of this species the anterior lumbar transverse processes are oriented more directly lateral in dorsal view, as is typically the case in *M. crassicaudata,* both species of *Phataginus, Smutsia temminckii,* and some individuals of *S. gigantea* (Gaudin et al., 2009). In some *S. gigantea*, these anterior transverse processes are actually directed posterolaterally, a condition apparently also present in *Cryptomanis*, judging from the preserved bases of the lumbar transverse processes. Although the last lumbar transverse process of *Patriomanis* is slightly shorter than that of the preceding vertebra, this extinct genus lacks the dramatic reduction of the last lumbar transverse process in modern pangolins, in which it may be greatly shortened in length (some *M. javanica* and *P. tricuspis*), anteroposterior breadth (*S. temminckii, P. tetradactyla,* some *S. gigantea,* and *P. tricuspis*), or even reduced to a small, rodlike element (*M. crassicaudata, M. pentadactyla,* and some *S. gigantea*; Gaudin et al., 2009).

The lumbar centra resemble those of the posterior thoracic vertebrae described above, although they are larger than the thoracic centra. They are wide and low, with a reniform cross section (Figure 17) indented dorsally by the transversely ovate vertebral canal. In *Patriomanis*, as in *Necromanis, Cryptomanis,* and some extant taxa (*M. crassicaudata, M. pentadactyla,* and *S. gigantea*), the anteroposterior length of the centra exceeds the dorsoventral depth by roughly a third (Table A3), whereas in other extant taxa (*M. javanica, S. temminckii,* and both species of *Phataginus*) the centra are more elongated, their length exceeding their depth by at least 1.5- fold.

Note that the sacral vertebrae are described with the pelvis below.

Caudal Vertebrae

Emry (1970) describes three caudal centra from the type specimen (F:AM 78999). In actuality, the type specimen includes at least four additional caudal vertebrae,

including one nearly complete anterior caudal and a partial caudal from the posterior part of the series. However, two other specimens have a much more complete caudal sequence. USNM-P 494439 preserves at least parts of 27 caudal vertebrae, with nearly 20 in series from the middle toward the anterior part of the sequence. We estimate this specimen had at least 31 caudals. USNM-P 299960 preserves 28, with nine complete caudal vertebrae clustered mostly anteriorly and many of the remainder comprising only centra or even partial centra, particularly toward the posterior end of the tail. The first five caudal vertebrae are present in sequence, separated by a gap from a more posterior sequence of six, with another gap separating a more posterior sequence of seven, a still more posterior sequence of eight following another gap, a couple more posterior caudals partially preserved, and the last few caudals likely missing. The specimen also preserves four or five partial chevron bones. We estimate that USNM-P 299960 had at least 34 caudals (despite the fact that only 31 are reconstructed in Figure 1, which also does not match exactly the sequence of gaps described above) and perhaps as many as 36. This many caudal vertebrae would mean that *Patriomanis* had a tail nearly as long as the extant African tree pangolins, which include the species with the largest number of caudals known for any extant mammal, *Phataginus tetradactyla*, with 47–49 caudal vertebrae (Flower, 1885; Gaudin, unpublished data), and a second species, *P. tricuspis*, with 35–39 caudals (Gaudin, unpublished data). In the other living pangolins, the number of caudals ranges from 24 to 29 (Flower, 1885; Gaudin et al., 2009; Gaudin, unpublished data; Flower, 1885, reports that some *M. javanica* have 30 caudal vertebrae). Gaudin et al. (2006) report 17 preserved caudals in the other patriomanid genus, *Cryptomanis*, but the series is much less complete in this specimen than in *Patriomanis,* and the actual number of caudals is hard to estimate. The tail is even less completely known in *Necromanis* (Koenigswald and Martin, 1990). The tail in *Eomanis waldi* is well preserved, with between 21 and 24 caudal vertebrae (Storch, 1978; Gaudin, unpublished data), but these are much shorter in the anteroposterior dimension than in the caudal vertebrae of other pholidotans, leaving this taxon with the shortest tail among known pangolins.

The anterior caudal vertebrae are reminiscent of the lumbars in many respects. The neural spines are tall, vertical, and broad anteroposteriorly, but with a rounded rather than a flat terminus. After Ca4 the neural spines become notably shorter and more posteriorly inclined. The wide, rectangular laminae support embracing zygapophyses like those of the lumbar vertebrae, the zygapophyseal processes themselves separated by deep U-shaped or V-shaped notches in dorsal view (Figure 20a). These enrolled zygapophyses are present in at least the first five caudals of USNM-P 299960. In modern manids, they are present in the anterior one-quarter to one-half of the caudal vertebrae (Gaudin, unpublished data), whereas in *Cryptomanis* they are known to be present in the first five caudals (Gaudin et al., 2006). The pedicles in the *Patriomanis* caudals are considerably lower than those in the lumbar vertebrae, and the vertebral canal is correspondingly smaller. The freestanding portions of the metapophyses are lower than in the lumbar vertebrae, leaving the neural spine much higher than the metapophyses, in contrast to the anterior caudals of modern manids, where the low neural spine is roughly the same height as the metapophyses. The centrum is shaped much as in the lumbar vertebrae, although as Emry (1970) noted, the centrum is roughly as wide as it is long (in fact, width slightly exceeds length in Ca1 from USNM-P 299960), and it bears blunt ventral articular processes for the chevron bones. These processes are paired, are situated at the anterior and posterior margins of the centra, and are connected to one another by a pair of longitudinal crests that cross the ventral surface of the centrum (Emry, 1970: fig. 13).

The primary difference between the lumbar vertebrae and anterior caudals, however, is the presence in the latter of greatly elongated transverse processes. As illustrated in Rose and Emry (1993: fig. 7.4) and our skeletal reconstruction (Figure 1), the tips of the caudal transverse processes actually extend laterally to a point even with the dorsal edge of the ischium. These processes are even broader in *Manis* (e.g., *M. javanica*, USNM 198852) and *Smutsia* (e.g., *S. temminckii*, AMMH 168955), extending well lateral to the ischium, whereas in *Phataginus* (e.g., *P. tricuspis*, CM 16206), they are large but do not extend to the lateral edge of the ischium (Gaudin et al., 2009). The transverse processes of the anterior caudal vertebrae are even smaller in *Eomanis* (e.g., SMF MEA 263) and *Euromanis* (Storch and Martin, 1994). The first caudal of *Patriomanis* has a thick, rectangular transverse process with a muscular fossa extending along its anterior edge for much of its length, ending laterally in a muscular boss (Figure 20a). It is oriented laterally and slightly posterior, with a straight or slightly convex distal edge that slants anterodorsolaterally. In succeeding vertebrae, the transverse processes become progressively narrower both mediolaterally and anteroposteriorly and have rounded (Ca2) or tapered tips (Ca3; Figure 1).

The caudal vertebrae from the middle of the caudal series differ strongly from the more anterior elements.

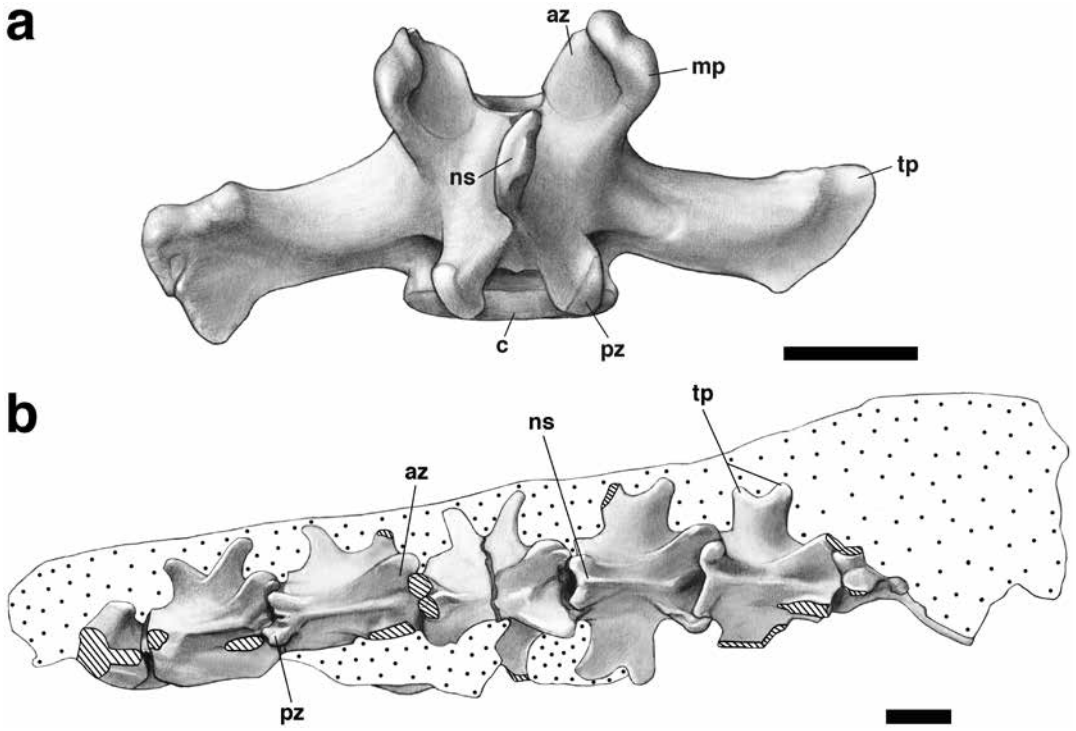

FIGURE 20. Caudal vertebrae of *Patriomanis americana*: (a) first caudal of USNM-P 299960 in dorsal view; (b) middle caudals of USNM-P 494439 in dorsal view, anterior toward right. Abbreviations: **az,** anterior zygapophysis; **c,** centrum; **mp,** metapophysis; **ns,** neural spine; **pz,** posterior zygapophysis; **tp,** transverse process. Stippled areas represent matrix; the cross-hatched areas show broken surfaces. Scale bars = 1 cm. Illustrations by Julia Morgan Scott for Smithsonian Institution.

The vertebral centra take on a cylindrical shape, as noted by Emry (1970), losing their reniform cross section and becoming more elongated, such that anteroposterior length is roughly one and a half to two times centrum transverse width, which is, in turn, roughly equal to centrum depth. The neural spines, although incomplete, are clearly much smaller than those from the more anterior caudals (Emry, 1970), with their bases restricted to the posterior half of the laminae. Although strong zygapophyses persist and form synovial joints at least through the midpoint of the tail (e.g., they are present in 16 of 27 preserved vertebrae in USNM-P 494439), they no longer possess the enrolled morphology, forming nearly flat surfaces facing dorsomedially in the case of the anterior zygapophyses and ventrolaterally in the smaller posterior zygapophyses (Figure 20b). Similar changes in centrum shape and zygapophyseal articulations are evident in modern pangolins.

The most striking feature of the mid-caudals in *Patriomanis* is the presence of double transverse processes. In USNM-P 299960 the twinned transverse processes begin in the 17th of 27 preserved vertebrae and are present in the next 7 preserved caudals (this section almost certainly incorporates a gap of at least 2 caudals), whereas in USNM-P 494439 the double processes begin with the 8th preserved caudal and include 14 more preserved caudals, including 11 consecutive vertebrae. In the more anterior examples, the transverse processes are anteroposteriorly broad, almost platelike, and diverge into separate processes only at the tips, but in more posterior vertebrae the transverse processes are deeply divided into two triangular, distally tapering and slightly recurved processes (Figure 20b). Double transverse processes have been noted in the two other patriomanid genera. In *Cryptomanis* the tips of the processes are broken, but a distinct gap can be seen between the bases of the doubled processes in at least one vertebra (Gaudin et al., 2006: fig. 5B). Double transverse processes have been described but not illustrated in one of the few preserved caudals of *Necromanis* (Storch

and Martin, 1994). Storch (1978) describes and illustrates divided transverse processes on at least one caudal vertebra in *Eomanis*, but they are considerably shorter than those in *Patriomanis* and do not appear to be present in other *Eomanis* caudals, although several succeeding vertebrae do have strongly hourglass-shaped centra.

Double transverse processes very similar to those of *Patriomanis* are present in semiarboreal or arboreal vermilinguan anteaters, in which they have been associated with the presence of a prehensile tail (Hirschfeld, 1976; Gaudin and Branham, 1998). Such twinned transverse processes are not found, however, in other mammalian taxa with prehensile tails (Argot, 2003; Youlatos, 2003; Organ, 2010), nor are they present in modern pangolins with prehensile tails, that is, in the African tree pangolins in the genus *Phataginus* (Gaudin et al., 2006), or in the scansorial pangolins of the genus *Manis* (Gaudin, unpublished data). Double processes are also known to occur on the caudals of semiaquatic mammals (e.g., pantolestids [Rose and Koenigswald, 2005], beavers, otters, and aquatic sloths [Muizon and McDonald, 1995]).

The posteriormost caudal vertebrae in modern pangolins are quite robust. Robust transverse processes (single, not double) extend nearly to the very tip of the tail; for example, in *M. javanica* USNM 198852 they are found in 28 of 29 vertebrae, in *Phataginus tetradactyla* USNM 481406 they are present in 46 of 49 vertebrae, and in *Smutsia gigantea* AMNH 53848 they are present in all 27 caudal vertebrae (there are actually double transverse processes found only on Ca27). Similarly, chevron articulations are found almost all the way to the tip of the tail: to Ca23/24 in *M. javanica* USNM 198852, to Ca44/45 in *Phataginus tetradactyla* USNM 481406, and to Ca25 in *Smutsia gigantea* AMNH 53848. The centra of these vertebrae are cylindrical like those of the mid-caudals but become not only smaller but also somewhat more dorsoventrally compressed posteriorly, and of course, they lose progressively their neural spines and zygapophyseal articulations. The zygapophyseal processes themselves persist, the posterior disappearing first; for example, in *Phataginus tricuspis* CM 16206, the last vestiges of the posterior zygapophyses are lost on the 36th of 37 preserved caudal vertebrae (the specimen is likely missing the last one or two caudals), whereas there are very small vestiges of the anterior zygapophyses on Ca37. The terminal caudals present in *Patriomanis,* as noted above, are the least well preserved, and many lack complete centra (Figure 21a). As in *Patriomanis*'s living relatives, the centra become smaller and somewhat more depressed posteriorly, the neural spines and vertebral canals disappear, and the zygapophyses are nonfunctional and reduced, the anterior being more robust and persisting farther posteriorly. They also retain ventral bosses or facets for the attachment of chevron bones nearly to the very end of the sequence. They lack, however, the robust transverse processes of the modern pangolins' distal caudals. Instead, they take on an hourglass shape with very short, rounded transverse processes near the anterior and posterior margins of the centra (Figure 19a), much like the posterior

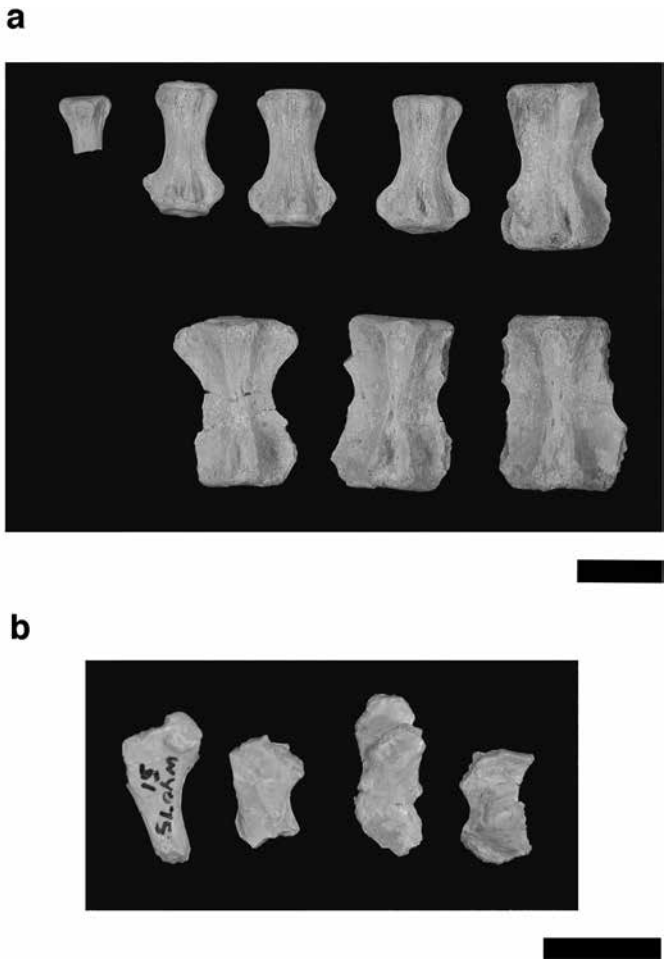

FIGURE 21. Distal caudal vertebrae and chevrons of *Patriomanis americana,* USNM-P 299960: (a) distal caudal vertebrae in ventral view, with posteriormost preserved caudal at upper left, progressively more anterior caudals to the right; lower left caudal anterior to vertebra at upper right, lower right vertebra representing the most anterior in the sequence; (b) chevrons in left lateral view, anterior to the left, with leftmost representing the first chevron in the caudal series (note single pair of dorsal facets). Scale bars = 1 cm. Photos by Tim Gaudin, composed and labeled by Julia Morgan Scott for Smithsonian Institution.

caudals of *Cryptomanis* (Gaudin et al., 2006) and *Eomanis* (Storch, 1978), although perhaps somewhat more robust than either. This morphology is very reminiscent of the pattern in vermilinguan anteaters with a prehensile tail (e.g., *Tamandua mexicana,* CM 76827), as well as prehensile-tailed marsupials, primates, and carnivorans (Argot, 2003; Youlatos, 2003; Organ, 2010), although in the latter the centra tend to be somewhat thinner and elongated anteroposteriorly.

Although Emry (1970) notes that no chevron bones were preserved with the type, a few chevron bones have been recovered from the other *Patriomanis* specimens (Figure 21b). These are generally rectangular, with their dorsoventral depth much greater than their anteroposterior length. They have robust processes that extend far ventrally beneath the hemal canal. Most are hourglass shaped in lateral view, expanding anteroposteriorly at the distal and proximal ends. The first, however, tapers distally and is recurved posteriorly in lateral view. It strongly resembles the condition in *M. javanica* USNM 198852, in which the first chevron is tapered and recurved posteriorly and the remainder are more hourglass shaped. Unlike the other chevrons, the first has but a single pair of dorsal facets near its posterior edge.

Axial Skeleton: Ribs and Sternum

FIGURES 22, 23

Ribs

Although Emry (1970) does not describe this portion of the axial skeleton in the type specimen, the type does preserve a few rib fragments, including a proximal end of a left rib and three fragments that are derived from mediolaterally expanded rib shafts (Figure 22a), like those described for *Cryptomanis* (Gaudin et al., 2006). USNM-P 494439 preserves additional ribs, including five fairly large fragments prepared free, plus three left and seven right ribs preserved in situ in the matrix. USNM-P 299960 includes 11 ribs for which the proximal ends are intact (two from the left, four from the right, five indeterminate), plus many rib fragments. Three nearly complete ribs from the middle of the series are illustrated in Figure 22b.

FIGURE 22. Ribs of *Patriomanis americana*: (a) large fragment from anterior, transversely expanded rib in F:AM 78999 (holotype), shown in anterior view, with proximal end pointed upward; (b) three nearly complete ribs from the middle of the series in USNM-P 299960, shown in posterior view—the ribs on the left and right have their proximal ends pointing upward, whereas in the middle specimen the proximal end is pointed downward. Abbreviations: **cap,** capitulum (= head); **ne,** neck; **rs,** rib shaft; **tub,** tubercle. Scale bars = 1 cm. Photos by Tim Gaudin, composed and labeled by Julia Morgan Scott for Smithsonian Institution.

Because there are three transversely expanded fragments in the type from three different ribs, it can be inferred that both the first and second rib shafts were expanded transversely relative to more posterior ribs, as is the case in *Eomanis, Euromanis*, the extant genera *Smutsia* and *Manis,* and at least the first rib in *Cryptomanis* (Gaudin et al., 2009). The capitular facets of the ribs are convex both anteroposteriorly and transversely, more so in the former plane, and are separated by a distinct neck of varying length from flatter tubercular facets, which are supported on a distinct tubercular boss and face dorsomedially (like the capitulum) and somewhat posteriorly. There is a small muscular fossa on the proximal and posterior surface of the shaft, just ventral to the tuberculum. The shaft itself is flattened anteroposteriorly and of varying curvature. *Cryptomanis* has very similar ribs, as does *Eomanis*, whereas in *Euromanis* the ribs are more cylindrical, and in modern pangolins the rib shafts are wider anteroposteriorly than they are mediolaterally (Gaudin, unpublished data).

Sternum

The only remnant of the sternum of *Patriomanis* appears to be a set of isolated bones from USNM-P 299960 (Figure 23). These include two articulated sternal elements, likely representing the penultimate (i.e., the sternebrae to which the xiphisternum is attached) and antepenultimate elements, and an isolated, more anterior sternebra. The two anterior sternebrae (i.e., the isolated and antepenultimate elements) are hourglass shaped in ventral view, with paired rib facets on their lateral surfaces at both anterior and posterior ends, the latter adjoining nearly identical facets on the anterior end of the next sternebra. The transverse widths of the anterior sternebrae are nearly equivalent to their anteroposterior lengths (e.g., 46.4 mm/52.2 mm = 0.89 in the antepenultimate segment), but what is more striking is the depth of the elements, which is nearly two-thirds their length. This depth gives the lateral rib facets of the adjacent sternebrae, when taken together, a deep U shape, with the opening of the U at the dorsal end (Figure 23b). The more posterior sternebra is taken to be the penultimate sternebra because it is twice the length of the anterior element and bears an extra pair of rib facets near its anteroposterior midpoint. It would then presumably have had a third pair of rib facets, along with a median distal articulation for the xiphisternum at its semicircular terminus, but these remain covered by matrix.

The morphology of the sternebrae in *Patriomanis* closely resembles that of *Cryptomanis* (Gaudin et al., 2006) but differs markedly from the morphology in modern pangolins. In *Phataginus,* the sternebrae are dorsoventrally flattened, whereas in *Manis, S. temminckii,* and some *S. gigantea* (the remainder of *S. gigantea* resemble *Phataginus*), the sternebrae have a deep anteroventral process, and the heads of the ribs overlap ventrally the posterior portions of the sternebrae (Gaudin et al., 2006, 2009). In *Eomanis* (Storch, 1978), the individual sternebrae are wider transversely than they are long, as in living manids but not patriomanids (Gaudin et al., 2006), and they appear flattened dorsoventrally, as in the modern species of *Phataginus* (Gaudin et al., 2009). The manubrium is preserved in the type of *Eomanis waldi* (Storch, 1978), and a partial manubrium and xiphisternum are preserved in *Cryptomanis* (Gaudin et al., 2006). The reader is referred to the original descriptions and to Gaudin et al. (2009) for more information on these elements.

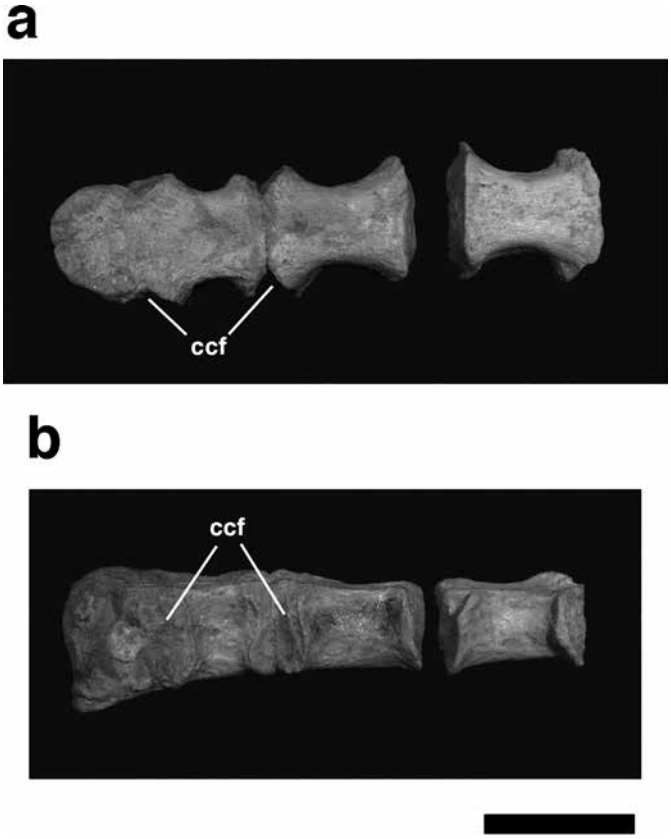

FIGURE 23. Sternebrae of *Patriomanis americana,* USNM-P 299960, including the penultimate (far left), antepenultimate, and a more anterior sternebra: (a) in ventral view; (b) in left lateral view. Abbreviation: **ccf,** costal cartilage facet. Scale bar = 1 cm. Photos by Tim Gaudin, composed and labeled by Julia Morgan Scott for Smithsonian Institution.

Hind Limb

FIGURES 24–40; TABLES A4–A8

Pedal Unguals

As noted by Emry (1970), very little of the pes is preserved in the type specimen of *Patriomanis* (F:AM 78999). None of the pedal unguals are preserved. However, some of the pedal unguals are preserved in USNM-P 494439. Some are apparently lost in this specimen, and a few have been prepared free of the matrix. A few pedal unguals are also available from USNM-P 531557. A virtually complete set of left and right pedal unguals has been preserved with USNM-P 299960 (Figure 24), and hence, the description that follows is based largely on that specimen.

The five unguals are broadly similar in size, the discrepancy between the largest and smallest being less in *Patriomanis* than in the modern pangolin species. As in the modern species, the third ungual is the largest, and the first and fifth are the smallest (Table A4).

The pedal unguals are deeply fissured (Figures 24, 25), as they are in all extinct and extant pholidotans (Figure 32c; Grassé, 1955; Guth, 1958; Gebo and Rasmussen, 1985; Koenigswald, 1969, 1999; Koenigswald and Martin, 1990; Gaudin et al., 2006, 2009) with the exception of *Eomanis* and *Euromanis* (Storch, 1978; Storch and Martin, 1994). The fissure measures as much as half the length of the ungual in dorsal view (Gaudin, unpublished data), as it does in the extant pangolin species. The unguals terminate in rather blunt rounded tips, a characteristic in which they differ from the living manids, where the unguals terminate in sharp points (Figure 32c). In dorsal view, the unguals are "waisted" in appearance, with a distinct constriction anterior to their base. The unguals expand slightly anterior to this constriction before narrowing again toward the tips (Figure 24). A very similar morphology is reported in *Necromanis* (Koenigswald, 1969, 1999; Koenigswald and Martin, 1990) and *Cryptomanis* (Gaudin et al., 2006) and is observed in *Eomanis*, *Euromanis,* and *Manis pentadactyla* but is not present in other extant manid species (Gaudin et al., 2009).

In lateral view, the unguals are roughly triangular, elevated proximally and tapering distally with a flat ventral surface and a gently convex dorsal surface (Figure 25a). The proximal surface is deeply concave in lateral view as in

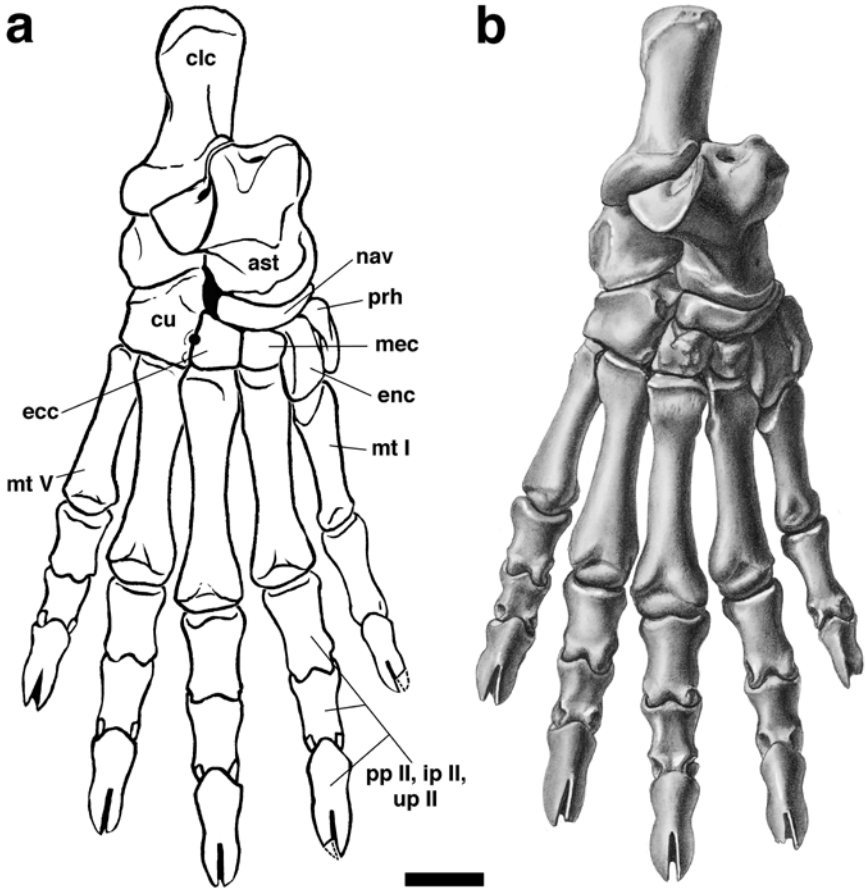

FIGURE 24. Pes of *Patriomanis americana*: (a) right pes of USNM-P 299960 in dorsal view; (b) labeled outline drawing of same. Abbreviations: **I–V,** digits I–V; **ast,** astragalus; **clc,** calcaneus; **cu,** cuboid; **ecc,** ectocuneiform; **enc,** entocuneiform; **ip,** intermediate phalanx; **mec,** mesocuneiform; **mt,** metatarsal; **nav,** navicular; **pp,** proximal phalanx; **prh,** prehallux; **up,** ungual phalanx. Scale bar = 1 cm. Illustration (a) by Julia Morgan Scott (JMS) for Smithsonian Institution (SI); (b) by Larry Isham, digitized by JMS for SI.

modern pangolins, with dorsal and ventral extensions that wrap around the distal articular surface of the intermediate phalanx. The ungual process is divided from the subungual process by a deep longitudinal groove on both the medial and lateral sides of the bone. A large vascular foramen is located at the proximal end of this groove (Figure 25a). The proximal articular surface is ovate, slightly broader transversely than it is tall. In this respect it resembles *Cryptomanis* and *M. pentadactyla* but differs markedly from other modern species in which the pedal unguals are compressed laterally (e.g., *M. javanica, Phataginus tricuspis*). The articular surface is divided by a prominent median ridge into two dorsoventrally elongate concave surfaces that receive the medial and lateral condyles of the intermediate phalanges.

In ventral view the pedal unguals have an extensive subungual process that occupies the proximal half of the bone (Figure 25b). The process takes the form of a rounded triangular platform separated by the aforementioned groove from the ungual process. The subungual process is perforated by two large oval subungual foramina at its proximal end. The left and right foramina are equivalent in size. These foramina connect to the grooves lying above the subungual process and presumably conveyed blood vessels toward the vascular foramina at the proximal ends of those grooves. Distally, the subungual process bears a short, low, rounded median crest flanked by two shallow concavities. This crest doubtless served as the insertion point for the tendons of the deep digital flexors (i.e., the tendons of the m. flexor fibularis, following Jouffroy, 1966). The subungual process of *Patriomanis* closely resembles that of *Cryptomanis* and the extant species *M. pentadactyla* and *M. javanica* but differs significantly from the narrower, strongly constricted subungual process of *Phataginus* (Gaudin et al., 2009).

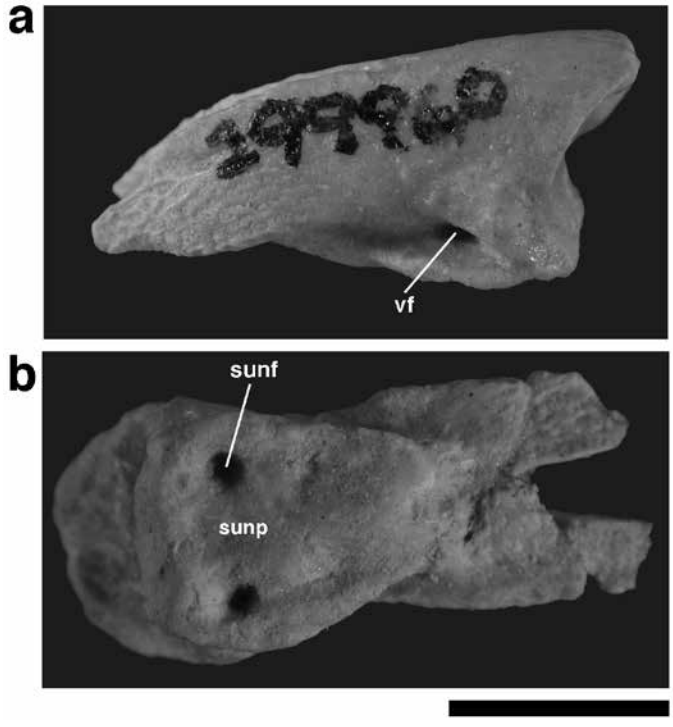

FIGURE 25. Ungual phalanx II of right pes of *Patriomanis americana* (USNM-P 299960): (a) in medial view; (b) in ventral view. Abbreviations: **sunf,** subungual foramen; **sunp,** subungual process; **vf,** vascular foramen. Scale bar = 0.5 cm. Photos by Tim Gaudin, composed and labeled by Julia Morgan Scott for Smithsonian Institution.

Pedal Intermediate Phalanges

These elements are not preserved in the type (Emry, 1970), but several intermediate phalanges are preserved and have been prepared in the right and left pes of USNM-P 494439. However, as a complete right and left series is available in USNM-P 299960 (Figure 24), the description that follows is based on that specimen.

As was the case with the ungual phalanges, the third intermediate phalanx is the longest, and the fifth is the shortest, although the second intermediate phalanx is approximately equal in length to the third in *Patriomanis* (Table A4). In dorsal view the intermediate phalanges are cylindrical and about half again as long as they are wide. They are slightly constricted in the middle and expanded at either end. Distally, they bear strongly convex, subequal medial and lateral condyles for articulation with the ungual phalanges. Immediately proximal to these condyles are paired dorsolateral concavities, presumably sites of origin for the collateral ligaments of the interphalangeal joint (based on anatomy of humans and dogs; Pick and Howden, 1977; Evans and Christensen, 1979). These concavities form distinct indentations behind the condyles visible in dorsal view (Figure 24). Although the concavities themselves are present in extant manids, they do not form dorsal indentations behind the condyles (Figure 32c; Gaudin et al., 2009).

The proximal articular surface is deeply concave in lateral view. It bears a single dorsal process and paired ventral processes that embrace the condyles of the proximal phalanges. The articular surface is approximately as wide as it is tall. The articular surface resembles those of the ungual phalanges in that it is divided by a central ridge into medial and lateral concavities that receive the medial and lateral condyles of the proximal phalanges. These concavities are flanked by well-developed lateral ridges in *Patriomanis*, a point of resemblance to *Cryptomanis*

lacking in modern pangolin species (Gaudin et al., 2009). In lateral view the intermediate phalanges are expanded proximally and distally and constricted in the middle, as in dorsal view. The base of the bone is triangular, and the condyles are pulley shaped.

Pedal Proximal Phalanges

Again, these elements are not preserved in the type (Emry, 1970). Proximal phalanges are preserved and have been prepared in the right and left pedes of USNM-P 494439 and USNM-P 299960. As before, the following description is based largely on the complete set available from the latter specimen (Figure 24).

The relative lengths of the proximal phalanges are more variable among living manids than was the case for the other phalanges. The fifth proximal phalanx is the shortest in all extant species, and the first is the longest in the majority of extant species (Gaudin et al., 2009). However, in *M. pentadactyla* the proximal phalanges become progressively shorter laterally, whereas in *P. tricuspis* the third proximal phalanx is approximately equal in length to the second and fourth (Figure 32c), and in *M. javanica, S. gigantea,* and *Cryptomanis* the third is decidedly longer than the second and fourth. In *Patriomanis* the first through third proximal phalanges are of approximately equal length, with the fourth shorter and the fifth shorter still (Table A4).

In dorsal view the proximal phalanges of *Patriomanis* closely resemble the intermediate phalanges, with a cylindrical shaft that is constricted in the middle and expanded at either end (Figure 24). As in *Cryptomanis*, the proximal phalanges are slightly longer than the intermediate phalanges in *Patriomanis* (Table A4). In every living species except *Manis javanica* the opposite is the case (Figure 32c). Indeed, in *S. gigantea, M. pentadactyla,* and *M. crassicaudata* the proximal phalanges are compressed proximodistally to the point that they no longer have a cylindrical shaft. The width of the proximal phalanges measured at the distal condyles in these taxa is as great as or greater than the overall length of the bone. The proximal phalanges have two subequal pulley-shaped distal condyles (Figures 24, 26d). These phalanges in *Patriomanis* lack a dorsal process at their proximal end that would serve to embrace the more proximal metatarsals, and hence, the metatarsal–phalangeal joint appears somewhat less stable than the interphalangeal joints. In manids, a large distal keel stabilizes the metatarsal–phalangeal joint (Figure 32c). As noted in subsequent descriptions, this keel is not developed dorsally in *Patriomanis* or in *Cryptomanis* or *Necromanis* (Gaudin et al., 2006, 2009).

The proximal articular surface itself is concave, although lacking the dorsal and ventral proximal prongs present in the other phalanges (Figure 26b). The lateral edge of the proximal end is actually slightly convex in lateral view. This articular surface also lacks the median keel that divides the proximal articular surface in the other phalanges. The facet is divided in its ventral half by a narrow midline depression that receives the keel of the distal metatarsals. This gives the articular surface a horseshoe-like shape, a shape that resembles that of *Cryptomanis* but differs from the extant species in which the entire articular surface is deeply divided by the metatarsal keel. In lateral view the proximal phalanges of *Patriomanis* are again shaped much like the intermediate phalanges, compressed in the middle with a triangular base and pulley-shaped condyles.

The first proximal phalanx differs somewhat in its morphology from the other four. It is more slender (Figure 24), with its maximum length more than twice its

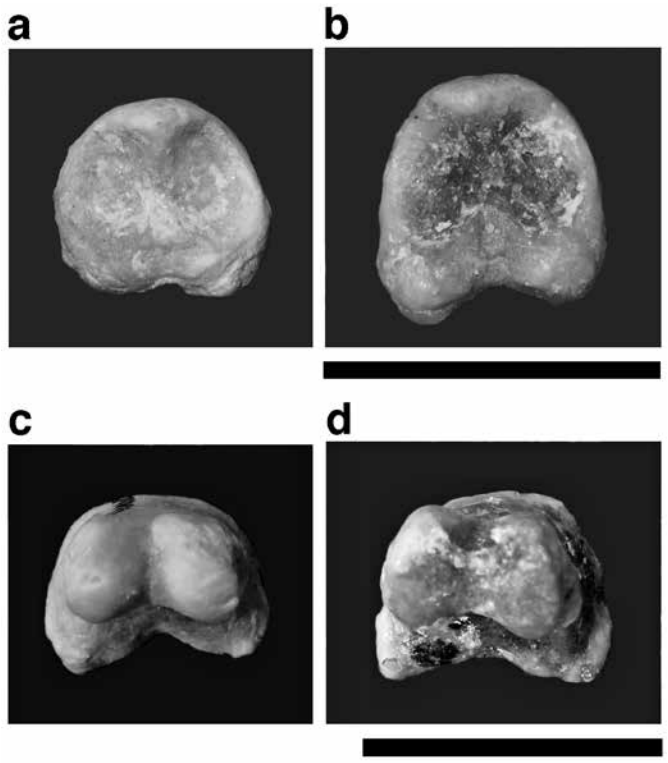

FIGURE 26. Proximal phalanges of *Patriomanis americana* (USNM-P299960): (a) proximal phalanx III of left manus in proximal view; (b) proximal phalanx III of right pes in proximal view; (c) proximal phalanx III of left manus in distal view; (d) proximal phalanx III of right pes in distal view. Scale bars = 1 cm. Photos by Tim Gaudin, composed and labeled by Julia Morgan Scott for Smithsonian Institution.

depth measured at the proximal end (its deepest point). In this respect it resembles the condition in *Cryptomanis* and *P. tricuspis* but differs from other extant species in which the first proximal phalanx is shorter and deeper (Gaudin et al., 2009). The ventral edge of the first proximal phalanx is gently concave in lateral view. In living pangolins (including *P. tricuspis*) the ventral edge is gently convex for roughly two-thirds its length, then indented sharply just proximal to the distal condyles. No such indentation is present in *Patriomanis*.

Metatarsals

In the type specimen, the only preserved portions of the metatarsals are the proximal ends of the right first and fifth metatarsals and the distal ends of the second and third metatarsals. In USNM-P 531556 the entire right fifth metatarsal is preserved, and USNM-P 531557 includes a distal end of what appears to be the second metatarsal on the right side. In USNM-P 494439 all five metatarsals are preserved intact on the left foot, although they remain embedded in the matrix ventrally. On the right pes, the third metatarsal is missing, and the other four are damaged to a certain extent. USNM-P 299960 preserves a complete series on the right (Figure 24). The first and second metatarsals are badly damaged on the left side. The left fifth metatarsal is also slightly damaged proximally and laterally.

As was the case for the proximal phalanges, there is some variation among pholidotans in the relative lengths of the metatarsals. In *Patriomanis*, the first metatarsal is the shortest, and the third is the longest (Table A4). These proportions are similar to those of *Cryptomanis* and of extant *Smutsia* and *Phataginus,* except that in the latter two genera the third and fourth metatarsals are subequal in length. Among *Manis* species the metatarsals exhibit several different patterns of relative lengths. The overall length of the digits relative to body size seems to be greater in *Patriomanis* and *Cryptomanis* (Gaudin et al., 2006) than in extant manids, a difference reflected in the lengths of the metatarsals. The length of the third metatarsal in *Patriomanis* is 35% that of the tibia, whereas in modern pangolins the third metatarsal is 25% or less of tibial length (Table A4).

Accompanying a shortening of the digits in the modern pangolins is an apparent increase in mobility of both the metatarsal–tarsal joints and the metatarsal–phalangeal joints. At the distal end of the metatarsals, extant pangolins have a robust median keel that extends dorsal and ventral to the shaft (Figure 32c). This keel increases the lateral stability of the metatarsal–phalangeal joint as well

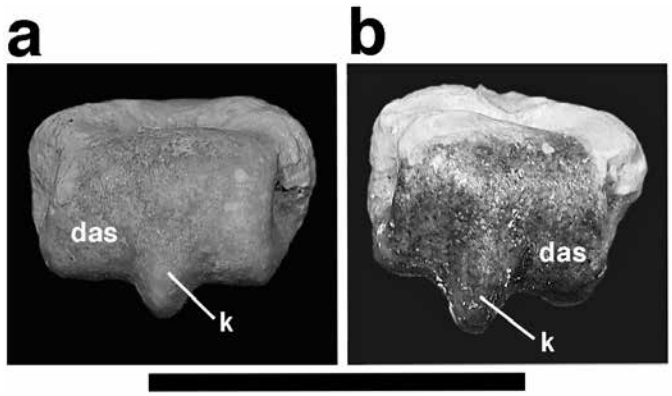

FIGURE 27. Metapodials of *Patriomanis americana* in distal view (USNM-P 299960): (a) left metacarpal III; (b) left metatarsal III. Abbreviations: **das,** distal articular surface; **k,** ventral keel. Scale bar = 1 cm. Photos by Tim Gaudin, composed and labeled by Julia Morgan Scott for Smithsonian Institution.

as its sagittal mobility. Such a keel is present on only the ventral half of the distal condyles of the metatarsals in *Patriomanis* (Figure 27b) and *Cryptomanis* (Gaudin et al., 2006) and is not as robust as the keel present in the modern species. With the exception of metatarsal I, the metatarsal articulations with the tarsals are flat in *Patriomanis*. They have a similar morphology in *Cryptomanis* (Gaudin et al., 2006) and apparently in *Necromanis* (Koenigswald and Martin, 1990). In extant pangolins the distal tarsals show extensive overlap onto the dorsal surfaces of both metatarsals I and III. They overlap metatarsals II and IV to a lesser degree (Figure 32c).

The shafts of the metatarsals of *Patriomanis* are wide and flat, their width exceeding their depth by 20% or more in all five digits. In *Cryptomanis*, the metatarsals are even wider, with all but digit I 50% wider than deep. Among modern pangolins, the depth at midshaft of the metatarsals is as great as or greater than the width for at least some of the digits, although the pattern varies among the living species (digits II–IV deepened in *Phataginus* and *S. temminckii*, digits I–IV in *S. gigantea, M. pentadactyla,* and *M. crassicaudata*, and only digit I in *M. javanica*). In dorsal view the metatarsals are roughly five times longer than wide, as in most manids, and most are slightly expanded both proximally and distally. The distal condyles appear slightly widened transversely and evenly convex in dorsal view. The condyles are distinctly narrower than the epicondyles (Figure 24), in contrast to the condition in the Manidae (Figure 32c; Gaudin et al., 2009). Immediately proximal to the condyles of metatarsals II–V is a midline depression on the dorsal surface. On their ventral surface each metatarsal has

a distal condyle bearing the aforementioned midline keel (Figure 27b). In addition, a robust plantar tubercle extends ventrally from the proximal end of each metatarsal.

Metatarsal I. In dorsal view the shaft of the first metatarsal is slightly bowed medially (Figure 24). At its proximal end the first metatarsal articulates laterally with metatarsal II and proximally with the entocuneiform. The proximal articular facet for the entocuneiform is triangular in proximal view. It is broad ventrally and narrows dorsally. It is strongly convex, the narrow dorsal portion overlapping extensively onto the dorsal surface of the shaft, as noted above. In all of these features *Patriomanis* resembles *Cryptomanis* (Gaudin et al., 2006) and the extant pangolin species. On the medial side of its proximal end, the first metatarsal bears a low, rugose proximodistally elongate ridge. A similar ridge is present in *Cryptomanis* and most extant manids (absent only in *Smutsia gigantea*).

Metatarsal II. Metatarsal II is the only metatarsal that is not markedly expanded proximally in dorsal view (Figure 24), a feature in which *Patriomanis* resembles *Cryptomanis* (Gaudin et al., 2006) and *Necromanis* (Koenigswald and Martin, 1990) but differs from extant manids (Figure 32c). On its proximal end it articulates medially with the first metatarsal and entocuneiform, proximally with the mesocuneiform, and laterally with the third metatarsal. The latter articulation is actually formed by two distinct facets, one carried dorsally on the shaft and a second carried ventrally on the plantar tubercle. Separate dorsal and ventral contacts between the second and third metatarsals are also present in *Cryptomanis, M. javanica,* and *M. crassicaudata* (Gaudin et al., 2009). The proximal articular surface is roughly rectangular, elongated dorsoventrally with indentations along its medial and lateral edges. A similar indentation along the lateral margin of the proximal articular surface is present in *P. tricuspis, S. gigantea, M. javanica,* and *M. crassicaudata.* Metatarsal II of *Patriomanis* bears a large depression on the posteromedial surface at its proximal end. Such a depression is also found in *Cryptomanis* (Gaudin et al., 2009), although it is not present among living pangolins, suggesting it may be a patriomanid feature.

Metatarsal III. This metatarsal articulates at its proximal end with metatarsal II medially, the ectocuneiform proximally, and metatarsal IV laterally. As was the case with its medial connection, its lateral connection to metatarsal IV is composed of a dorsal facet on the shaft and a ventral facet on the plantar tubercle, a point of resemblance to *Cryptomanis, Manis javanica,* and *M. crassicaudata* (Gaudin et al., 2009). In dorsal view the proximal articular surface is elevated along its lateral edge, as in manids (Figure 24). In proximal view, the articular surface for the ectocuneiform is vaguely dumbbell shaped, resembling the condition in *Cryptomanis* (Gaudin et al., 2009). It is broadly expanded dorsally and over the plantar tubercle ventrally and sharply constricted in between. In Manidae the facet lacks either the constriction or the ventral expansion or both and takes on a triangular or quadrangular appearance.

Metatarsal IV. The proximal end of the fourth metatarsal bears two medial facets for metatarsal III. It is deeply excavated on its lateral surface. Situated in the dorsal portion of this excavation is a kidney-bean-shaped facet for metatarsal V. In dorsal view the proximal end of the bone is elevated along its lateral edge, as is the third metatarsal (Figure 24). The dorsal surface itself is fairly flat, as in *Cryptomanis,* but contrasts with the condition in modern manid species in which this region of the fourth metatarsal is either markedly concave (*Manis, S. gigantea*) or deeply grooved (*Phataginus, S. temminckii*; Gaudin et al., 2009). In proximal view the articular facet for the cuboid is broad dorsally. It narrows ventrally but is slightly expanded at its ventral extremity. This ventral expansion helps to enclose a foramen formed between the proximal articular surfaces of the third and fourth metatarsals. This foramen is connected by a groove in the medial surface of the cuboid to a second foramen that opens more proximally between the dorsal surfaces of the cuboid and ectocuneiform. The arrangement in *Patriomanis* is very similar to the condition in *M. crassicaudata.* The latter species appears to be the only modern pangolin with the foramen between metatarsal III and IV, although the foramen between the cuboid and ectocuneiform is more widely distributed among the living species. Both foramina are absent in *Cryptomanis* (Gaudin et al., 2006, 2009). Given that the foramen between cuboid and ectocuneiform appears likely to have accommodated a ligament (see ectocuneiform description below), the foramen between metatarsals III and IV is likely related to the network of tarsal and metatarsal ligaments as well.

Metatarsal V. The proximal end of the fifth metatarsal is characterized not only by a broad plantar tubercle on its ventral surface but also by a prominent lateral process. This process lies at the same level as the proximal articular facet for the cuboid but is separated from this articular facet by a well-marked groove. The process is somewhat elongated dorsally and distally in lateral view. An even more prominent lateral process is present on metatarsal V in *Cryptomanis* and in modern pangolins (Figure 32c). The dorsal surface of metatarsal V is weakly concave at its proximal end in *Patriomanis* (Figure 24). Metatarsal V articulates with the cuboid proximally. The cuboid facet is D shaped in the type (F:AM 78999) and in USNM-P 299960, with a straight medial edge and a curved lateral margin. It is more elongate transversely in USNM-P 531556. The cuboid facet is contiguous on its

medial edge with the facet for metatarsal IV. However, the two facets are separated by a sharp ridge and are oriented at an obtuse angle to one another, with the cuboid facet facing mostly proximally, as well as dorsally and medially, and the facet for metatarsal IV facing mostly medially, as well as proximally and dorsally. The latter facet is L shaped, with one leg extended dorsoventrally and the other extending distally and dorsally. It is convex along its long axis. The morphology of these proximal articulations is generally similar in *Patriomanis* and manids, although the angle between cuboid and metatarsal IV facets and the shape of these facets varies somewhat among *Patriomanis* and the various extant species. In *Cryptomanis,* the division between the facets for the cuboid and metatarsal IV is much less marked, and the former facet is damaged so that its shape cannot be determined.

Prehallux

In USNM-P 299960 a sesamoid bone is preserved on the medial side of the right pes, abutting the entocuneiform (Figure 24). A similar element is present in *Cryptomanis* (Gaudin et al., 2006), all extant manid species (Figure 32c), and certain fossil armadillos (Scott, 1903–1904) and is termed by Szalay and Schrenk (1998) a "prehallux." We will follow the nomenclature of the latter authors. In *Cryptomanis* the prehallux is a rodlike element (Gaudin et al., 2006). However, in *Patriomanis,* as in extant pangolins, the prehallux is laterally compressed. In medial view it is roughly triangular in shape, narrow proximally and expanded distally, as in *Smutsia, M. javanica,* and *P. tetradactyla*. The prehallux of *Patriomanis* is convex medially and concave laterally and slightly twisted about its long axis, such that the dorsodistal corner is rotated medially approximately 20°. It lacks any definitive articular facets on its lateral side, and there are no obvious articular facets on the medial side of the entocuneiform. There is a small boss on the proximomedial surface of the navicular that may have served as a ligamentous attachment point. By contrast in some extant species there are well-developed articular facets on the proximal end of the prehallux for the navicular (*M. javanica, M. crassicaudata*) or the navicular and entocuneiform (*Phataginus*; Gaudin et al., 2009).

Entocuneiform

Although missing from the type and from the right side of USNM-P 299960, a nearly complete left entocuneiform is preserved in the latter specimen. In addition, both left and right entocuneiforms are intact and available for study in USNM-P 494439.

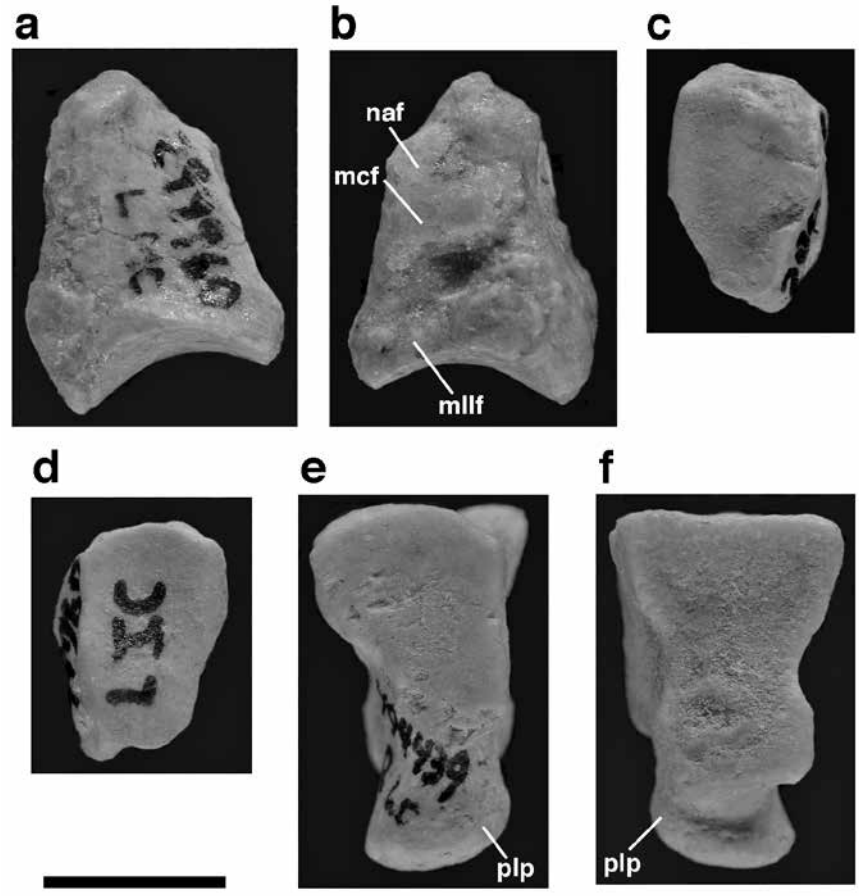

FIGURE 28. Distal tarsals of *Patriomanis americana*: (a) left entocuneiform in medial view (USNM-P 299960); (b) left entocuneiform in lateral view (USNM-P 299960); (c) left mesocuneiform in proximal view (USNM-P 299960); (d) left mesocuneiform in distal view (USNM-P 299960); (e) right ectocuneiform in proximal view (USNM-P 494439); (f) right ectocuneiform in distal view (USNM-P 494439). Abbreviations: **mcf,** mesocuneiform facet; **mIIf,** metatarsal II facet; **naf,** navicular facet; **plp,** plantar process. Scale bar = 0.5 cm. Photos by Tim Gaudin, composed and labeled by Julia Morgan Scott for Smithsonian Institution.

The morphology of this bone in *Patriomanis* is similar to that encountered in most extant pangolin species. It is a triangular element, broad distally and tapering proximally in medial view (Figure 28a). It is strongly compressed mediolaterally and bears a large concavity on its medial surface and a prominent boss on its ventrodistal corner. The distal articular facet for metatarsal I is strongly concave and, as noted previously, overlaps the dorsal surface of the shaft of the metatarsal (Figure 24). In distal view this articular facet is oval in outline, much like that of *Cryptomanis* and *Phataginus* (Gaudin et al., 2009). In other extant species the facet takes on a triangular (*Smutsia, M. crassicaudata*) or sigmoid shape (*M. javanica, M. pentadactyla*; Gaudin et al., 2009). Articular surfaces for three different bones, navicular, mesocuneiform, and metatarsal II, are present on its lateral side (Figure 28b). In *Patriomanis* the facets for navicular and mesocuneiform are contiguous and situated proximally along the dorsal edge of the lateral surface. These facets are almost circular and nearly the same size, the latter being slightly elongated dorsoventrally and hence slightly larger. The morphology of these facets is similar to that of *Cryptomanis* but differs notably from that of *Phataginus,* on the one hand, in which the mesocuneiform facet is greatly elongated dorsoventrally and clearly larger than the navicular facet, and *Smutsia* and *Manis,* on the other hand, in which it is the navicular facet that is enlarged along a dorsoventral axis and two separate and smaller mesocuneiform facets are present. The facet for metatarsal II lies along the distal edge of the entocuneiform in *Patriomanis*, well separated from the facet for the mesocuneiform. However, the shape and position of the facet differ somewhat in USNM-P 299960 and USNM-P 494439. In the former it is a round facet situated just ventral to the dorsoventral midline of the bone (Figure 28b). In the latter the facet begins at approximately the same place but appears to have a long low extension running along the distal edge toward its dorsal termination. In extant manids this facet is typically ovoid as in USNM-P 299960 but is situated near the dorsal edge of the entocuneiform, contiguous with the ventral edge of the mesocuneiform facet. It occurs in a similar position in *Cryptomanis,* where the facet is elongated proximodistally.

Mesocuneiform

The mesocuneiforms are missing from both the type and USNM-P 494437. However, both right and left mesocuneiforms are preserved in USNM-P 299960.

The mesocuneiform in *Patriomanis* is small and blocky. It has broad articular surfaces proximally and distally for the navicular and metatarsal II, respectively (Figure 28c,d), and smaller articulations medially and laterally with the entocuneiform and ectocuneiform. It has a rugose, nearly square exposure on the dorsal surface of the tarsus (Figure 24). In *Cryptomanis*, *Manis,* and *Smutsia,* the dorsal surface of the mesocuneiform is elongated mediolaterally (Gaudin et al., 2009). The navicular facet is ovate, slightly narrower ventrally than dorsally, with its dorsoventral axis somewhat longer than its greatest transverse diameter (ratio of depth/width = 1.3; Figure 28c). Among living pangolins it most closely resembles *Phataginus*. In *Cryptomanis,* the facet is more quadrangular, and in *Smutsia* it is elongated dorsoventrally and indented along its medial edge, whereas in *Manis* it is both elongated dorsoventrally (ratio of greatest depth/width ≥ 1.8) and L shaped, with a distinctive ventrolateral indentation (Gaudin et al., 2009). The facet for metatarsal II in *Patriomanis* is also wider dorsally than ventrally, giving it a rounded triangular appearance (Figure 28d). It closely resembles the facet for metatarsal II in living pangolins. On the medial surface of the mesocuneiform is a small teardrop-shaped facet for the entocuneiform. The facet lies in the dorsal and proximal corner of the medial surface and tapers ventrally, reaching approximately to the midpoint of the bone. On the lateral surface of the mesocuneiform is an ovate facet for the ectocuneiform. This facet is situated in the middle of the lateral surface and covers roughly half of its dorsoventral extent. The facet contacts both the proximal and distal margins of the lateral surface. The ectocuneiform facet resembles that of *Cryptomanis* and *Manis* but differs from the African pangolin species in which the facet is elongated dorsoventrally, occupying at least 75% of the dorsoventral extent of the lateral mesocuneiform (Gaudin et al., 2009).

Ectocuneiform

The ectocuneiforms are not preserved in the type, but both left and right ectocuneiforms are well preserved in USNM-P 494437 and USNM-P 299960.

Like the mesocuneiform, it is a blocky element, but it is substantially larger than the mesocuneiform. Its dorsal exposure on the tarsus is rugose and slightly wider than it is tall in a proximodistal direction (ratio = 1.2; Figure 24). In living pangolins the width of the dorsal surface of the ectocuneiform ranges from one and a half to two times greater than its height, whereas in *Cryptomanis* this surface is nearly square (Gaudin et al., 2009). The proximal end of the bone bears a robust plantar process that is separated by a distinct neck from the body of the bone (Figure 28e). This process is approximately circular in cross section. In

Cryptomanis and living pangolins the process is also present, although it is reduced in *Phataginus* and *S. temminckii,* and in *M. pentadactyla, Smutsia,* and *Phataginus* it lacks a distinct neck separating it from the body of the ectocuneiform. The ectocuneiform articulates proximally with the navicular and distally with metatarsal III. The proximal articular surface is in the shape of a rounded triangle in USNM-P 299960. In USNM-P 494439, the facet takes on more of an L shape, with a marked ventromedial concavity (Figure 28e). The distal facet is more angular and also varies somewhat in its shape between the two specimens. In USNM-P 299960, it is trapezoidal, almost triangular, with its dorsal width more than twice its ventral width. In USNM-P 494439 the ventral width of the facet is greater, with the dorsal end only one and a half times wider than the ventral end. The two ends of the facet are separated by sharp medial and lateral indentations (Figure 28f), perhaps a less developed form of the distinctive T-shaped metatarsal facet of the ectocuneiform in *Cryptomanis* and in *M. javanica* and *M. crassicaudata.* In other extant manids this facet is quadrangular or trapezoidal as in USNM-P 299960 (Gaudin et al., 2009). On its medial edge the ectocuneiform articulates with the mesocuneiform, as described above. On its lateral surface, the ectocuneiform of *Patriomanis* has two discrete facets for the cuboid. The more proximal facet is localized in the dorsal half of the lateral surface, and the more distal facet extends along the entire distal edge of the lateral surface. The proximal and distal facets are separated by a shallow groove that manifests itself on the dorsal surface of the tarsus as a large foramen between the ectocuneiform and cuboid (Figure 24). This foramen is present in *Necromanis* (Koenigswald and Martin, 1990) and most extant manids (except *Smutsia* and *P. tricuspis*) but is absent in *Cryptomanis* (Gaudin et al., 2006, 2009). In extant dogs, a similar foramen is present and appears to accommodate a branch of the proximal extensor retinaculum (Evans and Christensen, 1979).

Cuboid

The left cuboid is preserved intact in the type. In USNM-P 494439, both left and right cuboids are present, although neither has been prepared free of the matrix on its ventral surface. The right cuboid is well preserved in USNM-P 299960, but the left is badly damaged, with nearly the entire ventral half of the bone eroded away.

As is typical for eutherian mammals (e.g., Pick and Howden, 1977; Evans and Christensen, 1979; Ji et al., 2002; Kielan-Jaworowska et al., 2004), the cuboid is by far the largest element in the distal tarsal row (Figure 24). Its maximum height and width in *Patriomanis* are more than twice that of the next largest distal tarsal, the ectocuneiform. The cuboid articulates medially with the ectocuneiform and distally with metatarsals IV and V. At its proximal end it bears a complex series of articulations for the more proximal tarsals, including facets for the navicular, astragalus, and calcaneus (Figure 29a). As in *Cryptomanis* (Gaudin et al., 2006), *Necromanis* (Koenigswald and Martin, 1990), and living pangolins (Figure 32c), the dorsal surface of the cuboid is irregular, with a flat distal edge and a sharply angled proximal edge formed by the contact of the proximally and laterally oriented calcaneal facet and the proximally and medially oriented astragalar facet. On its ventral surface the cuboid carries a prominent plantar process (Figure 29a). The process is elongated transversely at its base and is oriented perpendicular to the proximodistal axis of the cuboid, in contrast to the condition in some extant manids in which this process

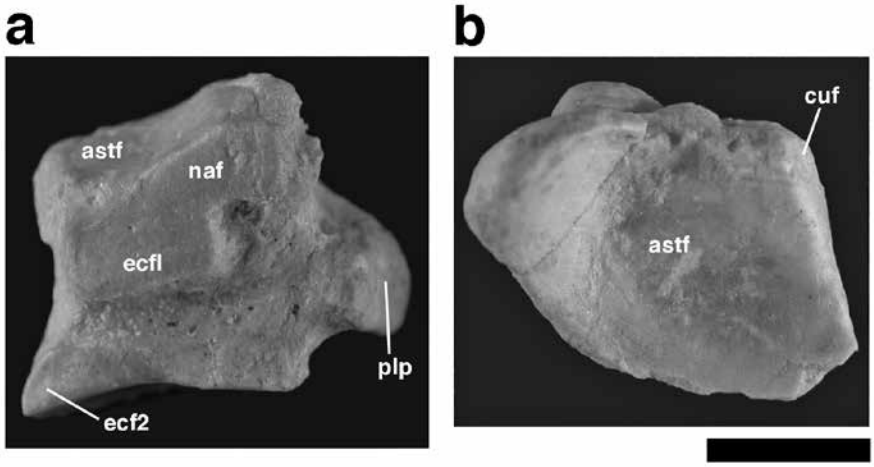

FIGURE 29. Tarsals of *Patriomanis americana* (USNM-P 299960): (a) right cuboid in medial view, dorsal to the left and proximal toward the top of photo; (b) left navicular in proximal view, lateral to the left, dorsal toward the bottom of the photo. Abbreviations: **astf,** astragalar facet; **cuf,** cuboid facet; **ecf1,** first (proximal) ectocuneiform facet; **ecf2,** second (distal) ectocuneiform facet; **naf,** navicular facet; **plp,** plantar process. Scale bar = 0.5 cm. Photos by Tim Gaudin, composed and labeled by Julia Morgan Scott for Smithsonian Institution.

tilts either proximomedially (*M. crassicaudata,* also *Cryptomanis*) or proximolaterally (*S. temminckii, P. tricuspis,* and *M. pentadactyla,* some *S. gigantea* and *M. javanica*; Gaudin et al., 2009).

The distal facet of the cuboid in *Patriomanis* is more elongate dorsoventrally in its medial portion, where it articulates with metatarsal IV, than in its lateral portion, where it articulates with metatarsal V. This is the case in *Cryptomanis* and all extant pangolins as well.

The calcaneal facet of the cuboid is strongly convex both dorsoventrally and proximodistally. It is ovate in shape, with its long axis oriented proximomedial to distolateral. It tapers to a point that extends ventrally, medially, and proximally slightly behind the astragalar facet. The calcaneal facet is particularly large in *Patriomanis* and *Cryptomanis* relative to that of extant manids. Its maximum length is approximately 80% of the maximum height of the cuboid bone itself. In modern pangolins the length of the calcaneal facet is only 50%–65% of the height of the cuboid (Gaudin et al., 2009). The astragalar facet is contiguous laterally with the calcaneal facet, with the ridge separating the two forming the highest point on the cuboid. It is ovate, with its long axis running dorsoventrally, and much smaller than the calcaneal facet. The astragalar facet lies at a slightly obtuse angle to the calcaneal facet, facing proximally and medially, as noted above, and is strongly concave both transversely and dorsoventrally. The astragalar facet is contiguous medially with a contact surface for the navicular. This latter articular surface is difficult to discern in the type since the relevant area is somewhat damaged in this specimen but is clearly evident in USNM-P 299960 (Figure 29a). The navicular facet is remarkably narrow proximodistally, although its dorsoventral length is greater than that of the astragalar facet. It faces medially, as does the facet for the ectocuneiform with which it shares its distal edge. The latter facet is one of two on the medial surface of the cuboid for the ectocuneiform. The upper facet is the larger of the two. It is oval, extends from the dorsal edge for somewhat more than half of the dorsoventral length of the medial surface, and is separated by a deep groove from the second ectocuneiform facet. This second facet is a small semicircular articular surface that is carried on a short process situated at the dorsal and distal corner of the medial cuboid surface (Figure 29a). The morphology of the medial surface of the cuboid and its astragalar, navicular, and ectocuneiform facets is highly variable among extant pangolin species (Gaudin et al., 2009). As noted above, some species lack the ectocuneiform–cuboid foramen and have only one facet for the ectocuneiform medially. In at least one modern species, *P. tetradactyla*, there is no contact between the navicular and cuboid. In addition, the shape and proportions of the astragalar and navicular facets are variable. As is the case with most other pedal elements, the anatomy of this region of the cuboid in *Patriomanis* is most similar to that of *Cryptomanis*.

Navicular

The navicular is not preserved in the type. In USNM-P 494439, the distal surface of the right navicular is visible within the matrix. Both the left and right naviculars are fully prepared and well preserved in USNM-P 299960.

The navicular articulates proximally with the astragalar head and laterally with the cuboid. On its distal surface it articulates with the entocuneiform, mesocuneiform, and ectocuneiform. In *Patriomanis*, as in *Cryptomanis* and living manids (Figure 32c; Gaudin et al., 2006, 2009), the navicular carries a prominent proximal extension along its medial edge. This extension wraps around the medial side of the astragalar head (Figure 24). As noted by Rose and Emry (1993), the head of the astragalus in *Patriomanis* lacks the distinctive concavity so characteristic of extant pangolins. Correspondingly, the astragalar facet of the navicular lacks any proximal convexity (Figure 29b). It is evenly concave both transversely and dorsoventrally and wider transversely than it is deep dorsoventrally. It is roughly ovate in shape with a rounded medial margin, although it is squared off along its lateral edge, where it articulates with the cuboid. The astragalar facet of the navicular in *Cryptomanis* is similar, albeit deeper dorsoventrally. As described in Gaudin et al. (2006:151), the facet in *Cryptomanis* bears a "weak proximal extension" on its dorsal margin that "may foreshadow the distinctive peg and socket articulation of modern manids." No such proximal extension is present in *Patriomanis*. The cuboid facet is narrow proximodistally and elongate dorsoventrally, much like the corresponding navicular facet on the cuboid described previously (Figure 29b). The distal surface of the navicular is rugose and carries a prominent knob on its proximomedial portion. This knob in all likelihood served as a point of ligamentous attachment for the prehallux. As noted above, in some living manids the prehallux forms a synovial joint with the navicular. As in *Cryptomanis,* the cuneiform facets are contiguous, separated from one another by low ridges. The mesocuneiform and ectocuneiform facets face distally, are quadrangular in shape, and are roughly equivalent in size. The mesocuneiform facet is convex, whereas the ectocuneiform facet is concave. The latter is a feature that is apparently unique

to *Patriomanis* among manids and patriomanids. The entocuneiform facet is decidedly smaller than the other two and directed distally and medially. The relative sizes and shapes of the cuneiform facets are difficult to discern in extant manids because of their tendency to fuse with one another, but they are clearly organized quite differently from those of *Patriomanis* and *Cryptomanis* and, indeed, vary considerably among the various extant species (Gaudin et al., 2009).

Astragalus

Although no astragalus is preserved in the type (Emry, 1970), both left and right astragali are preserved in USNM-P 494439. However, only the left has been prepared free of the matrix. In addition, a well-preserved, fully prepared right astragalus is available from USNM-P 29960. The latter has been figured previously by Rose and Emry (1993).

The most obvious difference between the astragalus of *Patriomanis* and living manids is the presence of a primitive convex head in the fossil form (Rose and Emry, 1993). In extant Manidae, the astragalar head bears a large lateral concavity that occupies almost its entire distal surface (Rose and Emry, 1993). The astragalar head of *Patriomanis* is hemispherical, is compressed in a dorsoventral plane, and extends narrowly onto the medial side of the neck (Figure 30). It has a width to height ratio greater than that of most other pangolins (Table A5). In *Cryptomanis* (Gaudin et al., 2006), the astragalar head is more convex dorsoventrally and deeper, extending farther ventrally than is the case in *Patriomanis*, with a broader exposure on the medial side of the neck. In *Necromanis* (Helbing, 1938; Koenigswald and Martin, 1990), the astragalar head is convex dorsoventrally but flat transversely. The astragalar head of *Euromanis krebsi* (Storch and Martin, 1994) is very primitive, with an almost spherical shape. The head of *Patriomanis* appears more primitive than that of *Cryptomanis* in several respects. The ventrolateral edge of the head of *Cryptomanis* bears a distinct facet for the cuboid (Gaudin et al., 2006) that is reduced and less clearly demarcated in *Patriomanis*. The head of *Cryptomanis* (Gaudin et al., 2006) also possesses a weak concavity at its dorsal margin leading to a weak groove descending along the lateral edge of the head, which Gaudin et al. (2006) suggest foreshadows the concavity found in extant pangolins. Both features are absent in *Patriomanis*.

The astragalar neck of *Patriomanis* is short, parallel sided, and more medially situated than is the case in most modern pangolins (Figure 30). A similar morphology is

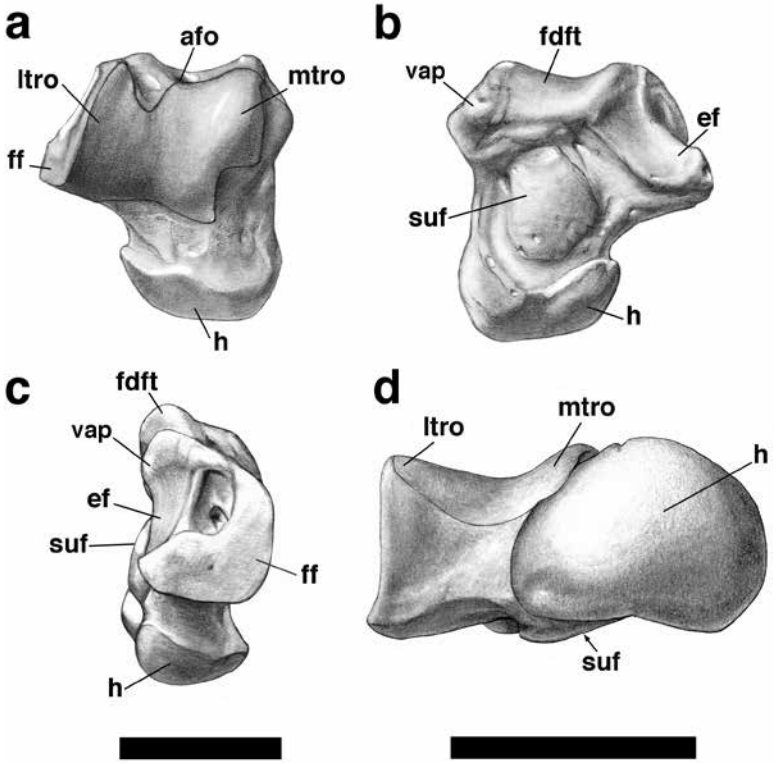

FIGURE 30. Right astragalus of *Patriomanis americana* (USNM-P 299960): (a) in dorsal view; (b) in plantar view; (c) in lateral view; (d) in distal view. Abbreviations: **afo,** astragalar foramen; **ef,** ectal facet; **ff,** fibular facet; **fdft,** fact for the m. flexor digitorum fibularis tendon; **h,** head; **ltro,** lateral trochlea; **mtro,** medial trochlea; **suf,** sustentacular facet; **vap,** ventral astragalar process. Scale bars = 1 cm. Illustrations by Julia Morgan Scott for Smithsonian Institution.

present in *Cryptomanis* (Gaudin et al., 2006), *Necromanis* (Helbing, 1938; Koenigswald and Martin, 1990), and *Euromanis krebsi* (Storch and Martin, 1994). In the fossil forms, the lateral edge of the neck is in line with the central trochlear depression. In extant pangolins the head lies much closer to the lateral edge of the astragalus, well lateral of the central trochlear depression (Figure 32c). The neck of all four fossil forms is narrow relative to the astragalar body, with a ratio of minimum neck width to maximum body width smaller than that of all extant manids except *Manis crassicaudata* (Table A5). *Cryptomanis* has a lower ratio than *Patriomanis* because of a distinct constriction halfway down the neck (Gaudin et al., 2006), and *Euromanis krebsi* has the lowest ratio of any pangolin owing to its small, cylindrical neck. In lateral view, the astragalar neck of *Patriomanis*, *Necromanis*, and *Euromanis krebsi* has an angular appearance, with a flat planar surface separated from the dorsal surface of the neck by a weak crest. In *Cryptomanis* this area is rounded and smooth.

The astragalar trochlea of *Patriomanis* has a rough hourglass shape, similar to that in most pangolins (Figure 30a). The trochlea is formed by two rounded swellings oriented proximodistally and separated by a central depression. The lateral trochlea forms a half circle with its lateral border defined by a sharp ridge. The medial trochlea has a more rounded medial edge that is interrupted by a steep concave depression at its distomedial corner. This depression is also present in *Cryptomanis* (Gaudin et al., 2006) and *Necromanis* (Helbing, 1938; Koenigswald and Martin, 1990) but is absent in *Euromanis krebsi* (Storch and Martin, 1994) and living manids (Figure 32c). The trochlea in *Patriomanis* is highly symmetrical compared to that of other pangolins, with a maximum proximodistal depth nearly equal for the medial and lateral trochleae (Table A5). A patent astragalar foramen is located proximal and slightly lateral to the central trochlear depression (Figure 30a; see also Rose and Emry, 1993). This primitive feature is also present in *Cryptomanis* (Gaudin et al., 2006) and *Necromanis* (Helbing, 1938; Koenigswald and Martin, 1990; Rose and Emry, 1993) but is rudimentary or absent in extant manids (Gaudin et al., 2009). An additional articular facet lies ventral to the medial trochlea at the proximal end of the astragalar body. This facet is narrow and slightly convex proximodistally and wide and concave transversely, with its central furrow directed in a proximal and medial direction (Figure 30b). This facet most likely served as the roof of a bursal cavity for the tendon of the m. flexor fibularis (Humphry, 1870; Jouffroy, 1966) and is a diagnostic character of the family Patriomanidae (Szalay and Schrenk, 1998; Gaudin et al., 2006), although it is also present in *Necromanis* (Helbing, 1938; Gaudin et al., 2009).

The fibular facet of *Patriomanis* is L shaped in lateral view with a deep pit ventral to the proximal end of the facet and a ventrally projecting arm that extends from the distal portion of the facet (Figure 30c). This morphology closely resembles that of *Cryptomanis* (Gaudin et al., 2006) but differs from the more U- or C-shaped facet of extant manids (Gaudin et al., 2009). The facet faces laterally and slightly proximally, so that it is less vertical than the fibular facet of *Cryptomanis* (Gaudin et al., 2006). It has a dorsal border that forms a sharp edge with the lateral trochlea. The more primitive fibular facet in *Euromanis krebsi* extends farther proximally, is broader and more rounded distally, and is much flatter than that in *Patriomanis*. The medial side of the astragalar body bears a strong process projecting medially from its ventral surface (labeled "vap" in Figure 30b,c). A similar process is present in *Necromanis* (Helbing, 1938; Koenigswald and Martin, 1990); both are much smaller than the prominent process in the same location in *Cryptomanis* (Gaudin et al., 2006). This process is absent in living manids. As noted in Gaudin et al. (2006), its function is unknown.

The ventral surface of the astragalus bears an elongate concave ectal facet that tapers along its long axis in a distolateral direction (Figure 30b). The distolateral extension of this facet abuts the ventral arm of the fibular facet. This facet is similar in shape to the ectal facet in *Necromanis* (Helbing, 1938; Koenigswald and Martin, 1990) and *Cryptomanis* (Gaudin et al., 2006) but is less concave than the latter. The ectal facet in extant manids is ovate and shortened anteroposteriorly (Gaudin et al., 2009). The sustentaculum in *Patriomanis* is an ovate facet with its long axis oriented proximodistally (Figure 30b). It is located in the center of the astragalus, resembling in this aspect the primitive placental condition (Szalay, 1977). The sustentaculum of *Necromanis* (Helbing, 1938; Koenigswald and Martin, 1990) is quite similar, whereas in *Cryptomanis* (Gaudin et al., 2006) the sustentaculum is larger, is more elongated distally, has migrated to the lateral side of the neck, and is separated by merely a shallow groove from the navicular facet. The sustentaculum in living manids may be dorsoventrally or transversely elongated and laterally or more centrally located and may lie distinct from the navicular and cuboid facets or may abut these facets (Gaudin et al., 2009). In many living species it is reduced in size, to the point of being completely absent

in some specimens of *M. pentadactyla* and *M. crassicaudata* (Gaudin et al., 2009).

Calcaneus

Only the distal portion of the right calcaneus is preserved in the type specimen of *Patriomanis* (Emry, 1970). However, a complete right calcaneus and a partial left calcaneus are preserved in USNM-P 299960. A complete left calcaneus is preserved in USNM-P 494439. The following description is based on the two complete calcanei (Figure 31; Table A6).

The calcaneus of *Patriomanis* (Emry, 1970) is similar to that of *Cryptomanis* (Gaudin et al., 2006) and *Necromanis* (Helbing, 1938; Koenigswald and Martin, 1990) but differs significantly from that of most extant manids. The most obvious difference between the fossil and modern forms is the arrangement of the calcaneal facets. The ectal facet of *Patriomanis* (Emry, 1970) is oblong, with a proximodistal length approximately twice that of its transverse width (Figure 31a,b). However, it is less elongate proximodistally than the ectal facet in *Cryptomanis* (Gaudin et al., 2006) and *Necromanis* (Helbing, 1938; Koenigswald and Martin, 1990). Most extant manids have an ectal facet that is wider, flatter, and more circular. Proximally, the ectal facet in *Patriomanis* is convex proximodistally, is flat transversely, and is directed medially and slightly dorsally. The distal portion of the ectal facet is flat and directed distomedially and slightly dorsally (Emry, 1970). This pattern is also present in *Cryptomanis* (Gaudin et al., 2006). In extant Manidae, the ectal facet is oriented more directly dorsad. The ectal facet extends well proximal to the fibular facet in *Patriomanis* (Emry, 1970), *Cryptomanis* (Gaudin et al., 2006), and *Necromanis* (Helbing, 1938; Koenigswald and Martin, 1990). In living pangolins, with the exception of *M. pentadactyla*, the proximal edge of the ectal facet lies even with or distal to the fibular facet. The ectal facet is much larger than the fibular facet, as it is in all pangolins except *P. tricuspis*, although this discrepancy is often slight in extant forms. The fibular facet in *Patriomanis* (Emry, 1970), *Cryptomanis* (Gaudin et al., 2006), and *Necromanis* (Helbing, 1938; Koenigswald and Martin, 1990) is ovate, with its long axis oriented in a distolateral direction. The shape and orientation of the facet vary within *Patriomanis*. In USNM-P 494439, the fibular facet is narrow proximodistally, convex transversely, and directed dorsally, whereas in USNM-P 299960 it is flat, nearly circular in outline, and directed dorsally and slightly distally (Figure 31a,b).

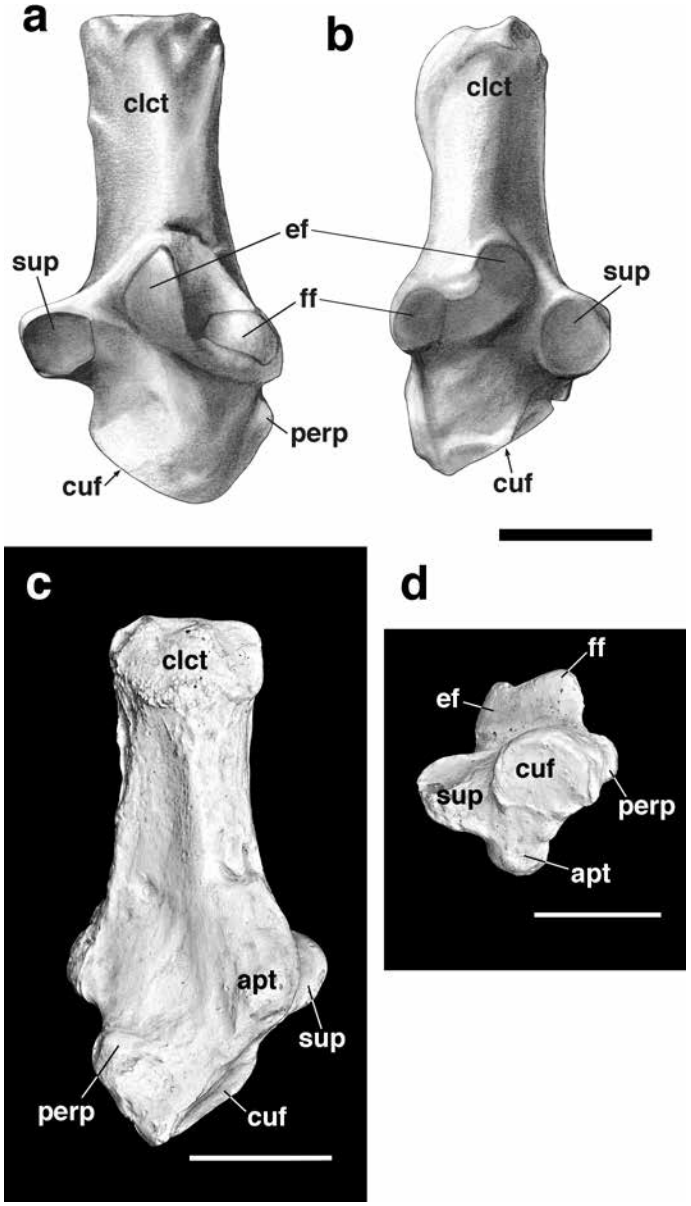

FIGURE 31. Calcaneus of *Patriomanis americana*: (a) left calcaneus of USNM-P 494439 in dorsal view; (b) right calcaneus of USNM-P 299960 in dorsal view; (c) left calcaneus of USNM-P 494439 (cast) in plantar view; (d) left calcaneus of USNM-P 494439 (cast) in distal view. Abbreviations: **apt,** anterior plantar tubercle**; clct,** calcaneal tuber; **cuf,** cuboid facet; **ef,** ectal facet; **ff,** fibular facet; **perp,** peroneal process; **sup,** sustentacular process and facet. Scale bars = 1 cm. Illustrations (a), (b) by Julia Morgan Scott (JMS) for Smithsonian Institution (SI); photos (c), (d) by Tim Gaudin, composed and labeled by JMS for SI.

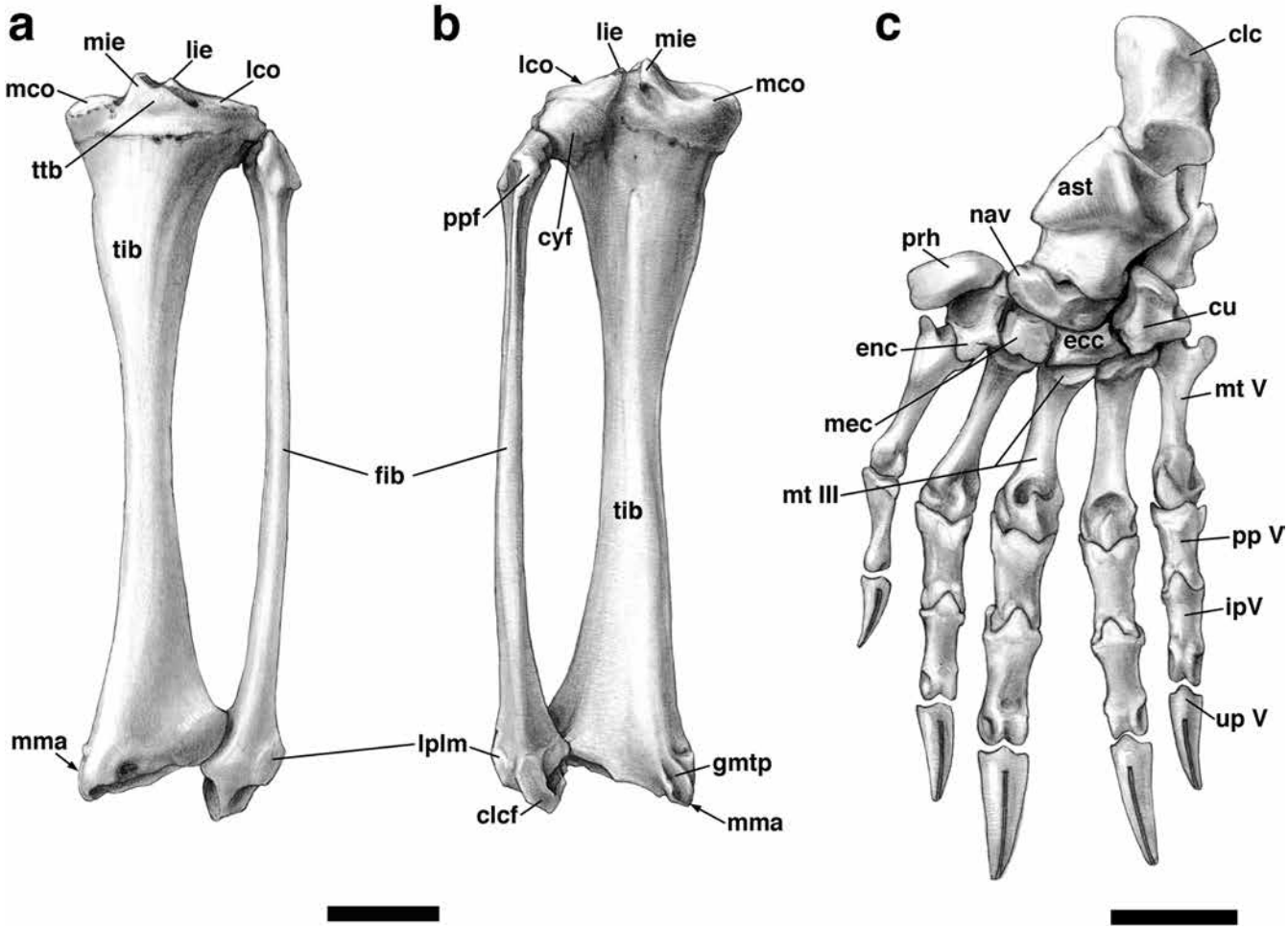

FIGURE 32. Right tibia and fibula and left pes of *Phataginus tricuspis* (CM 16206): (a) tibia and fibula in anterior view; (b) tibia and fibula in posterior view; (c) pes in dorsal view (unguals reconstructed on the basis of other specimens). Abbreviations: **I–V,** digits I–V; **ast,** astragalus; **clc,** calcaneus; **clcf,** fibular calcaneal facet; **cu,** cuboid; **cyf,** cyamelle facet; **ecc,** ectocuneiform; **enc,** entocuneiform; **fib,** fibula; **gmtp,** groove for m. tibialis posterior tendon; **ip,** intermediate phalanx; **lco,** lateral condyle; **lie,** lateral intercondylar eminence; **lplm,** lateral process of lateral malleolus of fibula; **mco,** medial condyle; **mec,** mesocuneiform; **mie,** medial intercondylar eminence; **mma,** medial malleolus of tibia; **mt,** metatarsal; **nav,** navicular; **pp,** proximal phalanx; **ppf,** posterior process of fibula; **prh,** prehallux; **tib,** tibia; **ttb,** tibial tuberosity; **up,** ungual phalanx. Scale bars = 1 cm. Illustrations by Julia Morgan Scott for Smithsonian Institution; parts (a), (b) modified from Gaudin et al. (2006), (c) modified from Gaudin et al. (2009).

The calcaneal tuber in both extant and fossil pangolins is large and expanded at its tip. In *Patriomanis*, the tuber is nearly cylindrical, but the dorsoventral axis remains longer than the transverse axis, whereas in *Cryptomanis* (Gaudin et al., 2006) the diameter of the tuber is significantly greater transversely than it is dorsoventrally. The tuber in living manids either resembles that of *Patriomanis* or is expanded obliquely along a dorsomedial to ventrolateral axis (Gaudin et al., 2009).

The anterior plantar tubercle lies on the ventral surface of the calcaneus medial to the cuboid facet in all pangolins, including *Patriomanis* (Emry, 1970). In *Patriomanis* (Emry, 1970), *Cryptomanis* (Gaudin et al., 2006), and *Necromanis* (Helbing, 1938; Koenigswald and Martin, 1990), it also lies proximal to the cuboid facet (Figure 31c), whereas its position is coincident with or distal to the cuboid facet in *Euromanis krebsi* (Storch and Martin, 1994) and all living manids except *S. gigantea* (Gaudin et al., 2009). The tubercle

is positioned at the same level as the distal edge of the sustentacular facet in USNM-P 494439 and is slightly distal to the sustentacular facet in USNM-P 299960. The tubercle is freestanding in all five fossil pangolin genera, whereas it is sessile in living manids. In *Patriomanis* (Emry, 1970), the tubercle is less prominent than in the other four fossil forms. A distinct groove is evident medial to the tubercle, on the ventral surface of the sustentacular process, allowing for the passage of the m. flexor fibularis. This groove is present in patriomanids and *Necromanis* but is absent in *Euromanis krebsi* (Storch and Martin, 1994) and the extant Manidae. The peroneal process in *Patriomanis* (Emry, 1970) is a knoblike eminence projecting from a dorsomedial ridge midway between the ectal and cuboid facets (Figure 31a,c). This process is highly reduced relative to that in *Cryptomanis* (Gaudin et al., 2006) and most extant Manidae but not as reduced as in *Necromanis* (Helbing, 1938; Koenigswald and Martin, 1990), in which it is nearly absent.

The cuboid facet in *Patriomanis* (Emry, 1970) forms an irregular circle, indented along its medial margin by a depression that separates it from the anterior plantar tubercle (Figure 31d). The facet is slightly concave transversely, is flat dorsoventrally, and is directed distomedially and somewhat ventrally. The facet is similar in shape to that of *Cryptomanis* but is less symmetrical than the circular facet of *Euromanis krebsi* (Storch and Martin, 1994). Modern African pangolins possess a cuboid facet similar to that of *Patriomanis* (Emry, 1970), although in *Smutsia* it tends to be more elongated transversely, whereas Asian pangolins possess a transversely ovate facet that is strongly concave transversely and directed more distally. The sustentacular facet in *Patriomanis* (Emry, 1970) is circular, is directed dorsally and slightly distomedially, and lies opposite the distal portion of the ectal and fibular facets (Figure 31a,b). It covers almost the entire dorsal surface of the sustentacular process, similar to the condition in *Euromanis krebsi* (Storch and Martin, 1994). The sustentacular facet is similar in shape to that of *Necromanis* (Helbing, 1938; Koenigswald and Martin, 1990) and *Euromanis krebsi* (Storch and Martin, 1994) but is smaller and less elongated distally than the sustentacular facet of *Cryptomanis* (Gaudin et al., 2006). In *Necromanis* (Helbing, 1938; Koenigswald and Martin, 1990) and, to a lesser degree, in *Cryptomanis* (Gaudin et al., 2006), the sustentacular process extends farther medially than the sustentacular facet. Among extant manids, the sustentacular process is usually positioned more distally but is variable in morphology. A large sustentacular process is present in all African pangolins except *P. tricuspis*, which bears a weak process, whereas in Asian pangolins the process is absent (with the exception of FMNH 57338, a juvenile *Manis crassicaudata* specimen). The sustentacular facet in Manidae is also variable. It may be distally elongated, transversely broadened, ovate, triangular, or entirely absent (Gaudin et al., 2009).

Fibula

As noted by Emry (1970), only the proximal portion of the right fibula is preserved in the type specimen. A distal portion of the left fibula is preserved in USNM-P 531557. An additional proximal right fibula and distal left fibula, although damaged, are available from USNM-P 494439. However, USNM-P 299960 preserves nearly complete right and left fibulae (Figure 30), although both are damaged at the proximal and distal ends.

The fibula in *Patriomanis* is significantly shorter than the tibia (Figure 33). In fact, the ratio of fibula to tibia length is lower in *Patriomanis* than in *Cryptomanis* (Gaudin et al., 2006) and all living manids (Table A7).

Emry (1970) describes the fibular head of *Patriomanis* as flattened laterally and elongated anteroposteriorly. In *Cryptomanis*, the head is expanded transversely and does not extend as far anteriorly or posteriorly (Gaudin et al., 2006). Among extant manids, the fibular head is somewhat variable in shape, but most possess a posterior process that extends farther posteriorly from the shaft and an anterior process that extends less far anteriorly than is the case in *Patriomanis* (Gaudin et al., 2009). Emry (1970) identifies a medially and dorsally facing proximal tibial facet that rests on an anterior projection of the head, displaced well anterior to the shaft. In *Cryptomanis* (Gaudin et al., 2006), the proximal tibial facet is more in line with the shaft, rather than being displaced anteriorly, and faces more posteriorly. In both the type and USNM-P 299960, there appears to be a second medially directed facet on the posterior portion of the head. This is likely a sesamoid facet for articulation with the cyamelle, similar to that in *Cryptomanis* (Gaudin et al., 2006) and some extant manids. This cyamelle facet is not described in Emry (1970), and Gaudin et al. (2006) assert on this basis that it is absent, but more thorough examination has revealed its presence (Figure 33a). The posterior process of the proximal fibula extends only slightly posterior to the sesamoid facet. This process consists of a lateral and a medial tubercle with a midline ridge in between that extends farther distally than in *Cryptomanis* (Gaudin et al., 2006) before merging with

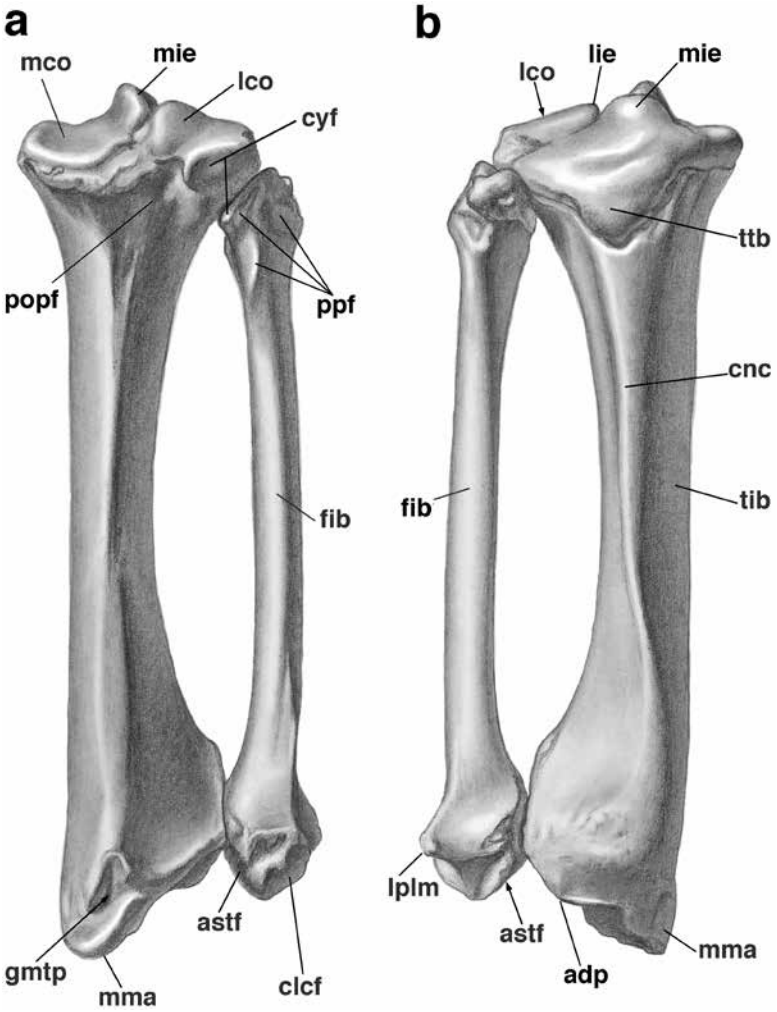

FIGURE 33. Right tibia and fibula of *Patriomanis americana* (USNM-P 299960): (a) in posterior view; (b) anterior view. Abbreviations: **adp,** anterior distal tibial process; **astf,** astragalar facet; **clcf,** fibular calcaneal facet; **cnc,** cnemial crest; **cyf,** cyamelle facet; **fib,** fibula; **gmtp,** groove for m. tibialis posterior tendon; **lco,** lateral condyle; **lie,** lateral intercondylar eminence; **lplm,** lateral process of lateral malleolus of fibula; **mco,** medial condyle; **mie,** medial intercondylar eminence; **mma,** medial malleolus of tibia; **popf,** popliteal fossa; **ppf,** posterior process of fibula; **tib,** tibia; **ttb,** tibial tuberosity. Scale bar = 1 cm. Drawn by Larry Isham, digitized and labeled by Julia Morgan Scott for Smithsonian Institution.

the medial edge of the fibula. In *Cryptomanis* (Gaudin et al., 2006), a similar morphology is present, although in this genus the lateral tubercle is larger and the medial tubercle is less pronounced than in *Patriomanis*, and there is a deep pit in between the lateral tubercle and the median ridge. In extant Manidae, a single large posterior process is present that may extend distally well down the shaft of the fibula (Figure 32b; Gaudin et al., 2009). As in all pholidotans (Gaudin et al., 2006), an eminence lies on the anterolateral surface of the proximal fibula. This eminence extends well forward of the tibial facet in *Patriomanis* and *Cryptomanis* (Gaudin et al., 2006) but not in extant manids (Gaudin et al., 2009).

On the basis of its proximal end, Emry (1970) describes the fibular shaft in *Patriomanis* as thin, straight, and cylindrical. The complete fibulae preserved in USNM-P 299960 confirm this description for the entire length of the fibular shaft. In *Cryptomanis* (Gaudin et al., 2006), the shaft is compressed anteroposteriorly and bowed laterally. In modern manids, the shape is variable—it is cylindrical in some taxa, whereas in others the shaft is compressed transversely; additionally, the shaft may be straight or bowed medially or laterally (Gaudin et al., 2009).

A lateral process is present on the lateral malleolus of all pholidotans (Figure 32a,b; Gaudin et al., 2006). In *Patriomanis*, the lateral process is rectangular in anterior view (Figure 33b). It is thin with a proximodistal length greater than its transverse width. In extant Manidae, the lateral process is usually even more elongated proximodistally. The lateral malleolus in *Patriomanis* is V shaped in anterior view and compressed along an anteromedial to posterolateral axis. In *Cryptomanis* (Gaudin et al., 2006), the lateral malleolus is less compressed transversely with a squared terminus. The distal tibial facet in *Patriomanis* is triangular and flat. The facet faces more anteriorly in *Patriomanis* and *Cryptomanis* (Gaudin et al., 2006) than

in extant manids, in which it faces more medially (Gaudin et al., 2009).

As noted in Gaudin et al. (2006), the astragalar and calcaneal facets of the fibula in all pangolins lie anterior and distal to the pit for the astragalo-fibular ligament. The astragalar facet in *Patriomanis* has a flat surface. Although angular, it is roughly C shaped, with a distal moiety that is less vertical than in *Cryptomanis* (Gaudin et al., 2006), which has an L-shaped astragalar facet that is markedly concave at its proximal extremity. The astragalar facet in most living pangolins is C shaped but less angular than in *Patriomanis*. The calcaneal facet is ovate and narrow transversely and is directed posteriorly and slightly distally and laterally. It is similar in shape to that in other pangolins except those in the genus *Manis,* in which the calcaneal facet is compressed proximodistally. Along its medial edge, the distal half of the calcaneal facet abuts the distal portion of the astragalar facet. From there it extends proximally nearly as far as the astragalar facet, much like the condition in *Phataginus* (Gaudin et al., 2009). In *Cryptomanis* (Gaudin et al., 2006), *S. temminckii,* and *Manis*, the proximal edge of the calcaneal facet is well distal to that of the astragalar facet. As noted by Gaudin et al. (2006, 2009), the calcaneus does not contact the fibula in *S. gigantea*.

Tibia

Most of the right and left tibiae are preserved in the type specimen and were described by Emry (1970). The right and left tibiae are also available from USNM-P 494439, although both are damaged. A complete pair of tibiae is available from USNM-P 299960 (Figures 33, 34).

Emry (1970) notes that the tibia of *Patriomanis* is expanded transversely at the distal and proximal ends like that of other pangolins (Figure 33). Its shape particularly resembles that of *Cryptomanis* (Gaudin et al., 2006). The most obvious difference between these two fossil forms and extant pangolins is the presence of a robust cnemial crest on the proximal portion of the tibial shaft (Figure 33b). As stated in the description of the type specimen, the cnemial crest in *Patriomanis* extends farther down the shaft than in extant pangolins (Emry, 1970). In fact, the crest extends approximately two-thirds down the length of the tibial shaft, where it forms a distinct, rounded angle before rejoining the shaft. Distal to this, the cnemial crest blends imperceptibly into a weak, rounded ridge that is in line with the anterior edge of the medial malleolus. A sharp cnemial crest is also present in *Cryptomanis* (Gaudin et al., 2006), but in this genus it terminates halfway down the tibial shaft in a prominent tubercle. In extant Manidae (except *M. pentadactyla*), the cnemial crest is greatly reduced, weak, and rounded if present at all (Figure 32a; Gaudin et al., 2009). Emry (1970) describes a prominent fossa lateral to the cnemial crest in *Patriomanis*. This fossa is also present in *Cryptomanis* (Gaudin et al., 2006), although it is less deep. This fossa is absent in most living manids, although a weak fossa is present in *M. pentadactyla* (Gaudin et al., 2009).

Additional surface markings are present on the tibial shaft that distinguish *Patriomanis* (Emry, 1970) and *Cryptomanis* (Gaudin et al., 2006) from living pangolins. Emry (1970) describes and illustrates a well-developed popliteal depression in *Patriomanis* immediately below the medial condyle on the posterior surface of the proximal tibia. The fossa is deep, narrow, and elongated

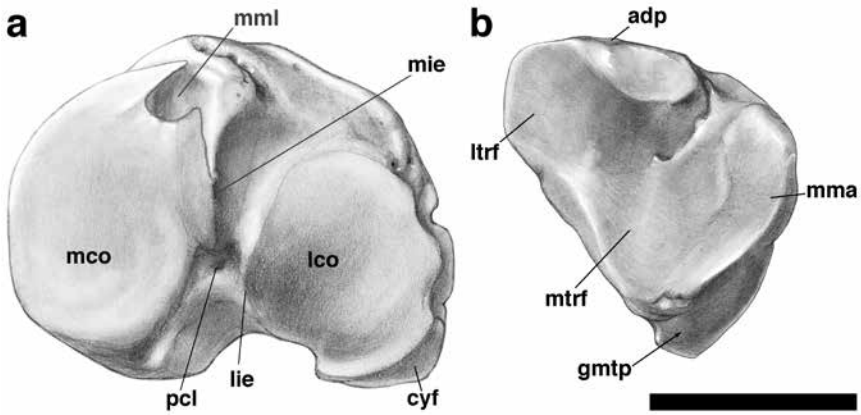

FIGURE 34. Right tibia of *Patriomanis americana* (USNM-P 299960): (a) in proximal view; (b) in distal view. Abbreviations: **adp,** anterior distal tibial process; **cyf,** cyamelle facet; **gmtp,** groove for m. tibialis posterior tendon; **lco,** lateral condyle; **lie,** lateral intercondylar eminence; **ltrf,** facet for lateral trochlea of astragalus; **mco,** medial condyle; **mie,** medial intercondylar eminence; **mma,** medial malleolus of tibia; **mml,** pit for attachment of medial meniscal ligament; **mtrf,** facet for medial trochlea of astragalus; **pcl,** pit for attachment of posterior cruciate ligament. Scale bar = 1 cm. Illustrations by Julia Morgan Scott for Smithsonian Institution.

distally for almost one-third the length of the shaft. It is bounded laterally by a sharp crest that marks the lateral edge of the shaft, descending from the lower margin of the proximal fibular facet to the midshaft region, where it nearly contacts a similar crest rising proximally from the distal fibular facet. A popliteal fossa is also present in *Cryptomanis* (Gaudin et al., 2006) and *M. pentadactyla* but is absent in other living manids. The posterior surface of the distal tibial shaft bears a broad, shallow concavity. In *Cryptomanis* (Gaudin et al., 2006), the concave posterior distal surface is interrupted by a rounded median ridge, creating two separate concavities. In most extant manids, the posterior distal tibial surface is convex (Figure 32b). The shaft itself is curved in medial view, such that the proximal and distal ends of the tibia lie posterior to the middle portion of the shaft. A similar condition prevails in *Cryptomanis,* whereas the tibial shaft is nearly straight in living pangolins.

As noted by Gaudin et al. (2006), both *Patriomanis* and *Cryptomanis* possess a robust tibial tuberosity that forms an elevated U-shaped eminence at its distal extent, where it abuts the proximal cnemial crest (Figure 33b). The tibial tuberosity in extant manids (except *M. crassicaudata*) is horizontally ovate or rectangular, positioned on the proximal portion of the anterior tibia but not extending distally (Figure 32a). Emry (1970:481) describes the medial tibial condyle in *Patriomanis* as "slightly convex" (anteroposteriorly), whereas that of *Cryptomanis* is flat (Gaudin et al., 2006). The medial condyle is concave transversely by virtue of a lappet forming much of the medial surface of the well-developed medial intercondylar eminence (Figures 33a, 34a). This lappet is bounded anteriorly by a discrete pit that has been interpreted by Gaudin et al. (2006) as a site for the attachment of the cranial tibial ligament of the medial meniscus (Figure 34a). The medial lappet is bounded posteriorly by a fossa for the posterior cruciate ligament. The fossa for the anterior cruciate ligament is located on the opposite side of the medial intercondylar eminence anterior and medial to the lateral condyle. All three of these fossae are present in all pangolins. As Emry (1970) also points out, the lateral tibial condyle is more convex than the medial condyle. The medial condyle is large and ovate, with its long axis oriented anteroposteriorly, whereas the lateral condyle is smaller and has an irregular outline, with its maximum width and depth roughly equivalent (Figure 34a). In contrast, the lateral condyle of *Cryptomanis* is widened transversely (Gaudin et al., 2006). Although the lateral condyle is elevated relative to the medial condyle in all pangolins, this characteristic is more pronounced in *Patriomanis* (Figure 33; Emry, 1970) and *Cryptomanis* (Gaudin et al., 2006). The medial intercondylar eminence in *Patriomanis* (Emry, 1970) is elongated anteroposteriorly, as in all pangolins, but is narrower transversely than in other forms. It is continuous anteriorly with the tibial tuberosity. The lateral intercondylar eminence is well developed but smaller than the medial intercondylar eminence (Figures 33, 34a), also a characteristic of all pangolins. In *Patriomanis* (Emry, 1970), the lateral intercondylar eminence is smooth and rounded and lies at the posteromedial extent of the lateral tibial condyle.

As related by Emry (1970), the proximal tibia bears a facet for the cyamelle (Figures 33a, 34a), a sesamoid bone that forms within the tendon of the mm. popliteus and peroneus longus (Jouffroy, 1966). This sesamoid facet projects posteriorly and slightly laterally from the posterolateral edge of the lateral tibial condyle. It is convex proximodistally and transversely and is elongated in a dorsolateral direction, whereas in *Cryptomanis* (Gaudin et al., 2006) the facet is nearly flat and deeper proximodistally. The orientation of this facet is variable in extant Manidae. The facet for the cyamelle is small compared to the femoral articular surfaces. The proximal fibular facet (Emry, 1970) is ovate and elongated anteroposteriorly. It is directed laterally and somewhat distally and anteriorly, similar to the condition of extant *Manis* and *Cryptomanis* (Gaudin et al., 2006, 2009) and differing from the proximal fibular facet in extant African pangolins, which is not visible in anterior view (Gaudin et al., 2009).

The distal end of the tibia in *Patriomanis* is triangular (Figure 34b; Emry, 1970) but much less expanded transversely than in other pangolins. In fact, *Patriomanis* has a ratio of distal maximum transverse width to anteroposterior depth less than that of all other pangolins (Table A7). The distal end of the tibia has undergone approximately 50° of torsion (clockwise on right tibia, counterclockwise on left tibia) relative to a transverse axis across the tibial head. Among other pangolins, only *Cryptomanis* (Gaudin et al., 2006), *Smutsia gigantea*, and *Manis javanica*, each with approximately 45° of torsion, have undergone such a large degree of twisting of the distal tibia (Gaudin et al., 2009).

The medial malleolus of *Patriomanis* (Emry, 1970) is large and occupies a larger portion of the distal tibial surface than in extant manids. However, *Cryptomanis* possesses an even more robust malleolus (Gaudin et al., 2006). The posteromedial surface of the malleolus in *Patriomanis* (Emry, 1970) and *Cryptomanis* (Gaudin et al., 2006) is impressed by a broad groove for the passage of the

m. tibialis posterior tendon (Figures 33a, 34b; inferred by analogy to *Smutsia gigantea* and *Manis pentadactyla*; see Humphry, 1870; Jouffroy, 1966; Gaudin et al., 2006). In living pangolins, this groove is more pronounced, in some taxa virtually enclosed in a bony tunnel, and may be accompanied by a second weaker and more anterior groove, presumably for the tendon of the m. flexor tibialis (Figure 32b; Jouffroy, 1966; Gaudin et al., 2009). The distal tibia bears two articular surfaces for the astragalar trochlea (Figure 34b). These surfaces are separated by a smooth ridge that is less pronounced than in *Cryptomanis* (Gaudin et al., 2006). The anterior distal tibial process that lies at the anterior end of this ridge (Figures 33b, 34b) is also less pronounced in *Patriomanis* than in *Cryptomanis* (Gaudin et al., 2006) but is larger than that in extant manids. The lateral trochlear facet is slightly concave anteroposteriorly and flat transversely, whereas this facet is concave transversely in *Cryptomanis* (Gaudin et al., 2006) and living pangolins. The concave medial trochlear facet is nearly centered on the distal end of the tibia and is slightly larger than the lateral facet. *Patriomanis* (Emry, 1970) is the only pangolin in which the anteroposterior depth of the medial trochlear facet exceeds that of the lateral facet (Figure 34b; Gaudin et al., 2009). The medial facet has a small anterior indentation that is present in *Cryptomanis* but absent in all living manids except *Manis pentadactyla*.

The distal fibular facet in *Patriomanis* (Emry, 1970) is a slender, transversely elongated surface that faces laterally and slightly posteriorly, similar to that in *Cryptomanis* (Gaudin et al., 2006). In both fossil species, the facet faces more posteriorly than in extant manids (Gaudin et al., 2009). The facet is not visible in distal view in either fossil form, whereas it can be seen in distal view in living pangolins (Gaudin et al., 2009).

Patella

Although no patellae are preserved in the type specimen, a left patella is available from USNM-P 494439. Left and right patellae are also available from USNM-P 299960 (Figure 35).

The patella in *Patriomanis* is roughly diamond shaped in anterior view. Like that of *Cryptomanis* (Gaudin et al., 2006), its height and width are roughly equivalent, whereas in extant manids and *Euromanis krebsi* (Storch and Martin, 1994), the patella is distinctly elongated proximodistally (Table A8). The patella is deeper anteroposteriorly than that of *Euromanis krebsi* (Storch and Martin, 1994) and most living manids (except *Manis crassicaudata*) but less so than the remarkably robust patella of *Cryptomanis* (Gaudin et al., 2006; Table A8). The patella in *Patriomanis* is sharply pointed distally, with angular lateral margins and a rugose anterior surface. Both the distal point and the surface rugosities are more strongly developed in *Cryptomanis* (Gaudin et al., 2006). The patella in *Euromanis krebsi* (Storch and Martin, 1994) and extant manids (Gaudin et al., 2009) is more ovate or rectangular and has a smooth anterior surface with rounded edges. The posterior surface of the patella in *Patriomanis* bears an articular facet that is divided nearly in half by a smooth, elevated ridge that is absent in all other pangolins (Figure 35). The rectangular articular surface is nearly flat proximodistally, whereas other pangolins possess a more concave articular surface. The medial facet is weakly concave transversely, whereas the lateral facet is almost flat. As in *Cryptomanis* (Gaudin et al., 2006) and in contrast to living pangolins, the medial portion of the patellar facet extends farther distally than the lateral portion.

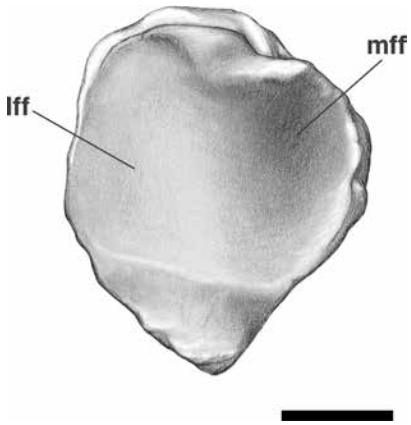

FIGURE 35. Right patella of *Patriomanis americana* (USNM-P 299960) in posterior view. Abbreviations: **lff,** lateral femoral facet; **mff,** medial femoral facet. Scale bar = 1 cm. Illustration by Julia Morgan Scott for Smithsonian Institution.

Femur

Although no femur is preserved in the type specimen (Emry, 1970), right and left femora are preserved in USNM-P 494439, the left still articulated in the acetabulum of the pelvis. Complete left and right femora (Figures 36, 37) are also preserved in USNM-P 299960 and have been prepared free of the matrix; thus, the description is largely based on these specimens.

The femoral head in *Patriomanis* is nearly hemispherical (Figure 36) but is slightly compressed along an anteromedial to posterolateral axis (Figure 37a). As in all pangolins, the head extends farther proximally than the greater trochanter. A fovea lies on the posteromedial surface of the head as in *Cryptomanis* (Gaudin et al., 2006) and *Euromanis krebsi* (Storch and Martin, 1994), although it is more medially positioned in the latter. A fovea is absent in living manids (Figure 38b,c; Gaudin et al., 2009). The femoral neck in *Patriomanis* is compressed anteroposteriorly, similar to the condition in *Cryptomanis* (Gaudin et al., 2006) and *Euromanis krebsi* (Storch and Martin, 1994).

The greater trochanter in *Patriomanis* is directed proximolaterally and is relatively narrow transversely compared to other pangolins (Table A8). Indeed, *Patriomanis* and *Cryptomanis* (Gaudin et al., 2006) differ from modern pangolins in having a greater trochanter with an anteroposterior depth greater than its transverse width. The greater trochanter in *Patriomanis* is

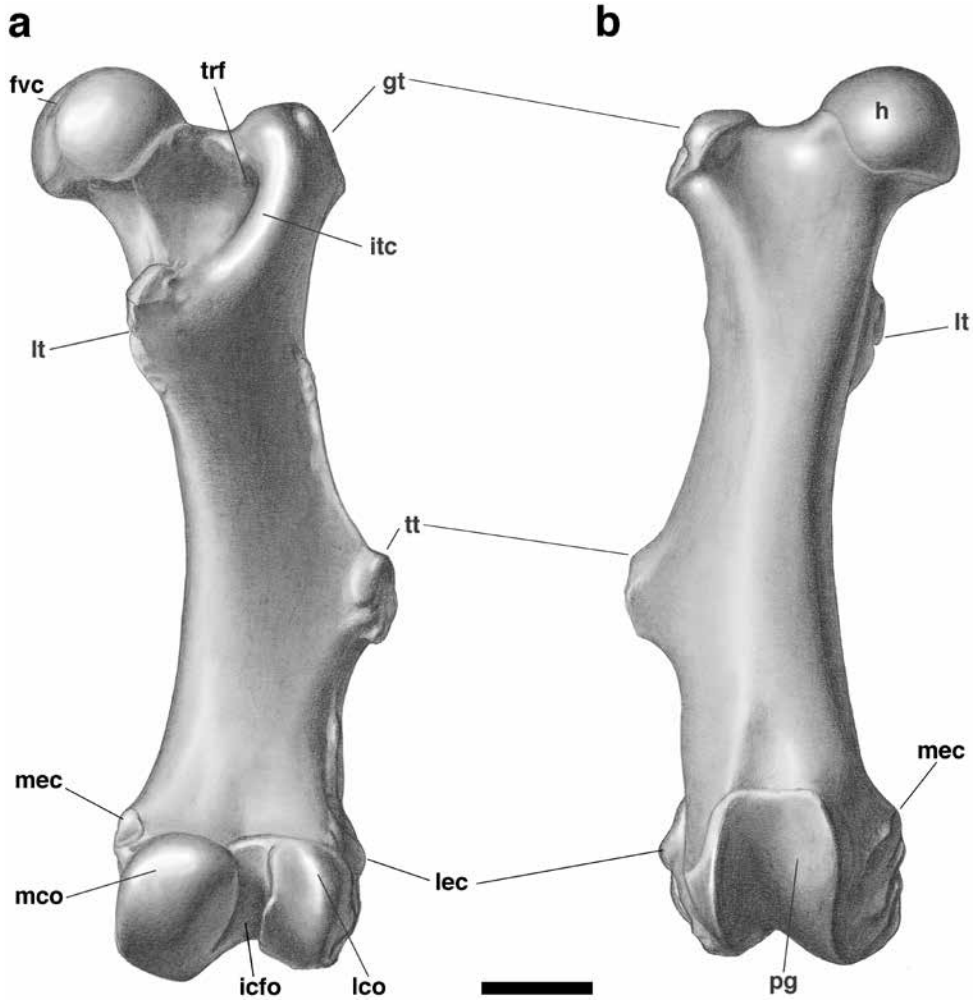

FIGURE 36. Right femur of *Patriomanis americana* (USNM-P 299960): (a) in posterior view; (b) in anterior view. Abbreviations: **fvc,** fovea capitis; **gt,** greater trochanter; **h,** head; **icfo,** intercondylar fossa; **itc,** intertrochanteric crest; **lco,** lateral condyle; **lec,** lateral epicondyle; **lt,** lesser trochanter; **mco,** medial condyle; **mec,** medial epicondyle; **pg,** patellar groove; **trf,** trochanteric fossa; **tt,** third trochanter. Scale bar = 1 cm. Illustrations drawn by Larry Isham, digitized and labeled by Julia Morgan Scott for Smithsonian Institution.

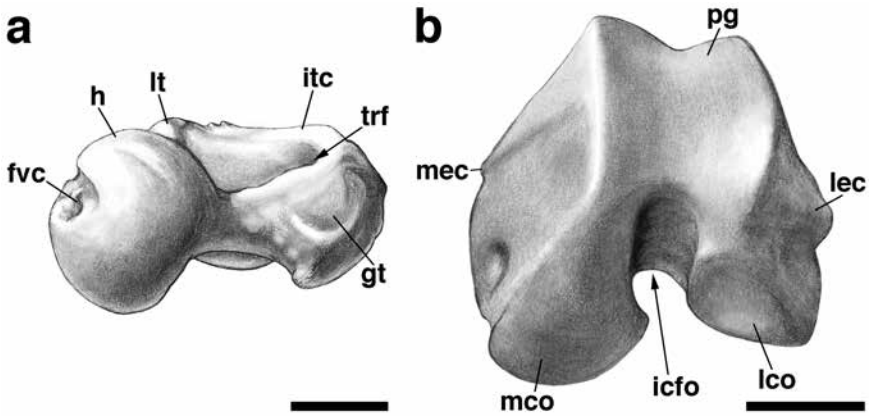

FIGURE 37. Left femur of *Patriomanis americana* (USNM-P 299960): (a) in proximal view; (b) in distal view. Abbreviations: **fvc,** fovea capitis; **gt,** greater trochanter; **h,** head; **icfo,** intercondylar fossa; **itc,** intertrochanteric crest; **lco,** lateral condyle; **lec,** lateral epicondyle; **lt,** lesser trochanter; **mco,** medial condyle; **mec,** medial epicondyle; **pg,** patellar groove; **trf,** trochanteric fossa. Scale bars = 1 cm. Illustrations by Julia Morgan Scott for Smithsonian Institution

connected to the femoral head by a narrow ridge (Figure 37a). The comparable ridge is much broader in *Cryptomanis* (Gaudin et al., 2006) and *Euromanis krebsi* (Storch and Martin, 1994). In the latter, an additional ridge extends distally from the greater trochanter on the anterior surface of the femur. The posterior surface of the proximal femur is impressed by a deep, ovate, proximodistally elongated trochanteric fossa (Figure 36a). This fossa is also present in *Necromanis* (Koenigswald, 1969, 1999; Koenigswald and Martin, 1990) and *Cryptomanis* (Gaudin et al., 2006) but is much reduced in the latter. Living pangolins lack a trochanteric fossa (Figure 38b,c; Gaudin et al., 2009). In *Patriomanis*, the trochanteric fossa is bordered posteriorly by a robust intertrochanteric ridge that extends from the greater trochanter to the lesser trochanter, although it is much less pronounced near the latter. This ridge is less developed in *Cryptomanis* (Gaudin et al., 2006) and is absent in extant manids (Gaudin et al., 2009). The lesser trochanter in *Patriomanis* projects posteromedially and lies posterior to the femoral neck (Figures 36, 37a). It is similar in morphology to that of *Necromanis* (Koenigswald, 1969, 1999; Koenigswald and Martin, 1990). In *Cryptomanis* (Gaudin et al., 2006), the lesser trochanter is more pronounced and is connected to the femoral head by a blunt ridge that is not present in *Patriomanis*. In extant pangolins the lesser trochanter tends to be more medially oriented (Figure 38b,c; Gaudin et al., 2009).

The femur in *Patriomanis* bears a robust, freestanding third trochanter that is nearly semicircular in outline with a rugose tubercle on its posterior surface (Figure 36). A similar morphology is present in *Cryptomanis* (Gaudin et al., 2006), although in this taxon the third trochanter is more robust, is broader proximodistally, and extends farther laterally. By considering the position of the third trochanter, pholidotans can be arranged in a series: *Eomanis* and *Euromanis* (Storch, 1978; Storch and Martin, 1994) have the most proximally situated third trochanter, positioned well proximal to the midshaft. In *Cryptomanis* (Gaudin et al., 2006), the third trochanter is just proximal to midshaft, whereas in *Patriomanis* it is just distal to midshaft. In *Necromanis* (Koenigswald and Martin, 1990; Koenigswald, 1999), it is well distal to midshaft. Finally, extant manids bear a third trochanter that is reduced in size and located at the distal end of the femur (Table A8; Emry, 1970; Gaudin et al., 2009). A thin, elevated ridge extends proximally from the third trochanter in *Patriomanis* and forms the lateral edge of the femur, ending just before it reaches the level of the lesser trochanter. A similar ridge extends distally from the third trochanter, terminating at the lateral epicondyle.

The femoral shaft in *Patriomanis* is more compressed anteroposteriorly than that of extant pangolins with the exception of *Smutsia gigantea* (Table A8). The femoral shaft is also somewhat compressed in *Necromanis* (Koenigswald, 1969, 1999; Koenigswald and Martin, 1990) and *Euromanis krebsi* (Storch and Martin, 1994). The femoral shaft in *Cryptomanis*, however, is significantly broader and more flattened than other pangolins (Gaudin et al., 2006). The femoral shaft in *Patriomanis* has a strongly convex anterior face, a flat posterior face, with a sharp lateral edge and a rounded medial margin connecting the medial epicondyle and the lesser trochanter. *Patriomanis* lacks any evidence of a supracondylar tuberosity like that which is prominently developed in *Cryptomanis* (Gaudin et al., 2006). *Cryptomanis* (Gaudin et al., 2006) also has an elevated ridge crossing the posterior distal surface of the femur that is absent in *Patriomanis*.

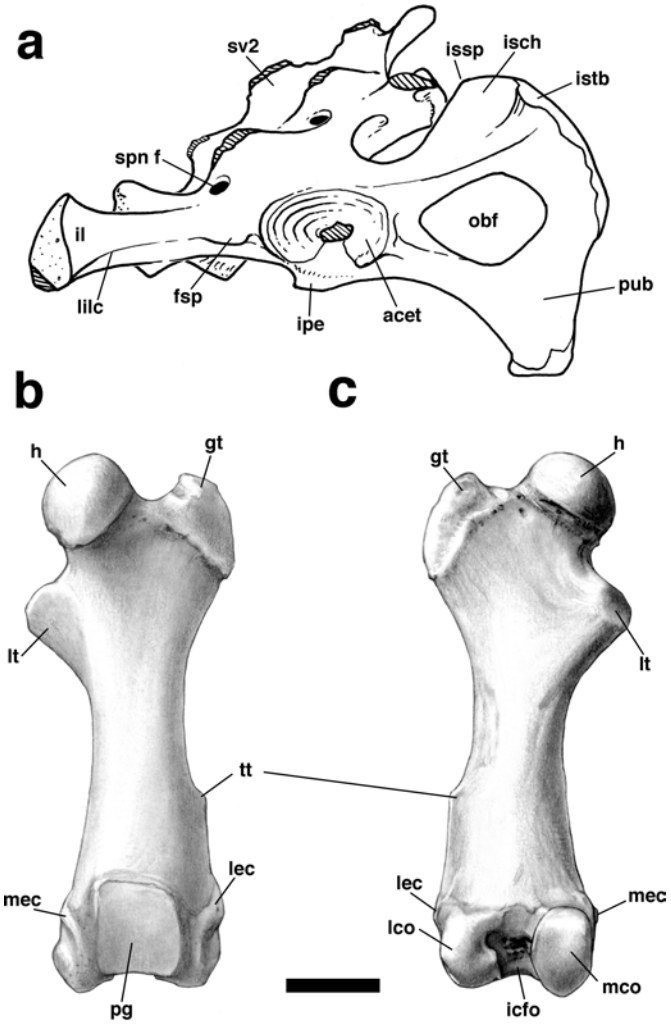

FIGURE 38. Pelvis, sacrum, and left femur of *Phataginus tricuspis* (CM 16206): (a) pelvis and sacrum in left lateral view; (b) femur in anterior view; (b) femur in posterior view. Abbreviations: **acet,** acetabulum; **fsp,** femoral spine; **gt,** greater trochanter; **h,** head; **icfo,** intercondylar fossa; **il,** ilium; **ipe,** iliopubic eminence; **isch,** ischium; **issp,** ischial spine; **istb,** ischial tuberosity; **lco,** lateral condyle; **lec,** lateral epicondyle; **lilc,** lateral iliac crest; **lt,** lesser trochanter; **mco,** medial condyle; **mec,** medial epicondyle; **obf,** obturator foramen; **pg,** patellar groove; **pub,** pubis; **spn f,** spinal nerve foramen; **sv2,** second sacral vertebra; **tf,** trochanteric fossa; **tt,** third trochanter. Scale bar = 1 cm. Illustrations by Julia Morgan Scott for Smithsonian Institution; (a) modified from Gaudin et al. (2009), (b) and (c) modified from Gaudin et al. (2006).

The distal end of the femur in *Patriomanis* is deeper than in other pangolins, with a maximum depth nearly equivalent to its maximum width (Figure 37b; Table A8). As in *Cryptomanis* (Gaudin et al., 2006) and *Smutsia gigantea* but unlike in other modern pangolins, the medial condyle is much wider than the lateral condyle (Table A8). In posterior view, the medial condyle in *Patriomanis* appears ovate, compressed transversely, and convex transversely and proximodistally. The lateral condyle is narrow transversely and rectangular in outline. It is convex proximodistally but flat transversely (Figure 36a). In *Cryptomanis* (Gaudin et al., 2006), the medial and lateral condyles have nearly the same shape but are wider transversely.

The patellar articular surface in *Patriomanis* is concave transversely, tapers slightly at its proximal end, and is inclined mediad so that it points toward the femoral head (Figures 36b, 37b). The medial edge of the facet is in line with the lateral edge of the femoral head and is slightly more elevated than the lateral edge. In *Cryptomanis* (Gaudin et al., 2006) and African tree pangolins (Figure 38b), the patellar surface is wider and less concave. In *Manis*, the patellar surface is almost flat. The intercondylar fossa in *Patriomanis* is deep and directed slightly laterally and has a uniform width throughout its extent (Figure 37b). In *Cryptomanis* (Gaudin et al., 2006), the fossa is broader and widens anteriorly.

Pelvis and Sacrum

The type specimen preserves only two small fragments of the pelvis, including the pubic symphysis and a fragment of the right acetabulum and pubis, but does not preserve the sacrum (Emry, 1970). However, a partial pelvis and sacrum are preserved in USNM-P 494439, although these have not been prepared free of the matrix. A complete pelvis and sacrum are preserved in USNM-P 299960 (Figure 39) and have been illustrated by Rose and Emry (1993).

The most obvious difference between the pelvis of *Patriomanis* and living manids is the presence of a large gluteal fossa. The ilium in *Patriomanis* is expanded medially and dorsally to form a large, deeply concave gluteal fossa that covers most of the lateral surface of the ilium. *Cryptomanis* (Gaudin et al., 2006) also possesses a large gluteal fossa. A weaker gluteal fossa is apparently present in *Necromanis* (Koenigswald and Martin, 1990). In *Euromanis krebsi* (Storch and Martin, 1994) and living pangolins (Figure 38a; Gaudin et al., 2009), however, the dorsolateral surface of the ilium is either flat or slightly convex and does not form an expanded surface.

The gluteal fossa is bordered laterally by a sharp, narrow lateral iliac crest (Figure 39b). The anterior end of the lateral iliac crest is confluent with a prominent, laterally projecting cranial ventral iliac spine. The posterior termination of the lateral iliac crest lies at the ventral

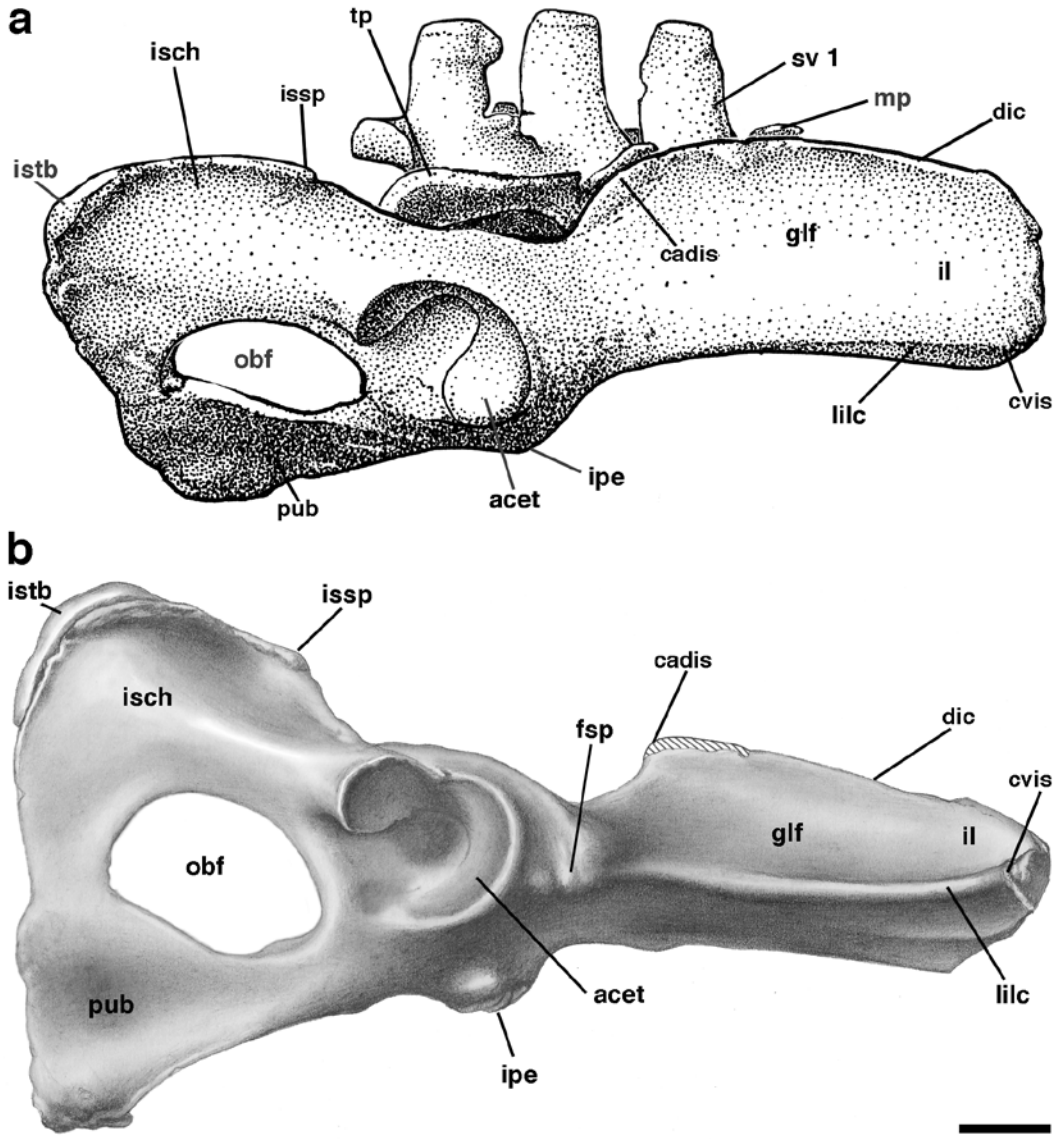

FIGURE 39. Right pelvis of *Patriomanis americana* (USNM-P 299960): (a) pelvis and sacral vertebrae in lateral view; (b) pelvis in ventrolateral view. Abbreviations: **acet,** acetabulum; **cadis,** caudal dorsal iliac spine; **cvis,** cranial ventral iliac spine; **dic,** dorsal iliac crest (= medial dorsal flange of ilium in Gaudin et al., 2009); **fsp,** femoral spine; **glf,** gluteal fossa; **il,** ilium; **ipe,** iliopubic eminence; **isch,** ischium; **issp,** ischial spine; **istb,** ischial tuberosity; **lilc,** lateral iliac crest; **mp,** metapophysis of first sacral vertebra; **obf,** obturator foramen; **pub,** pubis; **sv,** sacral vertebra; **tp,** transverse processes of third and fourth sacral vertebrae. Scale bar = 1 cm. Illustration (a) by Julia Morgan Scott (JMS) for Smithsonian Institution (SI); (b) drawn by Larry Isham, digitized and labeled by JMS for SI.

edge of the femoral spine. In *Euromanis krebsi* (Storch and Martin, 1994) the lateral iliac crest is developed to a similar extent, although it is less sharp than that of *Patriomanis,* and it appears to extend somewhat farther posteriorly, reaching the anterior margin of the acetabular eminence. The lateral iliac crest of extant manids is rounded and often poorly demarcated. The gluteal fossa in *Patriomanis* is bordered dorsally and medially by an elevated dorsal iliac crest (= medial dorsal flange of ilium in Gaudin et al., 2009) that is slightly folded over laterally along its upper edge. A weak cranial dorsal iliac spine lies just medial and ventral to the dorsal iliac crest near its

anterior end (not visible in Figure 39 because it lies on the medial surface of the ilium). Posteriorly, the dorsal iliac crest terminates at an elevated caudal dorsal iliac spine that projects slightly mediad. *Euromanis krebsi* (Storch and Martin, 1994) exhibits a weak caudal dorsal iliac spine but lacks a distinct dorsal iliac crest or cranial dorsal iliac spine. Living manids lack all of these structures (Gaudin et al., 2009).

The cranial surface of the ilium in *Patriomanis* bears a triangular iliac crest that reflects the roughly triangular shape of the body of the ilium. The ventrolateral iliac surface is flat, with sharp edges separating it from the dorsolateral and medial surfaces. The auricular surface is flat, oval, and rugose and covers the posterior half of the medial face of the ilium. This articular surface shares a broad border with the ventral edge of the ilium, whereas it contacts only the dorsal edge of the ilium at the caudal dorsal iliac spine and the sloping dorsal ridge behind it. The auricular surface terminates posteriorly just anterior to the leading edge of the acetabulum, resembling the condition in *Cryptomanis* (Gaudin et al., 2006) and *Euromanis krebsi* (Storch and Martin, 1994). In *Phataginus,* the sacroiliac attachment extends posteriorly to the center of the acetabular fossa (Figure 38a), whereas in *Manis* and *Smutsia* it extends even farther posteriorly (Gaudin et al., 2009). The body of the ilium runs nearly parallel to the sacrum (Figure 39a), the angle between the two approximating 10°, whereas in extant pangolins the dorsal margin of the pelvis is steeply inclined in an anterodorsal to posteroventral orientation (Figure 38a), with the angle between the pelvis and sacrum at least twice as large as that of *Patriomanis* (Gaudin et al., 2009).

The ventral junction of the ilium and pubis is marked by a robust, anteroposteriorly broad iliopubic eminence (Figure 39b). This process is well developed in all pangolins. The femoral spine is rounded and rather indistinct and lies on the acetabular eminence, nearly in line vertically with the iliopubic eminence. The femoral spine takes on a similar appearance in *Cryptomanis* and *Necromanis* (Koenigswald and Martin, 1990), although its position is difficult to compare because the iliopubic eminence is not preserved in available material of either taxon. In extant pangolins (except for *M. crassicaudata* and some *M. pentadactyla*; Gaudin et al., 2009), however, the femoral spine is often more robust and is situated well anterior to the iliopubic and acetabular eminences, displaced forward along the lateral iliac crest (Figure 38a).

The acetabular fossa in *Patriomanis* is broad and ovate, with a U-shaped articular (lunate) surface for the femoral head interrupted by a wide opening that faces posteriorly and ventrally (Figure 39). The posterodorsal limb of the lunate surface is undercut ventrally by a deep fossa that separates it from the lateral surface of the ischium. In both respects it closely resembles the condition in *Euromanis krebsi* (Storch and Martin, 1994). In living pangolins, the two arms of the lunate surface approach one another more closely and may even contact one another, while the opening between them rotates either posteriorly (*Manis, Smutsia*) or ventrally (*Phataginus*; Figure 38a; Gaudin et al., 2009).

The ischium in *Patriomanis* is flattened transversely, although, as in other pangolins, its lateral surface is marked by a rounded ridge connecting the posterodorsal arm of the acetabular lunate surface to the ischial tuberosity. The element appears deeper dorsoventrally than that of other pangolins because of the position and orientation of the ischial spine. The spine is erect, pointing dorsally. It is situated along the dorsal margin of the ischium, well anterior to the ischial tuberosity, lying over the anterior portion of the obturator foramen (Figure 39). It is connected by a crest to the ischial tuberosity and is roughly in line with the body of the ischium and the tuberosity, the latter being only weakly flared laterally. Gaudin et al. (2006) described a similar condition in *Cryptomanis* and noted that in modern pangolins the ischial spine is displaced posteriorly and inflected medially, whereas the ischial tuberosity is more strongly flared laterally (Figure 38a). *Euromanis krebsi* (Storch and Martin, 1994) shows a mixture of these conditions, with an anteriorly situated, medially inflected ischial spine and an ischial tuberosity that is not flared laterally.

As described by Emry (1970), the pubis extends ventrally and posteriorly from the iliopubic eminence toward the pubic symphysis. Its shaft is flattened transversely and flares strongly toward its posterior end in both a dorsal and ventral direction (Figure 39b). This is similar to the condition in other pangolins (Gaudin et al., 2009), although in *Euromanis krebsi* (Storch and Martin, 1994) the pubis is not strongly flattened, and in neither *Euromanis* nor *Eomanis* (Storch, 1978; Storch and Martin, 1994) is the pubis so strongly flared distally, whereas in modern pangolins the pubis is more strongly downturned ventrally as it approaches the symphysis (Figure 38a). All pangolins possess a short pubic symphysis. In *Patriomanis*, the pubic symphysis is extremely short and bears a triangular ossification on its posterior edge (Emry, 1970). In ventral view, the anterior edge of the pubic symphysis is narrow and V shaped, and the posterior edge takes the form of a broad, shallow U. *Eomanis* (Storch, 1978) displays a similar morphology. In extant manids, however, both edges

are broadly U shaped, with the posterior curvature being much shallower.

As in other pangolins, the obturator foramen in *Patriomanis* is relatively small and ovate, its maximum diameter only slightly more than 1.25 times the maximum diameter of the acetabulum (Figure 39b). By comparison, the diameter of the obturator foramen in the opossum *Caluromysiops* (Gaudin, unpublished data), the basal carnivoran *Nandinia,* and the palaeanodont *Metacheiromys* is approximately twice that of the acetabulum (Gaudin et al., 2009). The foramen is ovate, with its long axis running anteroposteriorly, similar to the condition in *Manis* or *Smutsia*. In *Phataginus* the opening is more circular, whereas in *Eomanis* and *Euromanis* (Storch, 1978; Storch and Martin, 1994) it is more triangular, tapering anteriorly.

The sacrum in *Patriomanis* comprises three fused vertebrae (Figure 40). As in *Euromanis krebsi* (Storch and Martin, 1994), *Cryptomanis* (Gaudin et al., 2006), and *Phataginus* (Gaudin et al., 2009), which also have three sacrals, only the anterior two sacral vertebrae are attached to the pelvis, and the attachment is restricted to the ilium (Figures 39a, 40b). In *Manis* and *Smutsia*, the sacrum incorporates three to four vertebrae, at least three are attached to the pelvis, and the attachment extends posteriorly to include the anterior part of the ischium (Gaudin et al., 2009). In fossil pangolins, the iliosacral junction is sutural, whereas the joint fuses in adults of extant taxa (Gaudin et al., 2009). The transverse process of the first sacral vertebrae and the anterior portion of the second are expanded dorsoventrally in *Patriomanis* to accommodate the auricular surface. In contrast, the transverse process of the third sacral vertebrae and the posterior portion of the second are thin dorsoventrally but greatly expanded anteroposteriorly to form a winglike structure. The lateral edges of these latter processes overlie the medial edge of the ischium. In most extant manids, the transverse process of the last sacral vertebra is cylindrical or rod shaped, is unexpanded anteroposteriorly, and extends far laterally beyond the body of the ischium (Gaudin et al., 2009). In living pangolins this transverse process also bears a process on its ventral surface for the sacrospinous ligament (Gaudin et al., 2009) that is absent in *Patriomanis*. The neural spines of the sacrum in *Patriomanis* are tall and robust, and the metapophyses are short, such that the heights of the former are more than twice that of the latter (Figures 39a, 40b). *Euromanis krebsi* (Storch and Martin, 1994) is similar, although the neural spines are somewhat lower and broader anteroposteriorly. In extant manids, the sacral metapophyses tend to be elongated so that they

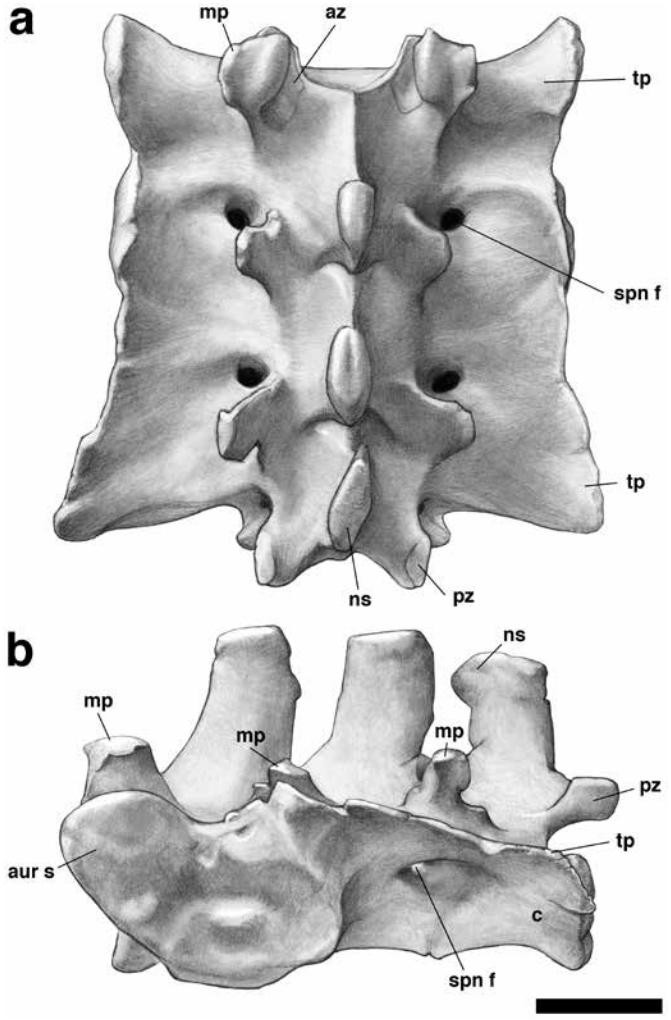

FIGURE 40. Sacrum of *Patriomanis americana,* USNM-P 299960: (a) in dorsal view; (b) in left lateral view. Abbreviations: **aur s,** auricular surface; **az,** anterior zygapophysis; **c,** centrum; **mp,** metapophysis; **ns,** neural spine; **pz,** posterior zygapophysis; **spn f,** foramen for spinal nerve; **tp,** transverse process. Scale bar = 1 cm. Illustrations by Julia Morgan Scott for Smithsonian Institution.

are nearly equal in height with the neural spines (Gaudin et al., 2009). The sacral neural spines and metapophyses are distinct and separate from one another in fossil pangolins, whereas in some modern pangolins these elements fuse to varying degrees (Gaudin et al., 2006, 2009). Gaudin et al. (2006) described the ventral surface of the sacral vertebrae in *Cryptomanis,* noting that the centra are "bulbous" with anteroposteriorly elongated ventral sacral foramina. They contrast this with the condition in extant forms, in which the centra have a flat surface and circular sacral foramina. In this respect the sacral vertebrae

in *Patriomanis* resemble the condition in modern forms rather than that of *Cryptomanis*.

Forelimb

FIGURES 41–52; TABLES A9–A13

Scapula

A complete scapula is not preserved. However, the morphology of nearly the entire element can be reconstructed on the basis of the available material, with the exception of the anterior edge (Figure 41c). Contrary to the initial report in Emry (1970), there is a substantial portion of the right scapula preserved in the type specimen. This specimen includes the entire scapular spine but for its ventral tip, as well as the central portion of the dorsal border and most of the glenoid, although the anterior and posterior scapular borders, along with most of the supraspinous and infraspinous fossae, are broken away (Figure 41b). In USNM-P 299960, a portion of the right scapula is also preserved, including nearly the whole ventral portion of the bone with an intact glenoid articulation, most if not all of the posterior border, and the ventral reaches of the scapular spine (Figure 41a). Once again, the ventral tip of the scapular spine has been worn away, so that the morphology of the acromion process cannot be unequivocally reconstructed. This specimen has been illustrated in Rose and Emry (1993: fig. 7.5). USNM-P 299960 also preserves the glenoid region from the left scapula. Portions of both the left and right scapula are preserved in USNM-P 494439, including, most importantly, the entire dorsal border posterior to the scapular spine, the posterior angle, and the dorsal portions of the posterior border on the left side (Figure 2). Neither scapula has been prepared free from the matrix in USNM-P 494439.

The scapula in modern pangolins tends to be broad and rectangular in shape (Figure 41d). Indeed, it is almost square in some taxa, with the maximum anteroposterior length roughly equal to the maximum dorsoventral height. More particularly, the supraspinous fossa is generally rectangular, whereas the infraspinous fossa is triangular, broad dorsally but narrowing ventrally, the straight posterior border of the scapula forming an acute (roughly 60°) angle with the dorsal border. The shape of the supraspinous fossa cannot be determined in *Patriomanis,* but the infraspinous fossa can be reconstructed in its entirety, and its shape resembles that of the modern forms. The posterior angle is more rounded than in extant manids and lacks the suprascapular ossification present in these taxa (Figure 41d), being marked instead in USNM-P 494439 by a series of jagged points that might be the result of postmortem breakage or damage incurred in preparation (Figure 41c). In both *Euromanis* and *Eomanis* (Storch and Martin, 1994; Storch, 2003) the scapula is much narrower and more triangular in appearance, largely because of the narrower supraspinous and infraspinous fossae. The latter is much less expanded dorsally, especially in *Eomanis,* so that the angle between the posterior and dorsal borders is approximately 75°. Only the region immediately around the glenoid is preserved in the known specimens of *Cryptomanis* (Gaudin et al., 2006) and *Necromanis* (Koenigswald and Martin, 1990), so the overall shape of the scapula cannot be compared to that of *Patriomanis*.

The supra- and infraspinous fossae of extant pangolins typically extend dorsally to contact the dorsal border of the scapula, whereas in *Patriomanis* there is a ridge marking the upper limit of these depressions that lies below the dorsal border, meaning that a small sliver of scapula would have been exposed above the infraspinatus and supraspinatus muscles. *Eomanis* and *Euromanis* (Storch and Martin, 1994; Storch, 2003) resemble the extant taxa in this regard. The scapular spine in *Patriomanis* is tall and folded over posteriorly along its lateral edge. When viewed distally, the height of the scapular spine is nearly equivalent to the maximum width of the glenoid fossa, much higher than that in modern pangolins, where scapular spine height ranges from 65% to 80% of the maximum width of the glenoid (Table A9; Gaudin et al., 2009). The spine is also more elongated than in modern forms, extending close to, but not quite reaching, the dorsal border of the scapula. In extant manids, the spine ends at a noticeably more ventral point. With respect to the height and length of the scapular spine, *Euromanis* and *Eomanis* more closely resemble *Patriomanis* than the condition in Manidae (Storch and Martin, 1994; Storch, 2003; Gaudin et al., 2009). As noted above, the acromial end of the scapular spine is damaged in both the type specimen and USNM-P 299960. The preserved portion of the acromion in the latter specimen (Figure 41a; Rose and Emry, 1993: fig. 7.5) closely resembles the morphology of the acromion in *Manis javanica* (USNM 198852; see Rose and Emry, 1993: fig. 7.5), in which the acromion is short, is bent slightly forward at its tip, and bears what appears to be a rudimentary metacromion process along its posterior margin. However, the damage to the lateral surface leaves open the possibility that a better-developed acromion and a better-developed metacromion were present in *Patriomanis*. Other living pangolins tend either to resemble the condition in *M. javanica* or to exhibit even

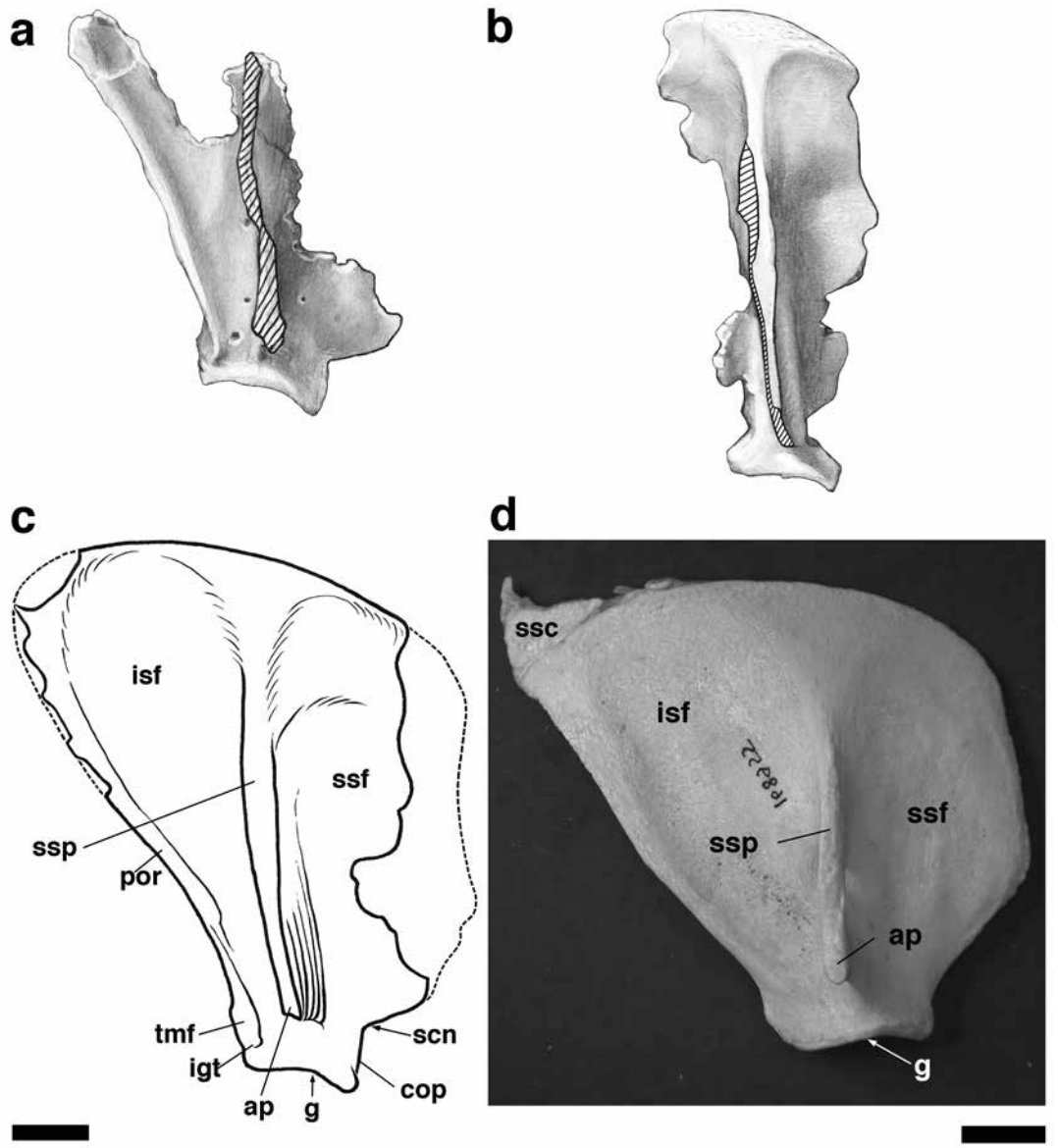

FIGURE 41. Scapula of *Patriomanis americana* and extant pangolin *Smutsia temminckii*: (a) right scapula of *P. americana*, USNM-P 299960, in lateral view; (b) right scapula of *P. americana*, F:AM 78999 (holotype), in lateral view; (c) composite reconstruction of right scapula of *P. americana* in lateral view; (d) left scapula (reversed image) of *S. temminckii* (AMNH 168955) in lateral view. Abbreviations: **ap,** acromion process; **cop,** coracoid process; **g,** glenoid cavity; **igt,** infraglenoid tubercle; **isf,** infraspinous fossa; **por,** posterior ridge of infraspinous fossa; **scn,** scapular notch; **ssc,** suprascapular ossification; **ssf,** supraspinous fossa; **ssp,** spine of scapula; **tmf,** teres minor fossa. Cross-hatched areas represent broken surfaces. Scale bars = 1 cm. Illustrations (a)–(c) by Julia Morgan Scott (JMS) for Smithsonian Institution (SI); photo (d) by Tim Gaudin, composed and labeled by JMS for SI.

less development of the acromion, with a blunt rounded process that lacks even the rudiment of a metacromion (Figure 41d). In contrast, both *Euromanis* and *Eomanis* (Storch and Martin, 1994; Storch, 2003) possess an extremely elongated acromion process, extending ventrally far past the glenoid to lie lateral to the proximal humerus (although not contacting the humerus), much as in the palaeanodont *Metacheiromys* (Simpson, 1931).

Neither *Eomanis* nor *Euromanis* shows any evidence of a separate metacromion, however, in strong contradistinction to *Metacheiromys*.

The posterior border of the scapula in *Patriomanis* is marked for most of its length by an elevated lateral crest that becomes sharper ventrally (Figure 41a,c). A prominent secondary scapular spine is present in *Eomanis* and *Euromanis* (Storch and Martin, 1994; Storch, 2003; Gaudin et al., 2009) but is lacking in living pangolins (Figure 41d). Instead, the posterior border is marked laterally by a low, rounded eminence in these taxa. The sharp, ventral portion of the posterior ridge in *Patriomanis* is marked by a shallow but distinct, dorsoventrally elongate fossa along its posterior surface (Figure 41a,c). This fossa is likely a site for muscle origin—in other placental mammals (e.g., *Canis,* Evans and Christensen, 1979; *Tenrec,* Neveu and Gasc, 2002) this area serves as the site of origin for the m. teres minor and the m. triceps brachii caput longum. Modern pangolins are known to possess both a scapular insertion of the m. triceps brachii long head (Humphry, 1870; Windle and Parsons, 1899) and a distinct m. teres minor (Windle and Parsons, 1899). In Gaudin et al. (2009: char. 203) this depression is called a "teres minor fossa" because of its position and its relatively small size, but in fact, it could have accommodated the origin of the teres minor along with the long head of the triceps in whole or in part. This depression is also present in *Euromanis* and *Eomanis* but is absent in *Necromanis* and extant pangolins (Gaudin et al., 2009). At the ventral terminus of the posterior ridge, the scapula of *Patriomanis* is marked by a prominent infraglenoid tuberosity (Figure 41a,c), a feature also present in *Cryptomanis* and living manids but not well developed in *Euromanis* or *Eomanis* (Storch and Martin, 1994; Storch, 2003).

The glenoid fossa in *Patriomanis* is generally egg shaped in outline, narrowing slightly at its anterior end. It is gently concave both transversely and anteroposteriorly, with its anterior terminus extending somewhat farther ventrally than its posterior end in lateral view. It differs in only minor respects from the glenoid morphology of other extinct and extant pangolins. For example, in *Cryptomanis* and in *Smutsia,* the outline of the glenoid is straighter along the medial edge and more convex along the lateral edge, whereas in *Euromanis* the glenoid outline is more rounded and does not narrow anteriorly as in other pangolins. *Cryptomanis* (Gaudin et al., 2006) is described as having a rudiment of the coracoid process in the form of a small but distinct tubercle. There is a rugosity on the anterior margin of the glenoid in *Patriomanis* that likely represents an even less developed version of the coracoid process (Figure 41a,c). A similar morphology exists in most modern pangolins, where a low knob or rugosity is often developed in this area, contrary to claims by Horovitz (2003) that no vestige of the process can be found in living pangolins.

Although most of the anterior edge of the scapula is lacking in the available *Patriomanis* specimens, USNM-P 299960 preserves enough of the ventral portion of the supraspinous fossa to show that it extended well anterior to the anterior edge of the glenoid and that the ventral edge of the supraspinous fossa was marked by a low, broad scapular notch like that in many extant pangolins (Figure 41a,c).

Clavicle

Although a clavicle is known to occur in both *Eomanis* (Storch, 1978) and *Euromanis* (Storch and Martin, 1994), it has not been recovered in either *Necromanis* or *Cryptomanis* and is definitely lacking in living Manidae (Gaudin et al., 2009). No vestige of the clavicle has been recovered with any of the known *Patriomanis* specimens. Given the completeness of this material, there is strong negative evidence that the clavicle was absent in *Patriomanis* as well.

Humerus

In the type specimen, only the distal portion and a partial shaft of the humerus are preserved (Emry, 1970). However, a complete left and partial right humerus are available from USNM-P 531556. A damaged right humerus is available from USNM-P 494439, and the essentially complete left humerus is also present, although still in place, incompletely prepared, on the underside of the block; a nearly complete right humerus is available from USNM-P 299960 (Figures 38, 39) and has been illustrated by Rose and Emry (1993).

The humeral head in *Patriomanis* is strongly convex both transversely and longitudinally and ovoid, with its long axis tilted slightly in a distomedial direction as in other pangolins (Figure 42b; Gaudin et al., 2006, 2009). The head is flanked by prominent greater and lesser tubercles and is separated from the former in proximal view by a deep, anteroposteriorly elongated fossa (Figure 43a). This fossa, which presumably accommodates the tendon of origin of the m. biceps brachii passing laterally to insert on the "outer surface … of the glenoid cup" (Humphry, 1870:37), is also present and even more sharply defined in modern *Manis* but is absent in living African pangolins.

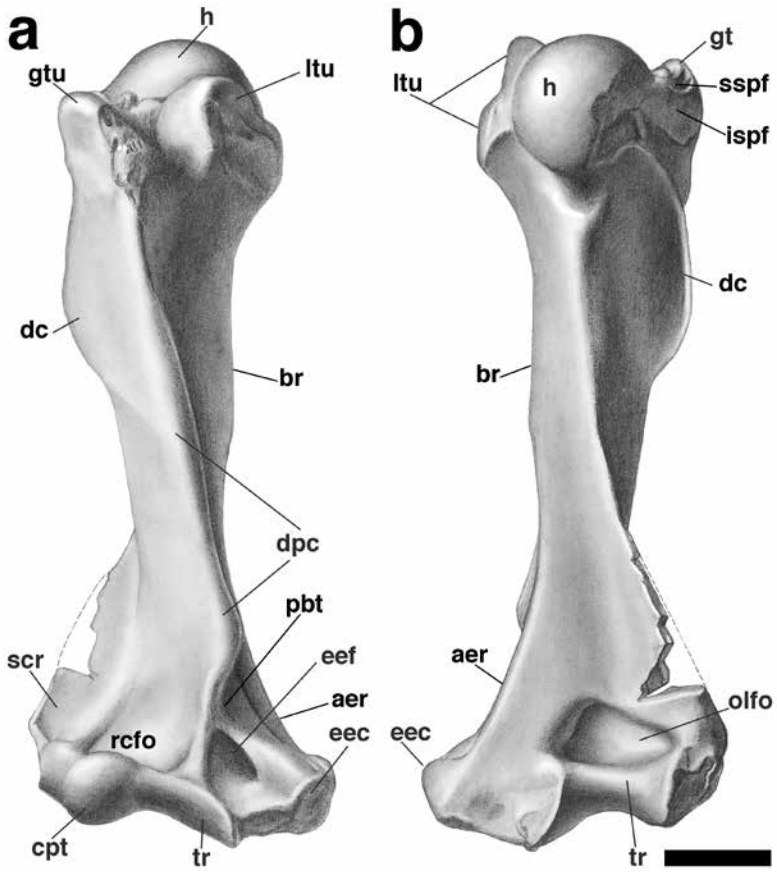

FIGURE 42. Right humerus of *Patriomanis americana* (USNM-P 299960): (a) in anterior view; (b) in posterior view. Abbreviations: **aer,** ascending entepicondylar ridge; **br,** bicipital ridge; **cpt,** capitulum; **dc,** deltoid crest; **dpc,** deltopectoral crest; **eec,** entepicondyle; **eef,** entepicondylar foramen; **gtu,** greater tubercle; **h,** head; **ispf,** fossa for m. infraspinatus; **ltu,** lesser tubercle; **olfo,** olecranon fossa; **pbt,** pulley for tendon of m. biceps brachii; **rcfo,** confluent radial and capitular fossa; **scr,** supinator crest; **sspf,** fossa for m. supraspinatus; **tr,** trochlea. Scale bar = 1 cm. Illustrations drawn by Larry Isham, digitized and labeled by Julia Morgan Scott for Smithsonian Institution.

The greater tubercle in *Patriomanis* is elongated along a posterolateral to anteromedial axis, beginning at the midpoint of the head and extending far anteriorly to form a freestanding process (Figure 43a). It is flat laterally and forms a sharp lateral crest along its proximal margin that is continuous with the proximal end of the pectoral crest at its most anterior and medial point (Figure 42a). It extends proximally just beyond the level of the lesser trochanter but not as far as the humeral head. The greater tubercle is similar in *Necromanis* (Koenigswald, 1969, 1999; Koenigswald and Martin, 1990) and extant manids, although in the living forms it typically does not extend as far anteriorly or medially. In *Cryptomanis*, the greater tubercle is divergent posterolaterally and extends farther posteriorly than in *Patriomanis* (Gaudin et al., 2006). (Note that Gaudin et al.'s description of the proximal humerus contains a lapsus. The fragment identified as the proximal right humerus is, in fact, the left proximal humerus. The greater tuberosity [= greater tubercle] has been correctly identified and described, but in the illustration of this element in their fig. 6 the proximal humerus should be transposed horizontally, so that the broken deltopectoral crest points toward the greater tubercle.) Two pits are present on the posterior end of the greater tubercle in USNM-P 531556 (Figures 42b, 43a). The proximal pit is elongated along the posterior one-third of the proximal tubercular crest and is likely an insertion surface for the m. supraspinatus (based on analogy with the dog; Evans and Christensen, 1979; see also Humphry, 1870). The larger, circular distal pit is likely an insertion for the m. infraspinatus and possibly the m. teres minor (Humphry, 1870; Evans and Christensen, 1979).

The lesser tubercle in *Patriomanis* projects from the anteromedial edge of the head and forms a prominent knob (Figures 42, 43a). It is blunt with a broad base that is elongated distally, posteriorly, and slightly laterally from its proximal tip. The process is compressed orthogonal to this axis. In *Necromanis* (Koenigswald and Martin, 1990; Koenigswald, 1999), the lesser tubercle is of similar size and position. In modern manids (Figure 44a,b), the lesser tubercle is larger and more elongated, is positioned more medially at its base, and does not extend as far proximally as in *Patriomanis* and *Necromanis*. A distinct U-shaped groove is present on the anterior surface of the proximal humerus in *Patriomanis*. This groove is formed by the anterior extensions of the greater and lesser tubercles and

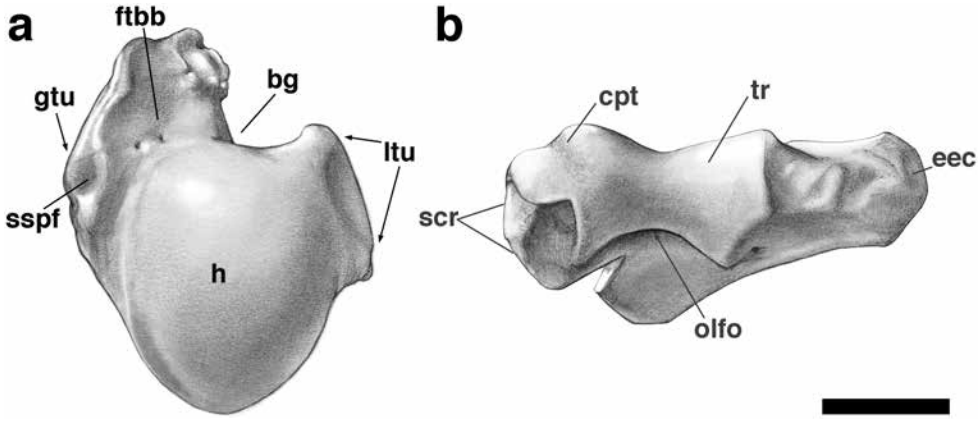

FIGURE 43. Right humerus of *Patriomanis americana* (USNM-P 299960): (a) in proximal view; (b) in distal view. Abbreviations: **bg,** bicipital groove; **cpt,** capitulum; **eec,** entepicondyle; **ftbb,** fossa for tendon of m. biceps brachii; **gtu,** greater tubercle; **h,** head; **ltu,** lesser tubercle; **olfo,** olecranon fossa; **scr,** supinator crest; **sspf,** fossa for m. supraspinatus; **tr,** trochlea. Scale bar = 1 cm. Illustrations by Julia Morgan Scott for Smithsonian Institution.

allows for the passage of the tendon of origin of the m. biceps brachii (Figure 43a; Humphry, 1870; Evans and Christensen, 1979). This groove is present in *Necromanis* (Koenigswald and Martin, 1990; Koenigswald, 1999), but it is strongly reduced or absent in extant Manidae (Gaudin et al., 2009).

The highly derived humeral shaft of fossil pangolins is very distinct from that of living manids. As described by Emry (1970) in the type specimen, the deltopectoral crest in *Patriomanis* extends from the greater tubercle to the proximal end of the entepicondylar bridge (Figure 42a) and is longer than that of any extant manid (Figure 44a,b; Table A10; Gaudin et al., 2009). Although the deltopectoral crest is incomplete in the type, the complementary portions in subsequently collected specimens confirm the reconstruction by Emry (1970). The deltopectoral crest projects farther medially than the shaft and is strongly folded over medially to form a deep concavity for the m. biceps brachii (Gaudin et al., 2006). Just proximal to the junction with the entepicondylar bridge, the deltopectoral crest ends abruptly in a pulley that accommodates the distal tendon of the m. biceps brachii (Figure 42a; Emry, 1970). *Cryptomanis* (Gaudin et al., 2006) and *Necromanis* (Helbing, 1938; Koenigswald and Martin, 1990; Koenigswald, 1999) also possess a robust deltopectoral crest with a distal pulley for the biceps tendon. In extant manids, the deltopectoral crest tends to be less robust than in patriomanids and *Necromanis*, whereas in *Eomanis* (Storch, 2003) a robust, broad deltopectoral platform is present that differs from the narrower, more elongate crest of the patriomanids and *Necromanis*. A distal pulley is present in *Manis* and *Smutsia gigantea* but is absent in *Eomanis* and the other modern African species (Gaudin et al., 2009). Like *Necromanis* (Koenigswald and Martin, 1990; Koenigswald, 1999), *Patriomanis* possesses a prominent deltoid crest extending from roughly the midpoint of the deltopectoral crest laterally and proximally, eventually turning posteriorly and continuing proximally before terminating at a point very close to the posterior edge of the greater tubercle (Figure 42). A similar deltoid crest is present in *Manis* and *Smutsia* but is absent in *Phataginus* (Gaudin et al., 2009).

The humeri of USNM-P 299960 and USNM-P 531556 confirm Emry's (1970) surmise, based on the type, of a crest extending from the posterior wall of the entepicondylar foramen to the lesser tubercle. The proximal portion of this crest is composed of a prominent bicipital ridge like that found in *Cryptomanis* (Gaudin et al., 2006) and *Necromanis* (Koenigswald and Martin, 1990; Koenigswald, 1999), extending distally from the lowermost edge of the lesser tubercle to the midshaft, where it is marked by a low, proximodistally elongate tuberosity. The lower edge of this tuberosity is joined by a crest ascending from the posterior wall of the entepicondylar foramen (Figure 42). The latter is sharp edged distally but becomes more rounded proximally. Together the bicipital ridge and this

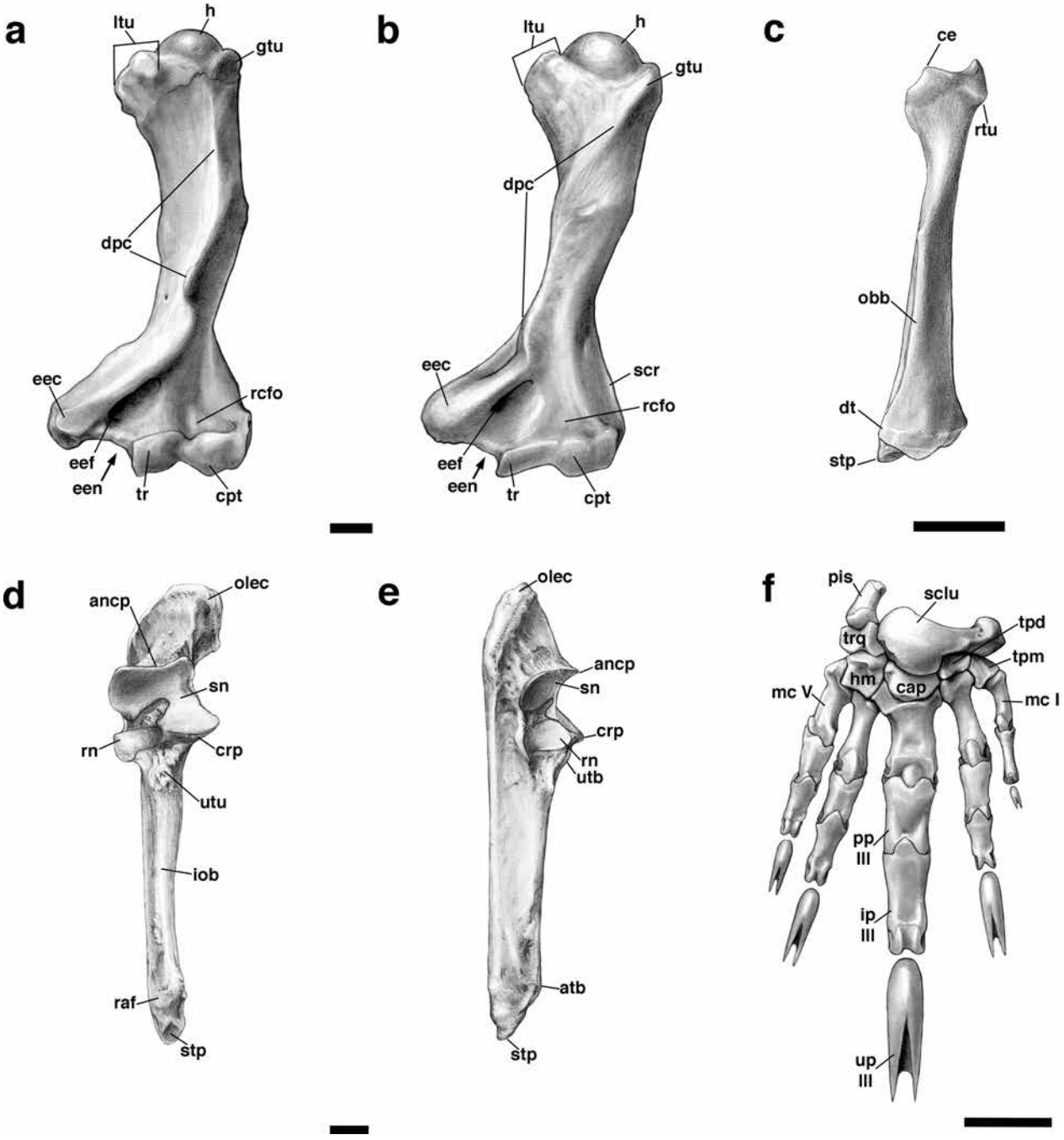

FIGURE 44. Forelimb skeleton of modern pangolins: (a) left humerus of *Phataginus tricuspis* (CM 16206) in anterior view; (b) left humerus of *Manis javanica* (USNM 198852) in anterior view; (c) left radius of *P. tricuspis* (CM 16206) in anterior view; (d) left ulna of *Smutsia gigantea* (AMNH 53858) in anterior view; (e) left ulna of *S. gigantea* (AMNH 53858) in lateral view; (f) right manus of *P. tricuspis* (CM 16206) in dorsal view (unguals reconstructed on the basis of other specimens). Abbreviations: **I–V,** digits I–V; **ancp,** anconeal process; **atb,** anterior tubercle; **cap,** capitate; **ce,** capitular eminence (= anterior proximal medial process of Gaudin et al., 2009); **cpt,** capitulum; **crp,** coronoid process; **dpc,** deltopectoral crest; **dt,** dorsal tubercle; **eec,** entepicondyle; **eef,** entepicondylar foramen; **een,** entepicondylar notch; **gtu,** greater tubercle; **h,** head; **hm,** hamate; **iob,** interosseous border; **ip,** intermediate phalanx; **ltu,** lesser tubercle; **mc,** metacarpal; **obb,** oblique border; **olec,** olecranon; **pis,** pisiform; **pp,** proximal phalanx; **raf,** radial facet; **rcfo,** confluent radial and capitular fossa; **rn,** radial notch; **rtu,** radial tuberosity; **sclu,** scapholunar; **scr,** supinator crest; **sn,** sigmoid notch; **stp,** styloid process; **tpd,** trapezoid; **tpm,** trapezium; **tr,** trochlea; **trq,** triquetrum; **up,** ungual phalanx; **utb,** ulnar tuberosity. Scale bars = 1 cm. Parts (a), (b), (c), and (f) modified from Gaudin et al. (2009) by Julia Morgan Scott (JMS) for Smithsonian Institution (SI); (d) and (e) created by JMS for SI.

ascending entepicondylar crest form the elevated posterior margin of the trough for the m. biceps brachii. In extant pangolins, the bicipital ridge is less pronounced.

The supinator crest in *Patriomanis* is damaged in both specimens, but enough is preserved to confidently infer its morphology. It begins in the middle of the posterior surface of the shaft and curves laterally to join the lateral edge of the ectepicondyle. The crest has a thin, sharp lateral margin and carries a weak distal concavity on its anterior surface just proximal to the anteroposteriorly e expanded ectepicondyle (Figure 42a). However, the supinator crest in *Patriomanis*, *Necromanis* (Koenigswald and Martin, 1990; Koenigswald, 1999), and extant Manidae (Figure 44a,b; Gaudin et al., 2009) is weakly developed compared to that in *Cryptomanis* (Gaudin et al., 2006) and *Eomanis* (Storch, 2003; Rose et al., 2005), in which the supinator crest is enlarged and flared laterally.

As described by Emry (1970), the trochlea in *Patriomanis* has a weakly concave distal margin in posterior view. It is strongly convex anteroposteriorly. As is typical for placental mammals (e.g., Homberger and Walker, 2004), the posterior surface of the trochlea is deeply concave in distal view (Figure 43b). In contrast, the anterior surface is slightly convex. The medial edge of the trochlea is sharp. It forms a small medial lappet along its distal surface that extends a short distance under the entepicondyle and represents the distalmost point on the humerus. *Necromanis* (Koenigswald and Martin, 1990; Koenigswald, 1999) and *Manis* (Gaudin et al., 2009) have a similarly shaped trochlea with a similar medial projection. The trochlea of *Cryptomanis* also has a slightly concave distal edge but lacks a medial projection (Gaudin et al., 2006). Emry (1970) describes the capitulum in *Patriomanis* as spherical and unkeeled, similar to that in living manids. A lateral extension is present on the capitulum in *Patriomanis* that covers a small part of the anterior and distal ectepicondylar surface (Figure 43b).

The entepicondylar bridge is subcylindrical, slightly flattened anteroposteriorly, lying anterior to a well-developed entepicondylar foramen (Figure 42a). This foramen is present in all pangolins (Figure 44a,b), with the exception of *Smutsia temminckii*. The entepicondylar process in *Patriomanis* (Emry, 1970) is prominent, thickened anteroposteriorly, and tapered medially, with a rugose surface. It does not extend as far medially as the entepicondyle of *Cryptomanis* (Gaudin et al., 2006), *Necromanis* (Koenigswald and Martin, 1990; Koenigswald, 1999), or extant pangolins (Table A10), so that the overall epicondylar width of the humerus is small in *Patriomanis* compared to that of other pangolins (Table A10). The distal edge of the entepicondylar process is irregular but roughly straight in *Patriomanis*, whereas *Cryptomanis, Necromanis,* and all extant manids possess a strongly concave entepicondylar notch (Figure 44a,b; Gaudin et al., 2009). In *Cryptomanis* (Gaudin et al., 2006) and *Necromanis* (Koenigswald and Martin, 1990; Koenigswald, 1999), the entepicondyle is flared distally.

The olecranon fossa in *Patriomanis* is large and expanded transversely, so that it is wider than the posterior trochlear surface (Figure 42b), resembling *Necromanis* (Helbing, 1938) in this respect. In *Cryptomanis* and extant Manidae, however, the olecranon fossa is substantially narrower (Gaudin et al., 2009). The olecranon fossa extends farther proximally in USNM-P 299960, in which it forms a somewhat triangular depression, than in USNM-P 531556, in which the olecranon fossa takes the form of a flattened oval. The radial and coronoid fossae are confluent, forming a large, shallow, roughly circular depression that lies proximal to the capitulum and the lateral half of the trochlea (Figure 42a). *Cryptomanis* and *Necromanis* display much the same condition, whereas in living manids the radial and coronoid fossae are more laterally situated, lying directly over the capitulum (Figure 44a,b; Gaudin et al., 2009).

Ulna

Only a small part of the right ulna is present in the type specimen (Emry, 1970). However, complete right and left ulnae are available from USNM-P 494439. An additional complete right ulna is preserved in USNM-P 299960 (Figures 45, 46). A partial right ulna is also preserved in both USNM-P 531556 and USNM-P 460256. The latter is the only *Patriomanis* specimen known from outside the Flagstaff Rim localities in Wyoming. It was recovered from Chadronian age deposits in Pipestone Springs, Montana. The ulna in *Patriomanis* is shorter relative to the humerus than in any of the extant pangolins (Table A10; Gaudin et al., 2009).

All pangolins possess a robust olecranon process (Gaudin et al., 2006). In *Patriomanis*, the olecranon is roughly rectangular in shape, deep anteroposteriorly, with a relatively straight posterior edge and a slight medial inflection (Figures 45, 46a,b). The olecranon of *Cryptomanis* is also deep but has no medial inflection, bending posteriorly instead, with both anterior and posterior edges inclined in this direction (Gaudin et al., 2006). In *Necromanis* (Koenigswald, 1969, 1999; Koenigswald and Martin, 1990) the olecranon is longer, less deep, and angled both medially and posteriorly, whereas in *Eomanis* and

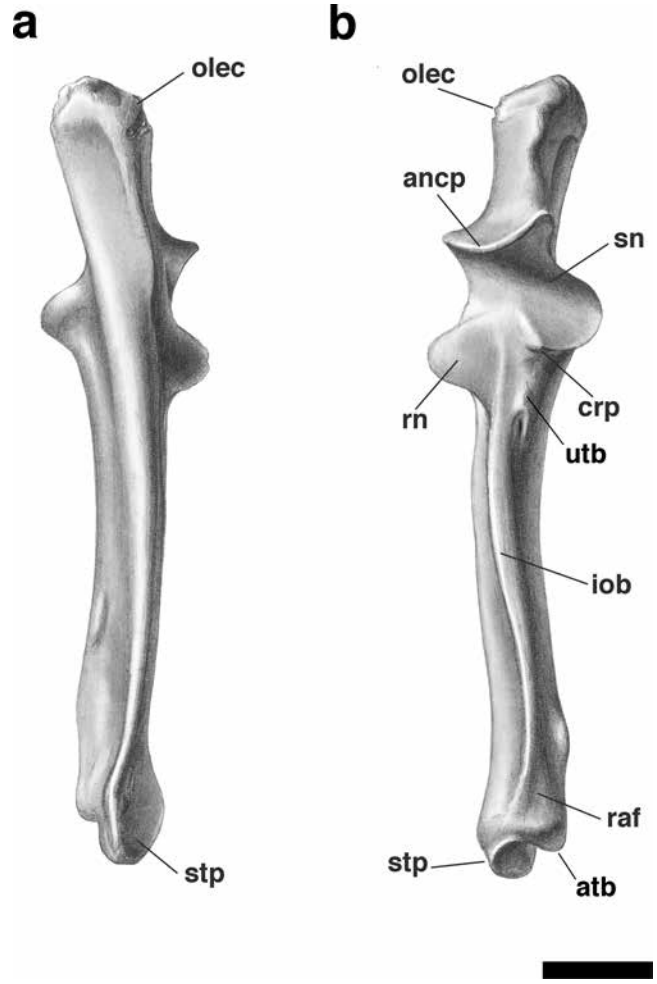

FIGURE 45. Right ulna of *Patriomanis americana* (USNM-P 299960): (a) in posterior view; (b) in anterior view. Abbreviations: **ancp,** anconeal process; **atb,** anterior tubercle; **crp,** coronoid process; **iob,** interosseous border; **olec,** olecranon; **raf,** radial facet; **rn,** radial notch; **sn,** sigmoid notch; **stp,** styloid process; **utb,** ulnar tuberosity. Scale bar = 1 cm. Drawn by Larry Isham, digitized and labeled by Julia Morgan Scott for Smithsonian Institution.

Euromanis the olecranon is more similar to that of *Patriomanis,* except that it has a stronger medial inflection and is actually bent somewhat anteriorly (Storch, 1978; Storch and Martin, 1994). Among living manids the olecranon has a more pronounced medial inflection than in any fossil pangolin, so that the process tends to be broader transversely than it is deep (Figure 44d,e). It is also posteriorly bent in most modern forms, but its length varies, so that in some taxa (*Phataginus*) the olecranon is shorter than that of *Patriomanis,* whereas in others it is longer (*M. crassicaudata* and *M. pentadactyla*; Gaudin et al., 2009).

As indicated by Emry (1970), the semilunar notch in *Patriomanis* is transversely expanded (Figure 45b). The anconeal process of *Patriomanis* (Emry, 1970) is wider than the coronoid process and extends farther anteriorly (Figures 45b, 46a). It extends laterally beyond the lateral edge of the shaft, almost as far laterally as the radial notch (Figure 45b). It is very similar in these respects to other pangolins (Figure 44d,e; Koenigswald, 1969, 1999; Koenigswald and Martin, 1990; Storch and Martin, 1994; Szalay and Schrenk, 1998; Storch, 2003; Gaudin et al., 2006, 2009). The medial edge of the anconeal process is slightly higher than the lateral and is connected to the proximal end of the olecranon by a distinct ridge. The coronoid process in *Patriomanis* is ovate, with its long axis oriented in a posteroproximal to anterodistal direction. The coronoid process is directed medially, as in all pangolins (Gaudin et al., 2006). It flares much farther medially than the shaft, and its lateral edge is well medial to the midline of the anconeal process (Figure 45b). The articular surface for the humeral trochlea has a complex shape. It is deeply concave proximodistally. Its proximal portion is strongly convex transversely and faces anteriorly and distally, whereas the distal portion is flat transversely, facing anteriorly and proximally. As noted by Emry (1970), the radial notch is contiguous with the humeral articulation. It is expanded transversely, narrow proximodistally, with a rounded lateral margin and a tapering medial extremity (Figures 45b, 46a). It extends far lateral to the ulnar shaft and is supported by a distinct lateral flange, as in other pangolins (Figure 44d; Koenigswald, 1969, 1999; Koenigswald and Martin, 1990; Szalay and Schrenk, 1998). It is flat and faces directly anteriorly, as in *Cryptomanis* (Gaudin et al., 2006), except for the most medial portion, which is curved anteriorly. In *Necromanis* the radial notch is more strongly concave (Koenigswald and Martin, 1990). In modern pangolins the radial notch faces more laterally. As described by Emry (1970), a distinct ulnar tuberosity lies distal to the semilunar notch on the anterior surface of the shaft just distal to the coronoid process (Figure 45b), a feature present in *Necromanis, Cryptomanis, Eomanis,* and all living pangolins (Figure 44d; Gaudin et al., 2006, 2009). The ulnar tuberosity serves as the site of insertion for the m. brachialis muscle in humans and for the mm. brachialis and biceps brachii in *Canis* (Evans and Christensen, 1979).

The ulnar shaft in *Patriomanis* (Emry, 1970) is flattened transversely and is concave on its medial and lateral sides (Figure 46a,b). The medial concavity begins just distal to the tip of the olecranon, where it occupies the posterior third of the process. It expands anteroposteriorly and deepens below the semilunar notch, then becomes

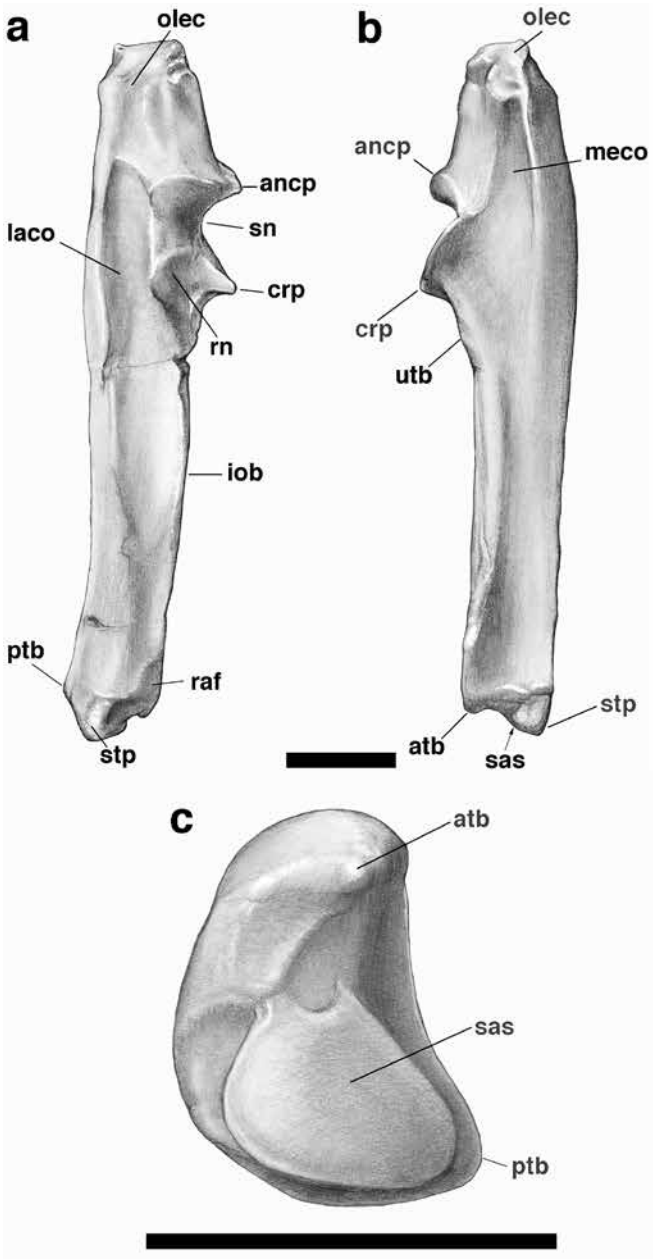

FIGURE 46. Right ulna of *Patriomanis americana* (USNM-P 299960): (a) in lateral view; (b) in medial view; (c) in distal view. Abbreviations: **ancp,** anconeal process; **atb,** anterior tubercle; **crp,** coronoid process; **iob,** interosseous border; **laco,** lateral concavity for mm. extensor digitorum profundus and abductor pollicis longus; **meco,** medial concavity for m. flexor digitorum profundus; **olec,** olecranon; **ptb,** posterior tubercle; **raf,** radial facet; **rn,** radial notch; **sas,** styloid articular surface; **sn,** sigmoid notch; **stp,** styloid process; **utb,** ulnar tuberosity. Scale bars = 1 cm. Illustrations by Julia Morgan Scott for Smithsonian Institution.

narrower and less deep toward the midshaft region, before expanding and deepening again in the distal third of the ulnar shaft, ending just proximal to the styloid process. The distal portion of this medial concavity is not present in most modern pangolins but is present in *Cryptomanis* and *Necromanis* (Koenigswald and Martin, 1990; Koenigswald, 1999; Gaudin et al., 2006). This medial concavity likely accommodates the m. flexor digitorum profundus (Jouffroy, 1966; Gaudin et al., 2006). A deep, sharp-e edged lateral concavity extends distally from the level of the anconeal process, becoming gradually less concave distally to terminate approximately three-fourths of the way down the shaft (Figure 41a). In *Cryptomanis* (Gaudin et al., 2006), this concavity extends much farther distally, whereas in the Manidae it terminates farther proximally. This concavity likely housed the mm. extensor digitorum profundus and abductor pollicis longus (Humphry, 1870; Jouffroy, 1966; Gaudin et al., 2006). The posterior surface of the ulna is flat proximally but tapers distally to form a narrow ridge (Figure 45a). The anterior surface of the ulnar shaft is marked by a sharp-e edged interosseous border that begins at the base of the radial notch and extends almost to the anterior tubercle at the distal end of the ulna. In its middle portion it is slightly folded over laterally, and it carries a slight concavity on its anteromedial surface. A second, very slight concavity on the anterolateral surface at the distal end represents the distal radial facet. *Cryptomanis* (Gaudin et al., 2006) has a very similar morphology. The ulnar shaft is straight and does not taper distally as it does in some modern pangolins (Figure 44e), but rather, as in *Cryptomanis* (Gaudin et al., 2006) and *Eomanis* (Storch, 2003), maintains a uniform depth.

The distal end of the ulna in *Patriomanis*, as in *Cryptomanis* (Gaudin et al., 2006), is flattened transversely and deep anteroposteriorly (Figure 46c). In fact, the distal end of the shaft in *Patriomanis* is deeper relative to maximum ulnar length than in all extant pangolins (Table A10). As in other pangolins (Gaudin et al., 2006), the distal end of the ulna in *Patriomanis* bears two distinct tubercles. The anterior tubercle lies on the anterior edge of the distal surface. A smaller posterior tubercle is situated midway up the lateral edge of the distal surface, just proximal to the lateral edge of the styloid process. The anterior tubercle represents the distal termination of the interosseous border that begins at the base of the coronoid process. The styloid process itself is capped by an ovate articular surface, its long axis oriented in an anterolateral to posteromedial direction. The styloid articular surface is thus wider than it is deep (Figure 46c), as it is in other therians (Gaudin et al., 2009). In contrast, in *Cryptomanis* and most living pangolins (with the sole

exception of *M. pentadactyla*), the styloid articular surface is compressed transversely. The articular surface is slightly convex both transversely and anteroposteriorly, and covers the posterior half of the distal ulnar surface, with its distalmost projection lying along its posterior edge. The articular surface faces distally and somewhat anteriorly, forming a 45° angle with the long axis of the ulna. The styloid process is shorter proximodistally than in living manids (Table A10) but extends farther distally than in *Cryptomanis*, in which the styloid articular surface forms a steep angle relative to the long axis of the ulna.

Radius

The type specimen preserves only partial radii, including the left proximal and left and right distal ends described and illustrated in Emry (1970). However, complete radii are available from USNM-P 494439 and USNM-P 299960, although the right radius of USNM-P 299960 is slightly damaged distally, missing its pseudostyloid process (Figures 47, 48). A complete right radius and a partial left radius are also available from USNM-P 531556.

The radius in *Patriomanis* is shorter relative to humeral length than in any extant pangolin (Table A10). The radial head is also transversely expanded more so than in modern manids (Figure 48a; Emry, 1970), with a depth to width ratio lower than that of all living pangolins (Table A10) but similar to that of *Necromanis* (Helbing, 1938; Emry, 1970). The proximal articulations were identified by Emry (1970). They include, on the proximal surface, a central capitular facet, a lateral shelf for articulation with the lateral extension of the capitulum, and a medial excavation for the trochlea, as well as an ulnar facet on the posterior surface and a sesamoid facet on the lateral surface (Figures 47a, 48a,c). In USNM-P 299960 the anterior edge of the proximal radius is deeply indented lateral to the capitular eminence (Figure 47b,c). This indentation is less well developed in USNM-P 531556 and is absent in the type (Emry, 1970). This indentation is also missing in *Necromanis* (Helbing, 1938) but is variably present in living pangolins. The capitular eminence is strongly developed in *Cryptomanis*, *Necromanis* (Helbing, 1938; Koenigswald and Martin, 1990; Gaudin et al., 2006), and extant manids (Figure 44c) except for *S. gigantea*. The triangular trochlear facet in *Patriomanis* (Emry, 1970) is wide, covering approximately one-third of the radial head. It is similarly well developed in *Cryptomanis* (Gaudin et al., 2006) and *Necromanis* (Helbing, 1938), whereas in extant manids the trochlear facet covers a much smaller portion of the proximal surface (Gaudin et al., 2009). The sesamoid facet identified by Emry (1970) in *Patriomanis* and *Necromanis* is small relative to that in modern pangolins. It also faces directly lateral in the two fossil genera, whereas in extant forms it is inclined distolaterally so that it becomes

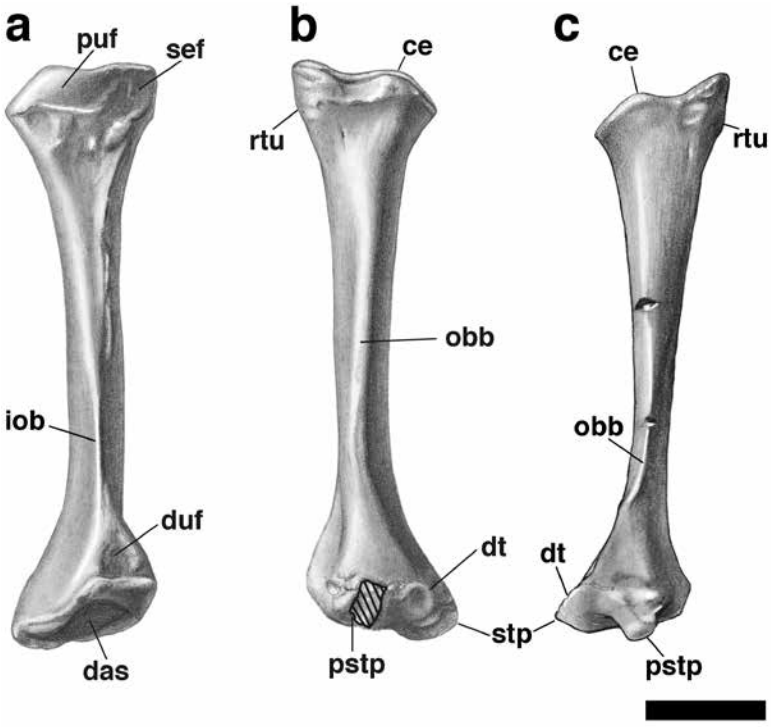

FIGURE 47. Radius of *Patriomanis americana*: (a) right radius of USNM-P 299960 in posterior view; (b) right radius of USNM-P 299960 in anterior view; (c) left radius of USNM-P 299960 in anterior view. Abbreviations: **ce,** capitular eminence (= anterior proximal medial process of Gaudin et al., 2009); **das,** distal articular surface; **dt,** dorsal tubercle; **duf,** distal ulnar facet; **iob,** interosseous border; **obb,** oblique border; **pstp,** pseudostyloid process; **puf,** proximal ulnar facet; **rtu,** radial tuberosity; **sef,** sesamoid facet; **stp,** styloid process. Cross-hatched areas represent broken surfaces. Scale bar = 1 cm. Illustrations (a), (b) drawn by Larry Isham, digitized and labeled by Julia Morgan Scott (JMS) for Smithsonian Institution (SI); (c) by JMS for SI.

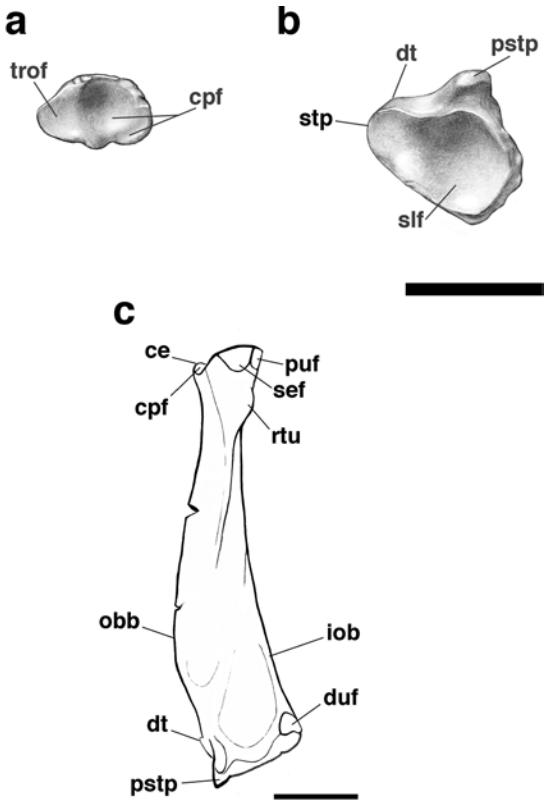

FIGURE 48. Left radius of *Patriomanis americana* (USNM-P 299960): (a) in proximal view; (b) in distal view; (c) in lateral view. Abbreviations: **ce,** capitular eminence; **cpf,** capitular facet; **dt,** dorsal tubercle; **duf,** distal ulnar facet; **iob,** interosseous border; **obb,** oblique border; **pstp,** pseudostyloid process; **puf,** proximal ulnar facet; **rtu,** radial tuberosity; **sef,** sesamoid facet; **slf,** scapholunar facet; **stp,** styloid process; **trof,** trochlear facet. Scale bar = 1 cm. Illustrations (a), (b) by Julia Morgan Scott for Smithsonian Institution and (c) by T. J. Gaudin.

visible in a proximal view of the radial head. The proximal ulnar facet in *Patriomanis* (Emry, 1970) is narrow proximodistally and elongated and convex transversely (Figure 47a). It abuts the sesamoid facet along its lateral margin, in contrast to the condition in extant manids, in which the two facets are clearly separate (Gaudin et al., 2009). Patriomanids and *Necromanis* lack a prominent radial tuberosity (Gaudin et al., 2009), but this process is strongly developed on the medial edge of the proximal radius in all modern manids except *S. temminckii* (Figure 44c). The function of this process in living manids is not entirely clear. In other placental mammals, the radial tuberosity serves as an insertion point for the m. biceps brachii (e.g., Evans and Christensen, 1979; Neveu and Gasc, 2002; Homberger and Walker, 2004). According to Emry (1970, based on Humphry, 1870, and Windle and Parsons, 1899), however, the biceps does not have a radial attachment, at least in *Manis*. Jouffroy (1966:266, discussion of m. pronator teres) implies that such an attachment is present in *S. gigantea*. The process may also serve as a site of origin for the very large m. flexor digitorum profundus (Humphry, 1870;Windle and Parsons, 1899; Jouffroy, 1966) of living pangolins.

The proximal radial shaft is transversely broad and anteroposteriorly compressed, reflecting the shape of the radial head. Distally, the shaft becomes increasingly compressed transversely and expanded anteroposteriorly (Figures 47, 48c), as noted by Emry (1970). At its deepest point, approximately three-fourths of the way down the shaft, its depth is three times greater than its width. The lateral compression of the radial shaft is much more pronounced in *Patriomanis* than in *Cryptomanis* (Gaudin et al., 2006), *Necromanis* (Helbing, 1938; Koenigswald and Martin, 1990), or living manids. As in other pangolins, the anterior surface is marked by a very sharp and elevated oblique border, which originates on the proximal quarter of the shaft and extends its entire length, curving sharply mediad as it approaches the distal margin of the radius (Figure 47b,c). The oblique border terminates in a weak tubercle, which, following the terminology of MacPhee (1994), we identify as the dorsal tubercle. A weaker, rounded ridge extends straight distally from the oblique border near the point where it begins to curve medially. This ridge terminates at the base of a prominent pseudostyloid process (Figure 47c; terminology of MacPhee, 1994; equal to "anteriorly directed tubercle" of Emry, 1970:480). The pseudostyloid process is rectangular, slightly wider than long, and is directed anteriorly, distally, and laterally. It is tilted somewhat so that its lateral edge is more elevated than its medial edge, and it extends farther distally than any other part of the radius. A prominent pseudostyloid process is also present in *Necromanis* (Koenigswald and Martin, 1990). In *Cryptomanis* (Gaudin et al., 2006), the median ridge extending distally from the oblique border is much more pronounced than in *Patriomanis*, but the region where a pseudostyloid process would be located is not preserved. The oblique border of living pangolins is, at best, weakly bifurcated distally, and there is no pseudostyloid process present (Figure 44c). Rather, the dorsal tubercle at the medial termination of the oblique crest is much more prominently developed than in *Patriomanis*.

The posterior surface of the radial shaft bears a sharp interosseous border distally (Figure 47a). This crest bifurcates proximally near the midshaft. The medial edge and more prominent lateral edge of the bifurcated interosseous

border are separated by a weak depression. In *Necromanis* (Helbing, 1938) and in extant pangolins, the interosseous border is similar in length but is undivided proximally. Multiple small, tubercular rugosities are situated around the proximal margin of the aforementioned posterior radial fossa in *Patriomanis*. These rugosities are also present in modern *Manis* but are absent in the extant African species. The distal ulnar facet lies near the distal margin of the posterior radial surface. Its medial edge is formed by the interosseous border. It is triangular and flat, as in all pholidotans, and is oriented posteriorly and somewhat laterally (Figures 47a, 48c).

Emry (1970:480) described the distal end of the radius as "strongly expanded and heavy … [with] a single concave, transversely oval articular surface." The articular surface is tilted distolaterally and slightly posteriad. In distal view (Figure 48b), the long axis of the articular surface appears twisted 45° relative to the long axis of the head (twisted counterclockwise on the right, clockwise on the left). *Cryptomanis* (Gaudin et al., 2006) likely shares a similar morphology judging by the preserved portions of the distal articulation, whereas in extant manids the distal articular surface is either circular (*S. gigantea*) or compressed transversely, so that its long axis is perpendicular to that of the radial head (Gaudin et al., 2009). As noted by Gaudin et al. (2006), this difference in orientation of the distal radius in the modern taxa may be related to the adoption of a pedolateral stance. The styloid process in *Patriomanis* is rudimentary, taking the form of a low, rounded tubercle situated near the posteromedial extremity of the distal radial articular surface. In living pangolins the styloid process is robust and forms a distinct process, confluent with, but set off by, indentations from the rest of the distal articular surface. It extends in either a ventral (*Phataginus*) or ventrolateral (*Manis* and *Smutsia*) direction from the medial or anteromedial margin of that surface (Gaudin et al., 2009).

Scapholunar

Although Emry (1970) reports finding only two manual proximal phalanges and an ungual phalanx (probably from digit III) in the type, several more pieces of the manus have since been recovered from the type specimen, including several carpals from both the left and right side (partial right scapholunar, right pisiform, left hamate), two proximal phalanges, at least one complete intermediate phalanx, and unguals from at least four different digits (I, II, III, and V). There are also a partial right manus largely prepared free from the matrix and a partial left manus still in the matrix in USNM-P 494439. The former includes the triquetrum, trapezium, capitate, hamate, metacarpals I and IV, proximal phalanges I and II, intermediate phalanx II, and unguals I, II, IV, and V. The latter includes most of digits II, III, and IV. However, the descriptions of the various elements in the manus that follow are based largely on USNM-P 299960, except where otherwise noted. This specimen includes an intact, articulated right manus (Figure 49), as well as much of the left manus. It is the only specimen with an intact scapholunar element (Figure 50).

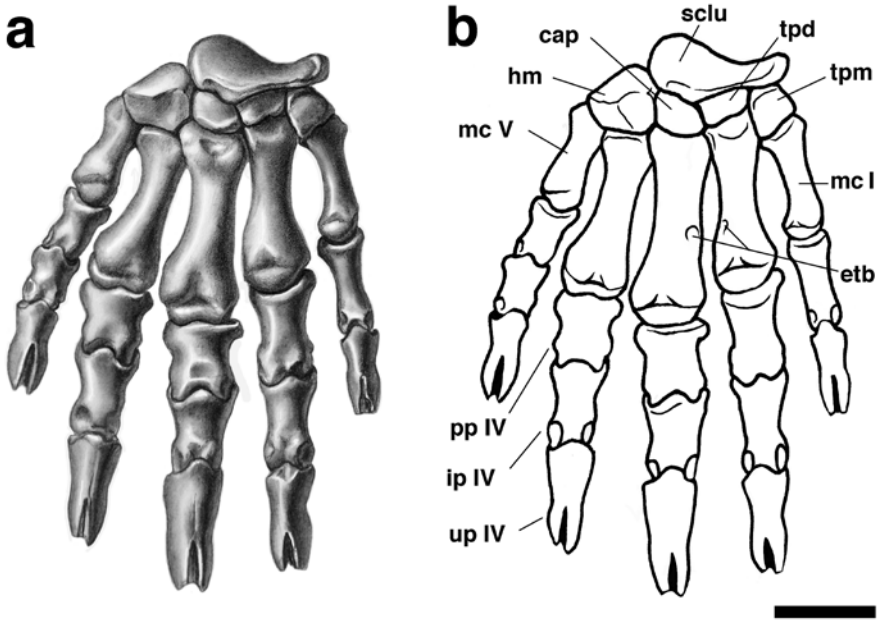

FIGURE 49. Right manus of *Patriomanis americana* (USNM-P 299960): (a) in dorsal view; (b) labeled line drawing of the same. Abbreviations: **I–V,** digits I–V; **cap,** capitate; **etb,** extensor tubercle; **hm,** hamate; **ip,** intermediate phalanx; **mc,** metacarpal; **pp,** proximal phalanx; **sclu,** scapholunar; **tpd,** trapezoid; **tpm,** trapezium; **up,** ungual phalanx. Scale bar = 1 cm. Illustration (a) drawn by Larry Isham, digitized by Julia Morgan Scott (JMS) for Smithsonian Institution (SI); (b) by JMS for SI.

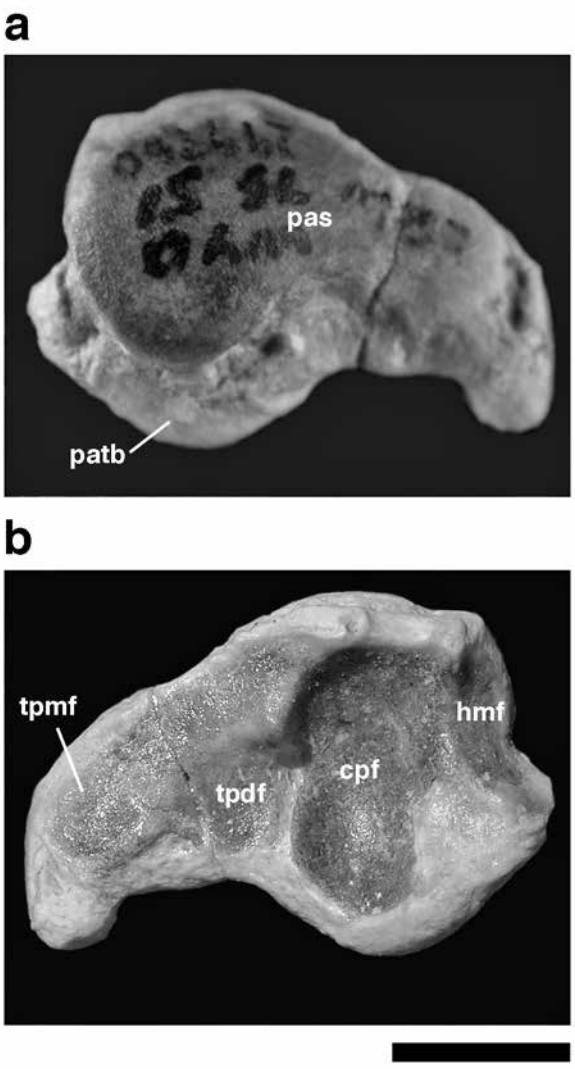

FIGURE 50. Left scapholunar of *Patriomanis americana* (USNM-P 299960): (a) in proximal view; (b) in distal view. Abbreviations: **cpf,** capitate facet; **hmf,** hamate facet; **pas,** proximal articular surface; **patb,** palmar tuberosity; **tpdf,** trapezoid facet; **tpmf,** trapezium facet. Scale bar = 1 cm. Photos by Tim Gaudin, composed and labeled by Julia Morgan Scott for Smithsonian Institution.

In modern pangolins, the scaphoid and lunate elements of the carpus are fused into a single bone, the scapholunar. It is possible that this element is actually a scaphocentrolunate, that is, that an embryologically separate centrale element forms an additional contribution to the adult element. However, in the manus of a 7.6-cm embryo of *Phataginus tricuspis* illustrated by Szalay and Schrenk (1998: fig. 25), there is no indication of a separate centrale element. It should be noted, however, that the scaphoid and lunate are already fused, perhaps indicating that this embryo represents too late a stage to be informative regarding the composition of the adult bone.

The scaphoid and lunate elements of the carpus are also fused in *Cryptomanis* (Gaudin et al., 2006) and *Necromanis* (Koenigswald and Martin, 1990) but not in *Eomanis* (Gaudin et al., 2009), although the evidence in the case of the latter is somewhat equivocal. In *Patriomanis,* as in the other Manoidea, the fused scapholunar element is clearly present, constituting the largest element by far in the carpus. The bone is half again as wide as it is deep in proximal view, much like the condition in modern pangolins (Figures 44f, 49, 50; Table A11). It articulates proximally with the radius and distally with the trapezium, trapezoid, capitate, and hamate. The proximal surface is dominated by the large articular facet for the radius (Figure 50a). This facet is much deeper dorsopalmarly in its lateral half than it is in its medial half, with the lateral portion roughly ovoid in outline and the medial portion tapering slightly toward the medial end, so that the facet resembles a rounded, sideways *L* in shape. The medial and lateral halves of the facet are separated in part by a strong concavity along the palmar margin. This concavity is also present in extant Manidae but is not present in *Cryptomanis* or *Necromanis,* in which the palmar margin is roughly straight (Gaudin et al., 2009). It is interesting that despite marked differences in the shape of the distal facet of the radius in modern pangolins versus *Patriomanis*, the shape of the proximal facet of the scapholunar does not generally reflect these differences but is instead generally similar among *Patriomanis* and most extant taxa.

In dorsal view, the scapholunar is very broad transversely and short proximodistally, with just a small sliver of a nonarticular dorsal surface exposed (Figure 49). In contrast to *Cryptomanis* and extant pangolins (Gaudin et al., 2009), there is no articular facet along the lateral edge for the triquetrum. The palmar surface of the bone is dominated by a large, rounded, smooth-surfaced palmar tuberosity. This protrusion covers the entire lateral half of the bone. It is ovate, with a transverse diameter much greater than its proximodistal extent. This is also the case in *Cryptomanis,* but in modern pangolins the palmar tuberosity tends to be more proximodistally elongated (Gaudin et al., 2009); in some taxa (e.g., *Manis javanica,* USNM 198852), the proximodistal diameter of the palmar tuberosity is nearly half the maximum width of the entire scapholunar.

In distal view, the surface of the scapholunar bears three facets separated from one another by prominent ridges

(Figure 50b). The facets are all strongly concave in both the transverse and dorsopalmar planes. Along its lateral edge, the scapholunar bears a crescent-shaped facet that faces distolaterally to articulate with the hamate. Medial to this is a larger facet with a roughly triangular outline (elongated in the dorsopalmar plane, apex on the palmar side) that contacts the capitate. Medial to this is a transversely wide, triangular facet (apex medial) for the trapezium and trapezoid. The trapezoid occupies the bulk of this last facet, with perhaps the medial third articulating with the trapezium, although there is no clear demarcation between these two regions on the surface of the facet itself. Both the capitate and trapezium–trapezoid facets face mainly distad, although the former is tilted slightly lateral and the latter slightly medial. The articulation between the scapholunar and hamate is missing in *M. javanica* and the extant African pangolins (Gaudin et al., 2009), and in all extant pangolin species the ridge separating the capitate and trapezium–trapezoid facet is lacking (Gaudin et al., 2009).

Triquetrum

Although not figured with the remainder of the manus (Figure 49), an isolated, slightly damaged right triquetrum is preserved in USNM-P 299960 (Figure 51a), along with a partial left triquetrum. There is also a complete right triquetrum that has been prepared free of the matrix in USNM-P 494439 (Figure 51a). The former is somewhat more compressed in the dorsopalmar plane than the latter, but they are otherwise quite similar.

The triquetrum articulates proximally with the ulna and pisiform and distally with the hamate. Of the two articular facets on the proximal surface, the facet for the styloid process of the ulna is situated more dorsal and faces more proximally, whereas the pisiform facet lies in a more palmar position. Both facets are elongated in the transverse plane, and both are relatively flat in USNM-P 494439, although the pisiform facet is slightly concave medially and slightly convex laterally in USNM-P 299960. The ulnar facet is roughly triangular or semicircular in outline, with the apex pointed dorsally. The ulnar facet is also elongated transversely in *Eomanis,* the extant pangolins in the genus *Phataginus,* and the extant species *Smutsia gigantea,* but in living Asian pangolins and *S. temminckii,* the transverse width is less than or equal to dorsopalmar depth (Gaudin et al., 2009). The ulnar and pisiform facets are contiguous along their entire transverse extent. They are situated well lateral to the medial edge of the bone, as in the extant pangolin genera *Manis* and *Smutsia* (Gaudin et al., 2009).

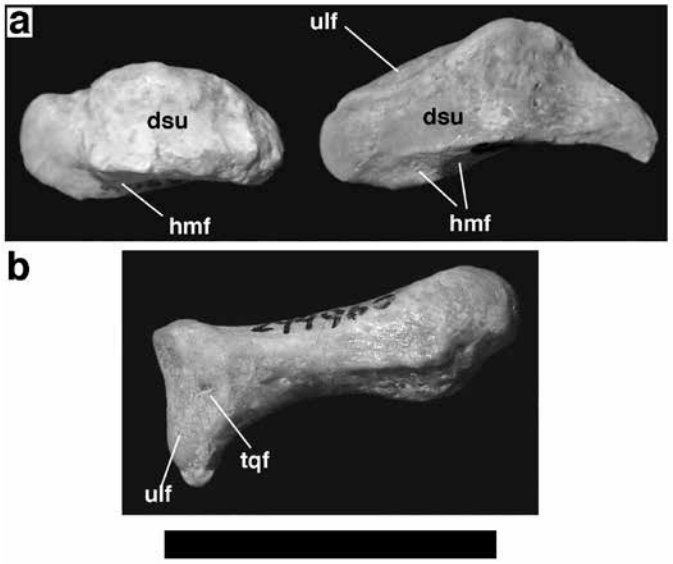

FIGURE 51. Triquetrum and pisiform of *Patriomanis americana*: (a) right triquetrum of USNM-P 299960 in dorsal view on right, right triquetrum of USNM-P 494439 in dorsal view on left; (b) right pisiform of USNM-P 299960 in medial view. Abbreviations: **dsu,** dorsal surface; **hmf,** hamate facet; **tqf,** triquetrum facet; **ulf,** ulnar facet. Scale bar = 1 cm. Photos by Tim Gaudin, composed and labeled by Julia Morgan Scott for Smithsonian Institution.

In dorsal view, the triquetrum is wide transversely and short proximodistally, much like modern pangolins. It has a quadrate outline in USNM-P 299960, whereas in USNM-P 494439 it is tapered at either end, giving it a triangular shape (Figure 51a). Its dorsal surface is convex transversely and slightly concave proximodistally, and it bears a strong, smooth-surfaced knob at its lateral end.

In distal view, the triquetrum bears a single, distally facing facet for the hamate. This facet is roughly triangular with a medial base and is gently concave.

Pisiform

The pisiform is not preserved in USNM 494439 but is known from two right pisiforms, one preserved with the type specimen (F:AM 78999) and the other with USNM-P 299960 (Figure 51b). The bone is elongated along its proximodistal axis, with a roughly rectangular outline. It has a blunt distal tip that is incised along its medial surface with a deep groove. This groove may very well have accommodated a tendon attaching the m. flexor carpi ulnaris to the outer metacarpals. In humans and dogs, the pisiform serves as the insertion point for the m. flexor carpi

ulnaris (Pick and Howden, 1977; Evans and Christensen, 1979), as well as the site of origin of several ligaments and, in humans, the m. abductor digiti minimi. However, in *Smutsia gigantea,* the insertion of the flexor carpi ulnaris is continued by a tendon or ligament that passes from the pisiform onto the ulnar border of the fourth metacarpal (Jouffroy, 1966). The presence of the distal groove in *Patriomanis* suggests it may have possessed a similar arrangement, although neither *S. gigantea* nor any other extant pangolin was observed to have a distal groove on the pisiform. The proximal end of the pisiform is roughly triangular (apex lateral) and slightly elongated transversely. It is marked by two articular facets separated by a sharp crest. One facet faces more toward the proximal side of the carpus and articulates with the ulna, and the other faces more toward the distal side of the carpus and articulates with the triquetrum (Figure 51b). The ulnar facet is ovate transversely, and the triquetral facet is semicircular in outline, with the flat side facing proximally in dorsal view. The pisiform has not been described in any other fossil pangolin.

Trapezium

The trapezium has been recovered from USNM-P 494439 and USNM-P 299960. It has a roughly triangular outline in dorsal view, with the base facing laterally and the apex medially, and its proximodistal length is greater than its transverse width (Figure 49). In *Manis javanica* and *M. pentadactyla,* the trapezium is deeper on the medial side, giving it a more trapezoidal outline, but the bone resembles that of *Patriomanis* in other extant pangolins (Figure 44f). The trapezium articulates with the scapholunar proximally, the trapezoid and second metacarpal laterally, and the first metacarpal distally. The dorsal surface is curved in *Patriomanis,* in such a manner that the dorsalmost point is at the distolateral corner, and the dorsal surface curves in a palmar direction toward both its medial and proximolateral corners. This dorsal point actually overlaps the dorsal surface of the first metacarpal, much as was the case with the entocuneiform and first metatarsal. The proximal surface of the trapezium bears a small, convex facet for the scapholunar that occupies the proximolateral corner of the bone. In most living pangolins (except *S. gigantea*), the scapholunar facet is much larger, covering the entire proximal surface of the trapezium, and in every living species except *M. crassicaudata* the facet is concave rather than convex (Gaudin et al., 2009). Along its lateral surface, the trapezium bears two facets: an upper facet for the trapezoid and a lower, larger facet for the second metacarpal. The upper facet is small, flat, and triangular; the lower facet is ovoid and concave. The distal surface carries the facet for the first metacarpal. This facet is compressed transversely and teardrop shaped, with a rounded palmar portion narrowing to a dorsolateral point. The outline of the distal facet for metacarpal I varies considerably among modern pangolins, even within species. In *M. javanica* (USNM 198852), the facet resembles that of *Patriomanis,* but in *M. pentadactyla* (USNM 308733) and *S. temminckii* (AMNH 244096) the facet is ellipsoidal, with a rounded dorsal margin, and in *S. gigantea* (AMNH 53851) it is almost triangular and is broader transversely than it is deep in a dorsopalmar plane.

Trapezoid

The trapezoid is known only from USNM-P 299960 (Figure 49). As in other pangolins, it is a transversely elongated element that articulates proximally with the scapholunar, medially with the trapezium, laterally with the capitate, and distally with the second metacarpal. In *Patriomanis,* as in *Cryptomanis* (Gaudin et al., 2006) and *Eomanis* (Gaudin et al., 2009), the dorsal surface of the trapezoid is rectangular in outline, with the distal and proximal articular surfaces roughly parallel to one another. In modern pangolins, the dorsal surface of the trapezoid is trapezoidal, with the distal and proximal surfaces converging on the medial side, largely because of the proximomedial tilt of the former (Gaudin et al., 2009).

The proximal surface of the trapezoid carries a large articular facet for the scapholunar. This facet is unusual in that it has a concave surface contour, in contrast to the condition in other known living and fossil pangolins, in which the facet is convex (Gaudin et al., 2009). This facet is roughly triangular in outline, narrowing at its palmar end. The distal surface is also triangular and bears two facets. On its medial edge, there is a small rectangular facet facing distomedially for the trapezium. This facet has a very similar orientation in *Cryptomanis,* whereas in extant African pangolins (*Smutsia* and *Phataginus*), the facet faces directly mediad (Gaudin et al., 2009). In Asian pangolins (*Manis*), the trapezium actually overlaps the trapezoid proximally, so that the trapezium facet faces proximally and medially (Gaudin et al., 2009). The bulk of the distal surface is occupied by a triangular facet for metacarpal II. This facet is concave in its dorsolateral corner, but the dorsomedial and palmar corners form part of a flat or slightly convex, crescent-shaped surface. This sort of complex, concavo-convex metacarpal II facet is common among pholidotans.

Capitate

A left capitate is available from USNM-P 531557, and a right capitate is available from USNM-P 494439, in addition to the left and right capitates of USNM-P 299960 (Figures 49, 52a,b). The element lies between the scapholunar dorsally, the hamate laterally, the trapezoid medially, and metacarpal III distally. Its maximum width is virtually identical to that of the trapezoid, but its dorsal surface is slightly deeper proximodistally, especially along its lateral border with the hamate (Figure 49). The palmar surface is marked by a prominent, rounded tuberosity (Figure 52b). The facet for the scapholunar that covers the proximal surface of the bone is strongly convex both transversely and in the dorsopalmar plane. It is fairly narrow compared to that of other pangolins, its maximum width roughly half of its maximum dorsopalmar depth (Figure 52a). In *Cryptomanis* and *Eomanis*, the width of the facet is more than 65% of its depth, in extant African pangolins more than 75% of its depth, and in extant Asian pangolins between 85% and 100% of its depth (Gaudin et al., 2009). The facet has a roughly triangular outline, although there is a steplike indentation approximately midway along its lateral margin. The facet takes on a similar shape in *Eomanis* and *Cryptomanis,* whereas in all modern pangolins except *M. javanica*, the facet is more L shaped, with a very deep and abrupt lateral indentation restricting the width of the palmar portion of the facet.

The capitate is roughly semicircular in outline in both medial and lateral views. It articulates with the trapezoid medially, but this facet is actually visible in proximal view because the trapezoid slightly overlaps the capitate proximally, so that the facet on the capitate faces proximomedially (Figure 52a). The overlap of the trapezoid on the capitate is also evident in *Eomanis, Cryptomanis,* and some *M. javanica,* but in other extant pangolins the reverse is the case, with the capitate showing a slight proximal overlap of the trapezoid (Gaudin et al., 2009). On its lateral surface, the capitate bears a small, triangular facet for the hamate near its dorsal and distal corner. *Eomanis* and *Cryptomanis* are similar, but in extant pangolins this triangular facet is displaced in a palmar direction, so that

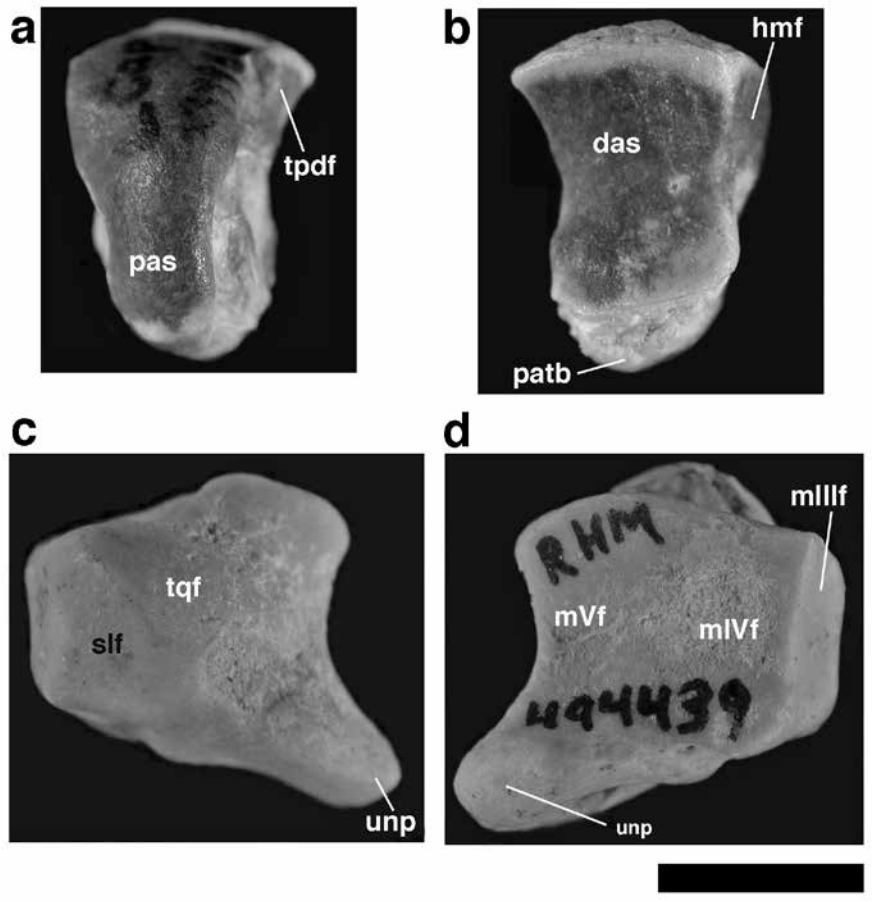

FIGURE 52. Capitate and hamate of *Patriomanis americana*: (a) left capitate of USNM-P 299960 in proximal view; (b) in distal view; (c) right hamate of USNM-P 494439 in proximal view; (d) in distal view. Abbreviations: **das,** distal articular surface; **hmf,** hamate facet; **mIIIf,** metacarpal III facet; **mIVf,** metacarpal IV facet; **mVf,** metacarpal V facet; **pas,** proximal articular surface; **patb,** palmar tuberosity; **slf,** scapholunar facet; **tpdf,** trapezoid facet; **tqf,** triquetrum facet; **unp,** unciform process. Scale bar = 1 cm. Photos by Tim Gaudin, composed and labeled by Julia Morgan Scott for Smithsonian Institution.

the facet comes to lie near the midpoint of the lateral surface (Gaudin et al., 2009).

The distal articular surface for metacarpal III has what Gaudin et al. (2009) term a "dumbbell shape" outline—it is roughly rectangular, compressed transversely, with relatively straight dorsal and palmar margins, but both lateral and medial margins are indented (Figure 52b). The outline is similar in *Eomanis* and *Cryptomanis* (Gaudin et al., 2009), whereas it differs in several respects in modern pangolins. In all extant taxa, the palmar edge is narrower than the dorsal edge. This is especially the case in *Manis* and *Smutsia*, where the distal capitate facet takes on a roughly triangular outline (Gaudin et al., 2009). In *Phataginus,* the palmar surface is only slightly narrower, whereas the medial border is indented and the lateral border is extended laterally into a blunt point, giving the whole articulation a bilobate appearance (Gaudin et al., 2009). The surface contour of the facet is complicated in pangolins. It is concave in a dorsopalmar plane in all taxa. In *Phataginus,* the facet is then convex transversely, especially its dorsal lobe. In *Patriomanis, Cryptomanis, Manis,* and *Smutsia,* the facet has a midline eminence that runs in a dorsopalmar direction and is flanked by two concavities, so that the overall transverse contour of the facet is concave medially and laterally and convex in the middle. In the modern taxa, there is a rounded knob at the dorsal end of this midline eminence that appears to form a stop, preventing hyperextension at the carpometacarpal joint. The fairly complex surface contour of the distal capitate facet exhibited by *Patriomanis* is likely the primitive condition for pangolins, rather than the somewhat simpler shape in *Phataginus*.

Hamate

The hamate is the second largest element in the carpus, behind only the fused scapholunar element. It has been recovered from the type specimen (F:AM 78999), as well as USNM-P 494439 and USNM-P 299960 (Figures 49, 52c,d). It articulates with the triquetrum and scapholunar proximally, the capitate medially, and the three lateral metacarpals (III, IV, V) distally. The hamate is blocky but carries a prominent unciform process that attaches to its distal, palmar, lateral corner and extends in a distal, palmar, and lateral direction toward a blunt, rounded tip (Figure 52c,d). A prominent unciform process is also found in *Eomanis* and in all extant pangolins except *M. pentadactyla*. In the modern taxa (except *M. pentadactyla* and some specimens of *S. gigantea*), however, the unciform process takes on a more complex shape, extending in a distal, palmar, and lateral direction at its base, before taking a distinct turn in the proximal direction, extending outward as a proximally, laterally, and palmarly oriented prong (Gaudin et al., 2009).

The dorsal surface of the hamate in *Patriomanis* is trapezoidal in outline, with the proximal and distal edges approaching one another laterally (Figure 49). Its transverse width is nearly half again greater than that of the capitate or trapezoid and is also somewhat greater than its maximum proximodistal height. Among the African pangolins (*Smutsia* and *Phataginus*) and *M. javanica,* the dorsal surface takes on a more pentagonal shape and is more compressed transversely, such that the maximum proximodistal height equals or exceeds its width (Figure 44f). In *M. crassicaudata* and *M. pentadactyla*, the dorsal surface is irregularly shaped but low, with its transverse width much greater than its height (Gaudin et al., 2009).

The proximal surface of the hamate bears two facets: a small, more medially directed facet for the scapholunar and a larger, more laterally sloping facet for the triquetrum (Figure 52c). Both are convex mediolaterally and in a dorsopalmar plane. The former is narrow transversely, and the latter is narrower in a dorsopalmar plane. The distal articular surface is quite complex (Figure 52d). It bears a rectangular, transversely narrow, distomedially oriented facet for metacarpal III. More laterally is an ovate facet, gently concave both transversely and in a dorsopalmar plane and more elongate in a dorsopalmar than transverse direction. This articulates with metacarpal IV. Last, there is a third, even more laterally situated facet for metacarpal V. This facet is strongly concave in the dorsopalmar plane. Transversely, it is relatively flat in USNM-P 494439, whereas it is concave in the type specimen, F:AM 78999. In both specimens it is broadly triangular, narrowing at its palmar end, where it overlaps onto the base of the unciform process. The distal hamate surface is basically similar to that of *Patriomanis* in *Eomanis* but shows numerous differences in modern pangolins. In *Phataginus,* the facet for metacarpal III is vertical and is carried on the medial rather than the distal surface of the hamate (see, e.g., Gaudin et al., 2009: fig. 5a). In *Phataginus* and *Manis,* the facet for metacarpal IV becomes much broader, so that its width equals or exceeds its dorsopalmar depth, and the facet comes to occupy most of the distal hamate surface. Moreover, in *Manis* this facet, which is generally concave as in *Patriomanis,* bears a distinct, convex eminence in its dorsomedial corner. This eminence is present but smaller in the African genera and *Patriomanis* and is located between the facets for metacarpals III and IV. The facet for metacarpal V is directed distolaterally in *M. javanica*

and *M. crassicaudata,* in contrast to the distally oriented facet of *Patriomanis,* whereas in the extant African taxa it has distinct distally and distolaterally facing facets for metacarpal V. Additionally, the facet for metacarpal V is not tapered at its palmar end in the extant pangolins but is of relatively uniform width throughout.

Metacarpals

The metacarpals are not preserved in the type specimen, and USNM-P 531557 preserves only the distal portion of metacarpal IV. In USNM-P 494439, the first and fourth metacarpals from the right manus are intact and have been prepared free of the matrix. Metacarpals II and III are preserved on the left side but remain partially embedded in the matrix ventrally. USNM-P 299960 preserves a complete series on the right (Figure 49). The third metacarpal is missing on the left side.

The third is the largest metacarpal in *Patriomanis,* in terms of its length, width, and depth (Table A12). This is also the case among extant manids (except *S. temminckii,* in which metacarpal IV is longest), whereas in *Cryptomanis* the second metacarpal is longer and equal in depth to the third (Table A12; Gaudin et al., 2006). However, if the ratio between width and length is considered, it becomes evident that the third and sometimes the second (*Cryptomanis*; Gaudin et al., 2006) or fourth metacarpals are greatly enlarged in other pangolins (Figure 44f). In *Patriomanis* the digits are relatively uniform in terms of metacarpal width versus depth, with values between 20% and 22% for all but metacarpal V (29%). In *Phataginus, M. javanica* and *M. crassicaudata,* and *Cryptomanis*, the ratio of width to depth for the third metacarpal exceeds 30%, and in *Smutsia* and *M. pentadactyla* it exceeds 40%. The fifth is the shortest metacarpal in *Patriomanis,* but the first is the narrowest, and the first and fifth are of equivalent midshaft depth (Table A12). There is considerable variation among pholidotans regarding the relative sizes of the fifth and first metacarpals, although these are invariably the smallest metacarpal elements. In *Phataginus, Smutsia,* and *M. javanica,* the first metacarpal is shortest, whereas in *M. pentadactyla* and *M. crassicaudata,* the fifth is shorter (Table A12; Gaudin et al., 2009). As was the case with the pes, the overall length of the digits relative to body size seems to be greater in *Patriomanis* and *Cryptomanis* (Gaudin et al., 2006) than in extant manids, as reflected in the lengths of the metacarpals. The length of the third metacarpal in *Patriomanis* is 28% that of the humerus, whereas in modern pangolins the third metacarpal is 25% or less of humeral length (Table A12). *Eomanis waldi* also has an elongated third metacarpal (Table A12; Gaudin et al., 2009), but its relatively short proximal and intermediate phalanges give it an appearance more like that of modern manids than the patriomanids.

Once again reminiscent of the condition in the pes, an apparent increase in the mobility of the metacarpophalangeal joints accompanies the shortening of the manual digits in modern pangolins. At the distal end of the metacarpals, extant manids have the same type of robust median keel that characterizes the metatarsals described above, extending dorsal and ventral to the metacarpal shaft (Figure 44f). This keel increases the lateral stability of the metacarpal–phalangeal joint as well as its sagittal mobility. Like *Cryptomanis* (Gaudin et al., 2006), *Patriomanis* has a keel extending only along the ventral and palmar surfaces of the distal condyles of the metacarpals, and this ventral keel is not as robust as that present in the modern species (Figure 27a). *Eomanis* and *Euromanis* resemble the patriomanids is this respect (Gaudin et al., 2009). In *Necromanis,* however, the median distal keel, although still restricted to the ventral half of the condyle, is elongated, thereby more closely resembling the robust condition of the keel in modern pangolins (Gaudin et al., 2009). The dorsal surfaces of the distal condyles of metacarpals II–IV in *Cryptomanis* are divided by a shallow median groove into two "hemicondyles" (Gaudin et al., 2006).

The metacarpal anatomy of *Patriomanis* is very reminiscent of the metatarsals in other respects as well. The shafts of the metacarpals tend to be relatively wide and flat or cylindrical, their minimum midshaft width equal to or exceeding their minimum midshaft depth. This mirrors the condition in metacarpals II–V of *Cryptomanis*, where width exceeds depth by an even greater amount (Gaudin et al., 2006; Table A12). Modern manids tend to have deeper metacarpals, with the midshaft depth exceeding the width for all digits, except in *Phataginus* and some *M. javanica*, in which the width is greater than or equal to the depth for only metacarpal III (Gaudin et al., 2009). The distal condyles appear slightly elongate transversely and are distinctly narrower than the epicondyles (Figure 49), in contrast to the condition in the Manidae (Figure 44f; Gaudin et al., 2009). Immediately proximal to the condyles of metacarpals II–V is a midline depression on the dorsal surface. This fossa is also present in *Cryptomanis* and *Necromanis* but is missing in modern pangolins (Gaudin et al., 2006, 2009). Nevertheless, it can be inferred from the myology of living forms that these depressions represent insertion sites for the m. extensor digitorum longus (Jouffroy, 1966).

The central metacarpals (II, III, and IV) of *Patriomanis* differ from those of other pholidotans in two additional aspects. In all three, the narrowest portion of the shaft in dorsal view lies proximal to the midpoint of the shaft, instead of at the midpoint. In addition, the shafts of these metacarpals are bowed dorsally, with a concave palmar profile. This dorsally bowed shaft can also be observed in metacarpals III and IV of *Cryptomanis* and metacarpal II in *M. javanica* but is otherwise unknown among other pholidotans.

Metacarpal I. In dorsal view the shaft of the first metatarsal is slightly bowed laterally toward its distal end (Figure 49). At its proximal end, metacarpal I articulates exclusively with the trapezium—*M. pentadactyla* is the only pholidotan that we have observed to retain an articulation between metacarpals I and II. The outline of the proximal articular facet for the trapezium takes on the form of an equilateral triangle, with a dorsal and palmar point, as well as a strong medial tuberosity. The facet is similar in shape in *Cryptomanis,* but in extant manids the medial tuberosity is small or absent, so that the facet takes on a more ovate or transversely narrow triangular outline. The proximal facet is strongly convex in the dorsopalmar plane, with the trapezium overlapping onto the dorsal surface of the metacarpal shaft. At the distal end, the condyle for the proximal phalanx is relatively broad in comparison to modern pangolins. The condyle is convex in a dorsopalmar plane, in contrast to the condition in *M. crassicaudata* and *M. pentadactyla,* in which the distal condyle has a flattened profile in medial view and the metacarpal–phalangeal joint is immobile. These two modern species have similarly immobile joints on digits II, III, and IV, whereas in *M. javanica* only the third metacarpal–phalangeal joint is immobilized. Other pangolins retain mobile metacarpal–phalangeal joints. In all *Manis* species as well as *P. tetradactyla,* the median keel is absent on the metacarpal I condyle, but it is retained in *Patriomanis* and other pangolins.

Metacarpal II. The second metacarpal articulates with the trapezium, trapezoid, and metacarpal III at its proximal end (Figure 49). The facet for the trapezium is carried on the medial surface of the bone and is crescent shaped, being elongated in a distodorsal to proximopalmar direction. The facet extends from the dorsal edge of the medial surface to approximately the midpoint of the medial surface, an arrangement shared in *S. gigantea* and *P. tricuspis*, although the shape of the facet is more triangular in these taxa. In other extant manids, the facet extends almost to the palmar edge of the bone (Gaudin et al., 2009). On the lateral surface, the facet for metacarpal III is crescent shaped, with its long axis oriented basically proximodistally. It is strongly concave, receiving a similarly shaped, strongly convex knob from metacarpal III. This morphology is similar to that in *Cryptomanis,* whereas in extant manids the articular surfaces between metacarpals II and III are flat (Gaudin et al., 2009). The proximal articulation for the trapezoid is triangular in outline, narrowing toward the palmar tuberosity. Its surface contour matches that of the distal trapezoid facet described above. In dorsal view, the proximal end of the metacarpal II shaft in *Patriomanis* lacks a concavity that is found in *Cryptomanis* and extant Manidae.

Metacarpal III. The third metacarpal articulates proximally with the capitate, the hamate, and metacarpals II and IV (Figure 49). The articulation with metacarpal II has been described above. The articulation with the metacarpal IV is carried on the lateral surface and is narrow and generally rectangular in outline, with its long axis oriented in a dorsopalmar plane. The facet extends from the dorsal edge of the bone nearly to its palmar edge. A facet for the hamate is situated on a lateral extension of the proximal end of the bone. This extension slightly overlaps metacarpal IV proximally. The overlap is even more pronounced in *Cryptomanis* and the extant African pangolins (Figure 44f) and is also present in *Eomanis* (Gaudin et al., 2009). In *Manis,* there is no overlap, although a hamate facet is present on the third metacarpal. The hamate facet itself is like that of most other pangolins, narrow transversely and elongated in a dorsopalmar plane, facing proximally and laterally. However, in *Phataginus* and some *S. gigantea,* the hamate facet takes on a very different shape, with a much shorter dorsopalmar extent (Gaudin et al., 2009). The proximal facet for the capitate in *Patriomanis* is rectangular in outline, slightly narrower transversely than in the dorsopalmar plane. It has a saddle-shaped surface contour and is concave transversely, with a strongly convex, semicircular profile in medial or lateral view. It is similar in *Cryptomanis* and modern manids, but in the latter group the dorsopalmar profile is sigmoid rather than semicircular (Gaudin et al., 2009). The sigmoid profile is created by a dorsal shelf that extends forward from the convex, palmar portion of the facet. This shelf presumably acts as a "stop" to prevent hyperextension at the capitate–metacarpal II joint and is presumably an adaptation to resist large forces generated at this joint when excavating termite nests. It is interesting to note that the stop is missing only in *S. temminckii,* which is the least fossorial of the living pangolins (Kingdon, 1974, 1997; Heath, 1992b; Nowak, 1999). The capitate facet in some modern

pangolins (*Smutsia, M. crassicaudata,* and *M. pentadactyla*; Gaudin et al., 2009) extends onto the palmar surface of the metacarpal shaft, allowing for increased plantar flexion at this joint. Such movement is prevented by the large palmar tuberosity of the metacarpal in *Patriomanis, Cryptomanis,* and other modern pangolins.

The proximal shaft of metacarpal III in modern manids has a distinctive T shape in dorsal view, with not only the aforementioned lateral extension abutting or overlapping metacarpal IV at its proximal end but also a corresponding medial extension contacting metacarpal II (Figure 44f). This second extension is missing in both *Patriomanis* (Figure 49) and *Cryptomanis* (Gaudin et al., 2006). *Patriomanis* bears a small extensor tubercle on the medial side of the shaft of metacarpal III, situated just distal to the midshaft region. A similar tubercle is found on the lateral side of the second metacarpal. *Cryptomanis* manifests a similar morphology (Gaudin et al., 2009), but extensor tubercles are largely lacking in *Eomanis* and modern pangolins. However, in *M. crassicaudata* and *M. pentadactyla,* the dorsal surface of metacarpal III is marked by a median crest that extends the entire length of the shaft. This crest bears a prominent tubercle at its proximal terminus (Gaudin et al., 2009).

Metacarpal IV. This element articulates with the hamate and with metacarpals III and V proximally. The facet for metacarpal III in *Patriomanis* is rectangular, elongate in a dorsopalmar plane. It is slightly convex proximodistally and nearly flat to slightly concave in its dorsopalmar aspect. It is similar in *Smutsia* and *Phataginus*, although in the former the convexity tends to be better developed. In *Manis*, it is strongly convex in both the proximodistal and dorsopalmar aspects (Gaudin et al., 2009). The facet for metacarpal V shows extensive shape variation among the pholidotans in which it is known. In *Patriomanis* it is teardrop shaped, with its long axis running in a dorsodistal to proximopalmar direction. The facet is concave in *Patriomanis* and *Cryptomanis,* whereas in most modern pangolins (except *S. gigantea*) it is convex at least in the dorsopalmar plane (Gaudin et al., 2009). The hamate facet is relatively simple in *Patriomanis,* as it is in *Cryptomanis*. It is rectangular in outline, is narrowest transversely, and is weakly convex in both the transverse and dorsopalmar planes. The facet varies considerably among extant Manidae. In African pangolins and *M. javanica,* it is triangular in outline, narrowing toward the palmar margin. In *M. crassicaudata* and *M. pentadactyla,* it takes on a semicircular shape, with the dorsal edge forming the base of the semicircle. Additionally, in all the extant species, the facet, although generally convex, bears a large concave pit near its dorsal edge (Gaudin et al., 2009).

As was the case with metacarpal III, metacarpal IV tends to be T shaped proximally in dorsal view in modern pangolins, with medial and lateral extensions at its proximal end that abut the adjacent metacarpals, although these are less prominent than in metacarpal III (Figure 44f). These are much less developed in patriomanids relative to extant pangolins, with only a weak extension evident on the lateral side (Figure 49).

Metacarpal V. The lateralmost metacarpal articulates only with the hamate proximally and metacarpal IV medially. All pholidotans, including *Patriomanis,* have a lateral tubercle projecting from the lateral margin of this bone at its proximal end (Figures 44f, 49), although it should be noted that this feature is present in early eutherians (Kielan-Jaworowska et al., 2004) and is thus likely a primitive feature for all placentals. In African manids, this tubercle appears to be displaced proximally relative to the other pholidotans, so that it comes to lie proximal to the distal edge for the hamate. In these taxa, the metacarpal V–hamate articulation is L shaped, with a vertical and horizontal moiety (Gaudin et al., 2009, describe this as a "peg-and-socket" articulation). In *Patriomanis* and *Manis,* the lateral tubercle lies slightly distal to the distal edge of the hamate, and the proximal facet on metacarpal V is either flat (*Manis*) or slightly convex in a dorsopalmar direction (*Patriomanis*). At the distal end of the bone, the median keel is reduced or absent in *Manis*, but it is retained in *Patriomanis, Cryptomanis,* and the extant African species.

Manual Proximal Phalanges

Emry (1970: fig. 20) illustrates and briefly describes two manual proximal phalanges recovered from the type specimen. Although he does not specify, these are the proximal phalanges from the second and third digits, the former the longer of the two. In addition, proximal phalanx IV is now known from the type specimen. Manual proximal phalanges I and II are preserved and have been prepared in the right manus of USNM-P 494439, and the left pes preserves proximal phalanges II–V still embedded in matrix. USNM-P 299960 includes a complete series of proximal phalanges from the left and right manus (Figure 49), except for digit III on the right. The following description is based largely on the complete set of elements available from the latter specimen.

The relative lengths of the proximal phalanges are variable among pholidotans. The fifth proximal phalanx

is the shortest in all extant species except *M. tetradactyla* (proximal phalanx I is slightly shorter) and *Patriomanis,* whereas in *Cryptomanis* the third is the shortest (Table A13). The longest is more variable. In *Patriomanis*, the second is generally longest, as it is in *M. crassicaudata* and *M. pentadactyla*. The third is longest in the extant African species and *M. javanica,* whereas the first is longest in *Cryptomanis* (Table A13).

The proximal phalanges of *Patriomanis* have a roughly cylindrical shaft that is constricted in the middle and expanded at either end in dorsal view, although in digits III and IV the elements are very broad, with a proximal width nearly 80% of their maximum length. In *Cryptomanis,* proximal phalanges II–IV are similarly short and broad, their width actually equaling or exceeding their length. Likewise, dramatic shortening and broadening of the proximal phalanges occurs in the extant genus *Smutsia* (digits II–V) and the extant species *M. crassicaudata* and *M. pentadactyla* (digits III–V; Table A13). As in *Cryptomanis, Euromanis,* and *Eomanis,* the width of the proximal phalanges is equal to or exceeds their depth, whereas in extant manids these bones are uniformly deepened, so that their dorsopalmar depth exceeds their transverse width (Gaudin et al., 2009).

At their proximal ends, the manual proximal phalanges resemble their pedal counterparts. They have a concave proximal facet that is divided ventrally by a median depression that in turn receives the keel of the distal metatarsals, giving the articular surface a horseshoe-like shape (Figure 26a). A similar morphology is present in *Cryptomanis,* whereas in extant species the entire articular surface is deeply divided by a median groove for the enlarged metatarsal keel. The absence of this keel in *Patriomanis* and other fossil pangolins (Gaudin et al., 2006, 2009) leaves the metatarsal–phalangeal joints appearing somewhat less stable than the interphalangeal joints.

At the distal ends, the proximal phalanges of *Patriomanis* are capped by a pair of subequal, pulley-shaped distal condyles, as in all other pangolins (Figure 26c). Lateral to each of these condyles are well-marked fossae (Figure 49), likely for the origin of collateral ligaments bracing the interphalangeal joints (based on anatomy of humans and dogs; Pick and Howden, 1977; Evans and Christensen, 1979). These fossae are also present in *Cryptomanis* and *Necromanis* but are missing in *Eomanis* and extant pangolins (Figure 44f; Gaudin et al., 2009).

As was the case in the pes, the first manual proximal phalanx is more elongate and slender than the other proximal phalanges (Table A13). This is true not just of *Patriomanis* but of all living and extinct pangolins. On digits II and IV, the proximal phalanges are slightly asymmetrical, the latter extending farther proximally on its medial side, the former extending farther proximally on its lateral side. Proximal phalanx III is marked in most extant pangolins (all but *M. javanica*; Gaudin et al., 2009) by a narrow transverse eminence that links the two distal condyles at their dorsopalmar midpoints. This eminence is lacking in patriomanids (Figure 26c).

Manual Intermediate Phalanges

There are no manual intermediate phalanges preserved in the type (Emry, 1970), but all five are preserved in the matrix surrounding the left manus of USNM-P 494439, along with several free elements from the right side. A complete right and left series is also available in USNM-P 299960 (except for the left intermediate phalanx IV; Figure 49). The description that follows is based largely on that specimen.

As was the case with the proximal phalanges, the manual intermediate phalanges are cylindrical in dorsal view, slightly constricted in the middle, and expanded at either end. In USNM-P 299960, the second is the longest, whereas in USNM-P 494439 the third is longest, as it is in all extant pangolin species. The fifth intermediate phalanx is the shortest in all pangolins except *P. tricuspis,* in which the second is marginally shorter than the fifth (Table A13). The manual intermediate phalanges are roughly equivalent in length to the proximal phalanges in *Patriomanis* (Table A13). In most instances, the intermediate phalanx is much longer (up to twice as long; Table A13) than the corresponding proximal element in living pangolins. This morphology is also evident in digit III of *Cryptomanis* (Gaudin et al., 2006: fig. 9). This appears to be due largely to the dramatic shortening and widening of the proximal phalanges that is so pronounced in *Cryptomanis, Smutsia,* and several Asian species, as described above. In these taxa, the proximal phalanges are often compressed proximodistally to the point that they no longer have a cylindrical shaft.

The proximal and distal articular surfaces are basically identical to those described above for the pedal intermediate phalanges. As in those elements, the proximal end comprises two shallow articular fossae for the proximal phalangeal condyles and dorsal and paired ventral processes that embrace the interphalangeal joint, although to a lesser extent than in modern forms. The dorsal processes are particularly elongated proximally in extant manids, so that they overshadow the proximal articular surface in dorsal view. The distal condyles are paired, subequal, and

strongly convex, flanked by pits for the interphalangeal collateral ligaments that are visible in dorsal view (Figure 49), in contrast to the condition in extant taxa, in which the distal condyles are parallel and the fossae for the collateral ligaments are oriented laterally (Figure 44f).

Manual Unguals

Emry (1970) described a single manual ungual in the type specimen of *Patriomanis* (F:AM 78999). Since that report, three additional unguals have been identified in the type, so that unguals from digits I, II, III, and V are now known. Manual unguals I, II, IV, and V have been prepared free from the right manus of USNM-P 494439, and manual unguals II and IV on the left are partially exposed in the matrix. A virtually complete set of left and right manual unguals has been preserved with USNM-P 299960 (Figure 49); hence, the description that follows is based largely on that specimen.

The third ungual is the largest, with the first and fifth nearly equivalent in size and smaller than the remaining unguals (Table A13). Among modern pangolins, the first ungual phalanx is notably smaller than the fifth in *Manis* and *Smutsia* and is dramatically reduced in *Phataginus,* in which its length is less than half that of the fifth (Figure 44f; Gaudin et al., 2009). Although ungual phalanx III is the largest manual ungual in *Patriomanis,* its length is only about 10% greater than the next largest ungual, so that overall, the unguals are of a fairly uniform length, as in the pes (Figure 49). However, in *Eomanis*, *Manis,* and *Phataginus,* the third ungual is greatly enlarged, being at least 30% longer than the next largest element (Figure 44f; Gaudin et al., 2009). In *Smutsia,* the second, third, and fourth unguals are all quite large. Consequently, the middle digit does not appear to be emphasized to the same degree

The anatomy of the manual unguals is virtually identical to that described above for the pedal unguals. They carry the characteristic deep fissures found in other extinct and extant pholidotans (Grassé, 1955; Guth, 1958; Gebo and Rasmussen, 1985; Koenigswald, 1969, 1999; Koenigswald and Martin, 1990; Gaudin et al., 2006, 2009) with the exception of *Eomanis* and *Euromanis* (Storch, 1978; Storch and Martin, 1994). As in the pes, the fissure occupies a little more than half the length of the ungual, as in other eupholidotans. The unguals are blunt tipped and waisted. *Necromanis* (Koenigswald, 1969, 1999; Koenigswald and Martin, 1990), *Cryptomanis* (Gaudin et al., 2006), and *Manis pentadactyla* also have waisted manual unguals, but *Eomanis* and *Euromanis* do not, in contrast to their pedal unguals, nor are waisted manual unguals found in other extant manids (Gaudin et al., 2009).

The proximal articular surface is as Emry (1970) described it and as it is described above for the pedal unguals. It has two strong concavities for medial and lateral distal condyles of the intermediate phalanges. The median crest on the subungual process is enlarged relative to that of the pedal unguals, taking the form of a large tubercle. In other respects, the subungual process and vascular foramina follow the pattern described above for the pedal unguals.

DISCUSSION

Species Comparisons Based on Size and Stratigraphy

To date, all the specimens of *Patriomanis* have been assigned at least implicitly to a single species, *Patriomanis americana*. Given that the holotype specimen is relatively incomplete (Emry, 1970) and subsequent investigations of *Patriomanis* have tended to focus only on a portion of the anatomy, either the skull (Gaudin and Wible, 1999; Emry, 2004) or other relatively circumscribed portions of the skeleton (Rose and Emry, 1993), this approach has made sense. However, now that a complete assessment has been made of the available material, it is reasonable to ask whether more than one species can be recognized.

There do not appear to be geographic grounds for recognizing more than one species. *Patriomanis* is known from only two locales, the Pipestone Springs Local Fauna in the Jefferson River Basin of southwestern Montana (USNM-P 460256) and the Flagstaff Rim area in Natrona County in central Wyoming (F:AM 78999 [holotype]; USNM-P 299960, 494439, 531556, 531557; see the Catalog of Specimens section of the Introduction). The two are roughly 500 km apart, certainly close enough to fall in the same species range if compared to the ranges of the extant forms (see, e.g., Kingdon, 1997). Moreover, the Pipestone Springs specimen is assigned to Chron 3 of the Chadronian NALMA (Janis et al., 2008; Rose, 2008), which is the case with all but one of the Flagstaff Rim specimens.

There are several positive arguments, however, that could be advanced for recognizing USNM-P 299960 as a second species relative to the other five specimens. USNM-P 299960 derives from Emry's (1973) Unit 4 of the White River Formation in the Flagstaff Rim area. The other specimens at that locality derive from Units 17 and 21 (see the Catalog of Specimens section). Janis et al. (2008) assign all the strata below Ash B at the Flagstaff Rim

site, including Unit 4, to Chron 2/3 of the Chadronian NALMA, and those levels between Ash B and F, including Unit 17, to Chron 3, with the two specimens from Unit 21 (holotype, F:AM 78999, and USNM-P 4894439) found only 5 m above Ash F, which would presumably also be in Chron 3 or, at the latest, the base of Chron 4. At first glance the clustering of all the *Patriomanis* in or around Chron 3 might further confirm the idea that they can be lumped into the same species. However, USNM-P 299960 sits some 45–46 m below the level containing USNM-P 531556, which in turn lies another 35 m below the holotype and USNM-P 494439 (Emry, 1973). Chrons 2 and 3 together span a period of roughly 2 million years, from 36.6 to 34.8 MYA (Janis et al., 2008; Rose, 2008). We think it unlikely that the *Patriomanis* remains from the Flagstaff Rim area span the entire range from the base of Chron 2 to the top of Chron 3, but it is not unreasonable to assume that either USNM-P 299960 comes from Chron 2 and the others from Chron 3 or at least that USNM-P 299960 comes from the base of Chron 3 and the others from substantially later in Chron 3 or even early Chron 4. Since Chron 3 itself is 1 million years in duration, it seems likely that the 80-m stratigraphic interval between Units 4 and 21 represents a time period of about 1 million years. This would certainly be enough time to recognize USNM-P 299960 as a chronospecies distinct from the type and USNM-P 494439, with the status of USNM-P 531556 less clear but closer to the latter than the former.

There is also some morphological support for recognizing USNM-P 299960 as a separate species. It is the smallest specimen of *Patriomanis*. There is only one complete skeletal element, the radius, held in common among USNM-P 299960, 531556, and 494439, the three specimens that define the stratigraphic range of *Patriomanis* at Flagstaff Rim. The greatest length of the radius is 48.9 mm in USNM-P 299960, 52.9 mm in USNM-P 531556, and 53.5 mm in USNM-P 494439 (Table A10), the last being 9% longer than the first, and the three specimens show an increase in size (at least for this element) through time. Although USNM-P 531556 preserves completely only the humerus (which is larger than USNM-P 299960, 63.4 versus 61.1 mm; Table A10), radius, and metatarsal V, more extensive comparisons can be carried out between USNM-P 299960 and USNM-P 494439, including the calcaneus, astragalus, most of the elements in the manus, the tibia, and the ulna. In every instance, the bones from USNM-P 494439 are between 8% and 29% larger than their counterparts in USNM-P 299960, with most being 15%–25% larger. Of course, it is possible that these size differences represent random interindividual size variation or even sexual dimorphism, as male pangolins are known to be larger than females (Heath, 1992a, 1992b; Nowak, 1999). Moreover, it is difficult to know what the expected magnitude of interspecific size differences might be on the basis of comparisons with extant taxa. In two of the three modern genera, *Phataginus* (Kingdon, 1997) and *Manis* (Heath, 1992a, 1995), the species broadly overlap in body size, and in *Smutsia* the giant pangolin is nearly twice the size of the ground pangolin (Kingdon, 1997). In the end, there are not enough specimens of *Patriomanis* to reliably discriminate among the various possibilities; indeed, distinguishing among individual differences, species-level differences, and gender-based differences remains a difficult problem for extinct taxa in general (see discussion in Pujos et al., 2012).

In the same stratigraphic interval occupied by *Patriomanis* (from just below Ash A to just below Ash G), the small ungulate artiodactyl *Leptomeryx* also shows a distinct increase in size (Emry, 1973: fig. 18; Emry and Gawne, 1986: fig. 5; Heaton and Emry, 1996: figs. 2–4, 6). However, unlike *Patriomanis*, *Leptomeryx* is represented by very large samples, which conclusively show that the increase in size of *Leptomeryx* from lower to higher stratigraphic levels is an evolutionary increase, with the whole population becoming larger, and not intrapopulation variation. This evidence suggests that the increase in size of *Patriomanis* through the same interval might also be evolutionary change rather than intrapopulation variation. The authors of the *Leptomeryx* studies faced the same question that we are faced with here regarding *Patriomanis*: whether to recognize these successive populations as distinct chronospecies when they are separated only by time and size and lack other obvious morphologic differences. Those authors declined to name new species of *Leptomeryx*, just as we decline to name a new species of *Patriomanis* here.

In an attempt to get a different perspective on morphological variation among the various *Patriomanis* specimens, we looked at character polymorphism in the Gaudin et al. (2009) phylogenetic analysis. The number of characters that were coded as polymorphic for extant pangolin species in that analysis ranged from 7 (*M. crassicaudata*) to 56 (*S. gigantea*). There did appear to be some correlation between polymorphisms and the number of specimens available for study. For example, the 305 postcranial characters in the study (out of a total of 395 characters) were coded in *M. crassicaudata* on the basis of only two specimens. It is noteworthy, then, that although *Patriomanis* was coded on the basis of more specimens than *M. crassicaudata* for the

postcranial data, only 10 polymorphisms were found. Of these, five were "false" polymorphisms, in the sense that the codings were not based on actual variation among specimens, but rather on the fact that the fossil specimens provided enough information to rule out one or more states but not enough to assign a definitive coding among remaining states. Thus, the various specimens of *Patriomanis* show very few morphological differences from one another, apart from size, when compared to modern species. This morphological uniformity is a strong argument against recognizing separate species on morphological grounds.

In summary, although there are reasonable grounds for recognizing USNM-P 299960 as a separate chronospecies from the other *Patriomanis* specimens on the basis of stratigraphic data, there is much less support for recognizing it on morphological grounds. The available specimens of *Patriomanis* are morphologically quite uniform, apart from a clear size difference between the geologically older, smaller USNM-P 299960 and the geologically younger, larger USNM-P 494439, perhaps with USNM-P 531556 intermediate in both age and size. There are not enough specimens, however, to establish this as a real size trend, as opposed to random individual variation or some form of sexual dimorphism. Therefore, until additional specimens are recovered, we choose to retain all the specimens in the single species *Patriomanis americana*.

Phylogeny, Taxonomy, and Biogeographic Origins

These aspects of the biology of *Patriomanis* have been thoroughly investigated and discussed by Gaudin et al. (2009), so we will offer no more than a summary of their results in the present study. *Patriomanis* is assigned by Gaudin et al. (2009) to the superorder Pholidotamorpha, which in turn encompasses two orders, Pholidota and Palaeanodonta. Pholidota is divided into three families, Eomanidae, Patriomanidae, and Manidae, with the genera *Eurotamandua* and *Euromanis* included in the order but not assigned to a particular family. Eomanidae is monotypic, accommodating only the genus *Eomanis,* whereas Manidae includes all the extant pangolins. The family Patriomanidae, to which, of course, *Patriomanis* is assigned, also includes the extinct Asian pangolin *Cryptomanis,* and Hoffmann (2011) suggests that the mid-Cenozoic European pangolin *Necromanis* should also be assigned to this family, although its familial affinities are not resolved in the Gaudin et al. (2009) study. The Patriomanidae represents the sister taxon to Manidae in Gaudin et al. (2009), the two together constituting a clade identified as the superfamily Manoidea. Eomanidae is in turn the sister taxon to this clade, forming a more inclusive clade called Eupholidota.

Gaudin et al. (2009) assert that the order Pholidota likely has its biogeographic origins in Europe, with the oldest pangolins (*Eomanis, Euromanis,* and *Eurotamandua*) coming from the middle Eocene (ca. 45 MYA) Messel deposits of Germany. The origin of Pholidotamorpha is less clear, as palaeanodonts have a North American origin (Rose and Lucas, 2000), as does the extant sister taxon to Pholidota, the Carnivora (Flynn and Wesley-Hunt, 2005), leaving the origin of Pholidotamorpha equivocal, although almost certainly located somewhere in Laurasia. It would appear that *Patriomanis* arrived in North America from the west, most likely over the Bering land bridge, as it is linked to the European birthplace of the order by the slightly older, late Eocene (ca. 40 MYA) pangolin from northern China, *Cryptomanis* (Gaudin et al., 2006). This further suggests that pangolins may have been distributed across all the Laurasian continents in the latter half of the Eocene epoch, although they are known to persist only in Europe after the Eocene, in the form of the Oligocene-Miocene genus *Necromanis*.

Paleobiology

As has been noted elsewhere (Gaudin et al., 2006, 2009), *Patriomanis* is quite similar anatomically to the slightly older patriomanid from northern China, *Cryptomanis*. Although it is generally smaller bodied and less robust in its skeletal construction, *Patriomanis* has many of the features presented as indicative of a fossorial lifestyle in *Cryptomanis* (Gaudin et al., 2006). Like the former, *Patriomanis* has a large gluteal fossa on the ilium and a large femoral greater trochanter and third trochanter (located somewhat more distad on the femoral midshaft region) with a robust intertrochanteric ridge, although the lesser trochanter is smaller and the femoral shaft is more cylindrical. The tibia has a prominent cnemial crest that is slightly longer but less robust than that of *Cryptomanis*; the fibula, with its cylindrical shaft, is sturdy but less robust than in *Cryptomanis*, and the patella is less massive. Like *Cryptomanis, Patriomanis* has a well-developed, fairly elongate olecranon on the ulna, but it is less flared along its proximal posterior edge. The humerus has a very strong deltopectoral crest that is longer but lower than that of *Cryptomanis*. The entepicondylar process is massive but less elongate than in *Cryptomanis,* and the supinator crest is well developed but not as prominent,

especially at its proximal end. *Patriomanis* also has a very tall scapular spine, much better developed than in living manids (the condition is unknown in *Cryptomanis*; Gaudin et al., 2009).

As in *Cryptomanis*, all these features are more robust in *Patriomanis* than in the extant forms, whereas the digits are considerably less robust than in the modern taxa, lacking the deeply keeled metapodials and greatly enlarged manual third digit and claw of the living manids. Indeed, the manual third digit of *Patriomanis* is weaker than that of *Cryptomanis*. Thus, both patriomanids share the characteristic of having more fossorially adapted proximal limb skeletons, that is, in the girdles and long bones, and less fossorially adapted distal limb skeletons in the manus and pes. Gaudin et al. (2006) suggest that there is a progressive transfer of digging adaptations from the proximal end of the limb to the distal end in pangolin evolution. This may be the case, but Patriomanidae is the sister taxon to Manidae and not necessarily its direct ancestor. Moreover, *Eomanis,* an older taxon and the sister taxon to both Manidae and Patriomanidae, is in some respects more like the modern manids than are patriomanids, with a weak gluteal fossa and third trochanter on the femur (albeit at the proximal rather than distal end) and a larger third manual ungual (Gaudin et al., 2009: chars. 128, 146, 303). It is therefore possible that the patriomanids are simply divergently specialized for digging relative to the living pangolins. This possibility would be consistent with Gaudin et al.'s (2006) suggestion that perhaps patriomanids dug in a different manner than the living taxa.

Cryptomanis is described as having a scansorial, semiarboreal mode of locomotion, lacking the prehensile tail of the arboreal African tree pangolins but with elongate digits, especially in the pes, that would have provided some grasping ability, although there is no evidence for opposability in the digits (Gaudin et al., 2006). The digits in *Patriomanis* are both absolutely and relatively shorter than those of *Cryptomanis,* but the tail is considerably longer. In fact, the evidence suggests that, unlike *Cryptomanis, Patriomanis* had a prehensile tail (see caudal vertebrae description above). It had a caudal vertebral count (31–36) commensurate with that of the modern prehensile-tailed African tree pangolin *Phataginus tricuspis* (35–39) and greater than that of any living pangolin that lacks a prehensile tail. In addition, it had very large transverse processes in the anterior caudal vertebrae, very large and elaborate double transverse processes in the mid-caudals reminiscent of those in prehensile-tailed vermilinguan anteaters, and ventral articulations for chevrons that extended nearly to the end of the caudal series, although they lacked the large transverse processes present in the terminal caudals of *Phataginus*. However, the morphology of the terminal caudals in *Patriomanis* was very similar to that of nonpholidotan extant mammals with prehensile tails, including vermilinguans, opossums, primates, and carnivorans (see caudal vertebrae description above). The prehensile tail demonstrates that *Patriomanis* was almost certainly an arboreal forest dweller. Additionally, it may have climbed in a different manner from its close relative *Cryptomanis*, with its longer digits but lack of a prehensile tail.

Unlike *Cryptomanis, Patriomanis* is represented by well-preserved skull material, including an edentulous rostrum and mandible (Emry, 1970, 2004). This morphology is a clear indication that like the modern forms, *Patriomanis* was myrmecophagous, feeding primarily on ants and termites. The older pangolin genus *Eomanis* is also edentulous and was also presumably myrmecophagous, although its preserved stomach contents contain more sand and plant remains than insect cuticle (Koenigswald et al., 1981). Like the living pangolins, the fossil forms lack both temporal lines and a frontal postorbital process (Gaudin et al., 2009) and therefore likely had the strongly reduced temporal fossa and concomitantly reduced temporalis muscle of the extant pangolins (note that in *Eurotamandua* temporal lines are also absent, but muscle scars on the braincase indicate a somewhat larger temporalis; Gaudin et al., 2009). However, both *Patriomanis* and *Eomanis* (Storch, 1978) preserve at least a small coronoid and angular process on the mandible, features missing in the modern forms. Moreover, the horizontal ramus of the mandible is somewhat more robust in *Patriomanis* than in the living taxa. We interpret this to mean that *Patriomanis* and *Eomanis* had somewhat better developed masticatory musculature and likely a wider gape than is the case in living pangolins.

The only fossil pangolin that preserves any portion of the xiphisternum is *Cryptomanis,* and it appears to possess the same elongated osseous xiphisternum found in the modern taxa, although, of course, we cannot say for certain whether it possessed the elongate cartilaginous extension found in extant forms (Grassé, 1955; Kingdon, 1974) or whether the tongue musculature attached to the xiphisternum or indeed any part of the sternum as in the modern taxa (Chan, 1995). In modern forms, this elongation of the tongue posteriorly facilitates the great protrusibility of the tongue during feeding.

Finally, we might make mention of the epidermal scales. Of course, the most recognizable feature of living

pangolins is their external covering of large, sharp-edged, overlapping scales that serve as an important defense mechanism, both from predators and from the often aggressive social insects that they feed upon (Kingdon, 1974, 1997; Heath, 1992a, 1992b, 1995; Nowak, 1999). Kingdon (1997) has speculated that the scaly covering evolved from an ancestral pangolin that had smaller scales only on its prehensile tail, like a modern opossum or murid or anomalurid rodents. From there the scales enlarged and spread to cover the dorsum, flanks, and limbs of the modern taxa. There is only one fossil pangolin for which scales are preserved, *Eomanis waldi,* from the fossil lagerstätten at Messel, but they are preserved as several isolated elements and reveal nothing about the extent of the scaly covering of the animal (Koenigswald et al., 1981). Storch (1978: plate 5, fig. 2) reconstructs the scaly covering much like that of the modern forms, covering the dorsum, flanks, and top of the head, although not covering the distal two-thirds of the tail or the distal portions of the limbs. In our reconstruction of *Patriomanis* (frontispiece), we have chosen to reconstruct the scales as Storch (1978) did for *Eomanis*, but in line with Kingdon's (1997) suggestion we have drawn a scale covering for the entire tail. We have also reconstructed more elongate pinnae for the ears and more and longer hair between the scales in *Patriomanis* than are found in any modern pangolin species. The longer ears and hair were intended as a kind of external reflection of its substantially more primitive skeletal anatomy, thus befitting an animal of its advanced geological age. It should be recognized, however, that all such reconstructions of the external anatomy are largely conjectural for the extinct pangolins.

Paleoecology, Climate, and Geographic Distribution

One of the curious aspects of the appearance of *Patriomanis* in the latest Eocene of North America is how the timing of its arrival relates to the paleoecology of this region. Modern pangolins are tropical creatures, their present distribution almost entirely encompassed within the belt between the Tropics of Cancer and Capricorn in Africa and South Asia (Macdonald, 2006). All but one of the extant species are forest dwellers, with only the African ground pangolin *Smutsia temminckii* habitually found in more open savannahs and grasslands (Kingdon, 1974, 1997; Heath, 1992a, 1992b, 1995; Nowak, 1999). Certainly, no modern pangolin could survive in the cool, dry, continental climes and open, scrubby habitat of today's Wyoming. However, the world of the Eocene was dramatically different from the modern world. The Eocene epoch was the warmest period of the Cenozoic era, with the Paleocene-Eocene Thermal Maximum (PETM) at the very beginning of this epoch representing the warmest single point in the past 65 million years. As noted by Blois and Hadly (2009:198), the PETM was characterized by the "lowest equator-to-pole temperature gradient" and "the greatest extent of tropical and subtropical forests ever achieved." These conditions persisted throughout the early Eocene, creating the kinds of habitats in northern Europe, Asia, and North America in which pangolins would certainly have thrived. However, from the beginning of the middle Eocene onward, there was a steady decline in global temperatures, culminating in a drastic drop known as the Terminal Eocene Event, when the northern climates became substantially drier and cooler (although still warmer than the present-day climate). In the late Cenozoic of western North America in particular, the tropical and subtropical forests of the Eocene were beginning to transition to the more open, grassy habits of the Oligocene epoch (Wing and Sues, 1992; Prothero, 1994; Blois and Hadley, 2009).

The fossil record of pangolins seems an ill fit in some regards when compared to this background of climate and vegetational change. As noted above, the oldest pangolins do not appear in the fossil record until the middle Eocene of Europe (*Eomanis, Euromanis, Eurotamandua*; Storch, 1978, 1981; Storch and Martin, 1994; Gaudin et al., 2009), when forests were still widespread in northern Laurasia but climatic deterioration was already well underway (Wing and Sues, 1992; Prothero, 1994; Blois and Hadley, 2009). The climate continued to become cooler and drier almost continually as, first, *Cryptomanis* made its appearance in the late Eocene of northern China (Gaudin et al., 2006) and, finally, *Patriomanis* made its appearance in North America in the latest Eocene (Rose, 2008). One might imagine that the warm tropical climes of the early Eocene would have been much more hospitable for the origin and spread of early pangolins than the middle and especially the late Eocene.

We offer two potential explanations for this apparent discrepancy between pangolin history and Eocene climatic history. Let us note at the outset that we do not imagine these to be the only possible explanations; although these appear plausible to us, other scenarios or contributing factors could certainly be imagined. That said, one possibility is to explain the discrepancy as the result of historical constraint. If the origin of the order is close to the age of its oldest fossils in the middle Eocene approximately 45 MYA, then the arrival of *Patriomanis* in North America occurs only 9–10 million years later. This is a long time,

but given the limitations noted in the Introduction—slow locomotory speeds, low reproductive rate, and low population densities, along with the apparently limited dispersal abilities of myrmecophagous mammals in general—it does not seem to be an unreasonable time lag to account for dispersal half a planet away. However, recent phylogenetic analyses postulate a much earlier origin for the pholidotan lineage. These analyses suggest an origin either in the vicinity of the Paleocene–Eocene boundary or in the early Paleocene. The former, from Meredith et al. (2011), is based on their estimate for the age of Carnivora, the extant sister group to Pholidota (their published estimate for Pholidota is much younger [25 MYA, late Oligocene] but refers only to the origin of Manidae; note that their figs. 1 and 2 suggest that Ferae [= Carnivora + Pholidota] may have an origin in the Paleocene or even the Cretaceous). The latter, from O'Leary et al. (2013), is based on ghost lineage analysis and the age of the extinct sister taxon to Pholidota, Palaeanodonta. The extra 10 or 20 million years provided for the origin of Pholidota by these hypotheses make the historical constraint hypothesis much less compelling.

Another possibility is that pangolins existed over much broader swaths of Laurasia much earlier in the Eocene (and Paleocene?) than is currently indicated by known fossils but that this results primarily from the incompleteness of their fossil record. The latter could be due to the difficulty in preserving, finding, and recognizing fossil pangolins. Patterson (1978) asserts that pangolins are less than ideal candidates for preservation, given their solitary lifestyle, preference for forested habitats, and lack of teeth, the most durable and readily recognizable part of mammalian skeletons. With the loss of teeth comes also a thinner and presumably less durable skull than that of comparably sized mammals. Pickford and Senut (1991) have also noted that mammalian paleontologists may overlook pangolin remains in the field or in the lab because of their edentulous nature and the difficulty of identifying fragmentary skulls or even well-preserved but isolated postcranial remains. This hypothesis is tantalizing to pangolin enthusiasts (an admittedly small group) because it suggests that more fossils remain to be found in Eocene, and perhaps even Paleocene, deposits in Europe, northern Asia, and North America. Nothing would form a more fitting ending for this monograph than that it should lead to the discovery of new fossil pangolins that will augment our understanding of this small but interesting and unusual group of mammals.

Appendix: Tables of Measurements

TABLE A1. Measurements of the skull and mandible in *Patriomanis americana* and related living and extinct (†) pangolins. A dash (—) indicates data are not available. GSL = greatest skull length; MML = maximum mandibular length.

Measurement	*Patriomanis americana*†, F:AM 78999 (type); USNM-P 494439	*Manis pentadactyla*, FMNH 32511	*Phataginus tricuspis*, USNM 537785, CM 86715	*Smutsia gigantea*, AMNH 53858	*Eomanis waldi*†, SMF MEA 263, Pohl specimen
Skull					
GSL (mm)	92[a]	89.6	68.6,[b] 69.6[c]	149.5	64.4[d]
Nasal length (mm)	—	28.10	24.1[c]	55.40	26[d]
Length of parietal-squamosal suture (mm)	27.1[e]	21.1	22.5[c]	32.2	13.5[d]
Length of parietal-squamosal suture versus GSL	~0.3	0.24	0.30	0.22	0.21
Mandible					
MML (mm)	>67[a,f]	57.9	46.9[b]	110.0	50.1[g]
Depth of horizontal ramus of the mandible (mm)	6.3	4.9	3.6[b]	5.7	4.9[g]
Depth of horizontal ramus of the mandible versus MML	<0.09	0.08	0.08	0.05	0.1

[a] Estimate.
[b] Based on USNM 537785.
[c] Based on CM 86715.
[d] Based on Pohl specimen.
[e] Based on only F:AM 78999.
[f] Based on only USNM-P 494439.
[g] Based on SMF MEA 263.

TABLE A2. Measurements of the atlas and axis in *Patriomanis americana* and living pangolins.

Measurement	*Patriomanis americana*†, F:AM 78999, USNM-P 299960	*Manis pentadactyla*, USNM 308733	*Phataginus tricuspis*, USNM 537785	*Smutsia gigantea*, AMNH 53848
Atlas				
Maximum transverse width, excluding transverse process (mm)	22.4[a]	26.1	21.7	41.1
Maximum dorsoventral height (mm)	16.4[a]	17.4	13.0	24.2
Ratio of height versus width	0.73	0.67	0.60	0.59
Maximum anteroposterior length, excluding transverse process (mm)	14.4[a]	14.4	9.1	26.1
Width versus length	1.50	1.90	2.40	1.60
Axis				
Maximum anteroposterior length, including dens (mm)	19.2[b]	15	8.9	22.3
Maximum transverse width, measured just behind anterior articular facets (mm)	16.7[b]	19.1	14.2	27.1
Length versus width	1.1	0.79	0.63	0.82

† Extinct.
[a] Based on only F:AM 78999.
[b] Based on only USNM-P 299960.

TABLE A3. Measurements of the thoracic and lumbar vertebrae in *Patriomanis americana* and related living and extinct (†) pangolins. A dash (—) indicates data are not available.

Measurement	*Patriomanis americana*†, USNM-P 299960	*Manis pentadactyla*, USNM 308733	*Phataginus tricuspis*, USNM 537785	*Smutsia gigantea*, AMNH 53848	*Cryptomanis gobiensis*†, AMNH 26140	*Eomanis waldi*†, SMF MEA 263 (cast)
Thoracic vertebrae[a]	ultimate or penultimate vertebra	T16 (of 16)	T14 (of 14)	T14 (of 14)	posteriormost preserved vertebra	—
Maximum transverse width of centrum (mm)	17.1	14.1	9.4	28.6	~22	—
Maximum dorsoventral height of centrum (mm)	9.3	8.2	5.6	17.0	~11	—
Ratio of height versus width	0.54	0.58	0.60	0.59	0.50	—
Maximum anteroposterior length of centrum	11.6	10.5	9.6	21.6	16.2	—
Width versus length	0.68	0.74	1.02	0.76	0.74	
Lumbar vertebrae[a]	L7	L3	L3	L3	L6	L4
Neural spine height (mm)	~13	10	4.7	28.3	~20	10.4
Neural spine anteroposterior length (mm)	8.4	9.8	8.2	17.6	8.2	6.5
Height versus length	1.5	1.02	0.57	1.6	2.4	1.6
Maximum dorsoventral height of centrum (mm)	11.6	8.4	6.6	19.3	13.2[b]	—
Maximum anteroposterior length of centrum (mm)	15	12.3	11	25	18.4[b]	—
Length versus height	1.29	1.46	1.67	1.3	1.39[b]	—

[a] Abbreviations: T14, T16 = 14th and 16th thoracic vertebrae; L3, L4, etc. = third lumbar vertebra, fourth lumbar vertebra, etc.
[b] Measurement taken at L3, not L6.

TABLE A4. Measurements of the metatarsals (mt) and pedal phalanges in *Patriomanis americana* and related living and extinct (†) pangolins. A dash (—) indicates data are not available.

Measurement	*Patriomanis americana*†, USNM-P 299960	*Manis pentadactyla*, USNM 308733	*Phataginus tricuspis* USNM 537785, CM 16206[a]	*Smutsia gigantea*, AMNH 53848, 53851[b]	*Cryptomanis gobiensis*†, AMNH 26140	*Eomanis waldi*†, SMF Me 84 (holotype), 15643[c]
Greatest length of mt						
Digit I (mm)	16.4	12.5	10.9	16.7	30.8	8.1
Digit II (mm)	26.6	14.4	14.3	22.6	36.6	15.2
Digit III (mm)	28.1	16	14.6	24.3	39.5	16.5
Digit III versus greatest length of tibia	0.35	0.24	0.25	0.2	0.43	0.31
Digit IV (mm)	27.4	15.6	14.9	24.8	38.7	13.6
Digit V (mm)	20.6	10	12.2	22.1	—	—
Greatest length of proximal phalanges						
Digit I (mm)	11.1	6.0	7.1	11.6	19.8	5.8
Digit II (mm)	11.2	4.2	6.3	7.3	16.2	6.3
Digit III (mm)	11.1	3.7	6.4	11.9	17.1	5.5
Digit IV (mm)	10.5	3.3	6.2	8.5	15.4	3.7
Digit V (mm)	9.0	3.2	5.8	6.6	14.1	2.4
Greatest length of intermediate phalanges (Ratio of intermediate/proximal phalanx length)						
Digit II (mm)	10.9 (1.0)	5.7 (1.4)	8.9 (1.2)	9.8 (1.3)	13.8 (0.9)	4.3 (0.7)
Digit III (mm)	11 (1.0)	7.3 (2.0)	8.6 (1.3) 10.5 (1.3)	10.5 (0.9)	12.6 (0.7)	6.3 (1.1)
Digit IV (mm)	9.8 (0.9)	6.9 (2.1)	8.6 (1.4) 10.7 (1.4)	10.6 (1.2)	14.2 (0.9)	4.0 (1.1)
Digit V (mm)	8.2 (0.9)	5.9 (1.8)	8.0 (1.2)	7.6 (1.2)	10.9 (0.8)	—
Greatest length of ungual phalanges						
Digit I (mm)	10.1	8.5	4.3	14.9	13.0	6.2
Digit II (mm)	11.4	10.8	12.1	20.4	15.0	9
Digit III (mm)	13.1	13.3	14.9	25.0	15.5	11.1
Digit IV (mm)	12.0	11.0	15.0	22.3	16.2	7.4
Digit V (mm)	9.6	8.7	10.8	15.8	—	4.1

[a] All measurements from USNM 537785 except for intermediate phalanges; first number under intermediate phalanges from USNM 537785, second number from CM 16206.
[b] Metatarsals from 53851, phalanges from 53848.
[c] Metatarsals: digit I from holotype, digits II–IV from 15643; phalanges: digits I, II from holotype, digits III–V from SMF Me 15643.

TABLE A5. Measurements of the astragalus in *Patriomanis americana* and related living and extinct (†) pangolins. A dash (—) indicates data are not available.

Measurement	*Patriomanis americana*†, USNM-P 299960	*Patriomanis americana*†, USNM-P 494439	*Manis pentadactyla*, USNM 308733	*Manis crassicaudata*, FMNH 244406	*Phataginus tricuspis*, USNM 537785
Maximum width of head (mm)	10.9	12.2	8.7	12.1	6.3
Maximum height of head (mm)	8	8.0	7.3	12.3	4.4
Height versus width of head	1.36	1.53	1.19	0.98	1.43
Minimum neck width (mm)	10.2	9.9	8.2	10.0	6.0
Maximum body width (mm)	17.2	18.0	13.4	19.3	8.5
Neck width versus body width	0.59	0.55	0.61	0.52	0.71
Maximum proximodistal depth of lateral trochlea (mm)	9.5	—	8.8	13.8	6.3
Maximum proximodistal depth of medial trochlea (mm)	9.4	—	6.6	8.0	4.0
Depth of medial trochlea versus depth of lateral trochlea	1.01	—	1.33	1.73	1.58
Maximum proximodistal length (mm)	18.5	21.5	14.5	22.6	10.3

Measurement	*Smutsia gigantea*, AMNH 53851	*Cryptomanis gobiensis*†, AMNH 26140	*Necromanis franconica*†, SMF M3379a+b	*Euromanis krebsi*†, SMF 94/1 (cast)
Maximum width of head (mm)	18.1	15.1	12.0	6.0
Maximum height of head (mm)	17.3	11.9	9.5	4.3
Height versus width of head	1.05	1.27	1.26	1.40
Minimum neck width (mm)	18.0	12.7	12.5	5.4
Maximum body width (mm)	27.5	25.4	22.5	14.1
Neck width versus body width	0.65	0.50	0.56	0.38
Maximum proximodistal depth of lateral trochlea (mm)	18.6	13.2	15.6	10.2
Maximum proximodistal depth of medial trochlea (mm)	12.5	11.1	12.9	9.3
Depth of medial trochlea versus depth of lateral trochlea	1.49	1.19	1.21	1.10
Maximum proximodistal length (mm)	28.2	25	23.9	15.5

TABLE A6. Measurements of the calcaneus in *Patriomanis americana* and related living and extinct (†) pangolins.

Measurement	*Patriomanis americana*†, USNM-P 299960	*Patriomanis americana*†, USNM-P 494439	*Manis pentadactyla*, USNM 308733	*Manis crassicaudata*, AMNH 244406	*Phataginus tricuspis*, USNM 537785
Maximum proximodistal length (mm)	30.0	33.0	22.0	35.0	16.5
Maximum proximodistal length of tuber (mm)	15.0	18.0	11.0	17.0	8.5
Proximodistal length of tuber as a percentage of proximodistal length	0.50	0.55	0.50	0.49	0.51

Measurement	*Smutsia gigantea*, AMNH 53851	*Cryptomanis gobiensis*†, AMNH 26140	*Necromanis franconica*†, SMF M3379c	*Eomanis waldi*†, SMF Me 15643A
Maximum proximodistal length (mm)	45.0	42.4	39.2	18.9
Maximum proximodistal length of tuber (mm)	16.7	22.0	21.0	7.9
Proximodistal length of tuber as a percentage of proximodistal length	0.37	0.52	0.54	0.42

TABLE A7. Measurements of the tibia and fibula in *Patriomanis americana* and related living and extinct (†) pangolins. A dash (—) indicates data are not available.

Measurement	*Patriomanis americana*†, USNM-P 299960, USNM-P 494439[a]	*Manis pentadactyla*, USNM 308733	*Phataginus tricuspis*, USNM 537785	*Smutsia gigantea*, AMNH 53858	*Cryptomanis gobiensis*†, AMNH 26140	*Eomanis waldi*†, SMF Me 84 (type)
Tibia						
Maximum length (mm)	79.6, 85.7	67.3	59.0	133.1	92.5	49.5
Maximum transverse width of distal end (mm)	16.9, 18.9	16.3	14.1	39.6	25.7	—
Maximum anteroposterior depth of distal end (mm)	11.7, 13.9	8.7	5.7	21.2	14.0	—
Anteroposterior depth versus transverse width of distal end	1.44, 1.36	1.87	2.47	1.87	1.84	—
Fibula						
Maximum fibula length (mm)	68.0	58.8	53.8	118.0	80.2	42.6
Fibula length versus tibia length	0.85	0.87	0.91	0.89	0.87	0.86

[a] First measurement for tibia and all fibula measurements from USNM-P 299960; second measurement for tibia from USNMP 494439.

TABLE A8. Measurements of the patella and femur in *Patriomanis americana* and related living and extinct (†) pangolins. A dash (—) indicates data are not available.

Measurement	*Patriomanis americana*†, USNM-P 299960	*Manis pentadactyla*, USNM 308733	*Phataginus tricuspis*, USNM 537785	*Smutsia gigantea*, AMNH 53858	*Cryptomanis gobiensis*†, AMNH 26140	*Euromanis krebsi*†, SMF Me 94/1	*Eomanis waldi*†, Pohl specimen
Patella							
Maximum patella height (mm)	15.5	18.7	10.4	32.3	21.4	11.8	—
Maximum patella width (mm)	13.7	11.5	7.7	23.5	18.4	9.4	—
Patella width versus patella height	1.13	1.63	1.35	1.37	1.16	1.26	—
Maximum patella depth (mm)	8.4	8.1	4.8	14.8	14.2	5.4	—
Patella depth versus patella height	0.56	0.43	0.46	0.46	0.66	0.46	—
Femur							
Maximum femur length (mm)	85.2	72.8	51.4	149.8	103.0	78.0	47.3, 50.3[a]
Proximodistal length of greater trochanter (mm)	10.4	12.3	9.8	28.7	15.2	—	—
Length of greater trochanter versus femur length	0.12	0.17	0.19	0.19	0.15	—	—
Distance from head to third trochanter (mm)	49.2	54.8	42.4	114.5	48.0	31.5	18
Distance from head to third trochanter versus femur length	0.58	0.75	0.82	0.76	0.47	0.40	0.38
Width at narrowest point on shaft (mm)	13.3	9.7	6.7	25.3	18.8	—	—
Depth at narrowest point on shaft (mm)	8.5	6.7	5.2	16.7	10.7	—	—
Depth versus width at narrowest point on shaft	1.56	1.45	1.29	1.51	1.76	—	—
Maximum width of distal end (mm)	23.7	21.6	15.4	48.4	35.3	22.1	16.5
Maximum depth of distal end (mm)	23.4	17.0	11.4	40.4	27.2	—	—
Depth versus width at distal end	1.01	1.27	1.35	1.20	1.30	—	—
Maximum width of medial condyle (mm)	10.0	9.5	6.4	21.6	15.2	—	7.5
Maximum width of lateral condyle (mm)	8.2	8.7	5.6	14.8	12.0	—	6.5
Width of lateral condyle versus width of medial condyle	1.22	1.09	1.14	1.46	1.27	—	1.15

[a] Second measurement from SMF Me 1573.

TABLE A9. Measurements of the scapula in *Patriomanis americana* and related living and extinct (†) pangolins. A dash (—) indicates data are not available.

Scapula measurement	*Patriomanis americana*†, USNM-P 299960	*Patriomanis americana*†, F:AM 78999	*Phataginus tricuspis*, USNM 537785	*Smutsia gigantea*, AMNH 53858	*Manis pentadactyla*, USNM 308733	*Euromanis krebsi*†, SMF Me 94/1	*Eomanis waldi*†, Pohl specimen
Dorsoventral length[a] (mm)	—	61.1	36.6	102.4	50.8	—	36.5
Height of scapular spine[b] (mm)	10.5	—	4.4	14.3	7.2	9	—
Maximum transverse width of glenoid fossa (mm)	11	—	6.6	19	9.3	9.20	—
Height of spine versus width of glenoid	0.95	—	0.67	0.75	0.78	0.98	—

[a] Measured from glenoid to dorsal border along spine.
[b] In distal view.

TABLE A10. Measurements of the humerus, radius, and ulna in *Patriomanis americana* and related living and extinct (†) pangolins. A dash (—) indicates data are not available.

Measurement	*Patriomanis americana*†, USNM-P 299960	*Patriomanis americana*†, USNM-P 531556	*Patriomanis americana*†, USNM-P 494439	*Manis pentadactyla*, USNM 308733	*Phataginus tricuspis*, USNM 537785	*Smutsia gigantea*, AMNH 53858	*Necromanis franconica*†, SMF Me 94/1	*Eomanis waldi*†, Pohl specimen
Humerus								
Length of deltopectoral crest (mm)	61.6	63.4	—	41.0	26.5	86.4	66.9	17.0
Maximum humerus length (mm)	76.9	81.0	—	62.3	48.4	121.2	84.2	47.3
Length of deltopectoral crest versus humerus lengt	0.79	0.78	—	0.66	0.55	0.71	0.79	0.47
Epicondyle width (mm)	28.8	29.4	—	28.8	22.0	59.4	44.0	18.0
Epicondyle width versus humerus length	0.37	0.36	—	0.46	0.45	0.49	0.52	0.38
Width of entepicondylar process (mm)	8.8	8.9	—	10.9	9.2	18.7	13.6	6.8
Width of entepicondylar process versus epicondyle width	0.31	0.30	—	0.38	0.42	0.31	0.3	0.4
Radius								
Maximum radius length (mm)	48.9	52.9	53.5	42.1	39.7	81.8	60.2	33.5
Radius length versus humerus length	0.64	0.65	—	0.68	0.82	0.67	0.90	0.71
Maximum depth of head (mm)	7.1	6.9	—	7.7	5.2	14.8	—	—
Maximum width of head (mm)	12.0	12.5	12.0	1.4	8.1	20.9	—	—
Width versus depth of head	0.59	0.55	—	0.68	0.64	0.71	—	—
Maximum depth of distal shaft (mm)	10.60	9.30	10.70	10.40	6.30	19.60	13.50	8.80
Depth of distal shaft versus radius length	0.22	0.18	0.20	0.25	0.16	0.24	0.22	0.26
Ulna								
Maximum ulna length (mm)	67.8	—	—	60.5	51.2	115.1	—	50.7
Ulna length versus humerus length	0.88	—	—	0.97	1.06	0.95	—	1.14
Maximum length of olecranon (mm)	18.1	—	—	20.7	9.3	23.4	—	13.8
Length of olecranon versus ulna length	0.27	—	—	0.34	0.18	0.20	—	0.27
Maximum depth of distal end of shaft (mm)	8.5	—	—	7.7	4.5	12.7	—	7.4
Depth of distal end of shaft versus ulna length	0.13	—	—	0.13	0.09	0.11	—	0.15
Length of styloid process (mm)	2.8	—	—	3.0	3.5	—	—	—
Length of styloid process versus ulna length	0.04	—	—	0.05	0.07	—	—	—

TABLE A11. Measurements of the scapholunar in *Patriomanis americana* and related living pangolins.

Scapholunar measurement	*Patriomanis americana*†, USNM-P 299960	*Manis pentadactyla*, USNM 308733	*Phataginus tricuspis*, USNM 537785	*Smutsia gigantea*, AMNH 53858
Maximum transverse width (mm)	14.5	15.3	13.1	28.5
Maximum dorsoventral depth (mm)	9.9	11.8	6.5	19.5
Depth versus width	0.68	0.77	0.5	0.68

†Extinct.

TABLE A12. Measurements of the metacarpals in *Patriomanis americana* and related living and extinct (†) pangolins. A dash (—) indicates data are not available.

Measurement	*Patriomanis americana*†, USNM-P 299960	*Patriomanis americana*†, USNM-P 494439	*Cryptomanis gobiensis*, AMNH 26140	*Manis pentadactyla*, USNM 308733	*Phataginus tricuspis*, USNM 537785	*Smutsia gigantea*, AMNH 53858	*Eomanis waldi*†, Pohl specimen
Greatest length of metacarpals							
Metacarpal I (mm)	13.3	14.8	25.5	9.6	6.5	11.5	—
Metacarpal II (mm)	19.2	—	~26	13.6	11.1	19.1	—
Metacarpal III (mm)	21.9	—	28.3	14.6	1.8	20.9	13.7
Length of metacarpal III versus maximum length of humerus	0.28	—	0.30	0.23	0.24	0.19	0.28
Metacarpal IV (mm)	19.3	21.4	28.9	12.4	11.0	17.8	10.2
Metacarpal V (mm)	12.6	—	—	8.6	10.2	17.2	—
Midshaft width of metacarpals							
Metacarpal I (mm)	2.6	2.7	3.6	1.6	4.1	2.3	—
Metacarpal II (mm)	3.8	—	6.0	2.2	1.8	4.6	—
Metacarpal III (mm)	4.8	—	10.0	5.8	3.8	9.3	—
Metacarpal IV (mm)	4.3	4.7	8.1	3.8	1.7	5.8	—
Metacarpal V (mm)	3.6	—	5.3	2.3	1.7	3.2	—
Midshaft depth of metacarpals							
Metacarpal I (mm)	2.6	2.7	4.0	2.3	1.6	4.1	—
Metacarpal II (mm)	3.7	—	4.5	3.9	2.1	4.9	—
Metacarpal III (mm)	4.7	—	5.5	6.4	3.7	10.1	6.0
Metacarpal IV (mm)	4.0	4.0	5.5	4.1	2.6	7.4	5.0
Metacarpal V (mm)	2.6	—	3.2	3.5	1.8	4.5	—
Ratio of metacarpal width to length							
Metacarpal I	0.20	0.18	0.14	0.14	0.18	0.2	—
Metacarpal II	0.20	—	0.23	0.16	0.16	0.24	—
Metacarpal III	0.22	—	0.35	0.4	0.32	0.44	—
Metacarpal IV	0.22	0.22	0.28	0.31	0.15	0.32	—
Metacarpal V	0.29	—	—	0.27	0.17	0.19	—

TABLE A13. Measurements of the manual phalanges in *Patriomanis americana* and related living and extinct (†) pangolins. A dash (—) indicates data are not available.

Measurement	*Patriomanis americana*†, USNM-P 299960	*Patriomanis americana*†, USNM-P 494439	*Patriomanis americana*†, F:AM 78999 (type)	*Manis pentadactyla*, USNM 308733	*Phataginus tricuspis*, USNM 537785	*Smutsia gigantea*, AMNH 53858	*Cryptomanis gobiensis*†, AMNH 26140	*Eomanis waldi*†, Pohl specimen
Greatest length of proximal phalanges								
Digit I (mm)	11.1	12.8	—	6.2	5.8	11.6	>13.5	—
Digit II (mm)	11.1	13.3	12.7	7.4	5.9	11.6	9.2	—
Digit III (mm)	9.6	9.7	10.0	6.4	8.7	14.3	7.2	5.5
Digit IV (mm)	8.7	12.0	10.2	5.2	6.1	11.8	9.8	—
Digit V (mm)	7.6	9.0	—	3.3	5.6	6.7	11.1	—
Maximum proximal width of proximal phalanges (Ratio of width/length)								
Digit I (mm)	4.7 (0.4)	4.5 (0.35)	—	2.5 (0.4)	1.4 (0.2)	4.3 (0.4)	6.3 (<0.5)	—
Digit II (mm)	6.4 (0.6)	8.3 (0.6)	7.3 (0.6)	3.7 (0.5)	2.9 (0.5)	8.4 (0.7)	9.4 (1.0)	—
Digit III (mm)	7.9 (0.8)	8.1 (0.8)	8.2 (0.8)	6.9 (1.1)	5.2 (0.6)	12.2 (0.85)	10.2 (1.4)	—
Digit IV (mm)	6.6 (0.8)	6.2 (0.5)	6.9 (0.7)	5.4 (1.0)	3.0 (0.5)	10.5 (0.9)	9.8 (1.0)	—
Digit V (mm)	5.6 (0.7)	5.6 (0.7)	—	3.5 (1.1)	2.7 (0.5)	5.6 (0.8)	7.9 (0.7)	—
Greatest length of intermediate phalanges (Ratio of intermediate/proximal phalanx length)								
Digit II (mm)	11.2 (1.0)	12.6 (1.0)	—	8.8 (1.2)	7.1 (1.2)	16.9 (1.5)	—	—
Digit III (mm)	10.6 (1.1)	13.0 (1.0)	—	12.5 (2.0)	11.9 (1.4)	18.3 (1.3)	13.1 (1.8)	4.8 (0.9)
Digit IV (mm)	10.1 (1.2)	12.6 (1.1)	—	9.2 (1.8)	8.7 (1.4)	17.2 (1.5)	—	—
Digit V (mm)	7.6 (1.0)	9.4 (1.0)	—	5.6 (1.7)	7.7 (1.4)	9.9 (1.5)	10.6 (1.0)	—
Greatest length of ungual phalanges								
Digit I (mm)	9.1	10.3	10.1	8.0	4.9	13.7	—	—
Digit II (mm)	12.2	15.8	—	16.5	11.6	32.3	—	15.8
Digit III (mm)	13.4	—	—	33.3	19.6	52.5	—	20.7
Digit IV (mm)	11.0	13.6	—	23.4	13.7	43.1	—	13.5
Digit V (mm)	9.2	—	—	11.6	10.8	19.0	—	—

References

Argot, C. 2003. Functional-Adaptive Anatomy of the Axial Skeleton of Some Extant Marsupials and the Paleobiology of the Paleocene Marsupials *Mayulestes ferox* and *Pucadelphys andinus*. *Journal of Morphology,* 255:279–300. http://dx.doi.org/10.1002/jmor.10062.

Blois, J., and E. A. Hadly. 2009. Mammalian Response to Cenozoic Climatic Change. *Annual Review of Earth and Planetary Sciences*, 37:181–208. http://dx.doi.org/10.1146/annurev.earth.031208.100055.

Bugge, J. 1979. Cephalic Arterial Pattern in New World Edentates and Old World Pangolins with Special Reference to Their Phylogenetic Relationships and Taxonomy. *Acta Anatomica,* 105(1):37–46. http://dx.doi.org/10.1159/000145104.

Chan, L.-K. 1995. Extrinsic Lingual Musculature of Two Pangolins (Pholidota: Manidae). *Journal of Mammalogy,* 76(2):472–480. http://dx.doi.org/10.2307/1382356.

Corbet, G. B., and J. E. Hill. 1991. *A World List of Mammalian Species*. Natural History Museum Publication. London: Oxford University Press.

Doran, G. A., and D. B. Allbrook. 1973. The Tongue and Associated Structures in Two Species of African Pangolins, *Manis gigantea* and *Manis tricuspis*. *Journal of Mammalogy,* 54(4):887–899. http://dx.doi.org/10.2307/1379083.

Emry, R. J. 1970. A North American Oligocene Pangolin and Other Additions to the Pholidota. *Bulletin of the American Museum of Natural History,* 142:459–510.

———. 1973. *Stratigraphy and Preliminary Biostratigraphy of the Flagstaff Rim Area, Natrona County, Wyoming*. Smithsonian Contributions to Paleobiology 18. Washington, D.C.: Smithsonian Institution Press. http://dx.doi.org/10.5479/si.00810266.18.1.

———. 2004. The Edentulous Skull of the North American Pangolin, *Patriomanis americanus*. *Bulletin of the American Museum of Natural History,* 285:130–138. http://dx.doi.org/10.1206/0003-0090(2004)285<0130:C>2.0.CO;2.

Emry, R. J., and C. E. Gawne. 1986. A Primitive, Early Oligocene Species of *Palaeolagus* (Mammalia, Lagomorpha) from the Flagstaff Rim Area of Wyoming. *Journal of Vertebrate Paleontology*, 6:271–280. http://dx.doi.org/10.1080/02724634.1986.10011622.

Evans, H. E., and G. C. Christensen. 1979. *Miller's Anatomy of the Dog*. 2nd ed. Philadelphia: W. B. Saunders.

Ferigolo, J. 1981. The Mesethmoid Bone and the Edentata. *Anais, Academia Brasileira de Ciências,* 53(4):817–824.

Frechkop, S. 1949. Notes sur les Mammiféres. XXXVI. Explication Biologique, Fournie par les Tatous, d'un des Caractères Distinctifs des Xénathres et d'un Caractère Adaptif Analogue chez les Pangolins. *Institut royal des Sciences naturelles de Belgique,* 25(28):1–12.

Flower, W. H. 1885. *An Introduction to the Osteology of the Mammalia*. London: Macmillan. http://dx.doi.org/10.5962/bhl.title.101537.

Flynn, J. J., and G. D. Wesley-Hunt. 2005. "Carnivora." In *The Rise of Placental Mammals: Origins and Relationships of the Major Extant Clades,* ed. K. D. Rose and J. D. Archibald, pp. 175–198. Baltimore: Johns Hopkins University Press.

Gaubert, P., and A. Antunes. 2005. Assessing the Taxonomic Status of the Palawan Pangolin *Manis culionensis* (Pholidota) Using Discrete Morphological Characters. *Journal of Mammalogy*, 86:1068–1074. http://dx.doi.org/10.1644/1545-1542(2005)86[1068:ATTSOT]2.0.CO;2.

Gaudin, T. J. 1995. The Ear Region of Edentates and the Phylogeny of the Tardigrada (Mammalia, Xenarthra). *Journal of Vertebrate Paleontology,* 15(3):672–705. http://dx.doi.org/10.1080/02724634.1995.10011255.

———. 2004. Phylogenetic Relationships among Sloths (Mammalia, Xenarthra, Tardigrada): The Craniodental Evidence. *Zoological Journal of the Linnean Society*, 140(2):255–305. http://dx.doi.org/10.1111/j.1096-3642.2003.00100.x.

———. 2010. "Pholidota." In *Cenozoic Mammals of Africa,* ed. L. Werdelin and W. J. Sanders, pp. 599–602. Berkeley: University of California Press. http://dx.doi.org/10.1525/california/9780520257214.003.0031.

Gaudin, T. J., and D. G. Branham. 1998. The Phylogeny of the Myrmecophagidae (Mammalia, Xenarthra, Vermilingua) and Relationship of *Eurotamandua* to the Vermilingua. *Journal of Mammalian Evolution*, 5(3):237–265. http://dx.doi.org/10.1023/A:1020512529767.

Gaudin, T. J., R. J. Emry, and B. Pogue. 2006. A New Genus and Species of Pangolin (Mammalia, Pholidota) from the Late Eocene of Inner Mongolia, China. *Journal of Vertebrate Paleontology*, 26(1):146–159. http://dx.doi.org/10.1671/0272-4634(2006)26[146:ANGASO]2.0.CO;2.

Gaudin, T. J., R. J. Emry, and J. R. Wible. 2009. The Phylogeny of Living and Extinct Pangolins (Mammalia, Pholidota) and Associated Taxa: A Morphology Based Analysis. *Journal of Mammalian Evolution*, 16(4):235–305. http://dx.doi.org/10.1007/s10914-009-9119-9.

Gaudin, T. J., and H. G. McDonald. 2008. "Morphology-Based Investigations of the Phylogenetic Relationships among Extant and Fossil Xenarthrans." In *Biology of the Xenarthra,* ed. J. Loughry and S. Vizcaíno, pp. 24–36. Gainesville: University of Florida Press.

Gaudin, T. J., and J. R. Wible. 1999. The Entotympanic of Pangolins and the Phylogeny of the Pholidota (Mammalia). *Journal of Mammalian Evolution*, 6:39–65. http://dx.doi.org/10.1023/A:1020538313412.

Gebo, D. L., and D. T. Rasmussen. 1985. The Earliest Fossil Pangolin (Pholidota: Manidae) from Africa. *Journal of Mammalogy*, 66:538–540. http://dx.doi.org/10.2307/1380929.

Grassé, P. P. 1955. "Ordre des Pholidotes." In *Traité de Zoologie*. Volume 17: *Mammifères,* ed. P. P. Grassé, pp. 1267–1282. Paris: Masson et Cie.

Guth, C. 1958. "Pholidota." In *Traité de Paléontologie*. Volume 2, no. 6: *Mammifères Évolution,* ed. J. Piveteau, pp. 641–647. Paris: Masson et Cie.

Heath, M. E. 1992a. *Manis pentadactyla*. *Mammalian Species*, 414:1–6. http://dx.doi.org/10.2307/3504143.

———. 1992b. *Manis temminckii*. *Mammalian Species,* 415:1–5. http://dx.doi.org/10.2307/3504220.

———. 1995. *Manis crassicaudata*. *Mammalian Species,* 513:1–4. http://dx.doi.org/10.2307/3504173.

Heaton, T. H., and R. J. Emry. 1996. "Leptomerycidae." In *The Terrestrial Eocene-Oligocene Transition in North America,* ed. D. R. Prothero and R. J. Emry, pp. 581–608. Cambridge: Cambridge University Press. http://dx.doi.org/10.1017/CBO9780511665431.028.

Helbing, H. 1938. Nachweis manisartiger Säugetiere im stratifzierten europäischen Oligocaen. *Eclogae Geologicae Helvetie,* 31:296–303.

Hirschfeld, S. E. 1976. A New Fossil Anteater (Edentata, Mammalia) from Colombia, S.A. and Evolution of the Vermilingua. *Journal of Paleontology,* 50:419–432.

Hoffmann, S. 2011. Revised Phylogeny of Pholidota: Implications for Ferae. *Journal of Vertebrate Paleontology*, 31(Suppl. 1):126A–127A.

Hoffmann, S., T. Martin, G. Storch, and M. Rummel. 2009. Skeletal Reconstruction of a Miocene Pangolin from Southern Germany. *Journal of Vertebrate Paleontology*, 29(Suppl. 1): 115A–116A.

Holroyd, P. A., and J. C. Mussell. 2005. "Macroscelidea and Tubulidentata." In *The Rise of Placental Mammals: Origins and Relationships of the Major Extant Clades,* ed. K. D. Rose and J. D. Archibald, pp. 71–83. Baltimore: Johns Hopkins University Press.

Homberger, D. G., and W. F. Walker. 2004. *Vertebrate Dissection*. 9th ed. Belmont, Calif.: Thomson Brooks/Cole.

Horovitz, I. 2003. Postcranial Skeleton of *Ukhaatherium nessovi* (Eutheria, Mammalia) from the Late Cretaceous of Mongolia. *Journal of Vertebrate Paleontology*, 23:857–868. http://dx.doi.org/10.1671/2399-10.

Humphry, G. M. 1870. The Myology of the Limbs of the Unau, the Aï, the Two-Toed Anteater, and the Pangolin. *Journal of Anatomy and Physiology*, 4:17–78.

Janis, C. M., G. F. Gunnell, and M. D. Uhen. 2008. *Evolution of Tertiary Mammals of North America*. Volume 2: *Small Mammals, Xenarthrans, and Marine Mammals*. New York: Cambridge University Press.

Ji, Q., Z.-X. Luo, C.-X. Yuan, J. R. Wible, J.-P. Zhang, and J. A. Georgi. 2002. The Earliest Known Eutherian Mammal. *Nature*, 416:816–822. http://dx.doi.org/10.1038/416816a.

Jollie, M. 1968. The Head Skeleton of a New-Born *Manis javanica* with Comments on the Ontogeny and Phylogeny of the Mammal Head Skeleton. *Acta Zoologica*, 49:227–305. http://dx.doi.org/10.1111/j.1463-6395.1968.tb00155.x.

Jouffroy, F. K. 1966. Musculature de l'Avant-bras et de la Main, de la Jambe et du Pied chez *Manis gigantea*, III. *Biologica Gabonica*, 2:251–286.

Kielan-Jaworowska, Z., R. L. Cifelli, and Z.-X. Luo. 2004. *Mammals from the Age of Dinosaurs: Origins, Evolution, and Structure*. New York: Columbia University Press.

Kingdon, J. 1974. *East African Mammals*. Volume 1. Chicago: University of Chicago Press.

———. 1997. *The Kingdon Field Guide to African Mammals*. Princeton, N.J.: Princeton University Press.

Koenigswald, W. von. 1969. Die Maniden (Pholidota, Mamm.) des europäischen Tertiärs. *Mitteilungen der Bayerischen*

Staatssammlung für Paläontologie und historische Geologie, 9:61–71.

———. 1999. "Order Pholidota." In *The Miocene Land Mammals of Europe*, ed. G. E. Rössner and K. Heissig, pp. 75–80. Munich: Verlag Dr. Friedrich Pfeil.

Koenigswald, W. von, and T. Martin. 1990. Ein Skelett von *Necromanis franconica*, einem Schuppentier (Pholidota, Mammalia) aus dem Aquitan von Saulcet im Allier-Becken (Frankreich). *Eclogae Geologicae Helvetiae,* 83:845–864.

Koenigswald, W. von, G. Richter, and G. Storch. 1981. Nachweis von Hornschuppen bei *Eomanis waldi* aus der "Grube Messel" bei Darmstadt (Mammalia, Pholidota). *Senckenbergiana lethaea,* 61:291–298.

Macdonald, D. W., ed. 2006. *The Princeton Encyclopedia of Mammals*. Princeton, N.J.: Princeton University Press.

MacPhee, R. D. E. 1994. Morphology, Adaptations, and Relationships of *Plesiorycteropus*, and a Diagnosis of a New Order of Eutherian Mammals. *Bulletin of the American Museum of Natural History*, 220:1–214.

Matthew, W. D. 1918. Edentata. A Revision of the Lower Eocene Wasatch and Wind River Faunas. Part V—Insectivora (continued), Glires, Edentata. *Bulletin of the American Museum of Natural History,* 38:565–657.

McKenna M. C., and S. K. Bell. 1997. *Classification of Mammals above the Species Level*. New York: Columbia University Press.

Meredith, R. W., J. E. Janec, J. Gatesy, O. A. Ryder, C. A. Fisher, E. C. Teeling, A. Goodbla, E. Eizirik, T. L. L. Simão, T. Stadler, D. L. Rabosky, R. L. Honeycutt, J. J. Flynn, C. M. Ingram, C. Steiner, T. L. Williams, T. J. Robinson, A. Burk-Herrick, M. Westerman, N. A. Ayoub, M. S. Springer, and W. J. Murphy. 2011. Impacts of the Cretaceous Terrestrial Revolution and KPg Extinction on Mammal Diversification. *Science*, 334:521–524. http://dx.doi.org/10.1126/science.1211028.

Muizon, C. de. 1998. *Mayulestes ferox,* a Borhyaenoid (Metatheria, Mammalia) from the Early Paleocene of Bolivia. Phylogenetic and Paleobiologic Implications. *Geodiversitas*, 20(1):19–142.

Muizon, C. de, and H. G. McDonald. 1995. An Aquatic Sloth from the Pliocene of Peru. *Nature,* 375:224–227. http://dx.doi.org/10.1038/375224a0.

Neveu, P., and J.-P. Gasc. 2002. Lipotyphla Limb Myology Comparison. *Journal of Morphology*, 252:183–201. http://dx.doi.org/10.1002/jmor.1098.

Novacek, M. J. 1986. The Skull of Leptictid Insectivorans and the Higher-Level Classification of Eutherian Mammals. *Bulletin of the American Museum of Natural History*, 183: 1–111.

———. 1993. "Patterns of Diversity in the Mammalian Skull." In *The Skull*. Volume 2: *Patterns of Structural and Systematic Diversity,* ed. J. Hanken and B. K. Hall, pp. 438–545. Chicago: University of Chicago Press.

Novacek, M. J., and A. R. Wyss. 1986. Higher-Level Relationships of the Recent Eutherian Orders: Morphological Evidence. *Cladistics,* 2:257–287.

Nowak, R. M. 1999. *Walker's Mammals of the World*. 6th ed. Baltimore: Johns Hopkins University Press.

O'Leary, M. A., J. I. Bloch, J. J. Flynn, T. J. Gaudin, A. Giallombardo, N. P. Giannini, S. L. Goldberg, B. P. Kraatz, Z.-X. Luo, J. Meng, X. Ni, M. J. Novacek, F. A. Perini, Z. Randall, G. W. Rougier, E. J. Sargis, M. T. Silcox, N. B. Simmons, M. Spaulding, P. M. Velazco, M. Weksler, J. R. Wible, and A. L. Cirranello. 2013. The Placental Mammal Ancestor and the Post-KPg Radiation of Placentals. *Science*, 339:662–667. http://dx.doi.org/10.1126/science.1229237.

Organ, J. M. 2010. Structure and Function of Platyrrhine Caudal Vertebrae. *Anatomical Record*, 293:730–745. http://dx.doi.org/10.1002/ar.21129.

Patterson, B. 1978. "Pholidota and Tubulidentata." In *Evolution of African Mammals,* ed. V. J. Maglio and H. B. S. Cooke, pp. 268–278. Cambridge, Mass.: Harvard University Press.

Patterson, B., W. Segall, and W. D. Turnbull. 1989. The Ear Region in Xenarthrans (= Edentata, Mammalia). Part I. Cingulates. *Fieldiana, Geology,* n.s., 18:1–46.

Patterson, B., W. Segall, W. D. Turnbull, and T. J. Gaudin. 1992. The Ear Region in Xenarthrans (= Edentata, Mammalia). Part II. Pilosa (Sloths, Anteaters), Palaeanodonts, and a Miscellany. *Fieldiana, Geology,* n.s., 24:1–79.

Pick, T. P., and R. Howden. 1977. *Gray's Anatomy*. 15th ed. New York: Bounty Books.

Pickford, M., and B. Senut. 1991. The Discovery of a Giant Pangolin in the Pliocene of Uganda. *Comptes Rendus de l'Académie des Sciences, Série II*, 313:827–830.

Prothero, D. R. 1994. *The Eocene-Oligocene Transition: Paradise Lost*. New York: Columbia University Press.

Prothero, D. R., and R. J. Emry. 1996. "Summary." In *The Terrestrial Eocene-Oligocene Transition in North America*, ed. D. R. Prothero and R. J. Emry, pp. 664–683. Cambridge, UK: Cambridge University Press.

———. 2004. "The Chadronian, Orellan, and Whitneyan North American Land Mammal Ages." In *Late Cretaceous and Cenozoic Mammals of North America,* ed. M. O. Woodburne, pp. 156–168. New York: Columbia University Press.

Prothero, D. R., and C. C. Swisher III. 1992. "Magnetostratigraphy and Geochronology of the Terrestrial Eocene-Oligocene Transition in North America." In *Eocene-Oligocene Climatic and Biotic Evolution,* ed. D. R. Prothero and W. A. Berggren, pp. 46–73. Princeton, N.J.: Princeton University Press.

Pujos, F., T. J. Gaudin, G. De Iuliis, and C. Cartelle. 2012. Recent Advances on Variability, Morpho-Functional Adaptations, Dental Terminology, and Evolution of Sloths. *Journal of Mammalian Evolution*, 19(3):159–169. http://dx.doi.org/10.1007/s10914-012-9189-y.

Rose, K. D. 1979. A New Paleocene Palaeanodont and the Origin of the Metacheiromyidae (Mammalia). *Breviora of the Museum of Comparative Zoology,* 455:1–14.

———. 2006. *The Beginning of the Age of Mammals*. Baltimore: Johns Hopkins University Press.

———. 2008. "Palaeanodonta and Pholidota." In *Evolution of Tertiary Mammals of North America*. Volume 2: *Small Mammals, Xenarthrans, and Marine Mammals,* ed. C. M. Janis, G. F. Gunnell, and M. D. Uhen, pp. 135–146. New York: Cambridge University Press.

Rose, K. D., and R. J. Emry. 1993. "Relationships of Xenarthra, Pholidota, and Fossil 'Edentates': The Morphological

Evidence." In *Mammal Phylogeny*. Volume 2: *Placentals,* ed. F. S. Szalay, M. J. Novacek, and M. C. McKenna, pp. 81–102. New York: Springer-Verlag.

Rose, K. D., R. J. Emry, T. J. Gaudin, and G. Storch. 2005. "Xenarthra and Pholidota." In *The Rise of Placental Mammals: Origins and Relationships of the Major Extant Clades,* ed. K. D. Rose and J. D. Archibald, pp. 106–126. Baltimore: Johns Hopkins University Press.

Rose, K. D., and W. von Koenigswald. 2005. An Exceptionally Complete Skeleton of *Palaeosinopa* (Mammalia, Cimolesta, Pantolestidae) from the Green River Formation, and the Other Postcranial Elements of the Pantolestidae from the Eocene of Wyoming (USA). *Palaeontographica, Abteilung A*, 273(3–6):55–96.

Rose, K. D., and S. G. Lucas. 2000. An Early Paleocene Palaeanodont (Mammalia, ?Pholidota) from New Mexico, and the Origin of the Palaeanodonta. *Journal of Vertebrate Paleontology*, 20:139–156. http://dx.doi.org/10.1671/0272-4634(2000)020[0139:AEPPMP]2.0.CO;2.

Schlitter, D. A. 2005. "Order Pholidota." In *Mammal Species of the World,* 3rd ed., ed. D. E. Wilson and D. M. Reeder, pp. 530–531. Baltimore: Johns Hopkins University Press.

Scott, W. B. 1903–1904. Mammalia of the Santa Cruz Beds. Part 1: Edentata. *Reports of the Princeton Expeditions to Patagonia*, 5:1–364.

Segall, W. 1970. Morphological Parallelisms of the Bulla and Auditory Ossicles in Some Insectivores and Marsupials. *Fieldiana: Zoology*, 51:169–205. http://dx.doi.org/10.5962/bhl.title.2899.

Simpson, G. G. 1931. *Metacheiromys* and the Edentata. *Bulletin of the American Museum of Natural History*, 59:295–381.

Slijper, E. J. 1946. Comparative Biologic-Anatomical Investigations on the Vertebral Column and Spinal Musculature of Mammals. *Verhandelingen der Koninklijke Nederlandsche Akademie van Wetenschappen, Afdeeling Natuurkunde, Tweede Sectie*, 17:1–128.

Solomon, E. P., L. R. Berg, and D. W. Martin. 2011. *Biology*. 9th ed. Belmont, Calif.: Cengage Learning.

Storch, G. 1978. *Eomanis waldi*, ein Schuppentier aus dem Mittel-Eozän der "Grube Messel" bei Darmstadt (Mammalia: Pholidota). *Senckenbergiana lethaea*, 59:503–529.

———. 1981. *Eurotamandua joresi*, ein Myrmecophagidae aus dem Eozän der "Grube Messel" bei Darmstadt (Mammalia, Xenarthra). *Senckenbergiana lethaea,* 61:247–289.

———. 2003. Fossil Old World "Edentates." In *Morphological Studies in Fossil and Extant Xenarthra (Mammalia),* ed. R. A. Fariña, S. F. Vizcaíno, and G. Storch. *Senckenbergiana biologica*, 83:51–60.

Storch, G., and J. Habersetzer. 1991. Rückverlagerte Choanen und akzessorische Bulla tympanica bei rezenten Vermilingua und Eurotamandua aus dem Eozän von Messel (Mammalia: Xenarthra). *Zeitschrift für Säugetierkunde*, 56:257–271.

Storch, G., and T. Martin. 1994. *Euromanis krebsi*, ein neues Schuppentier aus dem Mittel-Eozän der Grube Messel bei Darmstadt (Mammalia: Pholidota). *Berliner geowissenschaftliche Abhandlungen*, E13:83–97.

Swisher, C. C., III, and D. R. Prothero. 1990. Single-Crystal $^{40}Ar/^{39}Ar$ Dating of the Eocene-Oligocene Transition in North America. *Science*, 249:760–762. http://dx.doi.org/10.1126/science.249.4970.760.

Szalay, F. S. 1977. "Phylogenetic Relationships and a Classification of the Eutherian Mammals." In *Major Patterns in Vertebrate Evolution,* ed. M. K. Hecht, P. C. Goody, and B. M. Hecht, pp. 315–374. New York: Plenum Press.

Szalay, F. S., and F. Schrenk. 1998. The Middle Eocene *Eurotamandua* and a Darwinian Phylogenetic Analysis of "Edentates." *Kaupia: Darmstädter Beiträge zur Naturgeschichte*, 7:97–186.

Vaughan, T. A., J. M. Ryan, and N. J. Czaplewski. 2011. *Mammalogy*. 5th ed. Sudbury, Mass.: Jones and Bartlett.

Weber, M. 1928. *Die Säugetiere*. Jena, Germany: Gustav Fischer.

Wible, J. R. 1990. Petrosals of Late Cretaceous Marsupials from North America, and a Cladistic Analysis of the Petrosal in Therian Mammals. *Journal of Vertebrate Paleontology*, 10(2):183–205. http://dx.doi.org/10.1080/02724634.1990.10011807.

———. 2008. On the Cranial Osteology of the Hispaniolan Solenodon, *Solenodon paradoxus* Brandt, 1833 (Mammalia, Lipotyphla, Solenodontidae). *Annals of the Carnegie Museum*, 70(3):321–402. http://dx.doi.org/10.2992/0097-4463-77.3.321.

———. 2010. Petrosal Anatomy of the Nine-Banded Armadillo, *Dasypus novemcinctus* Linnaeus, 1758 (Placentalia: Xenarthra: Dasypodidae). *Annals of Carnegie Museum*, 79:1–28. http://dx.doi.org/10.2992/007.079.0101.

Wible, J. R., and T. J. Gaudin. 2004. On the Cranial Osteology of the Yellow Armadillo *Euphractus sexcinctus* (Dasypodidae, Xenarthra, Placentalia). *Annals of the Carnegie Museum of Natural History*, 73(3):117–196.

Wible, J. R., M. J. Novacek, and G. W. Rougier. 2004. New Data on the Skull and Dentition in the Mongolian Late Cretaceous Mammal *Zalambdalestes*. *Bulletin of the American Museum of Natural History*, 281:1–144. http://dx.doi.org/10.1206/0003-0090(2004)281<0001:NDOTSA>2.0.CO;2.

Wible, J. R., G. W. Rougier, M. J. Novacek, and R. J. Asher. 2009. The Eutherian Mammal *Maelestes gobiensis* from the Late Cretaceous of Mongolia and the Phylogeny of Cretaceous Eutheria. *Bulletin of the American Museum of Natural History*, 327:1–123. http://dx.doi.org/10.1206/623.1.

Windle, B. G., and F. G. Parsons. 1899. Myology of the Edentata. *Proceedings of the Zoological Society of London*, 1899:314–338, 990–1017.

Wing, S. L., and H.-D. Sues. 1992. "Mesozoic and Early Cenozoic Terrestrial Ecosystems." In *Terrestrial Ecosystems through Time: Evolutionary Paleoecology of Terrestrial Plants and Animals,* ed. A. K. Behrensmeyer, J. D. Damuth, W. A. DiMichele, R. Potts, H.-D. Sues, and S. L. Wing, pp. 327–416. Chicago: University of Chicago Press.

Wyss, A. R., and J. J. Flynn. 1993. "A Phylogenetic Analysis and Definition of the Carnivora." In *Mammal Phylogeny*. Volume 2: *Placentals,* ed. F. S. Szalay, M. J. Novacek, and M. C. McKenna, pp. 32–52. New York: Springer-Verlag. http://dx.doi.org/10.1007/978-1-4613-9246-0_4.

Youlatos, D. 2003. Osteological Correlates of Tail Prehensility in Carnivorans. *Journal of Zoology, London*, 259:423–430. http://dx.doi.org/10.1017/S0952836903003431.

SUMMARY OF REQUIREMENTS FOR SMITHSONIAN CONTRIBUTIONS SERIES

For comprehensive guidelines and specifications, visit www.scholarlypress.si.edu or Open SI (http://opensi.si.edu).

ABSTRACTS must not exceed 300 words.

TEXT must be prepared in a recent version of Microsoft Word; use a Times font in 12 point for regular text; be double spaced; and have 1" margins.

REQUIRED ELEMENTS are title page, abstract, table of contents, main text, and references.

FIGURES should be numbered sequentially (1, 2, 3, etc.) in the order called out; have components lettered consistently (in size, font, and style) and described in captions; include a scale bar or scale description, if appropriate; include any legends in or on the figure rather than in a caption. Figures must be original and submitted as individual TIF or EPS files.

FIGURE FILES must not be embedded in the main text. Resolution for art files must be at least 300 dpi for grayscale and color images, and at least 1200 dpi for line art. Color images should be requested only if required.

TAXONOMIC KEYS in natural history papers should use the aligned-couplet form for zoology. If cross referencing is required between key and text, do not include page references within the key but number the keyed-out taxa, using the same numbers with their corresponding heads in the text.

SYNONYMY IN ZOOLOGY must use the short form (taxon, author, year:page), with full reference at the end of the paper under "References."

REFERENCES should be in alphabetical order, and in chronological order for same-author entries.
Each reference should be cited at least once in main text. Complete bibliographic information must be included in all citations. Examples of the most common types of citations are provided on SISP's "Author Resources" page at www.scholarlypress.si.edu.